On the Probabilistic Time-Dependent Axial Shortening of Tall Concrete Buildings - Volume 1

by

Michael Koutsoukis, BE(Hons)

Submitted in fulfilment of

the requirements for the degree of

Doctor of Philosophy

Dept of Civil & Mechanical Engr

University of Tasmania

July, 1996

ORIGINALITY

This thesis contains no material which has been accepted for a degree or diploma by the University of Tasmania or any other institution, except by way of background information and duly acknowledged in the thesis, and to the best of the candidate's knowledge and belief no material previously published or written by another person except where due acknowledgment is made in the text of the thesis.

Signed: 

(Michael Koutsoukis)

AUTHORITY OF ACCESS

This thesis may be made available for loan and limited copying in accordance with the Copyright Act 1968.

PREFACE

This thesis is in two volumes. Volume 1 contains the body of the research. Volume 2 contains published work in the form of conference papers and research reports resulting from the research.

ABSTRACT

Tall concrete buildings experience time-dependent axial shortening which may be interpreted as either absolute or differential, the former being with respect to a single column or core element, the latter being with respect to adjacent elements. The types of analyses undertaken to determine axial shortening would normally be deterministic, the rigour being commensurate with the degree of shortening likely to be experienced. Mathematical rigour, however, may or may not be justified in the context of the natural variability of constituent parameters and thus a closer examination of the probabilistic uncertainties associated with axial shortening, particularly for tall buildings, is warranted. Shortening is influenced by, amongst other things, the complex load history of a building during its construction cycle. In this context the properties of concrete are investigated to determine those that are critical to any axial shortening analysis. The work here describes three probabilistic techniques, namely, Monte Carlo simulation, and first- and second-order moment analyses. Each incorporates random constitutive information in addition to a rigorous procedure for obtaining the representative shortening values. Element behaviour is modelled by the composite models of either Faber, Trost and Bazant, Dischinger or improved Dischinger, combined with the recommendations of the ACI, CEB-FIP, AS-3600 and other sources for describing creep and shrinkage. These models are coupled with the detailed load history of each successive element, based on the construction sequence of the building, and the usual environmental effects, resulting in a procedure capable of analysing fully the axial shortening effects to a high level of detail and with a measured degree of certainty. A software program has been developed to do this analysis.

The probabilistic distributions of axial shortening results are subsequently determined using standard goodness of fit tests. With numerous predictive methods available for column behaviour, the author sets out to examine their differences in the context of axial shortening behaviour. An assessment of the sensitivity of each input parameter, in addition to comparisons with other predictive procedures is made. Conclusions follow from these studies. Finally, the probabilistic models are, to a limited extent, compared to field data of column shortenings.

ACKNOWLEDGMENTS

I would like to specially thank the following people:

Allan Beasley: For his continuous support, encouragement, guidance, advice and the invaluable discussions throughout this entire project. This included discussions on structural concrete, probability and statistical theory, conference preparation and technical report writing, to name a few.

Edmund Melerski: For his helpful discussions on probability theory, technical report writing and conference preparation.

Brian Cousins: For his useful discussions on statistical theory and TurboPascal programming.

Violet Koutsoukis: For typing up the majority of this thesis.

Ashay Prabhu: For his beneficial discussions throughout the project and his continuous support as a friend.

Reza Izadnegahdar: For his support as a friend.

Mum and Dad: For their support throughout my entire university study, especially at the times of need.

and for the many others who helped on the way.

CONTENTS

CHAPTER 1

CHAPTER 1

INTRODUCTION

1.1 GENERAL

Tall buildings add to architectural appearance of large cities. They enhance the views given to the cityscape by adding major landmarks, and the efficiency at which tall buildings use landspace is quite high, allowing large concentrations of human population to inhabit central city areas. Especially with the increasing urbanisation of the world's population, tall buildings play a vital role in providing space to meet this trend. The technology to design and construct buildings up to 150 storeys already exists [1], although *concrete* buildings up to 90 storeys only have thus been constructed. In Australia, some thirty buildings whose heights from the basement level to the top storey exceed 150m can be seen on the skyline of most capital cities [2], whilst the tallest concrete building currently is the 60 storey Rialto Tower in Melbourne, completed in 1985 at a height of 242m [2].

On the international scene, the 1990 world's tallest reinforced concrete building was constructed at 311 South Wacker Drive, Chicago [3]. The total height of this building is 296m, and comprises 70 storeys of mainly commercial office space. More recently (1993), the reinforced concrete Central Plaza building was completed in Hong Kong [4]. At 78 storeys, and with a total height to the upper storey of 309m, making it the 1993 world's tallest reinforced concrete building.

As the international market, particularly the Asian market, remains active with more buildings being planned, in addition to those already under construction, a study focussed on improving design standards and more rigorously quantifying the shortening phenomena of tall buildings becomes increasingly important. Axial deformations become more critical as the columns and the service cores of concrete buildings become more slender [5].

The current hiatus in tall building construction in Australia would appear to be only transient as Australia develops its economic and cultural links with the stronger economies in the region. It is, therefore, certain that a requirement exists

to maintain a high level of technology and technological expertise in construction of tall buildings. The work described here is part of this effort.

1.2 SCOPE OF THE PROJECT

This project is concerned with the derivation of probabilistic models which predict the time-dependent shortening in the vertical elements of concrete buildings; a significant component of the design process for tall buildings. These models are more rationally utilised in design since any uncertainty associated with design parameters such as creep and shrinkage coefficients can be quantified, and thus used to assess structural, and especially, serviceability performance.

As concrete is a visco-elastic material, time-dependent shortening in part results from the effects of creep and drying shrinkage, whilst the presence of reinforcement in the elements resist these influences. The parameters mentioned are investigated in some detail. Temperature effects on concrete also induce a time-dependent response, however, this is beyond the scope of the project and is not reported here.

The concrete constitutive parameters required for shortening analyses, as is well known, exhibit natural variability which, in turn, results in uncertainty in their use in deterministic approaches to the solutions. This obligates a probabilistic approach for which randomness in the critical design variables can be taken into account. For example, the coefficient of variation of some concrete properties can be shown to be as much as 15% to 25%. A complete computational model which purports to give sensible predictions of axial shortening should account for this variability in a probabilistic sense. Randomness is also implicit in the environmental parameters which influence structural response, for example relative humidity. This has an obvious impact on creep and shrinkage response and further strengthens the need for a more rational approach to axial shortening in tall buildings.

The methods of analysis currently available to determine the axial shortening of reinforced concrete column elements include any of the four concrete constitutive models as follows: Faber [6], Trost and Bazant [7], Dischinger [8] and Improved Dischinger [9]. Whilst some of these models have been employed previously in deterministic analyses [10-17], work on probabilistic models is, to the best of the author's knowledge, non-existent. Preliminary work by the author with Beasley [18-25] has been presented at recent conferences, and forms part of this

submission (see Vol 2). Further developments of the building construction model described in Chapter 2 can be found in Koutsoukis and Beasley [21]. In addition, probabilistic modelling of planar bar structures by Koutsoukis and Melerski [26] have also been included as part of the thesis. This study was completed in preliminary work prior to developing the Monte Carlo axial shortening models described in Chapter 6.

The probabilistic basis of the project concerns the development of three separate procedures, namely first- and second-order moment analyses and a Monte Carlo simulation. The two former procedures utilise Taylor's series expansion as an approximation for obtaining probabilistic outcomes such as moments of distributions, while the latter samples the results from a large number of repetitive deterministic analyses. All three procedures form the basis for the software which is documented in Chapter 7, with further details in [27] and [28]. The latter two references form part of the research work conducted for this project. For each probabilistic model considered, the concrete properties describing elastic, creep and shrinkage behaviour are modelled as random.

To further the project a number of parametric studies are carried out to determine variable sensitivities within analytical concrete column models, including the ranking of variables in order of sensitivity relative to the shortening outcomes.

The numerous concrete constitutive models and properties currently available in the literature, and to be reported later in Chapters 4 and 5, can be used to determine analytical models for time-dependent reinforced column shortening. Figure 1.1 shows the relation between *concrete properties*, *constitutive models* and *analytical models*, as defined in this thesis. Here, the latter describe the load-deflection behaviour of reinforced concrete columns, whilst constitutive models describe the stress-strain relation of concrete. Finally, the concrete properties refer to the elastic, creep and shrinkage characteristics of concrete. The objectives of this project thus include a study of constitutive models and properties, leading to recommendations regarding their applicability. That is, of the elemental models, which are the most appropriate for the analysis of tall buildings, taking account of the information available through their probabilistic characterisation.

To assess the validity of the probabilistic analytical column models developed, comparisons with experimental column shortening data are made. The data

employed in these comparisons have been measured by Brady [29] on building columns at the University of Technology Sydney.

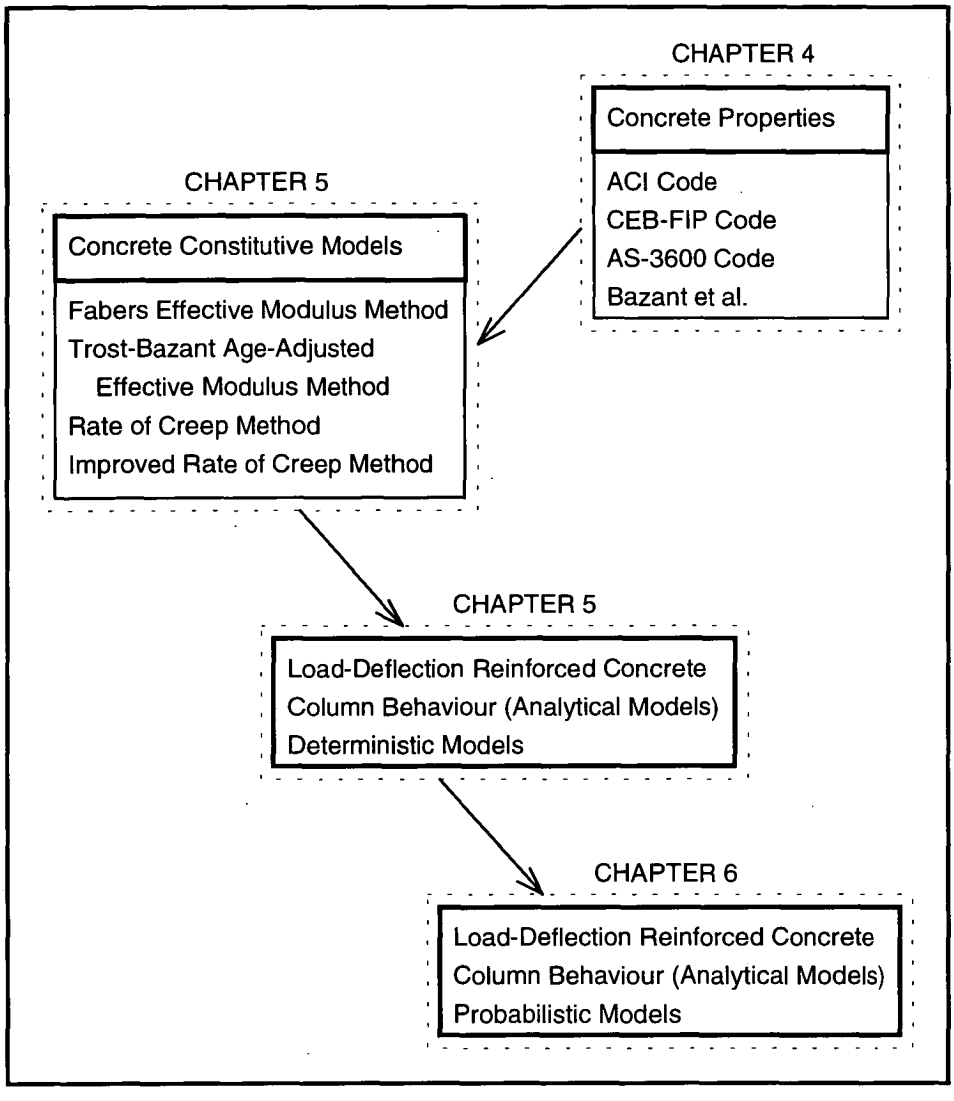

Figure 1.1 - Flow chart showing relation between concrete properties, constitutive models and analytical models.

1.3 SIGNIFICANCE OF AXIAL SHORTENING

With the accumulation of deformations in both the columns and core of a concrete building with respect to height, a variety of problems can arise both during and after construction [5,30-32]. Generally affected are the vertical services including ventilation systems, water pipes, sewerage pipes and heating systems. For example, in the Tower Building in Sydney [33], operational problems of elevators due to service core shortening required the lift guide rails to be shortened by more than 76.2mm. Other components of buildings affected include the exterior cladding, curtain walling and/or precast facade units fixed to the spandrel frame.

Design detailing decisions for the installation of services also rely on knowledge of shortening deflections.

To emphasise the quantitative significance of axial shortening in buildings, the total absolute long-term shortening of a 4m high reinforced concrete column may be 4mm [5]. In the context of a 160m high building, this value can be 160mm.

Axial shortening also manifests itself as differential shortening between adjacent column pairs or service core and outer spandrel frame columns within the same storey [5,30-32]. This type of shortening has been observed also on the Tower Building in Sydney [33]. Differential shortening arises due to different elemental properties, environmental effects and applied load differences, including the construction scheduling, for each element. With differential shortening, internal stresses can develop in connecting beams and slabs, depending on the connection detailing. For example, rigid beam connections at the service core and outer spandrel frame cause internal axial loads in the columns to redistribute. This may not be insignificant and must feature in the overall column and beam design. Careful concrete mix design and structural detailing in this case is necessary. The same principle applies to spandrel beams and header beams which connect major core elements. Diagonal bracing which provides the structure for the lateral wind loads is often a major problem in the event of differential shortening. Accurate design information in this case is extremely important and has been associated with at least one major building currently under construction [34,35].

As a consequence of differential shortening, the floor slabs connecting adjacent columns, or the core to the outer spandrel frame, develop cambers as time-dependent shortening occurs [5,31,32]. Although buildings generally remain structurally sound, camber in the slabs may lead to serviceability problems and possible loss of function. Mitigation of this problem may begin at the design stage with the appropriate information on the likely pre-cambering requirements of floor slabs at the time of slab installation at each stage of construction [5,31]. The obvious task is to minimise differential deflections resulting in a scenario in which all floor slabs are horizontal at a pre-determined time in the post-construction period. As inelastic strains can vary continuously with time, rectification of the problems associated with differential axial shortening in buildings in the post-construction period is generally difficult and expensive.

1.4 REQUIREMENTS FOR SHORTENING ANALYSES

Both total cumulative and differential shortenings are determined from the absolute time-dependent shortening of each column on a discrete incremental basis. The idealisation of a building structure, representing the complete sequential construction cycle, and including differential construction rates between adjacent structural elements, is essential [5]. This enables an accurate definition of the loading history of each adjacent element to be employed in the prediction of differential behaviour. Thus, the final outcomes of a cumulative and differential axial shortening analysis of the columns depend in the main on two criteria, namely the idealisation of the building with its idealised construction cycle, and the analytical column model containing the concrete and steel properties (i.e. concrete constitutive and property models).

1.5 LITERATURE SURVEY

Several concrete constitutive models are available in the literature which incorporate the effects of creep and shrinkage for describing axial shortening behaviour. Four of these models are described in detail in Chapter 5 and include:

Rate of Creep Method (RCM) [8],
Improved Rate of Creep Method (IRCM) [9],
Fabers Effective Modulus Method (FEMM) [6], and
Trost-Bazant Age-Adjusted Effective Modulus Method (TBEMM) [7].

FEMM and TBEMM are similar in form with the latter requiring an additional coefficient which incorporates the aging of concrete for creep.

Previous studies on theoretical developments to predict the axial shortening of tall buildings has been conducted by Fintel and Khan [10,30,36]. The Fintel-Khan model [10] is simple, requiring knowledge of the column properties, environmental parameters and the properties of the concrete and steel. The Fintel-Khan model allows for the interaction effects of beams which are attached to columns and which cause frame type action. The final form of the theoretical model is a summation of the elastic, creep and shrinkage shortenings, whilst the governing equations include correction factors to take into account the effects of humidity, as well as cement content and air content in the concrete. These correction factors are given graphically. With new and more sophisticated theoretical developments, the use of the Fintel-Khan model may be too simplistic for some structures currently being proposed or in construction.

More recently, Beasley [12,13] has developed software to predict the axial shortening in tall concrete buildings. This work is based on the Trost-Bazant Age-Adjusted Effective Modulus Method [7] and includes options for selecting the appropriate creep and shrinkage models from any of the ACI 1978 [37], CEB-FIP 1978 [38] or AS-3600 [39] codes. The procedure employed recognises the construction cycle, and hence loading history, of each of the column and core elements of the building. Following Beasley, the work here employs a similar modelling approach to the staged construction sequence which is generally typical of tall buildings. The method of analysis implemented by Beasley calls for the determination of an aging coefficient recommended by the CEB-FIP [40].

Pre-empting this work, the author [16] developed a software package which was based on a simpler method of analysis, employing Fabers Effective Modulus Method [6]. The idealisation of the construction cycle of the building was based on that of Beasley, but extended to give an option of obtaining final predictions of axial shortening at any stage of construction. This work is based on the implementation of the creep and shrinkage characteristics recommended by the ACI code [37]. A result of this work was a comparison between the two analytical models (i.e. FEMM and TBEMM) to determine any significant differences. This result was of minor significance but exposed some of the questions being addressed here.

Both criteria (i.e. idealising a building and its construction cycle, and the analytical column model) have been considered by Fintel and Khan [10], Beasley [12,13] and Koutsoukis [16]. Additional studies have been conducted on modelling reinforced concrete column behaviour. These have also included the creep buckling of slender columns and, the analysis of rectangular and circular cross-sectional columns. The effects due to slenderness of columns and off-set applied loads are also beyond the scope of this research.

Some important work has been carried out by Manuel and MacGregor [41]. They considered columns in a frame structure. The work involved establishing a model for the time-dependent analysis of columns which interacted with the beams. This model allowed for the interactive beam and column effects on the shortening of the columns. Their theoretical model was partially verified by the experimental data measured. Warner [11] considered the analysis of a short reinforced concrete column, where two methods were proposed. The first was based on a rate-of-creep analysis, whilst the second was based on a superposition analysis. Also the first is

shown to be suitable for a hand calculation, and the second is more suited for computer.

More studies on column behaviour have been done by McAdam and Behan [15] and Pan *et al.* [17]. These were based on applying the constitutive model of TBEMM to short columns. Both concluded that the TBEMM is a simple method to implement for design purposes. Pan *et al.* also compared the results of the theoretical column model with those measured on the University of Technology Sydney building [29]. The comparisons were found to be in good agreement.

Reinforced concrete column deformations due to elastic and creep behaviour of concrete have been considered by Samra [42]. In this work, a theoretical model was developed for column behaviour based on an iterative approach, and incorporates yielding of the reinforcement. Later, Samra [43] also derived a closed form column shortening model based on the TBEMM. This model was verified employing long-term column shortenings measured by others, where close correlations between computed values and field data were observed.

Research conducted on slender columns has been carried out by Mauch and Holly [44], Rangan [45], Gilbert [14,46] and, Gao and Bradford [47]. In general, these works were based on rectangular columns with eccentrically applied loads. Bradford and Gilbert [48] also presented studies on slender circular reinforced concrete columns. Slender columns may result in additional axial shortening due to secondary effects, but this is not considered here.

The literature has shown that time-dependent column models for different loading and boundary conditions have been developed, but only at deterministic levels of analysis. The reported research thus far has not considered randomness of concrete properties in axial shortening models nor the application of probabilistic models to tall buildings. This is the subject of this thesis.

Work in the area of probabilistic prediction models for concrete, steel and timber members are available in the literature and can be found, for example, in [49]. Structural reliability theory considers the degree of overlap between the distributions of capacity (resisting) and demand for any structural system. Reliability theory covered in the literature can be found in [50-52]. With probabilistic predictions only one distribution derives from the analysis. Studies on probabilistic predictions in structural members describing long-term time-

dependent deflections of reinforced concrete beams can be found in [53-56], although these are not directly related to the developments here. They have been included to acknowledge the body of structural reliability theory and probabilistic methods of analysis that currently exist and to provide a framework within which the material here must fit.

1.6 ORGANISATIONAL OUTLINE OF THESIS

The organisation of the thesis is described here. Figure 1.2 shows a thesis flow chart for Volume 1 (Chapters 1 to 10). Volume 2 contains research papers written during the execution of the project and presented at a number of recent international and national conferences. Also included in Volume 2 are two research reports.

Chapter 2 outlines the assumptions regarding the structural configuration and construction sequence of tall concrete buildings for the purposes of the analyses proposed here. Each column is discretised at each storey level, and the applied loads with corresponding loading ages are defined from the construction cycle. The idealisation assumed is representative of, and include the techniques generally employed in tall building construction. An example building is used for illustration purposes.

Chapter 3 examines the theoretical and experimental work available in the literature for describing the visco-elastic constitutive nature of concrete. Definitions for the parameters used in time-dependent analyses are outlined and include the creep coefficient, specific creep, creep function, relaxation function and elastic modulus. Different theories related to creep and shrinkage mechanisms and the significant factors which affect them are also outlined. Finally, the principle of superposition of deformations is presented with direct reasoning for its application to the shortening prediction of buildings.

Chapter 4 examines the restrictions of the concrete property models (describing the elastic, creep and shrinkage characteristics of concrete) recommended by the ACI [37,57], CEB-FIP [38,58] and AS-3600 [39] codes, and other sources. A comparison of the different concrete strength, elastic modulus, creep and shrinkage models is made at a deterministic level.

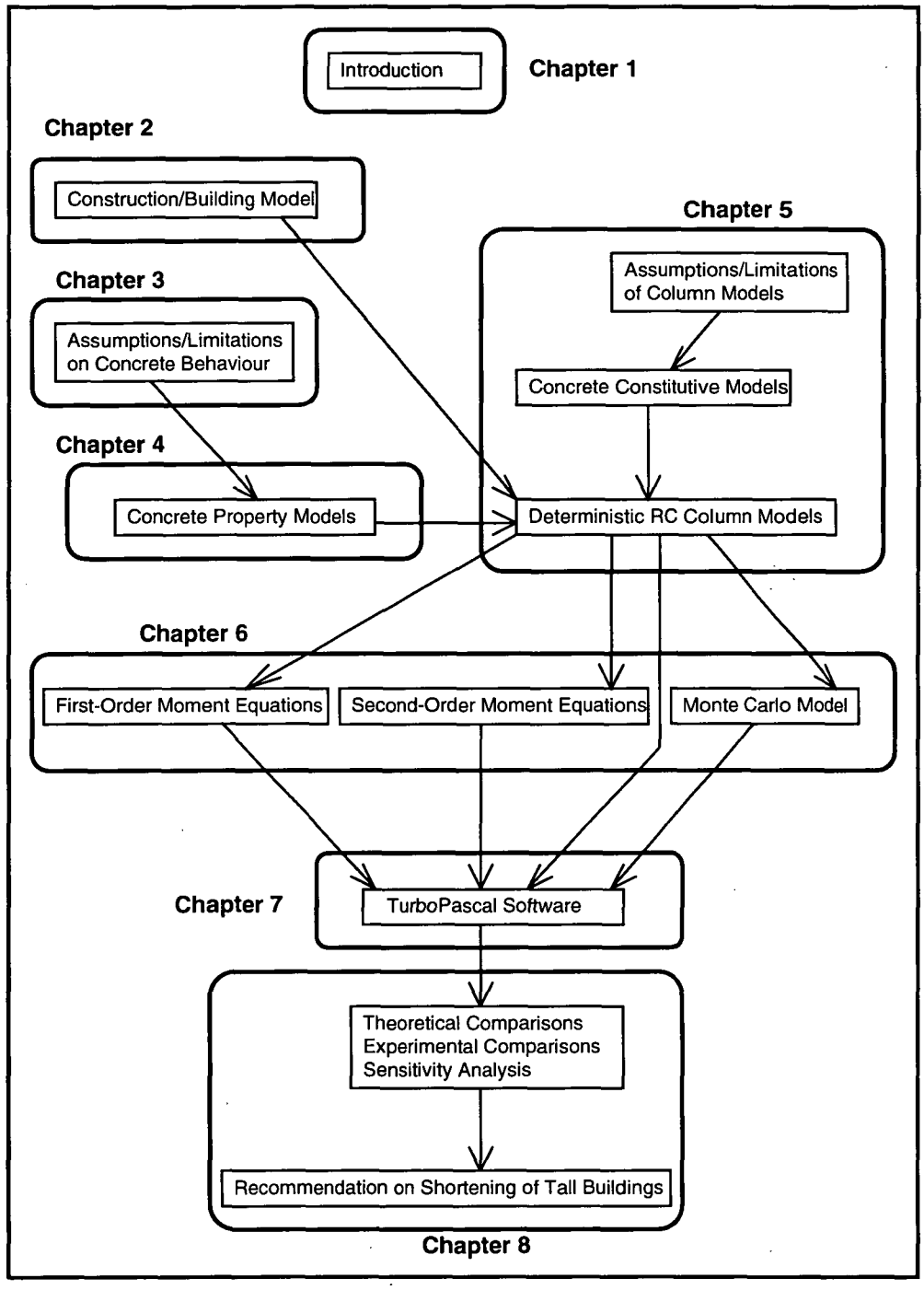

Figure 1.2 - Flow chart of entire project (thesis) showing connectivity between chapters.

In Chapter 5, the assumptions and limitations of the four concrete constitutive models, together with their mathematical form, are given. These models, as cited earlier, include the proposals of Faber, Trost and Bazant, Dischinger and improved Dischinger. A discussion on the applicability of each constitutive model is given, however, further recommendations are given in Chapter 8. The equations for reinforced concrete column behaviour are derived from each of the constitutive

models. Here, the principle of superposition outlined in Chapter 3 is employed, thus any finite number of applied loads are able to be modelled by these equations.

In Chapter 6, three probabilistic methods are applied to the modelling of column behaviour incorporating random concrete properties. Monte Carlo simulation is employed firstly, whilst the first- and second-order moment analyses follow. Characterisation of each random parameter distribution and associated numerical values is examined. A comparison between the three probabilistic models is presented which establishes numerical accuracy. Finally, this chapter sets out to derive new probabilistic time-dependent axial shortening reinforced concrete column models which are an extension of those previously derived in Chapter 6. The extension being to allow the new models to incorporate stochastic variations in relation to the time-dependent parameters in the analyses. The three independent concrete properties are each modelled by Gaussian processes using the first- and second-order moment analyses, and a Monte Carlo simulation. A comparison between the three probabilistic models is presented which establishes numerical accuracy.

In Chapter 7, two software programs, one developed for predicting axial shortening in concrete buildings and the other for the statistical analysis of Monte Carlo data, are described. The first (Axial Shortening Software Package - AXS) incorporates the deterministic and probabilistic theoretical column models derived, and has the capacity to resolve shortening values for complete buildings. The latter program (Statistical Analysis Software Package - STATS) samples Monte Carlo data to establish output distributions specifically for axial shortening. A more detailed description of both programs is found in [27] and [28] for STATS and AXS respectively. These are embodied in this submission in the form of separate reports (see Vol 2).

Chapter 8 examines a procedure developed here for comparing probability density functions, and in particular those of axial shortening predictions. STATS is used to examine the Monte Carlo axial shortening data, which includes the assessment of long-term shortening distributions determined for a range of analytical column models. Having once established the form of distributions, comparisons between the different concrete constitutive models and properties are made utilising the probabilistic comparison technique outlined here. Comparisons of experimental shortening data are achieved with the probabilistic models developed here. Parametric studies to determine variable sensitivities in the reinforced concrete

column models are performed. Finally, a recommendation on axial shortening prediction methods for tall concrete buildings is made.

Chapter 9 presents the conclusions drawn from the project, based on the deterministic comparisons of the concrete property models, the probabilistic comparisons of the analytical column models, the parametric study of these models and the comparisons of probabilistic shortening predictions with field data.

CHAPTER 2

CHAPTER 2

IDEALISATION OF BUILDING AND CONSTRUCTION CYCLE

This chapter outlines the assumptions made in idealising a tall building structure into discrete vertical elements for the purpose of an axial shortening analysis. An idealised construction cycle is defined, representative of the usual cycle generally employed on tall buildings, which characterises the specific load history for each vertical element. An example five storey building is considered (for illustration purposes only) to depict the stage by stage erection sequence of a structure, and hence define the total characteristic set of loads which are assumed to apply to each column as they are analysed within the whole process.

2.1 BUILDING STRUCTURE

In general, most tall buildings are simple in configuration and thus structural idealisation for creep and shrinkage analysis is, in the main, easily achieved. For structurally complex buildings, it is often possible to resolve these into elementary components. In others, the presence of cross-bracing or other forms of structural interaction can pose difficult design problems, details of one such project can be found in [34]. Figure 2.1 illustrates the general structure of the class of multi-storey buildings being considered here, and indicates two main structural elements representing firstly, the service (or central) core, and secondly the spandrel (or outer) frame. This idealisation follows on from that reported in Beasley [12].

The service core is laterally rigid. It resists wind load and supports significant proportions of live and dead load, depending on the buildings configuration [59,60]. Although the service core is treated as a single member normally, in reality the configuration is often more of a multi-element system joined with stiff header beams in order to transfer vertical shear loads arising from wind action. Individual core elements sometimes require special attention for an axial shortening analysis in order to resolve implicit stresses in header beams due to differential action, however it is the core as a whole which is normally idealised to a single column and discretised at each storey, see Figure 2.1.

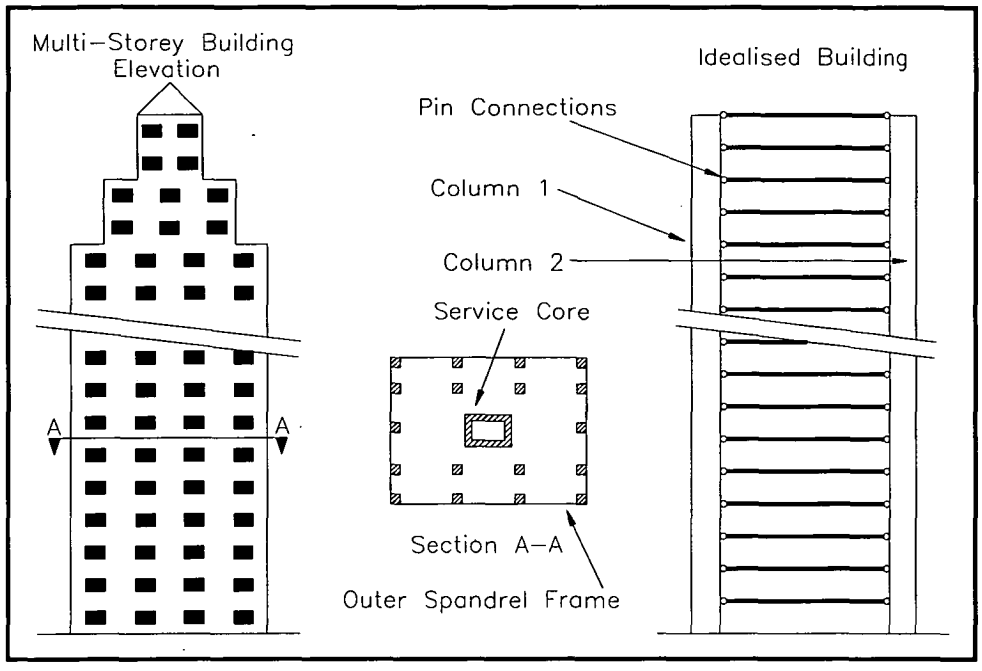

Figure 2.1 - The idealisation of a concrete building.

The spandrel frame contains numerous columns within any particular storey (refer to Figure 2.1), and for the purposes of analysis may be treated wholly or as individual columns, with the requisite loading.

Connection details at the service core and spandrel frame for beams and slabs are important in any shortening analysis. The presence or absence of axial load transfer between the two separate elements is a function of the connections (refer to Figures 2.2 to 2.4 inclusive), and thus the complexity of structural analysis is also dependent. Pinned connections are typically assumed for tall buildings in recognition of unwanted load transfer effects and also subsequent complex stress paths and long-term deflection effects. This is reflected in the model proposed herein.

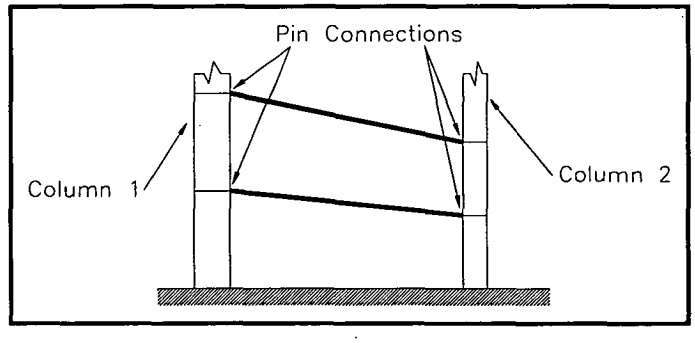

Figure 2.2 - The effect of slab and beam deformations, when differential shortening occurs between columns 1 and 2 for the given connections.

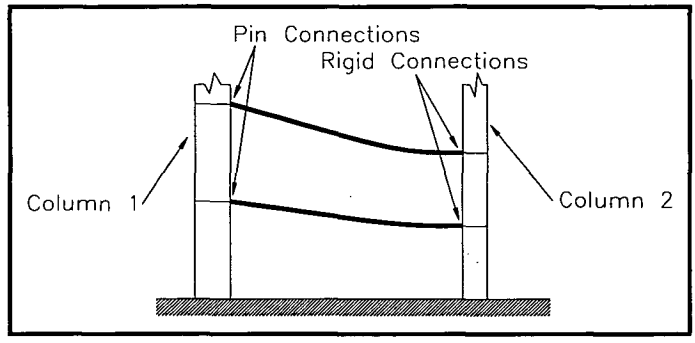

Figure 2.3 - The effect of slab and beam deformations, when differential shortening occurs between columns 1 and 2 for the given connections.

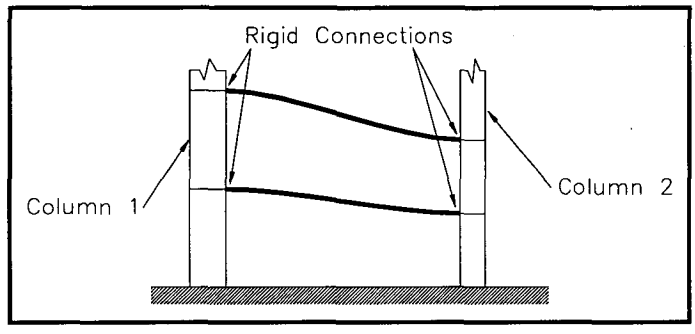

Figure 2.4 - The effect of slab and beam deformations, when differential shortening occurs between columns 1 and 2 for the given connections.

2.2 CONSTRUCTION CYCLE

Before outlining this process, some important construction practices are discussed and how they influence any time-dependent structural analysis. These practices are modelled and then merged into the idealisation of the sequential construction of the building.

Efficient construction methods can be achieved, in terms of time and money, if the core is fabricated in advance of the outer frame [59,60]. This idea permits two construction crews to work simultaneously, although independently, and a much faster construction rate is then feasible. The difference between the number of service core and outer spandrel frame storeys erected at any stage of construction is defined as the *floor difference*, which is postulated to be constant. Also, the construction period of each floor (i.e. floor cycle $\mathbf{T}_c$) is assumed constant, which generally lies between four to six days.

As construction of buildings can take several years, the load history of elements vary widely depending on several factors, including the taking up of occupancy

(representing service loads as distinct from construction loads). As the construction cycle is set by established work practices on the project, the installation of services is normally adapted to this cycle, and thus tenancy is geared to the cycle also. The difference between the outer spandrel frame's storey in construction and the highest storey in full occupancy at any stage is referred to as the *service difference* here, and is assumed constant.

2.3 LOADS ON STRUCTURE

Gravity loads in tall buildings are assumed to monotonically increase throughout construction until full occupancy is achieved. To simplify the modelling of the load history for each element, whilst retaining representation as regards incremental element loads, three load types are contemplated here. These are the column element self-weights, elemental construction loads and elemental in-service loads. Each discrete load is assumed to be applied instantaneously. Further, it is postulated that the self-weight acts one day after casting column, and drying shrinkage simultaneously initiates.

The construction loads are derived from additional dead loading from the structure (other than column self-weights) and the assessed construction live load. These loads represent a significant proportion of the total service loading and are therefore critical to axial shortening owing to their application on relatively fresh concrete. The in-service loads are defined for the purpose here as the increase in load from construction load to full design occupancy load. These loads represent further additional dead load as storeys of the building are brought to completion, plus the balance of total service live loading beyond that applied during construction.

The estimated loads for an axial shortening analysis need to be representative of actual working loads rather than conservative values thereof. This is particularly critical in the case of differential deformations between adjacent columns where load conservatism can result in inaccurate predictions leading to oversight of potential problems. Defining the total dead and live load estimates as **DL** and **LL** respectively, the construction and in-service loads can be expressed respectively as follows

$$\text{Construction load} = \alpha_1 \, \mathrm{DL} + \beta_1 \mathrm{LL} \tag{2.1}$$

$$\text{In–service load} = \alpha_2 \, \mathrm{DL} + \beta_2 \, \mathrm{LL} \tag{2.2}$$

Here, the constants α_1, α_2, β_1 and β_2 define certain portions of building loads. For differential analyses, these constants would be certain ratios which would give rise to the most probable applied loads in the structure.

2.4 EXAMPLE FIVE STOREY BUILDING

To illustrate the construction cycle adopted for the class of buildings being considered here, an example five storey building is examined (see Figure 2.5). The age of the building is defined from the time when the service core on level 1 is poured, and is denoted by $\mathbf{T_a}$ days. Both the *floor difference* and *service difference* are 1 storey, with a construction cycle period of $\mathbf{T_c}$ days. The service core and outer spandrel frame are denoted by columns 1 and 2 respectively. To differentiate between columns on different storeys, $\mathbf{C_{ab}}$ refers to column **a** (i.e. either column 1

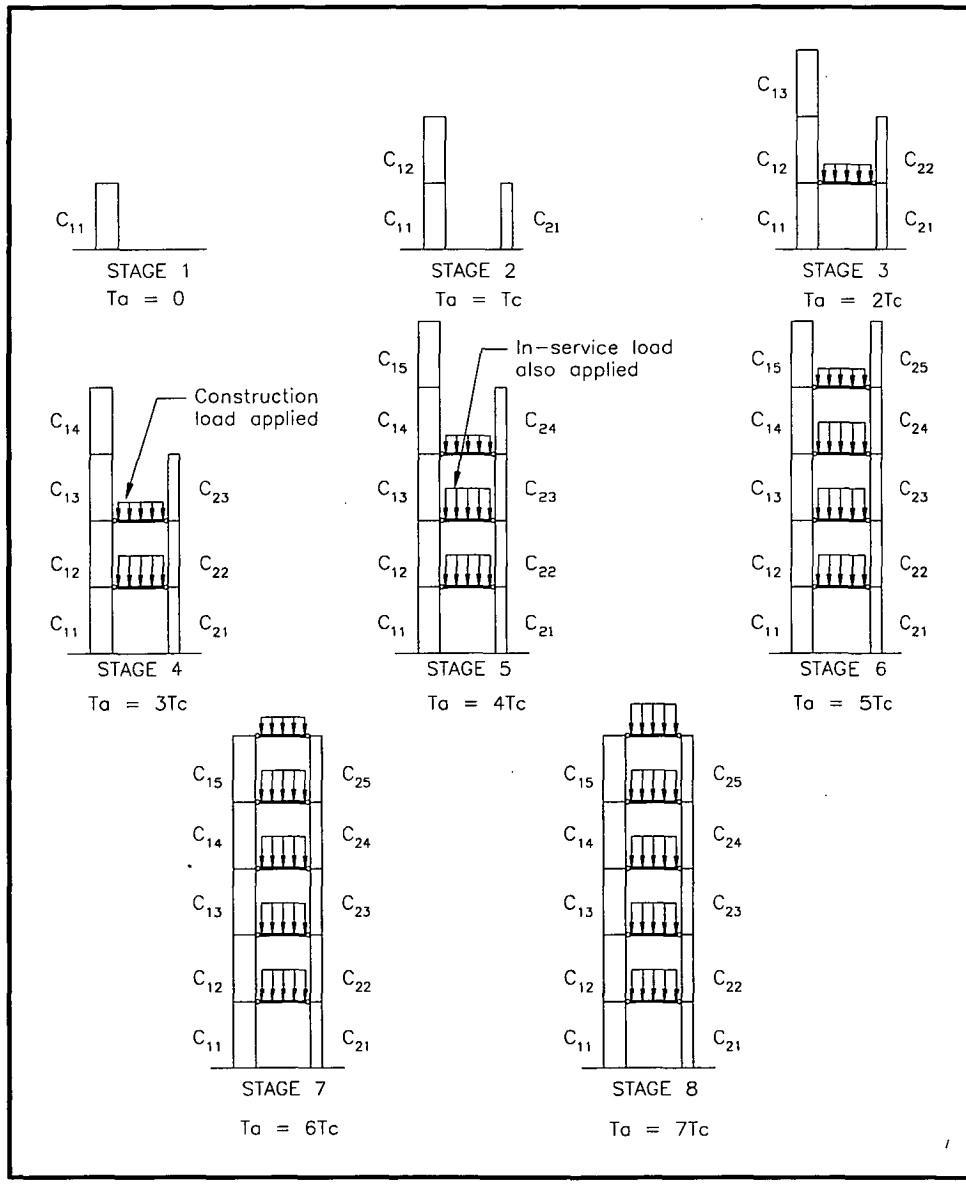

Figure 2.5 - The construction cycle of an example five storey building.

or 2) on storey **b**. The construction stages which are critical to a shortening analysis can now be defined.

2.4.1 Stage 1

This represents the start of construction of the building in question. At age $\mathbf{T_a} = 0$ days, column 1 on the first storey is poured (i.e. column $\mathbf{C_{11}}$). The form-work supports the column, and thus at this stage there are no loads applied to it. However, at $\mathbf{T_a}$ = 1 day, the form-work is removed and this results in the self-weight of the column being the first applied load. From when the column was poured up until the form-work is removed, the column is moist cured. After this period (i.e. $\mathbf{T_a} > 1$ day), shrinkage strains begin to affect the concrete column.

2.4.2 Stage 2

At the age $\mathbf{T_a} = T_c$ days, $\mathbf{C_{12}}$ is poured simultaneously with $\mathbf{C_{21}}$. The second load applied to $\mathbf{C_{11}}$ is the weight of $\mathbf{C_{12}}$. Shrinkage strains in $\mathbf{C_{12}}$ and $\mathbf{C_{21}}$ have not begun yet, but shrinkage is continuously occurring in $\mathbf{C_{11}}$. At the age $\mathbf{T_a} = (T_c + 1)$ days, the self-weight of $\mathbf{C_{12}}$ and $\mathbf{C_{21}}$ act on each column respectively. Also, shrinkage has been initiated in both $\mathbf{C_{12}}$ and $\mathbf{C_{21}}$.

2.4.3 Stage 3

The age of the building is $\mathbf{T_a} = 2T_c$ days. At this age, $\mathbf{C_{13}}$ and $\mathbf{C_{22}}$ together with the floor slab on storey 1 are cast simultaneously. The weight of $\mathbf{C_{13}}$ is applied to both $\mathbf{C_{11}}$ and $\mathbf{C_{12}}$, while the weight of $\mathbf{C_{22}}$ is applied to $\mathbf{C_{21}}$. A new load is introduced into the system which is the construction load. This load acts on $\mathbf{C_{11}}$ and $\mathbf{C_{21}}$. Again, shrinkage is continuously taking place in $\mathbf{C_{11}}$, $\mathbf{C_{12}}$ and $\mathbf{C_{21}}$. When the age of the building is $\mathbf{T_a} = (2T_c + 1)$ days, the self-weight of $\mathbf{C_{13}}$ and $\mathbf{C_{22}}$ act on each column, while shrinkage commences in both of these columns.

2.4.4 Stage 4

With the age of the building being $\mathbf{T_a} = 3T_c$ days, $\mathbf{C_{14}}$ and $\mathbf{C_{23}}$ are poured together with the floor slab on storey 2. The weight of $\mathbf{C_{14}}$ acts on $\mathbf{C_{11}}$, $\mathbf{C_{12}}$ and $\mathbf{C_{13}}$, while the weight of $\mathbf{C_{23}}$ acts on $\mathbf{C_{21}}$ and $\mathbf{C_{22}}$. As the slab on storey 2 is cast, the construction load of storey 2 is applied to $\mathbf{C_{11}}$, $\mathbf{C_{21}}$, $\mathbf{C_{12}}$ and $\mathbf{C_{22}}$. Another new load is introduced into the construction cycle which is the in-service load of storey 1 due to the full occupancy of this storey. Thus, the in-service load acts on $\mathbf{C_{11}}$ and $\mathbf{C_{21}}$. When the age of the building is $(3T_c + 1)$ days, shrinkage strains begin in $\mathbf{C_{14}}$ and $\mathbf{C_{23}}$, while the self-weight of these columns act on them.

2.4.5 Stage 5

The age of the building is $4T_c$ days, with $\mathbf{C_{15}}$ and $\mathbf{C_{24}}$ being cast simultaneously with the floor slab on storey 3. The weight of $\mathbf{C_{15}}$ acts on $\mathbf{C_{11}}$, $\mathbf{C_{12}}$, $\mathbf{C_{13}}$, and $\mathbf{C_{14}}$, while the weight of $\mathbf{C_{24}}$ acts on $\mathbf{C_{21}}$, $\mathbf{C_{22}}$ and $\mathbf{C_{23}}$. Column $\mathbf{C_{15}}$ is the top storey of the service core. The construction load of storey 3 acts on $\mathbf{C_{11}}$, $\mathbf{C_{12}}$, $\mathbf{C_{13}}$, $\mathbf{C_{21}}$, $\mathbf{C_{22}}$ and $\mathbf{C_{23}}$, while the in-service load of storey 2 acts on $\mathbf{C_{11}}$, $\mathbf{C_{12}}$, $\mathbf{C_{21}}$ and $\mathbf{C_{22}}$. At the age $(4T_c + 1)$ days, again the self-weight of $\mathbf{C_{15}}$ and $\mathbf{C_{24}}$ act, together with shrinkage commencing.

2.4.6 Stage 6

This is similar to stage 5, except the service core is completed and only the final outer frame (i.e. column 2) is cast. Only the weight of $\mathbf{C_{25}}$ has to be contemplated. The construction load of storey 4 acts on the columns below, while the in-service load of storey 3 acts on the columns below. The self-weight of $\mathbf{C_{25}}$ acts at the age $\mathbf{T_a} = (5T_c + 1)$ days with shrinkage strains also being initiated.

2.4.7 Stage 7

Similar to stage 6, except the both the core and outer frame have been completed with the floor slab of storey 5 being the only construction (i.e. roof of building) taking place. The construction load of storey 5 and the in-service load of storey 4 act on the columns below. Construction of the building has now finished.

2.4.8 Stage 8

The age of the building is $7T_c$ days when the in-service load of storey 5 (i.e. roof load) acts on the columns below. The building is now in full occupancy. A summary of the entire load sets with corresponding loading ages for each column, when $\mathbf{T_a} = 7T_c$ days, are given in Table 2.1.

Column	(t - s)	t	load	Column	(t - s)	t	load
C_{11}	1	$7T_c$	SW	C_{12}	$4T_c$	$6T_c$	SL
C_{11}	T_c	$7T_c$	CW	C_{12}	$5T_c$	$6T_c$	CL
C_{11}	$2T_c$	$7T_c$	CW	C_{12}	$5T_c$	$6T_c$	SL
C_{11}	$2T_c$	$7T_c$	CL	C_{12}	$6T_c$	$6T_c$	SL
C_{11}	$3T_c$	$7T_c$	CW	C_{13}	1	$5T_c$	SW
C_{11}	$3T_c$	$7T_c$	CL	C_{13}	T_c	$5T_c$	CW
C_{11}	$3T_c$	$7T_c$	SL	C_{13}	$2T_c$	$5T_c$	CW
C_{11}	$4T_c$	$7T_c$	CW	C_{13}	$2T_c$	$5T_c$	CL
C_{11}	$4T_c$	$7T_c$	CL	C_{13}	$3T_c$	$5T_c$	CL
C_{11}	$4T_c$	$7T_c$	SL	C_{13}	$3T_c$	$5T_c$	SL
C_{11}	$5T_c$	$7T_c$	CL	C_{13}	$4T_c$	$5T_c$	CL
C_{11}	$5T_c$	$7T_c$	SL	C_{13}	$4T_c$	$5T_c$	SL
C_{11}	$6T_c$	$7T_c$	CL	C_{13}	$5T_c$	$5T_c$	SL
C_{11}	$6T_c$	$7T_c$	SL	C_{14}	1	$4T_c$	SW
C_{11}	$7T_c$	$7T_c$	SL	C_{14}	T_c	$4T_c$	CW
C_{12}	1	$6T_c$	SW	C_{14}	$2T_c$	$4T_c$	CL
C_{12}	T_c	$6T_c$	CW	C_{14}	$3T_c$	$4T_c$	CL
C_{12}	$2T_c$	$6T_c$	CW	C_{14}	$3T_c$	$4T_c$	SL
C_{12}	$2T_c$	$6T_c$	CL	C_{14}	$4T_c$	$4T_c$	SL
C_{12}	$3T_c$	$6T_c$	CW	C_{15}	1	$3T_c$	SW
C_{12}	$3T_c$	$6T_c$	CL	C_{15}	$2T_c$	$3T_c$	CL
C_{12}	$3T_c$	$6T_c$	SL	C_{15}	$3T_c$	$3T_c$	SL
C_{12}	$4T_c$	$6T_c$	CL				

Table 2.1 - Summary of all loads applied to each column in example five storey building, together with loading ages, **s**, and age of column, **t**, when building age is $\mathbf{T_a} = 7T_c$ days, where :

SW = Self weight CW = Column weight CL = Construction load and SL = In-service load.

Column	(t - s)	t	load	Column	(t - s)	t	load
C_{21}	1	$6T_c$	SW	C_{22}	$3T_c$	$5T_c$	SL
C_{21}	T_c	$6T_c$	CW	C_{22}	$4T_c$	$5T_c$	CL
C_{21}	T_c	$6T_c$	CL	C_{22}	$4T_c$	$5T_c$	SL
C_{21}	$2T_c$	$6T_c$	CW	C_{22}	$5T_c$	$5T_c$	SL
C_{21}	$2T_c$	$6T_c$	CL	C_{23}	1	$4T_c$	SW
C_{21}	$2T_c$	$6T_c$	SL	C_{23}	T_c	$4T_c$	CW
C_{21}	$3T_c$	$6T_c$	CW	C_{23}	$2T_c$	$4T_c$	CL
C_{21}	$3T_c$	$6T_c$	CL	C_{23}	$2T_c$	$4T_c$	CW
C_{21}	$3T_c$	$6T_c$	SL	C_{23}	$3T_c$	$4T_c$	CL
C_{21}	$4T_c$	$6T_c$	CW	C_{23}	$3T_c$	$4T_c$	SL
C_{21}	$4T_c$	$6T_c$	CL	C_{23}	$4T_c$	$4T_c$	CL
C_{21}	$4T_c$	$6T_c$	SL	C_{23}	$4T_c$	$4T_c$	SL
C_{21}	$5T_c$	$6T_c$	CL	C_{23}	$5T_c$	$4T_c$	SL
C_{21}	$5T_c$	$6T_c$	SL	C_{24}	1	$3T_c$	SW
C_{21}	$6T_c$	$6T_c$	SL	C_{24}	T_c	$3T_c$	CW
C_{22}	1	$5T_c$	SW	C_{24}	$2T_c$	$3T_c$	CL
C_{22}	T_c	$5T_c$	CW	C_{24}	$3T_c$	$3T_c$	CL
C_{22}	T_c	$5T_c$	CL	C_{24}	$3T_c$	$3T_c$	SL
C_{22}	$2T_c$	$5T_c$	CW	C_{24}	$4T_c$	$3T_c$	SL
C_{22}	$2T_c$	$5T_c$	CL	C_{25}	1	$2T_c$	SW
C_{22}	$2T_c$	$5T_c$	SL	C_{25}	$2T_c$	$2T_c$	CL
C_{22}	$3T_c$	$5T_c$	CW	C_{25}	$3T_c$	$2T_c$	SL
C_{22}	$3T_c$	$5T_c$	CL				

Table 2.1 (con't) - Summary of loads applied to example five storey building.

2.5 CONCLUDING REMARKS TO CHAPTER

An idealised building and construction cycle model has been presented. This model together with the load-deflection reinforced concrete column equations derived in Chapters 5 and 6 are employed in Chapter 8 to assess axial shortening predictions for the class of buildings considered here. The idealised construction model was implemented into computer algorithms for the software developed in Chapter 7.

CHAPTER 3

CHAPTER 3

CREEP AND SHRINKAGE IN CONCRETE

In this chapter, current theoretical and experimental work on modelling a variety of concrete properties are investigated. Some of the properties include visco-elastic effects, aging and shrinkage characteristics. The time-dependent behaviour of concrete necessitates several fundamental definitions which initially need defining. These include the creep coefficient, specific creep, creep function, relaxation function and elastic modulus. Mechanisms and theories on the creep and shrinkage characteristics of concrete are outlined. Also, a summary of the factors which influence these time-dependent properties are discussed. Finally, the validity of the principle of superposition in relation to concrete deformations and indeed necessity in rationalising tall building analyses is examined.

3.1 INTRODUCTION

The total axial deformation of concrete may be expressed as the summation of instantaneous, creep and shrinkage strains as follows

$$\varepsilon(t) = \varepsilon_e(t) + \varepsilon_c(t) + \varepsilon_{sh}(t) \tag{3.1}$$

where

$\varepsilon(t)$ = total concrete strain

$\varepsilon_e(t)$ = instantaneous strain

$\varepsilon_c(t)$ = creep strain

and $\varepsilon_{sh}(t)$ = shrinkage strain

A diagrammatic representation of the strain components is shown in Figure 3.1. In this definition, creep and shrinkage are treated as independent, however, some interdependence may be present, though has as yet to be fully quantified in the general research. For the purpose of analysis, creep strains are stress dependent, whilst shrinkage strains are independent of stress. Thermal strains are not considered, however they can be incorporated into the shrinkage components. The temperature variation is cyclic and changes in temperature on average are zero in

most cases, and is disregarded here. However, the influence of temperature on creep and shrinkage is examined here.

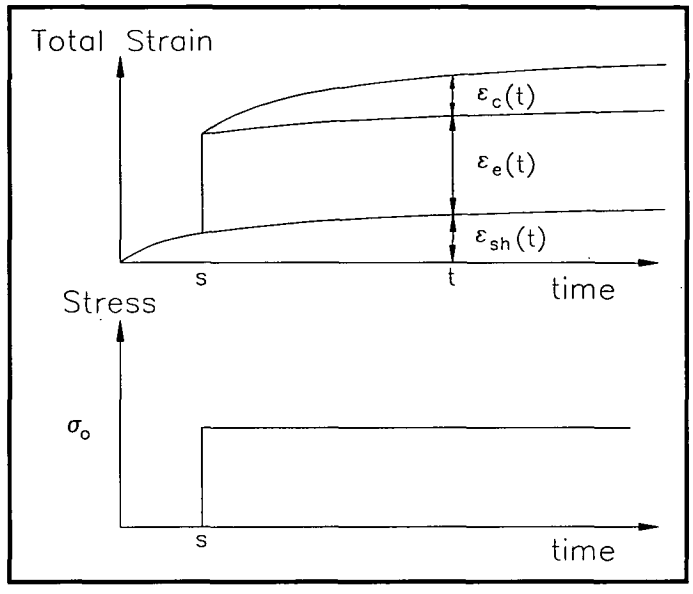

Figure 3.1 - Total concrete strain at time **t**, for an applied stress σ_0 at **s**.

The creep coefficient is defined in Neville *et al.* [61] as the ratio of creep strain to elastic (instantaneous) strain, i.e.

$$\phi(t,s) = \frac{\varepsilon_c(t,s)}{\varepsilon_e(t)} \tag{3.2}$$

where

$\varepsilon_c(t,s)$ = creep strain

and $\varepsilon_e(t)$ = elastic strain

Equation (3.2) has been defined such that the creep strain is linearly related to the applied stress through the elastic strain term. The creep coefficient is independent of applied stress and relies on a time function [14]. Backstrom [62] observed that the creep strains become non-linear when the ratio of applied stress to ultimate strength is greater than 0.7. This value is generally much greater than the design stress range for concrete. Smerda and Kristek [63] therefore concluded that for values of the ratio less than 0.5, linearity of creep is held.

Specific creep is defined in Neville *et al.* [61] as the creep strain at time **t** due to an applied unit stress, i.e.

$$C(t,s) = \frac{\varepsilon_c(t,s)}{\sigma(t)} \tag{3.3}$$

where

$C(t,s)$ = specific creep

and $\sigma(t)$ = applied stress

The creep function at time **t** is defined in Neville *et al.* [61] as the summation of the instantaneous and creep strains due to a sustained applied load at time **s**, or

$$J(t,s) = \frac{1+\phi(t,s)}{E_c(s)} \tag{3.4}$$

where

$J(t,s)$ = creep function

and $E_c(s)$ = elastic modulus

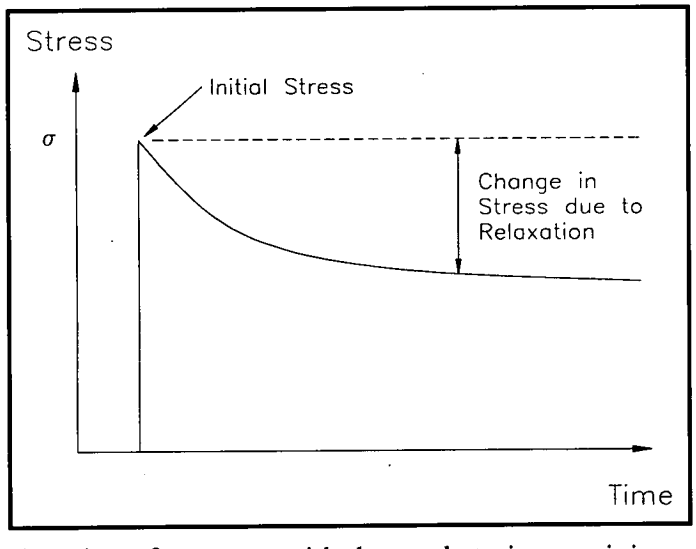

Figure 3.2 - Relaxation of concrete with the total strain remaining constant.

To define the relaxation function, an explanation of relaxation is firstly necessary. For example, for a concrete specimen not allowed to freely deform due to creep, then the initial stress in the concrete decreases with time (refer to Figure 3.2). This decrease is referred to as relaxation. The relaxation function is defined in Bazant [64] by the following equation

$$\sigma(t) = \int_0^t R(t,s)\, d\varepsilon_c(t,s) \tag{3.5}$$

where

$R(t,s)$ = relaxation function

and $\sigma(t)$ = concrete stress at time t

It follows that the creep and relaxation functions are related.

3.2 CREEP

Concrete creep can be sub-divided into smaller constituents. One approach divides creep into basic and drying portions, whilst a second distinguishes between delayed elastic and flow components [65]. The latter can further separate into rapid initial, basic and drying. To further complicate the procedure, separation into recoverable and irrecoverable creep constituents can be made.

With the first approach, basic creep is measured as the time-dependent deformation of a concrete specimen which is in a sealed condition (i.e. no moisture exchange occurs with the environment), whilst drying creep is measured as the additional deformation the specimen undergoes subject to the drying conditions of the environment [65]. The total creep is the summation of both components and can be expressed as

$$\varepsilon_c(t) = \varepsilon_{bc}(t) + \varepsilon_{dc}(t) \tag{3.6}$$

where

$\varepsilon_{bc}(t)$ = basic creep strain

and $\varepsilon_{dc}(t)$ = drying creep strain

This approach is employed in the concrete property models proposed by Bazant and Panula [66-75] and Bazant *et al.* [76-86]. ACI [37] and AS-3600 [39] modify (3.6) to a slightly different form, given by

$$\varepsilon_c(t) = k_{dc}\varepsilon_{bc}(t) \tag{3.7}$$

where

k_{dc} = modification factor for the drying environment

The appropriate application of either definition (3.6) or (3.7) depends on the experimental testing procedures employed. Creep models are empirical equations resulting from experimental curve fitting techniques, with the exception of the Bazant and Panula [66-75] and Bazant *et al.* [76-83] models. The latter models are semi-empirical and based on diffusion theory and thermodynamic restrictions, fitted to experimental data.

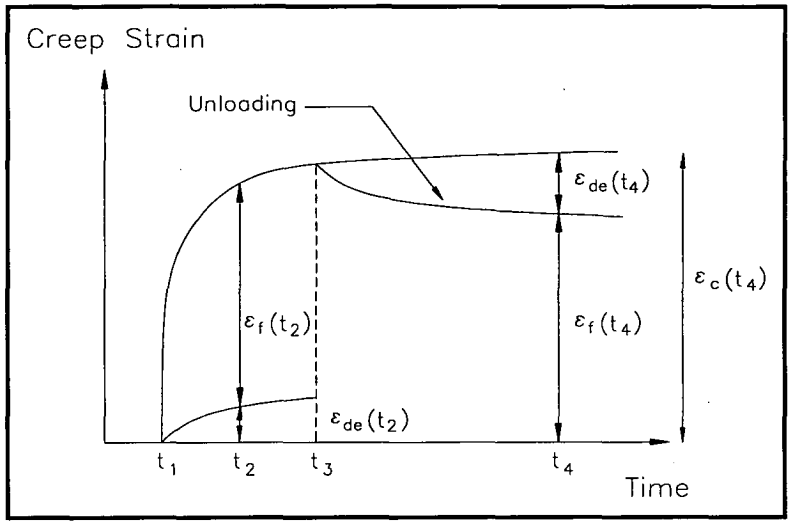

Figure 3.3 - The break-down of creep into flow and delayed elastic components, after CEB-FIP 1978 model [38] (Figure 16.6 on page 251 of Neville *et al.* [61]).

The second approach divides creep into flow and delayed elastic components [65], as mentioned. Considering a concrete specimen loaded at time t_1, the creep at time t_2 is shown schematically in Figure 3.3. This can be expressed as

$$\varepsilon_c(t_2) = \varepsilon_{de}(t_2) + \varepsilon_f(t_2) \tag{3.8}$$

where

$\varepsilon_{de}(t_2)$ = delayed elastic creep strain

and $\varepsilon_f(t_2)$ = flow creep strain

On removing the load at some time, say t_3, the entire delayed elastic creep constituent is recovered in the long-term, whilst the remaining component (i.e. flow creep) is irrecoverable. Temperature and thickness of the specimen do not greatly influence the delayed elastic constituent, however, the latter is dependent on the degree of hydration of the cement paste.

The flow component of creep is further broken down into rapid initial, basic and drying flow components [65]. This can be written as

$$\varepsilon_f(t) = \varepsilon_{if}(t) + \varepsilon_{fb}(t) + \varepsilon_{fd}(t) \tag{3.9}$$

where

$\varepsilon_{if}(t)$ = initial rapid flow creep strain

$\varepsilon_{fb}(t)$ = basic flow creep strain

and $\varepsilon_{fd}(t)$ = drying flow creep strain

The initial rapid flow is the flow component which occurs in the first twenty four hours after loading. This constituent is mainly irreversible and is independent of the specimen size, but is highly dependent on the environmental temperature and the degree of hydration. With the dependence on the latter, the initial rapid flow is more pronounced in concretes loaded at relatively young ages. Basic flow is defined as flow creep which occurs by analogy in a sealed concrete specimen. This portion is irreversible and highly dependent on ambient temperature. The degree of hydration of the cement paste affects basic flow, while the thickness of the specimen does not influence this component. Finally, drying flow is defined as the additional flow due to the drying environment, and is partially recoverable once the specimen is re-wetted. The degree of hydration has no significant influence on drying flow, but the size of the concrete specimen does.

All the creep constituents for the second approach can be represented by the following formula

$$\varepsilon_c(t) = \varepsilon_{de}(t) + \varepsilon_{if}(t) + \varepsilon_{fb}(t) + \varepsilon_{fd}(t) \tag{3.10}$$

The CEB-FIP 1978 code [38] adopts this approach for predicting creep of concretes and also describes the behaviour for cases of unloading. The break-down of creep into the fundamental constituents modelled by (3.6) or (3.10) is not essential to the analysis of tall buildings as the applied vertical loads are assumed to be monotonically increasing. However, these components help explain creep processes, and are the basis for all concrete properties presented in Chapter 4.

Several mechanisms have been described for creep behaviour of concrete [61]. These include: mechanical deformation theory (Freyssinet [87,88]), plastic theories (Bingham and Reiner [89], Glanville and Thomas [90], Jensen and Richart [91], Glanville [8], Lynam [92] and Vogt [93]), viscous and visco-elastic flow theories (Arnstein and Reiner [94], Thomas [95], Reiner [96] and Hansen

[97]), solid solution theory (Lea and Lee [98]) and seepage theory (Lea and Lee [98], Lynam [92], Seed [99]).

None of these theories fully model creep, they only account for some of the experimental observations [61]. It is more probable that creep can be fully described by a combination of two or more processes. Some of these hypotheses were made by: Kesler [100,101], Ruetz [102,103], Cilosani [104], Powers [105,106], Bazant [107] and the ACI [108].

The exact nature of creep is still unknown, although the ACI [108] has theorised a model in which four main processes are described. The bulk of creep is due to viscous flow and consolidation of cement paste. Water contributes to creep, but its mechanism is still in debate. Water does not have to be present for creep to occur, creep having been observed at high temperatures. Some of the viscous flow refers to the cement paste's microstructure sliding or shearing with and without the lubrication of water within the cement paste. The second mechanism refers to some of the seepage due to consolidation of the cement paste. The third process is due to the two phase modelling of concrete as a rigid elastic aggregate in a matrix of viscous cement paste. Finally, the last mechanism is due to the permanent breakdown of bonds in the cement paste with a possibility of new bonds forming. The knowledge of the true mechanism or combination of mechanisms is not however necessary to derive solutions to axial shortening problems here.

3.3 GOVERNING PARAMETERS FOR CREEP BEHAVIOUR

Factors which significantly influence creep of concrete are summarised here, although more detailed discussions can be found in Neville *et al.* [61], Smerda and Kristek [63], Bazant [64] and Rusch *et al.* [65]. Experimental data has shown that loading age is given to be the most crucial factor for determining creep strain, see Neville *et al.* for some examples.

A summary of the factors which influence creep and which are critical to the analyses to follow are:

(i) loading age; increasing loading age decreases ultimate creep coefficient.

(ii) ambient humidity; reduces creep if humidity increases.

(iii) ambient temperature; reduces creep if temperature decreases. However, Marzouk [109] has found this not to always be the case for certain temperature ranges. The effects of temperature in the ranges -10°C to 40°C are not very pronounced [63].

(iv) type of aggregate; reduces creep if limestone is used instead of sandstone.
(v) cement content; reduces creep if this portion increases.
(vi) water-cement ratio; reduces creep if this ratio decreases.
(vii) cement type; reduces creep if high early-strength instead of normal types are employed.
(viii) specimen size; thick specimens are prone to less creep at any given time.
(ix) method of curing; reduces creep if specimens are steam cured instead of moist cured.

The majority of these factors are included in most standards and codes, with loading age, relative humidity and member size being the three most important factors found in these codes.

3.4 SHRINKAGE

Shrinkage is defined as the reduction in volume of a concrete specimen at constant temperature, which is unloaded and unrestrained. This reduction is mainly attributed to water lost to the surrounding environment, in addition to chemical reactions within the cement paste [61]. The magnitudes of shrinkage are greatest at the surface of the specimen which is normally exposed to the drying environment. Shrinkage magnitudes vary throughout the cross-section of a member (refer to Figure 3.4) warranting the use of an average value for the purpose of structural analysis.

For the purpose of definition, shrinkage can be sub-divided into four components [61], as follows

$$\varepsilon_{sh}(t) = \varepsilon_{shd}(t) + \varepsilon_{shc}(t) + \varepsilon_{shh}(t) + \varepsilon_{shcp}(t) \tag{3.11}$$

where

$\varepsilon_{shd}(t)$ = drying shrinkage strain
$\varepsilon_{shc}(t)$ = carbonation shrinkage strain
$\varepsilon_{shh}(t)$ = hydration shrinkage strain
and $\varepsilon_{shcp}(t)$ = capillary shrinkage strain

The drying constituent is attributed to loss of moisture to the environment and is partially recoverable on re-wetting. As the specimen is subjected to carbon dioxide at low relative humidity, carbonation shrinkage occurs. Hydration shrinkage occurs as water is removed internally by chemical reaction during hydration in a

sealed condition. Finally, the capillary component of shrinkage occurs due to water loss of the concrete in a plastic state. The individual shrinkage components are not essential to the analysis of tall buildings, however, they help explain the different types of shrinkage deformations possible in concrete columns.

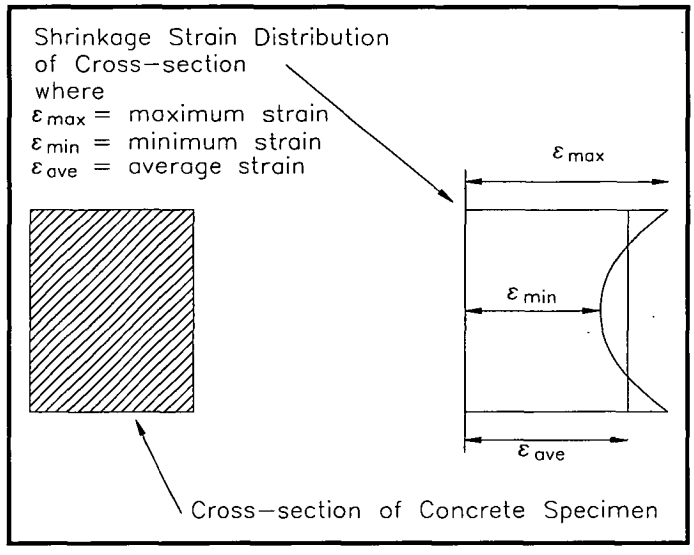

Figure 3.4 - Variation of shrinkage through a concrete member.

3.5 GOVERNING PARAMETERS FOR SHRINKAGE BEHAVIOUR

The factors influencing shrinkage are summarised here, although further details can be found in [61,63-65]. These factors are similar to those for creep, except loading age is not included. Exposure age of the specimen to the drying environment replaces the latter.

Factors which influence shrinkage and which are critical to the analyses to follow include:

(i) ambient humidity; reduces shrinkage if humidity increases.
(ii) curing period; reduces shrinkage if this period increases.
(iii) specimen size; thick specimens are prone to less shrinkage at any given time. Consequently, L'Hermite [110] first introduced a hypothetical thickness definition as simply the volume to surface area ratio.
(iv) water-cement ratio; reduces shrinkage if this ratio decreases.
(v) cement type; insignificant effect on shrinkage.
(vi) ambient temperature; reduces shrinkage if temperature decreases.

The factors which influence shrinkage are numerous, although most are not significant enough to be considered in any concrete property equation. The three

most important factors are relative humidity, member size and specimen age at onset of drying.

3.6 INSTANTANEOUS DEFORMATIONS

Instantaneous strains are those which occur at the instant of load application. For stresses less than $0.5f_c(s)$, strains produced are mainly recoverable with a very small portion irrecoverable [63]. Concrete structures are generally designed within the working stress range, and this includes tall buildings. As a result, most of the instantaneous strains can be considered elastic. For the purposes here, elastic strain is defined as instantaneous and depends on applied stress, concrete age and application rate of stress. Elastic strain is then refined as follows

$$\varepsilon_e(t) = \frac{\sigma(t)}{E_c(t)} \tag{3.12}$$

where

$\varepsilon_e(t)$ = elastic strain

$\sigma(t)$ = applied stress

and $E_c(t)$ = elastic modulus

The stress-strain relation for concrete is non-linear. Several models are available in the literature which describe this and can be found in Neville [111] for example. For the purposes of design, the initial curve is approximated by a straight line and is commonly referred to as the elastic modulus. For an axial shortening analysis of a tall building, a non-linear representation invalidates the application of superposition which is central to the overall analysis and in particular determining deformations as a result of highly complex incremental load histories for the entire set of column elements become complicated. Thus, the research here involves formulations which are based on the notion of linearity.

3.7 ELASTIC MODULUS

3.7.1 Normal Strength Concrete Models

Determining the elastic modulus from tests requires application of a load for a period of up to five minutes with the concrete stress at 40% of its ultimate value [61]. This procedure has been employed by various researchers to determine concrete moduli.

Most mathematical models used for the formulation of the elastic modulus are a function of concrete strength. With the dependence on strength, the variation of the modulus with time is implicit, for example [38,58]. The strength dependent model proposed by the CEB-FIP 1970 code [58] is

$$E_c(t) = 5.94\sqrt{f_c(t)} \quad \text{(GPa)} \tag{3.13}$$

whilst the later model of CEB-FIP 1978 code [38] is

$$E_c(t) = 9.5\sqrt[3]{f_c(t)} \quad \text{(GPa)} \tag{3.14}$$

where

$E_c(t)$ = elastic modulus at time t

and $f_c(t)$ = strength of concrete (MPa)

In 1960, Pauw [112] suggested that the modulus depended on the density of the concrete. A light-weight concrete having a lower modulus than normal weight concrete, as would be expected. Experimental data on concretes which were normal weight, light-weight and sand light-weight were analysed employing linear regression, the resulting formula being

$$E_c(t) = \rho^{1.5} 0.043\sqrt{f_c(t)} \quad \text{(MPa)} \tag{3.15}$$

where

ρ = density of concrete

Equation (3.15) is applicable up to 40% of the ultimate concrete strength, and is incorporated into the ACI [37] and AS-3600 [39] codes.

Concrete can be regarded as a material with a high elastic modulus aggregate embedded in a matrix of lower elastic modulus mortar. In 1965, Hansen [113] applied this concept to model concrete as a two phase material, and proposed the following model

$$E_c(t) = \frac{1}{\left(\frac{V_m}{E_m(t)} + \frac{V_a}{E_a(t)}\right)} \tag{3.16}$$

where

$E_m(t)$ = elastic modulus of cement mortar

V_m = volume fraction of cement mortar

$E_a(t)$ = elastic modulus of coarse aggregate

V_a = volume fraction of coarse aggregate

and $V_a = 1 - V_m$

Equation (3.16) is crude, and requires values for the modulus of the mortar and aggregate respectively. More recently, Rusch *et al.* [65] suggested that the modulus depends on the type of aggregates used. Stiffer aggregate produces a higher modulus for concrete, and the equation proposed by Rusch *et al.* was

$$E_c(t) = 4.3\beta_a \rho \sqrt[3]{f_c(t)} \qquad \text{(MPa)} \tag{3.17}$$

where

β_a = coefficient which depends on the aggregate type used

$\beta_a \cong 0.7$ for sandstone

$\beta_a \cong 0.9$ for limestone and granite

$\beta_a \cong 1.0$ for quartzite

and $\beta_a \cong 1.1$ for basalt or dense limestone

Equation (3.17) was obtained by considering normal weight and high strength concretes most typically utilised in concrete structures. The values of β_a were obtained from a limited number of tests, and are thus approximate. Rusch *et al.* recommended that more experimental data was needed to determine precise values of β_a for different types of aggregates.

3.7.2 High Strength Concrete Models

Design and construction of tall concrete buildings have led to the use of high strength concretes. Knowledge of the moduli for high strength concretes (up to 83 MPa) is thus necessary for the analysis of these buildings.

The modulus of the cement mortar approaches that of the aggregate for higher strength concretes [114]. La Rue [115] suggested that the elastic modulus of concrete must lie within an upper and lower limit. The limits are based on idealising the concrete as a two phase material. The upper value is the elastic modulus of the aggregate, whilst the lower limit is the elastic modulus of the

cement mortar. Setunge *et al.* [114] have concluded from experiments conducted on very high strength concretes (60 MPa to 120 MPa) that the elastic modulus of concrete is very sensitive to the type of aggregate.

The ACI code [57] has introduced an empirical model for predicting the elastic modulus of high strength concretes based on the proposal by Carrasquillo *et al.* [116]. Both high and normal strength concretes were investigated by Carrasquillo *et al.* and proposed the following expression for instantaneous modulus

$$E_c(t) = 3320\sqrt{f_c(t)} + 6900 \quad \text{(MPa)} \tag{3.18}$$

where the concrete strength ranges from 21 MPa to 83 MPa.

Empirical equations proposed by others include

$$E_c(t) = \rho^{1.5} 0.0337\sqrt{f_c(t)} \quad \text{(MPa)} \tag{3.19}$$

and

$$E_c(t) = \rho^{2.5}\ 3.3789 \times 10^{-5} [f_c(t)]^{0.325} \quad \text{(MPa)} \tag{3.20}$$

Equation (3.19) has been proposed by Jobse and Moustafa [117], and is similar in form to the model proposed by Pauw [112], but accurate for higher strength concretes. Ahmad and Shah [118] proposed (3.20).

From experimental findings [114,116], the elastic modulus predicted using (3.15) substantially overestimates the value of modulus for high strength concretes. Even considering the ±20% variation of this equation, as required by the AS-3600 [39], the lower limit is still on the higher side of experimental data [114]. In this case, the constant in (3.15) reduces from 0.043 to 0.0344. The final conclusion is that (3.15) is not accurate for high strength concretes.

At this stage the preceding discussion on concrete elastic moduli has more or less suggested that recent higher strength models should be considered in axial shortening analyses if high strength concretes are used. However, the assessment of these models in the context of predicting long-term deformations in building columns is made in Chapter 8.

3.8 PRINCIPLE OF SUPERPOSITION

The principle of superposition is one of the most commonly used assumptions in the linear analysis of structures. Boltzmann [119] first introduced the principle of superposition for non-aging materials. Applying this principle to aging materials was then followed by Volterra [120]. McHenry [121] was first to apply this principle to concrete. The principle can be stated for deformations as *"The total strain in concrete due to n stresses applied is the sum of the individual strains due to each stress applied independently"* [14]. The strain for any particular applied stress is independent of the previously administered stresses, or on those that will be applied. This principle is illustrated diagrammatically in Figure 3.5, where the total strain variation is shown with time for applied stresses σ_1 and σ_2 at times s_1 and s_2 respectively. At time t_1, the total strain is given by

$$\varepsilon(t_1) = \varepsilon_e(t_1) + \varepsilon_c(t_1) + \varepsilon_{sh}(t_1) \tag{3.21}$$

With the application of the principle of superposition, the total strain at time t_2 is

$$\varepsilon(t_2) = \varepsilon_e(t_1) + \varepsilon_e(t_2) + \varepsilon_c(t_1) + \varepsilon_c(t_2) + \varepsilon_{sh}(t_1) \tag{3.22}$$

Equation (3.22) represents total strains due to two monotonically increasing loads. This principle can also be extended to describe decreasing load histories. Experimental findings [63] have suggested that superposition yields satisfactory results for increasing stress histories, with predictions overestimating experimental data. For decreasing stress histories, the difference between predicted and experimental results is greater (i.e. prediction overestimates creep recovery) than that for increasing stresses.

To obtain accurate predictions from superposition, certain conditions must be satisfied [64]. The most important prerequisite requires that the stresses remain within the service range, and this is generally met in the design of concrete buildings. The second condition discourages decreasing stress histories, and this is again satisfied as tall buildings generally experience monotonically increasing loads due to the construction process. There should be insignificant changes in moisture distribution of concrete during creep, and in practice this is generally violated. However, the research here assumes that ambient conditions of the environment remain constant with respect to time, thus changes in moisture distribution are negligible. Finally, there should be no large sudden stress increase after initial loading. This condition is the least important of the above four. The

latter condition is generally not violated, as incremental building loads defined by the construction cycle are small in comparison with the working stress capacity of the column elements. In summary, application of superposition to tall building analyses has been justified.

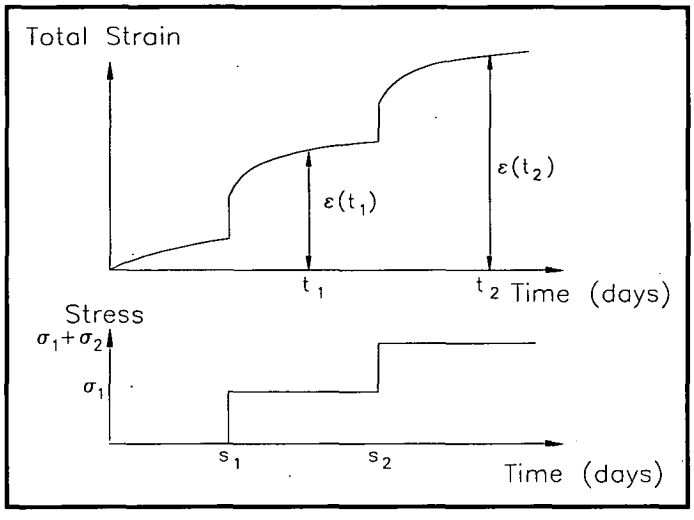

Figure 3.5 - The principle of superposition for concrete deformations loaded with stresses σ_1 and σ_2 at times s_1 and s_2 respectively.

3.9 RELAXATION FUNCTION

The concept of relaxation has been described earlier in this chapter, and the relaxation function was defined by (3.5) as the stress at time **t** due to a constant sustain applied strain at time **s**. This formula is known as the Volterra integral. The relaxation function depends on two variables, i.e. concrete age and loading age, however Bazant [64] comments that it cannot be written as a function of one variable, i.e. time lag. From the solution of the Volterra integral for a unit stress step at time **s**, the creep function and coefficient can be evaluated. More commonly, the relaxation function is determined by solving the Volterra integral for a given creep function. The relaxation function is then used to obtain the aging coefficient, which is subsequently employed in predicting column deformations based on the constitutive model of Trost and Bazant [7].

The solution to the Volterra integral can be carried out numerically, and one of these methods is given in Appendix A3.1. The calculation of the relaxation function by these numerical procedures is time consuming however. Bazant and Kim [122] have proposed an empirical equation for determining the relaxation function. This model results in approximate values for the relaxation function, for

which the values are within 2% of the exact values. This approximation applies to typical creep curves in use today, and is given as

$$R(t,s)=\frac{1-\Delta_o}{J(t,s)}-\frac{0.115}{J(t,t-1)}\left(\frac{J(s+\xi,s)}{J(t,t-\xi)}-1\right) \tag{3.23}$$

where

$$\xi=\frac{t-s}{2}$$

and $$\Delta_o=0.009\left(\frac{J(s+1,s)}{J(29,28)}\right)^2\left(\frac{J(t,s)-J(s+0.01,s)}{J(t,s)-0.9J(s+0.01,s)}-1\right) \quad \text{for } t>(s+0.01)$$

3.10 CONCLUDING REMARKS TO CHAPTER

The visco-elastic character of concrete, its aging and its shrinkage properties have been investigated by various researchers. Recently, the concentration has been on obtaining physically and experimentally justified creep and shrinkage predictions. In this chapter, the discussion has been on deterministic time-dependent models for behaviour of concrete properties, whilst probabilistic and statistical information are given in Chapter 6.

In obtaining deterministic and probabilistic axial shortening models, derived later in Chapters 5 and 6 respectively, the elementary parameter definitions required are given in this chapter. These shortening models depend on the elastic, creep and shrinkage deformation mechanisms for concrete behaviour and their influencing factors. The critical factors are made self-evident in this chapter, whilst later in Chapter 8 the sensitivity of these parameters are assessed with respect to the concrete property models presented in Chapter 4 when applied to axial shortening analyses. The superposition principle is central to the overall analyses of tall buildings where incremental deformations are accumulated due to the complex load history of each vertical element, thus a critical assessment of this principle was a necessary inclusion.

APPENDIX

TO

CHAPTER 3

APPENDIX A3.1

The numerical evaluation of the relaxation function **R(t,s)** can be carried out using a step by step procedure [7,40,122], requiring the creep coefficient and elastic modulus. Originally Trost assumed that the elastic modulus remained constant for evaluating the relaxation function and consequently calculating the aging coefficient. Bazant [7] found this assumption incorrect, and the variation of the elastic modulus with time must be included in the procedure outlined here. Once the relaxation function is determined, then the corresponding aging coefficient is evaluated by (A5.9).

Employing the rectangular rule for approximating the Volterra integral given by (3.5), the relaxation function is

$$R(t,s) = \sum_{j=1}^{n} \Delta R(t_j, s) \tag{A3.1}$$

where

$$\Delta R(t_1, s) = \frac{1}{J(s,s)} = E_c(s) \tag{A3.2}$$

and

$$\Delta R(t_k, s) = \frac{\sum_{i=1}^{k-1} \left(\Delta R(t_i, s)[J(t_k, t_i) - J(t_{k-1}, t_i)] \right)}{J(t_k, t_k)} \tag{A3.3}$$

$$\text{for } k = 2,3,4,\ldots$$

Equation (A3.1) is determined by a recurrence relation where the time interval between **s** and **t** is divided into **n** steps. Bazant [7] suggested that this time interval be chosen such that

$$\frac{\Delta t_r}{\Delta t_{r-1}} = 10^{1/16} \tag{A3.4}$$

where Δt_r is the time step.

An improved routine for evaluating the relaxation function is using the trapezoidal rule for approximating the Volterra integral. Equations (A3.1) and (A3.2) remain the same, but (A3.3) is expanded to

$$\Delta R(t_k,s)=\frac{\sum_{i=1}^{k-1}\left(\Delta R(t_i,s)[J(t_k,t_i)+J(t_k,t_{i-1})-J(t_{k-1},t_i)-J(t_{k-1},t_{i-1})]\right)}{J(t_k,t_k)+J(t_k,t_{k-1})} \tag{A3.5}$$

The above procedure has been implemented into the software described in Chapter 7 for predicting shortening of columns and cores in tall concrete buildings.

CHAPTER 4

CHAPTER 4

ADVANCED CONCRETE PROPERTY MODELS

In this chapter, the concrete property models are presented which describe the elastic modulus, concrete strength and creep and shrinkage behaviour, and are based on the recommendations of the American Concrete Institute [37,57], Comite Euro-International du Beton [38,58] and Australian Standards [39], and also the proposals of Bazant *et al.* [66-86]. Some of these concrete properties are empirical, whilst others are semi-empirical with a theoretical basis. The refinements made by Bazant *et al.* [72-75] to the original model are included, as well as two more recent proposals based on *solidification* theory [78-86]. Finally, comparisons between the concrete properties are made showing significant differences in predicted behaviour.

In the accompanying Appendix A4.1, the concrete properties which are required for *reinforced* concrete column behaviour are given. These models are presented in a manner which are readily implemented into the axial shortening formulations as derived in Chapter 5 and Chapter 7 in a software format.

4.1 INTRODUCTION

The concrete properties being considered here are obtained from National Standards currently used in practice, or from recent published research. Concrete property models not included are those obtained from experimental curve fitting of short-term creep and shrinkage data for specific concrete mixes. In this case, power or logarithmic forms for modelling time-dependent properties result in good predictions, and can be seen in [65]. Cridland *et al.* [123] found that if creep and shrinkage test data are used, the comparison of time-dependent deformations in concrete columns are in good agreement with experimental results. If test data is not utilised, they concluded that the discrepancies are more significant.

A number of concrete models are presented in Appendix A4.1, and may be defined as simple to highly complex. These models include the recommendations of the ACI [37,57], CEB-FIP [38,58] and AS-3600 [39] codes. In addition, a number of other models have filtered through the literature from Bazant and

others. These include the following Bazant models: the BP [66-68], BPs [69,70], BPh [71], BPc [72], BPdpll [73], BPtpl [75], BPX [78-82], BPXs [83] and B3 [84-86] models. A simple flow chart (see Figure 4.1) shows the relationships between the different models of Bazant and co-researchers [66-86].

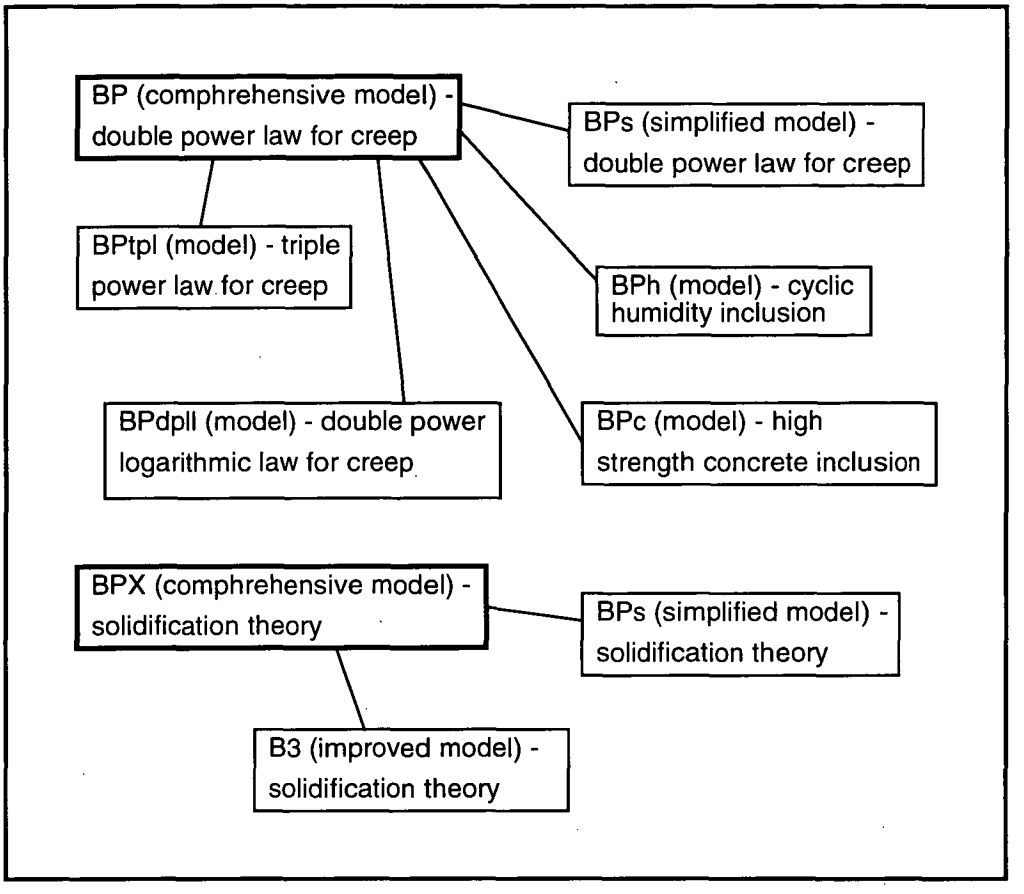

Figure 4.1 - A flow chart showing connections between the different concrete property models proposed by Bazant *et al.* [66-86].

As can be seen, several concrete property models are available ranging from elementary to intricate and model selection is a difficult task. Complex models usually require a greater number of input parameters which does not necessarily lend transparency to the analysis. A critical assessment of each concrete property model becomes warranted and follows below.

4.2 CRITICAL ASSESSMENT OF CONCRETE PROPERTY MODELS

The ACI model [37,57] was derived from experimental data of normal and light-weight concrete mixes. Light-weight concrete mixes are not used in columns and cores of high rise buildings and this limits the accuracy of the ACI code data

directly. Field data of course can be incorporated to improve this situation. The concrete modulus of Pauw [112] has been shown to be inaccurate for normal and high strength concretes [114,116], and a refined model has been recommended by the ACI on high strength concretes [57].

The CEB-FIP 1978 code [38] for creep prediction allows for both increasing and decreasing stress histories. However, the latter case is not relevant to the study here as the loads applied to tall concrete buildings are assumed to be monotonically increasing. Concrete properties of the CEB-FIP model are presented in forms of curves, however Smerda and Kristek [63], Gilbert [14] and CEB-FIP [40] have given independent analytical expressions for these curves. Recently, CEB [124] has stated that the form the CEB-FIP 1978 model is controversial, and thus unsuitable for current application.

The CEB-FIP [38] has recommended a ±20% variation of the final values for creep, shrinkage, strength and elastic modulus for design purposes. These limits are deemed to incorporate the randomness of concrete properties in a very crude manner and gives no information about the final output distributions obtained from a structural analysis. In the case of column shortening predictions, correlations exist between deformations for each independently applied load, as the analysis is time-dependent. Thus, these correlations must be included for accurate analyses.

The CEB-FIP 1970 code [58], having been superseded by the 1978 version [38], does not have the rigour of the new model. The older model is restricted in terms of the range of humidities which can be included, and has the major draw back of not adequately modelling the variation of shrinkage with member size. This aspect is examined later in this chapter.

The AS-3600 code [39] offers a relatively simple model, but recommends the use of the outdated concrete modulus model of Pauw [112]. A variation of ±30% for creep and shrinkage and, ±20% for elastic modulus needs consideration for design purposes. Adopting these limiting values results in a very simplistic approach to the incorporation of randomness of properties and may be less than advantageous in terms of the output obtained.

Bazant *et al.* [66-86] examined time-dependent deformations in concrete at a detailed level, and this is shown to some extent by the complex form of the

models. These models have been derived from semi-empirical equations with some theoretical basis. Derivation of the *Bazant* equations employed over 10,000 data points from the published research. These models would appear to be accurate because of their highly complex nature, however, it must be noted that the equation constants evaluated by Bazant *et al.* for their model would generally require more test data than if curve fitting fewer constants to a simple model. Time-dependent behaviour of different concrete mixes which have similar strength characteristics but may exhibit unrelated creep and shrinkage properties can be accounted for, as the Bazant *et al.* models are given as functions of concrete composition amongst other things.

An important recent development has been the concrete property model of Bazant and Baweja [84-86]. This latest model (B3) is a revision of that previously reported by Bazant *et al.* [78-83] in 1991. The B3 model is based on solidification theory [76,77] for creep and diffusivity theory [128] for shrinkage. However, the concrete parameter equations, which are functions of concrete composition and strength, were derived from 15,000 test data, substantially more than were used in the BPX [78-82] model. In addition, the B3 model is shown to agree better with test data than previous models, and is found to be simpler to use. The concrete parameter expressions were derived by consideration of the sensitivities of the output predictions for creep and shrinkage with respect to the input mix and strength parameters [84,85].

Coefficient of variation values were determined by Bazant and Baweja [84,85] for the creep and shrinkage B3 models and were found to be 23.6% and 34.3% respectively compared with 17.05% and 27.0% by Bazant *et al.* [78-83]. There seems to be an apparent contradiction that higher coefficient of variation values are associated with the improved B3 model, however, one should remember that the B3 model allows for a wider range of possible concrete mixes than the BPX model and in that sense can be more readily applied in situations when concrete test data is unavailable.

4.3 COMPARISON OF CONCRETE PROPERTY MODELS

The comparison of concrete property models at a deterministic level has been carried out by the author, in which four separate concrete mixes have been chosen with strengths of 30, 40, 50 and 60 MPa. Table 4.1 lists the concrete mix portions respectively.

Concrete Mix	f'_c (MPa)	c (kg/m³)	w/c ratio	a/c ratio	s/c ratio	Aggregate type	a (%)
30 MPa	36.1	325	0.52	5.91	2.31	basalt	3.5
40 MPa	47.8*	395	0.43	4.8	1.68	basalt	2.5
50 MPa	59.8*	485	0.35	3.79	1.13	basalt	2
60 MPa	71.8*	520	0.33	3.47	0.99	basalt	1.5

Table 4.1 - Concrete mixes which have been used in construction projects.
* denotes that the coefficient of variation adapted is 10 %. A slump of 100mm is assumed.

f'_c = mean concrete compressive strength (MPa)
c = cement content (kg/m³), w/c = water-cement ratio
a/c = total aggregate-cement ratio, s/c = sand-cement ratio, and
a = percentage of air content by volume (%)

Comparisons of concrete strength models proposed by the ACI [37] and CEB-FIP 1978 [38] are made in Figure 4.2. Both models show close agreement to approximately 70 days, after which a significant difference is apparent, as each model converges to different ultimate values. The 28-day concrete strength does not directly affect deformations in columns, but does so indirectly through the correlation with the elastic modulus. This strength parameter also influences the creep models of AS-3600, BP, BPs, BPX, BPXs and B3.

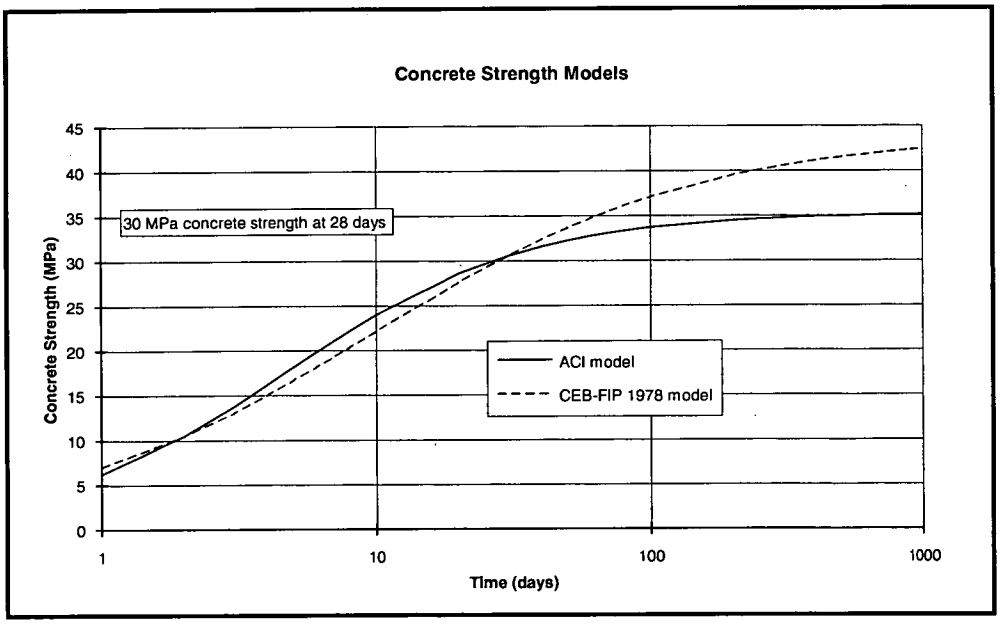

Figure 4.2 - Variation of concrete strength with time for the ACI [37] and CEB-FIP 1978 [38] models.

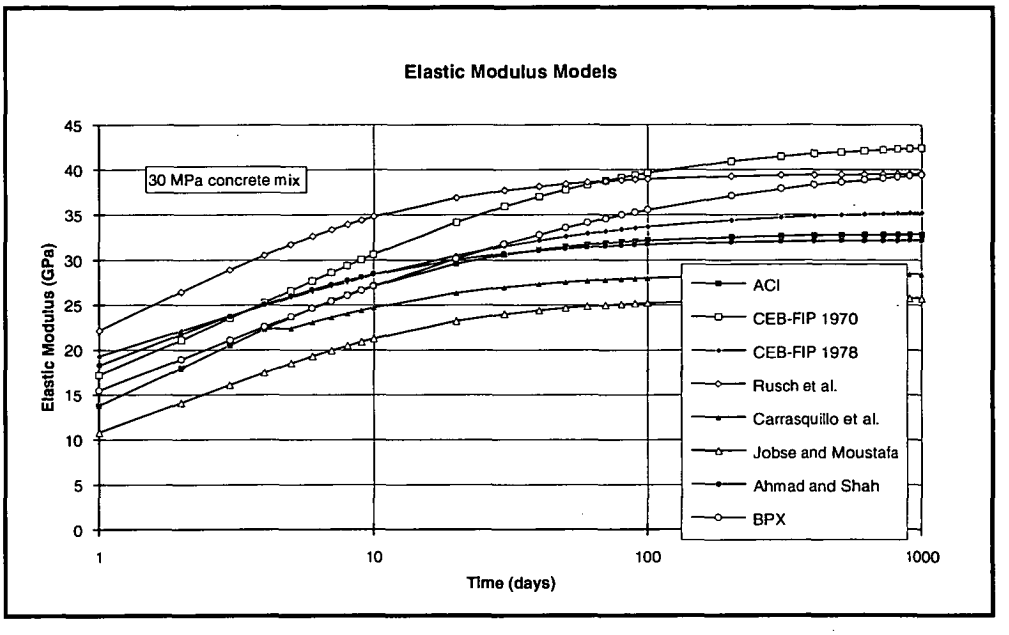

(a)

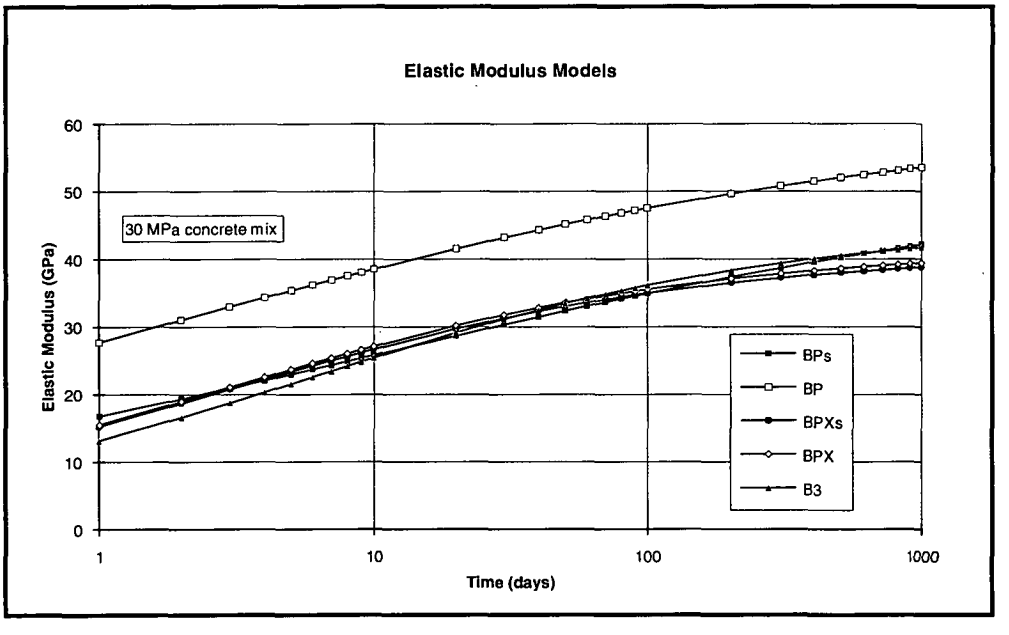

(b)

Figure 4.3 - Variation of elastic modulus with time for the ACI [37], CEB-FIP 1970 [58], CEB-FIP 1978 [38], Rusch *et al.* [65], Carrasquillo *et al.* [116], Jobse and Moustafa [117], Ahmad and Shah [118], BPs [69,70], BP [66-68], BPXs [83], BPX [78-82] and B3 [84-86] models for a 30 MPa concrete mix.

In Figure 4.3, a comparison is shown between the elastic modulus models for a 30 MPa concrete. The models of Bazant are a function of concrete composition, and Figure 4.4 compares the modulus of a 30 and 60 MPa mix. From the latter two Figures, it can be seen that all models lie within a 15 GPa bandwidth, except for the BP model [66-68] which is predicting significantly higher values. The testing

of models defined by Bazant should be done by comparing the total elastic and inelastic responses (i.e. comparing creep functions), as the creep function, creep coefficient and modulus are inter-related. However, this is not attempted here.

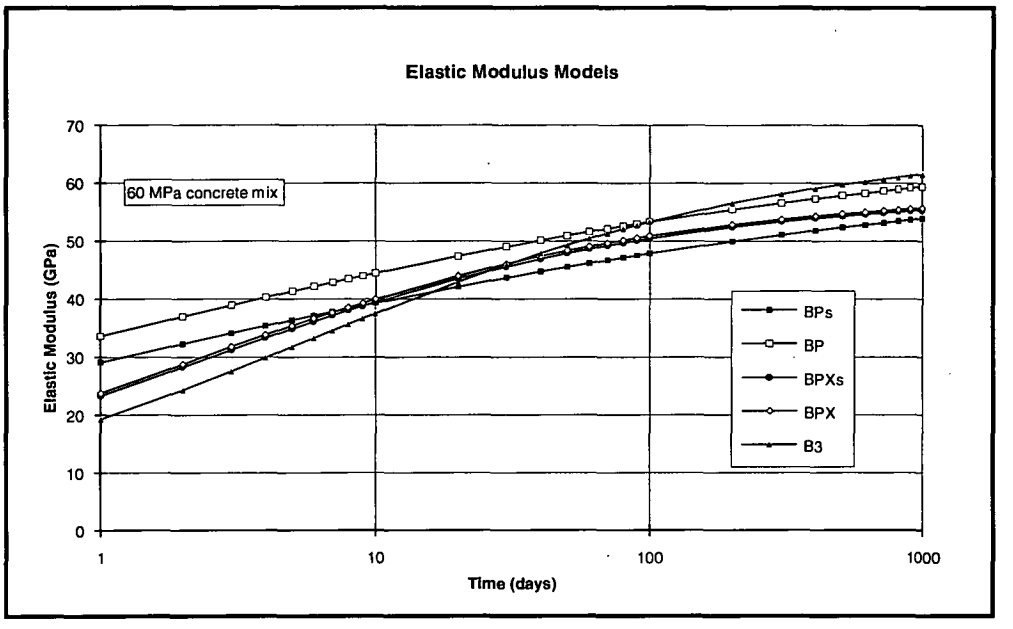

Figure 4.4 - Variation of elastic modulus with time for the BPs [69,70], BP [66-68], BPXs [83], BPX [78-82] and B3 [84-86] models for a 60 MPa concrete mix.

For the creep coefficient and shrinkage model comparisons, the specimens used are assumed to be 500mm long square prismatic section which is subjected to 60% relative humidity. Variation of creep coefficient with loading duration, relative humidity and volume-surface area ratio are shown in Figures 4.5 to 4.7 respectively. There is a large scatter of predictions. The BP model [66-68] predicts higher values of creep. However, the combined elastic and creep components of this model are comparable with other models as the elastic deformations are small.

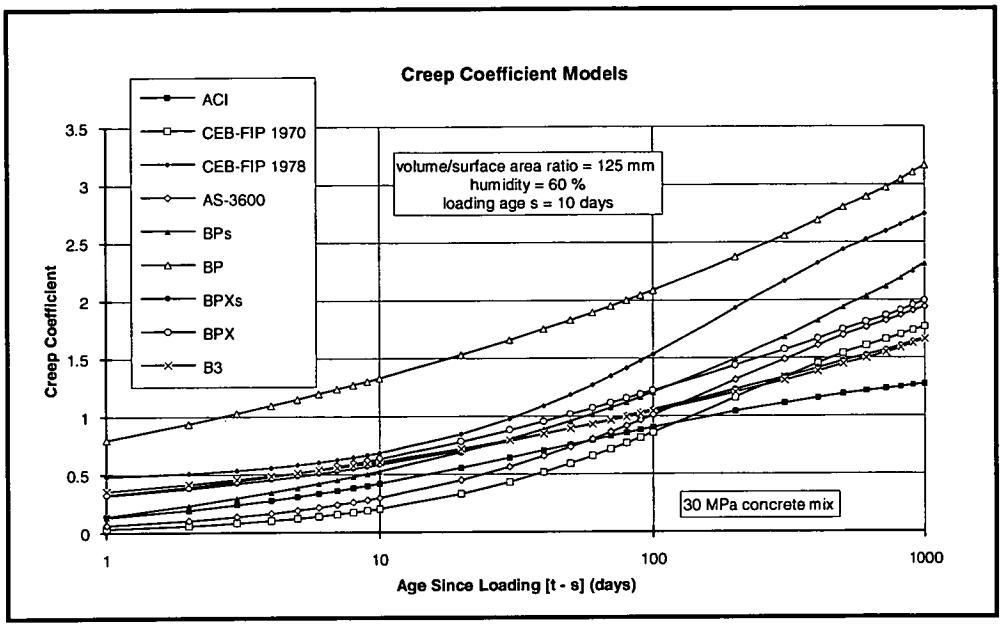

Figure 4.5 - Variation of creep coefficient with loading duration for the ACI [37], CEB-FIP 1970 [58], CEB-FIP 1978 [38], AS-3600 [39], BPs [69,70], BP [66-68], BPXs [83], BPX [78-82] and B3 [84-86] models for a 30 MPa concrete mix.

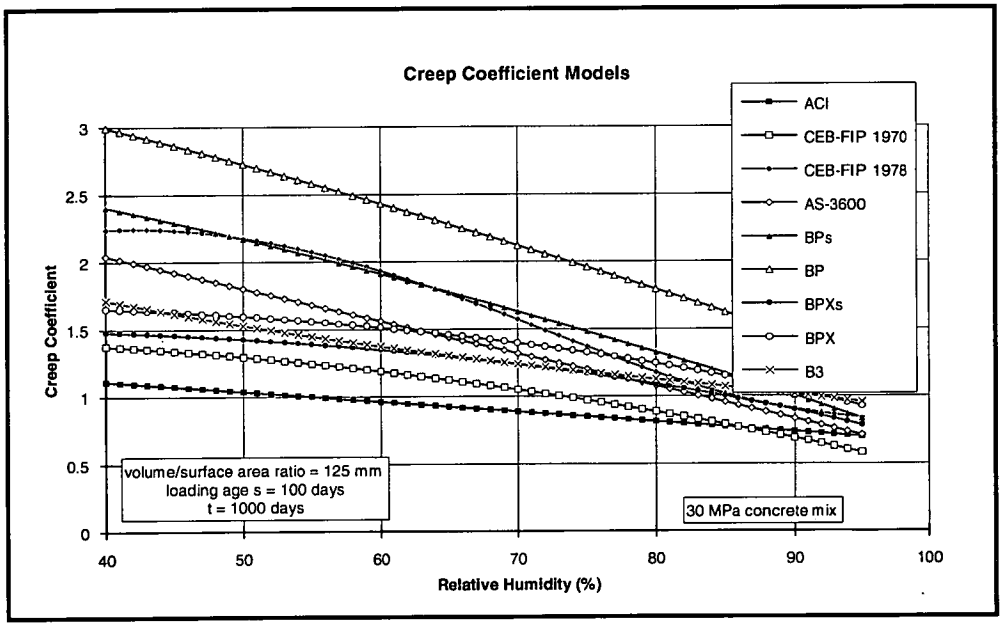

Figure 4.6 - Variation of creep coefficient with relative humidity for the ACI [37], CEB-FIP 1970 [58], CEB-FIP 1978 [38], AS-3600 [39], BPs [69,70], BP [66-68], BPXs [83], BPX [78-82] and B3 [84-86] models for a 30 MPa concrete mix.

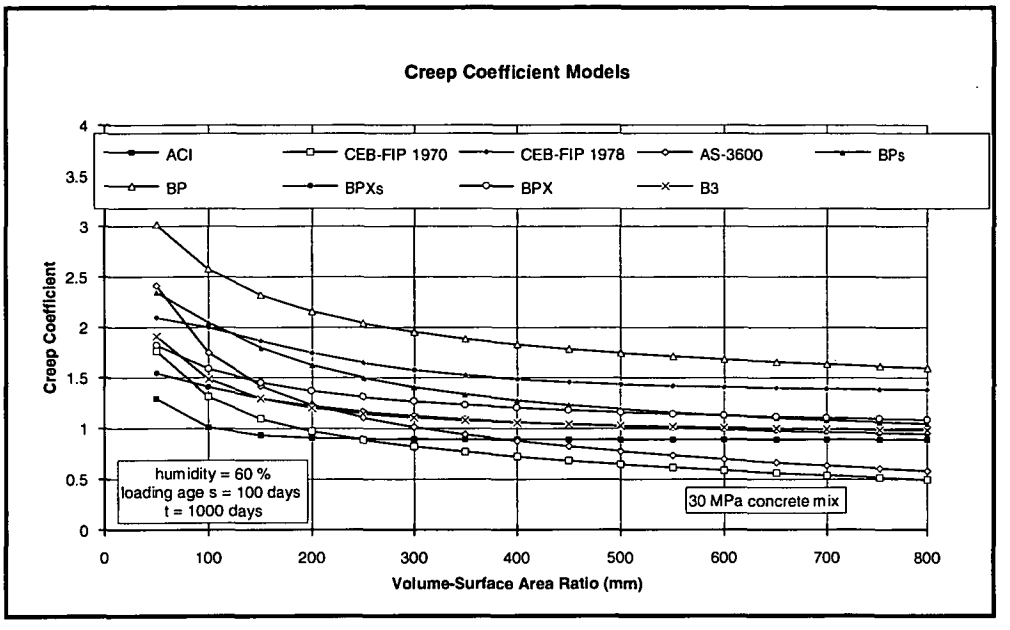

Figure 4.7 - Variation of creep coefficient with volume-surface area ratio for the ACI [37], CEB-FIP 1970 [58], CEB-FIP 1978 [38], AS-3600 [39], BPs [69,70], BP [66-68], BPXs [83], BPX [78-82] and B3 [84-86] models for a 30 MPa concrete mix.

Comparisons of shrinkage variations with drying period, relative humidity and volume-surface area ratio are shown in Figures 4.8 to 4.10 respectively. There is a large scatter of predictions, as was for the case of creep. The shrinkage prediction from the CEB-FIP 1970 code [58] follows the same decreasing trend as that for the other models, i.e. shrinkage decreases as the volume-surface area ratio increases to a value of 300mm, see Figure 4.10. After reaching 300mm, the shrinkage model incorrectly predicts an increase in shrinkage strain. This observation suggests that the equation in the CEB-FIP 1970 code for incorporating effects of member shape is inadequate for thick elements.

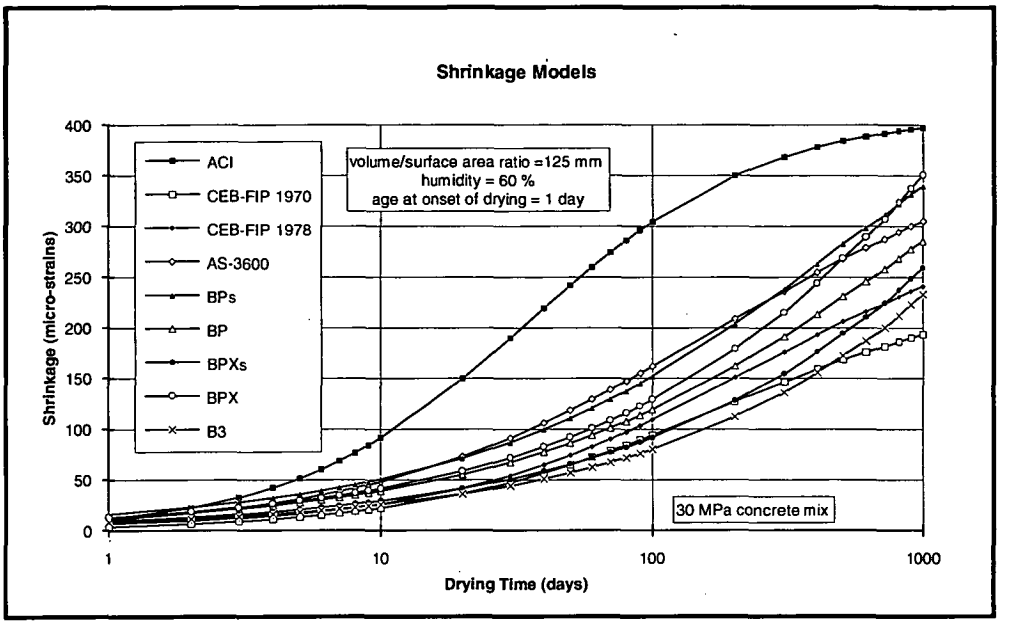

Figure 4.8 - Variation of shrinkage with drying time for the ACI [37], CEB-FIP 1970 [58], CEB-FIP 1978 [38], AS-3600 [39], BPs [69,70], BP [66-68], BPXs [83], BPX [78-82] and B3 [84-86] models for a 30 MPa concrete mix.

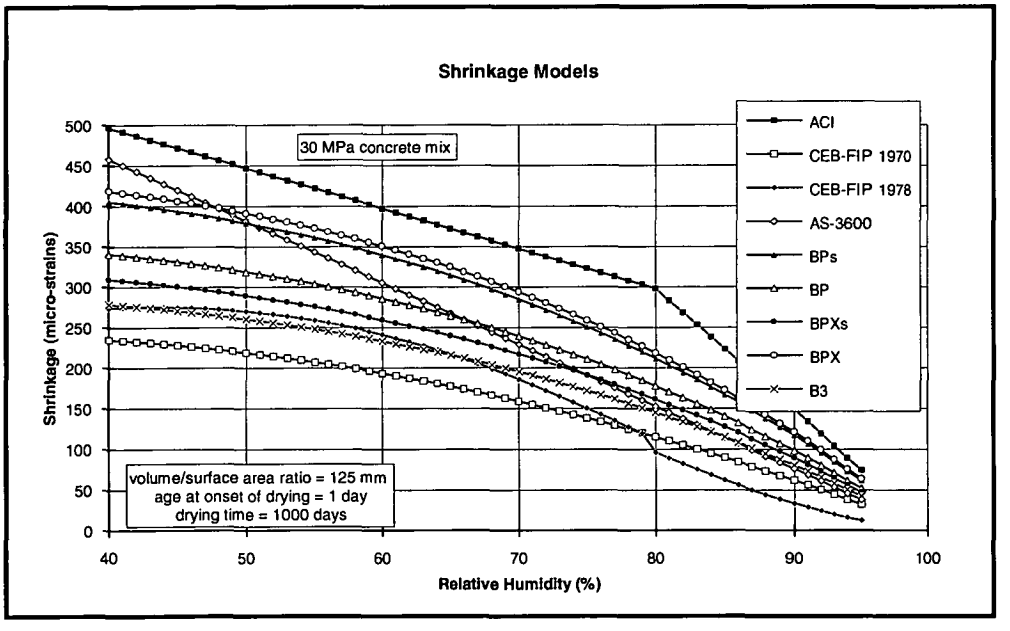

Figure 4.9 - Variation of shrinkage with relative humidity for the ACI [37], CEB-FIP 1970 [58], CEB-FIP 1978 [38], AS-3600 [39], BPs [69,70], BP [66-68], BPXs [83], BPX [78-82] and B3 [84-86] models for a 30 MPa concrete mix.

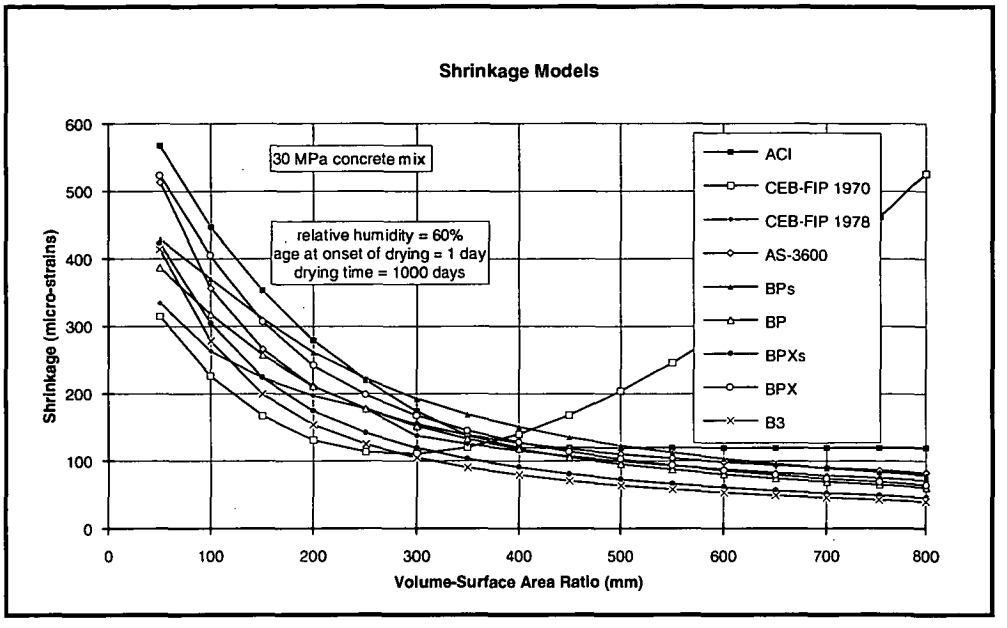

Figure 4.10 - Variation of shrinkage with volume-surface area ratio for the ACI [37], CEB-FIP 1970 [58], CEB-FIP 1978 [38], AS-3600 [39], BPs [69,70], BP [66-68], BPXs [83], BPX [78-82] and B3 [84-86] models for a 30 MPa concrete mix.

In summary, it was found that prediction methods for concrete properties offered by some codes and recommendations have shown large discrepancies. These comparisons were made at a deterministic level. Similar observations were made by Hilsdorf and Muller [125] who also found great differences in some prediction models of creep and shrinkage for concretes loaded at early ages, small volume-surface area ratios and low humidities.

4.4 CONCLUDING REMARKS TO CHAPTER

There are numerous models which describe the properties of concrete including the ACI [37,57], CEB-FIP [38,58] and AS-3600 [39] codes, as well as the proposals of Bazant *et al.* [66-86]. These properties include the concrete strength, elastic modulus, creep coefficient and shrinkage. Deterministic comparisons of the models have shown large differences. The limitations of each concrete property model was also examined. Selection of models based on this review and the comparisons are not made at this stage, as the influence of concrete properties at a probabilistic level on the final axial shortening response of columns are further investigated in Chapter 8.

APPENDIX

TO

CHAPTER 4

APPENDIX A4.1

A4.1.1 ACI 1978 CODE

A4.1.1.1 Introduction

The method for predicting concrete property behaviour given in ACI [37] is based on the work by Branson *et al.* [126]. This approach is a simplified procedure, where average ultimate parameter values are used for modelling the basic shrinkage strain and creep coefficient. These ultimate values are then modified by a time ratio and coefficients to incorporate the influence of governing factors. The time ratio is hyperbolic for shrinkage, whilst a combined hyperbolic and power expression is employed for creep. Branson *et al.* measured and individually fitted experimental creep and shrinkage data to three curves. One curve being for normal weight concretes, a second for sand light-weight concretes, whilst the remaining were for other light-weight concretes. These three curves were combined to obtain average final equations for time-dependent behaviour. Branson *et al.* concluded that the variation of either creep or shrinkage for different weight concretes was not consistent. The concrete strength equation proposed by the ACI modifies the 28-day compressive strength for time, where a hyperbolic time ratio is utilised.

These models yield reasonable results, but correlations between field and predicted values have been shown to be inconsistent [37]. For almost uniform temperature and humidity field conditions, as for example, found in laboratories, close correlations can be expected. The most important environmental factor according to the ACI code which influences creep and shrinkage is humidity, whilst temperature being the second. For temperatures which are significantly different to 21°C, the influence of this factor should be embodied into the ACI model.

A4.1.1.2 Concrete Strength

The ACI [37] recommends the following equation for modelling concrete strength at age **s**

$$f_c(s) = \frac{s}{(\alpha + \beta s)} f_c' \qquad \text{(A4.1)}$$

where

f_c' = 28-day concrete strength

The constants α and β depend on the type of cement and method of concrete curing. For normal and high early strength cements and moist cured, the value of these constants are respectively

$$\left.\begin{array}{lll} & \alpha = 4.0 & \beta = 0.85 \\ \text{and} & \alpha = 2.3 & \beta = 0.92 \end{array}\right\} \quad \text{(A4.2)}$$

Equation (A4.1) applies to normal weight, sand light-weight and all light-weight concretes, with all experimental data used in deriving the previous falling within 20% of its predictions.

A4.1.1.3 Elastic Modulus

The ACI [37] employs the following formula for predicting the elastic modulus of concrete at age s

$$E_c(s) = \rho^{1.5} 0.043 \sqrt{f_c(s)} \quad \text{(A4.3)}$$

where

$f_c(s)$ = concrete strength (MPa)

ρ = concrete density (kg/m^3)

and $E_c(s)$ = concrete modulus (MPa)

This model was developed by Pauw [112], and incorporates the density of concrete. The static modulus here is defined as the secant modulus at $0.4f_c(s)$ for a loading period of between one to five minutes. Recent work by Carrasquillo *et al.* [116] has been included in the ACI high strength concrete code [57], which models the modulus of normal and high strength concretes.

A4.1.1.4 Creep Coefficient

The creep coefficient proposed by the ACI [37] includes basic and drying creep, and is given by

$$\mu_t = \frac{(t-s)^{0.6}}{10+(t-s)^{0.6}} \mu_u \quad \text{(A4.4)}$$

where

μ_u = ultimate creep coefficient

t = total age of concrete

and s = age of concrete when load is applied

The ultimate creep coefficient is

$$\mu_u = 2.35\gamma_s\gamma_\lambda\gamma_{v/s}\gamma_\xi\gamma_\psi\gamma_a \qquad \text{(A4.5)}$$

where

$\gamma_s = 1.25 s^{-0.118}$ for $s > 7$ days for moist

$\gamma_s = 1.0$ (assume) for $s \le 7$ days cured concrete

$\gamma_\lambda = 1.27 - 0.0067\lambda$ for $\lambda > 40\%$

$\gamma_\lambda \ge 1.0$ for $\lambda < 40\%$

h_o (mm)	50	75	100	125	150
$\gamma_{v/s}$	1.30	1.17	1.11	1.04	1.00

Note: linear interpolation is used for values not given in table $(50 \le h_o \le 150)$

$\gamma_{v/s} = 1.14 - 0.00092 h_o$ for $(t-s) \le 365$ days

$\gamma_{v/s} = 1.10 - 0.00067 h_o$ for $(t-s) > 365$ days $\qquad (150 < h_o < 380)$

$$\gamma_{v/s} = \frac{2}{3}(1 + 1.13 e^{-0.0213 v/s}) \qquad (380 \ge h_o)$$

$\gamma_\xi = 0.82 + 0.00264\xi$

$\gamma_\psi = 0.88 + 0.0024\psi$

$\gamma_a = 0.46 + 0.09a \ge 1.0$

$h_o = 4\frac{V}{S}$

$\frac{V}{S}$ = volume to surface ratio (mm)

λ = relative humidity (%)

ξ = slump of concrete (mm)

ψ = percentage of fine aggregates in total aggregate (by mass)

and a = percentage of air content by volume in concrete

A4.1.1.5 Shrinkage Model

The basic shrinkage strain of concrete, for a drying period $\mathbf{t_d}$ and moist cured concrete, as recommended by the ACI [37] is

$$(\varepsilon_{sh})_t = \frac{t_d}{35 + t_d}(\varepsilon_{sh})_u \qquad \text{(A4.6)}$$

where

$(\varepsilon_{sh})_u$ = ultimate shrinkage (μstrains)

and t_d = concrete age from onset of drying (days)

The ultimate shrinkage value is

$$(\varepsilon_{sh})_u = 780\gamma'_{cp}\gamma'_{\lambda}\gamma'_{v/s}\gamma'_{\xi}\gamma'_{\psi}\gamma'_{c}\gamma'_{a} \qquad \text{(A4.7)}$$

where

$$\left.\begin{aligned} \gamma'_{\lambda} &= 1.4 - 0.01\lambda \quad \text{for } 40\% \le \lambda \le 80\% \\ \gamma'_{\lambda} &= 3.0 - 0.03\lambda \quad \text{for } 80\% < \lambda \le 100\% \\ \gamma'_{\lambda} &\ge 1.0 \quad \lambda < 40\ \%, \end{aligned}\right\}$$

h_o (mm)	50	75	100	125	150
$\gamma'_{v/s}$	1.35	1.25	1.17	1.08	1.00

Note: linear interpolation is used for values not given in table $(50 \le h_o \le 150)$

$$\left.\begin{aligned} \gamma'_{v/s} &= 1.23 - 0.0015\,h_o \quad \text{for } t_d \le 365 \text{ days} \\ \gamma'_{v/s} &= 1.17 - 0.00114\,h_o \quad \text{for } t_d > 365 \text{ days} \end{aligned}\right\} \quad (150 \le h_o < 380)$$

$$\gamma'_{v/s} = 1.2e^{-0.00472\,v/s} \ge 0.2 \qquad (380 \ge h_o)$$

$$\gamma'_{\xi} = 0.89 + 0.00161\xi$$

$$\left.\begin{aligned} \gamma'_{\psi} &= 0.30 + 0.014\,\psi \quad \text{for } \psi \le 50\% \\ \gamma'_{\psi} &= 0.90 + 0.002\,\psi \quad \text{for } \psi > 50\% \end{aligned}\right\}$$

$$\gamma'_{c} = 0.75 + 0.00061c$$

$$\gamma'_{a} = 0.95 + 0.008a$$

T_c (days)	1	3	7	14	28	90
γ'_{cp}	1.2	1.1	1.0	0.93	0.86	0.75

T_c = initial moist curing period (days)

and c = cement content (kg/m^3)

A4.1.2 CEB-FIP 1978 CODE

A4.1.2.1 Introduction

This theory is based on the work by Rusch *et al.* [65]. A ±20% variation of the final values for creep, shrinkage, strength and elastic modulus must be contemplated in design.

A4.1.2.2 Concrete Strength

The CEB-FIP [38] recommends the following equation for concrete strength at age **s**

$$\frac{f_c(s)}{f_c(\infty)} = \frac{s^{0.73}}{5.27 + s^{0.73}} \tag{A4.8}$$

If **s** = 28 days, the previous equation is simplified to

$$\frac{f_c(28)}{f_c(\infty)} = \frac{28^{0.73}}{5.27 + 28^{0.73}} = 0.6836 \tag{A4.9}$$

Dividing the latter two expressions, results in

$$f_c(s) = \frac{1.4628 s^{0.73}}{5.27 + s^{0.73}} f_c(28) \tag{A4.10}$$

This formula relates the concrete strength at **s** to the 28-day strength.

A4.1.2.3 Elastic Modulus

The elastic modulus of concrete at age **s**, proposed by the CEB-FIP [38] is

$$E_c(s) = 9.5 \sqrt[3]{f_c(s)} \quad \text{(GPa)} \tag{A4.11}$$

where

$f_c(s)$ = concrete strength (MPa)

A4.1.2.4 Creep Coefficient

The CEB-FIP [38] defines the creep strain by

$$\varepsilon_c(t,s) = \frac{\sigma_o}{E_c(28)} \phi(t,s)_{CEB} \tag{A4.12}$$

where

$\phi(t,s)_{CEB}$ = creep coefficient for CEB-FIP 1978 code

and σ_o = constant stress applied at time s

Rearranging (A4.12), the general creep coefficient can be expressed as

$$\phi(t,s) = \frac{E_c(s)}{E_c(28)}\phi(t,s)_{CEB} \qquad \text{(A4.13)}$$

The CEB-FIP creep coefficient is given by

$$\phi(t,s)_{CEB} = \phi_d\,\beta_d(t-s) + \beta_a(s) + \phi_f\left[\beta_f(t) - \beta_f(s)\right] \qquad \text{(A4.14)}$$

The first term represents the delayed elastic component, the second term models the rapid initial flow, whilst the final term describes the subsequent flow. Expressions for each of the parameters can be found in [14], and are given below:

$$\phi_d = 0.4$$

$$\beta_d(t-s) = 0.27 + 0.73\left(1 - e^{-0.01(t-s)}\right)$$

$$\beta_a(s) = 0.8\left(1 - \frac{f_c'}{f_c(\infty)}\right)$$

$$\phi_f = \phi_{f1}\phi_{f2}$$

$$\phi_{f1} = \frac{1}{9}\left(0.0002\,h^3 - 0.043\,h^2 + 2.57\,h\right) - 2.2$$

$$\phi_{f2} = 1.12\left(1 + e^{-0.044\,h_c^{0.58}}\right)$$

$$\lambda = 1.0 + 0.00049\,e^{0.1\,h} \qquad \text{for } h \le 98\%$$

$$\lambda = 30 \qquad \text{for } h = 100\%$$

$$h_c = \lambda_c \frac{2A_t}{u}$$

$$\beta_f(t) = \sqrt[3]{\frac{t^\alpha}{t^\alpha + \beta}}$$

$$\alpha = 0.8 + 0.55\,e^{-0.003\,h_c}$$

$$\beta = 770 + 210\,e^{-0.0043\,h_c}$$

h = relative humidity (%)

h_c = notional thickness of member (mm)

A_t = cross-sectional area of member

u = perimeter exposed to drying

and λ_c = humidity coefficient

A4.1.2.5 Shrinkage Model

The CEB-FIP [38] recommends the following equation for concrete shrinkage at time **t** when drying begins at $\mathbf{t_{sh}}$, by

$$\varepsilon_{sh}(t,t_{sh}) = \varepsilon_{sho}[\beta_{sh}(t) - \beta_{sh}(t_{sh})] \qquad \text{(A4.15)}$$

Expressions for each of the terms given in the previous equation can be found in [14], and now follow:

$$\varepsilon_{sho} = \varepsilon_{sh1}\,\varepsilon_{sh2}$$

$$\varepsilon_{sh1} = \frac{1}{3}\left(0.41h^2 - 37.1h - 372\right) \qquad \text{for } h \le 98\% \quad (\text{in } \mu\text{strains})$$

$$\varepsilon_{sh1} = 100 \qquad \text{for } h = 100\% \quad (\text{in } \mu\text{strains})$$

$$\varepsilon_{sh2} = 0.7 + 1.42\,e^{-0.18h_c^{0.45}}$$

$$\beta_{sh}(t) = \frac{t^{0.8}}{t^{0.8} + 0.25\,h_c} \qquad (50 \le h_c \le 600)$$

and

$$\beta_{sh}(t) = \frac{t^{1.25}}{t^{1.25} + 8\,h_c} \qquad (600 < h_c \le 1600)$$

A4.1.2.6 Alternative Expressions for Creep and Shrinkage Models

Alternative expressions for the parameters in (A4.14) and (A4.15) by Smerda and Kristek [63] are given below:

$$\beta_d(t-s) = 0.28 + 0.5\arctan(0.011(t-s))^{2/3}$$

$$\beta_a(s) = 0.95\,s^{-0.3} - 0.1$$

$$\phi_{f2} = 1.1089 + 0.8469\,e^{-0.0027h_c}$$

$$\beta_f(t) = 1 - e^{-(A_f t)^{B_f}}$$

$$A_f = 0.078\,e^{-1.22\log h_c}$$

$$B_f = 0.528\,e^{-0.13\log h_c}$$

$$\varepsilon_{sh2} = 0.7001 + 0.6292\,e^{-0.0046h_c}$$

$$\beta_{sh}(t) = 1 - e^{-(A_s t)^{B_s}}$$

$$A_s = 3.16\,e^{-2.98\log h_c}$$

and

$$B_s = 0.18\,e^{0.49\log h_c}$$

More expressions for the parameters in (A4.14) and (A4.15) by CEB-FIP [40] now follow:

$$\frac{f_c(s)}{f_c(\infty)} = \left(\frac{s}{s+47}\right)^{\frac{1}{2.45}}$$

$$\beta_d(t-s)=\left(\frac{t-s}{t-s+328}\right)^{\frac{1}{4.2}}$$

$$\beta_f(t)=\left(\frac{t}{t+A_{bf}}\right)^{B_{bf}}$$

$$A_{bf}=\exp\left(\frac{5.02}{h_o}+\ln\left(6.95\,h_o{}^{1.25}\right)\right) \qquad \text{note: } h_o \text{ is in cm}$$

$$B_{bf}=\exp\left(0.00144\,h_o-\frac{1.1}{h_o}-\ln\left(1.005\,h_o{}^{0.2954}\right)\right)$$

$$\phi_{f1}=4.45-0.035\,h$$

$$\phi_{f2}=\exp\left(4.4\times10^{-5}\,h_o-\frac{0.357}{h_o}-\ln\left(\frac{h_o{}^{0.1667}}{2.6}\right)\right)$$

$$\beta_s(t)=\left(\frac{t}{t+A_{bs}}\right)^{B_{bs}}$$

$$A_{bs}=11.8\,h_o+16$$

$$B_{bf}=\exp\left(-0.00257\,h_o+\frac{0.32}{h_o}+\ln\left(0.22\,h_o{}^{0.4}\right)\right)$$

$$\varepsilon_{shl}=\left(-0.00775\,h^3+1.565\,h^2-110.325\,h+3032.5\right) \qquad (\text{in } \mu\text{strains})$$

and $$\varepsilon_{sh2}=\left(0.00174\,h_o-\frac{0.32}{h_o}-\ln\left(\frac{h_o{}^{0.251}}{1.9}\right)\right)$$

A4.1.3 CEB-FIP 1970 CODE

A4.1.3.1 Introduction

This method [58] is limited to working stress ranges for concrete, an environmental temperature approximately 20°C with relative humidity between 55% and 75%.

A4.1.3.2 Concrete Strength

The CEB-FIP [58] recommends (A4.10) for concrete strength.

A4.1.3.3 Elastic Modulus

The CEB-FIP [58] proposes the following equation for elastic modulus of concrete at age s

$$E_c(s)=5.94\sqrt{f_c(s)} \qquad (\text{GPa}) \qquad (A4.16)$$

where

$f_c(s)$ = concrete strength (MPa)

A4.1.3.4 Creep Coefficient

The general creep coefficient is determined by (A4.13), in which the CEB-FIP [58] creep coefficient is

$$\phi(t,s)_{CEB} = k_1 k_2 k_3 k_4 k_5 \qquad \text{(A4.17)}$$

In the previous equation, the variables $\mathbf{k_2}$, $\mathbf{k_3}$ and $\mathbf{k_4}$ represent modifying factors due to loading age, concrete composition and member size respectively. A standard creep value is defined by $\mathbf{k_1}$, and $\mathbf{k_5}$ represents a time ratio. Expressions for parameters in (A4.17) can be found in [14], and are given below:

$$k_1 = 3 + 0.01\lambda - 0.0003\lambda^2$$

$$k_2 = 0.45 + 1.76e^{-0.267s^{0.44}}$$

$$k_3 = (1.3 + 0.007c)(w/c) - 0.85$$

$$k_4 = 0.7 + 0.77e^{-0.009h_o}$$

$$h_o = \frac{2A_t}{u}$$

$$k_5 = \frac{(t-s)^{0.8}}{(t-s)^{0.8} + 0.25h_o}$$

(w/c) = water to cement ratio

λ = relative humidity (%)

c = cement content (kg/m^3)

h_o = hypothetical thickness of member (mm)

A_t = cross-sectional area of member

and u = perimeter exposed to drying

A4.1.3.5 Shrinkage Model

The CEB-FIP [58] recommends the following formula for predicting shrinkage with a drying period $\mathbf{t_d}$, as follows

$$\varepsilon_{sh}(t_d) = k_1^* k_3 k_4^* k_5 \qquad \text{(A4.18)}$$

In this equation, the variables $\mathbf{k_3}$ and $\mathbf{k_4^*}$ represent modifying factors due to concrete composition and member shape respectively. A standard shrinkage strain value is given by $\mathbf{k_1^*}$, and $\mathbf{k_5}$ defines a time ratio. Expressions for each parameter in (A4.18) can be found in [14], and now follow:

$$k_1^* = 360 + 4.4\lambda - 0.08\lambda^2$$

$$k_4^* = 3\times10^{-6}\, h_o{}^2 - 0.0031 h_o + 1.3$$

and $$k_5^* = \frac{t_d{}^{0.8}}{t_d{}^{0.8} + 0.25 h_o}$$

A4.1.4 AS-3600 CODE

A4.1.4.1 Introduction

The AS-3600 [39] proposal is based on the CEB-FIP 1970 code [58] for time-dependent behaviour. Basic values of creep and shrinkage are modified to incorporate the effects of humidity and member size. A variation of ±30% for creep and shrinkage and, ±20% for elastic modulus is recommended for design.

A4.1.4.2 Concrete Strength

No recommendations are made by AS-3600 [39] for concrete strength, either (A4.1) or (A4.10) can be employed.

A4.1.4.3 Elastic Modulus

AS-3600 [39] recommends the equation proposed by Pauw [112], and is given by (A4.3).

A4.1.4.4 Creep Coefficient

The creep coefficient utilised by AS-3600 [39] is

$$\phi(t,s) = k_2 k_3 \phi_{cc.b} \qquad \text{(A4.19)}$$

where

$\phi_{cc.b}$ = basic creep factor

$$\phi_{cc.b} = -0.00002446\, f_{cc}'^{\,3} + 0.005217\, f_{cc}'^{\,2} - 0.3758\, f_{cc}' + 10.796$$

and f_{cc}' = characteristic concrete strength (MPa)

The author has obtained the expression for $\phi_{cc.b}$ by fitting a third-order polynomial based on the tabulated values in AS-3600. Expressions for the other terms given in (A4.19) can be found in [14], and are given below:

$$k_2 = \frac{k_7 k_8 (t-s)^{0.7}}{(t-s)^{0.7} + k_9}$$

$$k_7 = 0.76 + 0.9 e^{-0.008 h_o}$$

$$k_8 = 1.37 - 0.011 h$$

$$k_9 = 0.15 h_o$$

$$h_o = 2\frac{A_t}{u} \qquad \text{(in mm)}$$

$$k_3 = 0.9 \qquad \text{for} \frac{f_c(s)}{f_c'} \geq 1.4$$

$$k_3 = -0.5\frac{f_c(s)}{f_c'} + 1.6 \qquad \text{for} \; 1.0 \leq \frac{f_c(s)}{f_c'} \leq 1.4$$

$$k_3 = -0.8\frac{f_c(s)}{f_c'} + 1.9 \qquad \text{for} \; 0.5 \leq \frac{f_c(s)}{f_c'} \leq 1.0$$

h = relative humidity (%)

A_t = cross-sectional area of member

and u = perimeter exposed to drying

A4.1.4.5 Shrinkage Model

Shrinkage from onset of drying t_d, recommended by AS-3600 [39] is given as

$$\varepsilon_{sh}(t_d) = 700\, k_1 \qquad (\mu\text{strains}) \qquad \text{(A4.20)}$$

Equations for determining k_1 are found in [14], as follows:

$$k_1 = \frac{k_4 k_5 t_d^{0.7}}{t_d^{0.7} + k_6}$$

$$k_4 = 0.62 + 1.5 e^{-0.005 h_o}$$

$$k_5 = \frac{4 - 0.04 h}{3}$$

and $$k_6 = \frac{h_o}{7}$$

A4.1.5 BAZANT CONCRETE PROPERTY MODELS

A4.1.5.1 Introduction

Bazant and Panula [66] commented that the database for available creep and shrinkage data is large, and that current codes and standards only use a fraction of this data with the selection being arbitrary and very narrow. This might suggest that prediction of concrete properties from these codes do not agree well with the available experimental data.

Bazant and Panula [66-70] based their concrete property models on semi-empirical equations developed from diffusivity theory, thermodynamic restrictions and activation energy theory. The term *'thermodynamic restrictions'* firstly needs some explanation and is given in the form of equations. Some of these obvious restrictions are found in Bazant [64], and now follow

$$\frac{\partial J(t,s)}{\partial t} \geq 0 \qquad \text{(A4.21)}$$

$$\frac{\partial^2 J(t,s)}{\partial t^2} \leq 0 \qquad \text{(A4.22)}$$

and $$\left[\frac{\partial J(t,s)}{\partial s}\right]_{t=s} \leq 0 \qquad \text{(A4.23)}$$

Further thermodynamic restrictions are beyond the scope of this thesis. The term *'activation energy theory'* refers to the rate at which chemical reactions are taking place in hydrating or aging concrete, whilst *'diffusivity theory'* is the process of water/moisture flow through concrete.

Evaluation of the constants in the Bazant and Panula models [66-70] was made using over 10,000 data points, where the material constants are a function of concrete composition. Models proposed at a later date by Bazant and Chern [73-75] are improvements of the original Bazant and Panula models [66-70]. More recently, Bazant *et al.* [76-86] proposed a new creep model based on solidification theory and an improved shrinkage formula. In this context, *'solidification theory'* refers to modelling concrete as a solidifying material for describing the aging process. In deriving the new model, more creep and shrinkage data were utilised. The Bazant *et al.* property models [66-86] seem to be statistically better than those found in codes, and this was reported in [127] for the case of shrinkage in

particular. Application of the Bazant *et al.* creep models are even valid for extremely small loading ages (i.e. **s** = 10^{-7} days).

A4.1.5.2 Shrinkage (model 1)

Bazant and Panula [66] proposed the following model for shrinkage at time t_d from onset of drying

$$\varepsilon_{sh}(t_d) = k_h \varepsilon_{\infty sh} \sqrt{\frac{t_d}{\tau_{sh} + t_d}} \quad (\mu\text{strains}) \qquad \text{(A4.24)}$$

where

$$k_h = 1 - 10^{-6} h^3 \qquad \text{for } h \le 98\%$$

$$k_h = -0.2 \qquad \text{for } h = 100\%$$

$$\varepsilon_{\infty sh} = \varepsilon_{sh} \frac{E(7+600)}{E(t_{sh} + \tau_{sh})}$$

$$E(t') = E(28) \sqrt{\frac{t'}{4.0 + 0.85 t'}}$$

$$\varepsilon_{\infty sh} = 1.0805 \varepsilon_{sh} \sqrt{\frac{4.0 + 0.85(t_{sh} + \tau_{sh})}{t_{sh} + \tau_{sh}}}$$

$$\varepsilon_{sh} = (1210 - 880\, y) \quad (\mu\text{strains})$$

$$y = \frac{1}{390 z^{-4} + 1}$$

$$z = \left(1.25\sqrt{(a/c)} + 0.5(g/s)^2\right) \sqrt[3]{\frac{1 + s/c}{w/c}}\, 0.381\sqrt{f_c'} - 12 \ge 0$$

$$\tau_{sh} = 600 \left(\frac{k_s}{150} D\right)^2 \frac{10}{C_1(t_{sh})}$$

$$D = 2V/S \quad (\text{in mm})$$

$$k_s = 1.25 \quad (\text{a square prism})$$

$$C_1(t_{sh}) = C_7 k_T' \left(0.05 + \sqrt{\frac{6.3}{t_{sh}}}\right) \qquad \text{mm}^2/\text{day}$$

$$k_T' = \frac{T}{T_o} \exp\left(\frac{5000}{T_o} - \frac{5000}{T}\right)$$

$k_T' = 1$ for excluding temperature in this model

$$C_7 = \frac{(w/c)c}{8} - 12 \qquad (\text{where } 7 \le C_7 \le 21)$$

(sand is defined as the aggregate which will pass through a 4.7 mm sieve)

h = relative humidity (%)

V / S = volume/surface area ratio (mm)

w / c = water/cement ratio

a/c = total aggregate/cement ratio

and g/s = gravel/sand ratio

A4.1.5.3 Creep (model 1) - Double Power Law

Bazant and Panula [66-68] derived this model based on thermodynamic restrictions for the creep function, as well as activation energy theory. The general creep coefficient follows

$$\phi(t,s) = E_c(s)\phi_{bp}(t,s) - 1 \qquad \text{(A4.25)}$$

The creep function $\phi_{bp}(t,s)$ is based on the double power law, and determined by Bazant and Panula to be

$$\phi_{bp}(t,s) = \frac{1 + \phi_{bo}(t,s) + \phi_{do}(t,s,t_{sh}) - \phi_{po}(t,s,t_{sh})}{E_o} \qquad \text{(A4.26)}$$

where

$$\phi_{bo}(t,s) = \phi_T\left(s_e^{-m} + \alpha\right)(t-s)^{n_T}$$

$$\phi_{bo}(t,s) = \phi_1\left(s^{-m} + \alpha\right)(t-s)^{n} \qquad \text{(excluding temperature effects)}$$

$$\phi_T = \phi_1(1 + C_T)$$

$$\phi_1 = \frac{10^{3n}}{2(28^{-m} + \alpha)}$$

$$\alpha = \frac{1}{40\,w/c}$$

$$m = 0.28 + 47.541 f_c'^{-2}$$

$$n_T = B_T\, n$$

$$B_T = \frac{0.25}{1 + \left(\frac{74}{T - 253.2}\right)^7} + 1$$

$$n = 0.12 \qquad \text{for } x \le 4$$

$$n = 0.12 + \frac{0.07x^6}{5130 + x^6} \qquad \text{for } x > 4$$

$$x = \left(2.1\frac{(a/c)}{(s/c)^{1.4}} + 0.005523 f_c'^{1.5}\sqrt[3]{(w/c)}\,(a/g)^{2.2}\right)a_1 - 4$$

$a_1 = 1.00$ for type 'A' cements

$a_1 = 0.93$ for type 'C' cements

$$s_e = \int_0^s \beta_T(t')\,dt'$$

$$\beta_T = \exp\left(\frac{4000}{T_o} - \frac{4000}{T}\right)$$

$$C_T = c_T\,\tau_T\,c_o$$

$$c_T = \frac{19.4}{1+\left(\frac{100}{T-253.2}\right)^{3.5}} - 1$$

$$\tau_T = \frac{1}{1+60\,t_T^{-0.69}} + 0.78$$

$$c_o = \frac{(w/c)^2\,(a/c)\,a_1}{8}$$

$$\frac{1}{E_o} = 145.0\times10^{-6}\left(0.09+\frac{1}{1.7\,z_1{}^2}\right) \quad (\text{MPa}^{-1})$$

$$z_1 = 2.822\times10^{-8}\,\rho^2\,f_c'$$

$$\phi_{do}(t,s,t_{sh}) = \phi_d'\,k_h'\,s_e^{-m/2}\varepsilon_{\infty sh}\left(1+\frac{10\,\tau_{sh}(T)\,k_T{}^{1/4}}{t-s}\right)^{-c_d\,n/K_T^2}$$

$$\phi_{do}(t,s,t_{sh}) = \phi_d'\,k_h'\,s^{-m/2}\varepsilon_{\infty sh}\left(1+\frac{10\,\tau_{sh}}{t-s}\right)^{-c_d\,n} \quad \text{(excluding temperature)}$$

$$\phi_d' = \frac{1}{\sqrt{\left(1+\frac{\Delta\tau'}{10}\right)}}\phi_d$$

$$\phi_d' = \frac{1}{\sqrt{\left(1+\frac{s-t_{sh}}{10\,\tau_{sh}}\right)}}\phi_d \quad \text{(excluding temperature effects)}$$

$$\phi_d = 0.008+\frac{0.027}{1+0.7\,r^{-1.4}} \quad \text{for } r>0$$

$$\phi_d = 0.008 \quad \text{for } r\le 0$$

$$r = 31378\left((s/a)\,f_c'\right)^{0.3}(g/s)^{1.3}\left(\frac{(w/c)}{\varepsilon_{sh}}\right)^{1.5} - 0.85$$

$$\Delta\tau' = \frac{t_T - t_{sh}}{\tau_{sh}(T_o)} + \frac{s-t_T}{\tau_{sh}(T)}\,k_T''$$

$\tau_{sh}(T)$ = value of τ_{sh} at temperature T

$$k_T'' = (k_T)^{5/4}$$

$$k_T = \frac{17.6}{1+\left(\frac{100}{T-253.2}\right)^4} + 0.42$$

$$K_T = \frac{0.4}{1+\left(\frac{93.5}{T-253.2}\right)^4} + 1$$

$$c_d = 2.8-7.5\,n$$

$$k_h' = 1-10^{-3}\,h^{1.5}$$

$$\phi_{po}(t,s,t_{sh}) = c_p\, k_h''\, \phi_{bo}(t,s)\left(1+\frac{100}{\Delta\tau}\right)^{-n}$$

$$\phi_{po}(t,s,t_{sh}) = c_p\, k_h''\, \phi_{bo}(t,s)\left(1+\frac{100\,\tau_{sh}}{t-t_{sh}}\right)^{-n} \qquad \text{(excluding temperature)}$$

$c_p = 0.83$

$k_h'' = 1-10^{-4}\,h^2$

$\Delta\tau = \dfrac{t_T - t_{sh}}{\tau_{sh}(T_o)} + \dfrac{t-t_T}{\tau_{sh}(T)}$

$\phi_{bp}(t,s) =$ in units of $(MPa)^{-1}$

E_o = asymptotic modulus

$\phi_{bo}(t,s) =$ basic creep

$\phi_{do}(t,s,t_{sh}) =$ additional drying creep

$\phi_{po}(t,s,t_{sh}) =$ decrease in creep after drying

t_T = time when temperature T is applied (days)

and T = temperature in Kelvin

The *'BP'* notation denotes time-dependent behaviour according to (A4.24) and (A4.26).

Further refinements to the original creep model were made by Bazant and Wang [71] to firstly embody the effects of cyclic humidity, this model is designated by *'BPc'*. A correction factor κ is employed to the original BP model, and the creep function given by Bazant and Wang is

$$\phi_{bp}(t,s) = \frac{1+\phi_{bo}(t,s)+\kappa\phi_{do}(t,s,t_{sh})-\phi_{po}(t,s,t_{sh})}{E_o} \qquad \text{(A4.27)}$$

where

$$\kappa = 1+\kappa_1\frac{D_p}{D_p+V/S}$$

$$\kappa_1 = 2.5\frac{\Delta_h}{100}\left(1-\exp\left(\frac{-(t-s)}{10}\right)\right)\left(1-\exp\left(\frac{-T}{5}\right)\right)$$

$D_p \cong \sqrt{6C_1T}$

D_p = Depth of penetration of cyclic humidity (mm)

T = period of humidity cycle (days)

$C_1 \cong 10\,mm^2/day$

and Δ_h = peak to peak amplitude of humidity (%)

The second modification incorporates high strength concretes [72], for which this model is denoted by *'BPh'*. Refined equations only affect the drying creep components and are adjusted as follows

$$\phi'_d = \frac{1}{\sqrt{\left(1+\frac{s-t_{sh}}{a_d\,\tau_{sh}}\right)}}\phi_d \qquad \text{(A4.28)}$$

$$\phi_{do}(t,s,t_{sh}) = \phi'_d\, k'_h\, s^{-m/2}\varepsilon_{\infty sh}\left(1+\frac{b_d\,\tau_{sh}}{t-s}\right)^{-c_d\, n} \qquad \text{(A4.29)}$$

where

$a_d = 10 \quad (f'_c \le 41.37\,\text{MPa}), \qquad a_d = 1 \quad (f'_c \ge 68.95\,\text{MPa})$

$b_d = 10 \quad (f'_c \le 41.37\,\text{MPa}), \qquad b_d = 100 \quad (f'_c \ge 68.95\,\text{MPa})$

and linear interpolation is utilised for values of $\mathbf{f'_c}$ between 41.37 MPa and 68.95 MPa.

A4.1.5.4 Elastic Modulus (model 1)

The corresponding elastic modulus for the BP model can be evaluated by replacing (t-s) = 0.001 days into (A4.26). The drying constituent does not affect the modulus for small loading periods, and basic creep needs to be included. The resulting equation is

$$E_c(s) = \frac{E_o}{1+10^{-3n_T}\,\phi_T\,(s_e^{-m}+\alpha)}\ (\text{MPa}) \qquad \text{(A4.30)}$$

Bazant [64] stated that a value of (t-s) = 0.1 days agrees better with the ACI [37] and CEB-FIP 1978 [38] formulas.

A4.1.5.5 Shrinkage (model 2)

The original Bazant and Panula model [66] has been defined by numerous complicated equations. Bazant and Panula [69,70] proposed a simplified model, which is denoted by *'BPs'*. The shrinkage at time $\mathbf{t_d}$ from onset of drying can be determined by (A4.24), where the parameters in this equation have been simplified to

$$k_h = 1 - 10^{-6} h^3 \qquad \text{for } h \le 98\%$$

$$k_h = -0.2 \qquad \text{for } h = 100\%$$

$$\varepsilon_{\infty sh} = (1330 - 970\,y) \quad (\mu\text{strains})$$

$$y = \frac{1}{390\,z^{-4} + 1}$$

$$z = \left(1.25\sqrt{(a/c)} + 0.5(g/s)^2\right)\sqrt[3]{\frac{1 + s/c}{w/c}}\,0.381\sqrt{f_c'} - 12 \ge 0$$

$$\tau_{sh} = 4\left(k_s\,V/S\right)^2 \frac{1}{C_1(t_{sh})}$$

$$k_s = 1.25 \qquad \text{(a square prism)}$$

$$C_1(t_{sh}) = 2.4 + \frac{120}{\sqrt{t_{sh}}}$$

(sand is defined as the aggregate which will pass through a 4.7 mm sieve)

h = relative humidity (%)

V/S = volume/surface area ratio (mm)

w/c = water/cement ratio

a/c = total aggregate/cement ratio

and g/s = gravel/sand ratio

A4.1.5.6 Creep (model 2) - Double Power Law

The corresponding simplified Bazant and Panula creep function [69,70] is

$$\phi_{bp}(t,s) = \frac{1 + \phi_{bo}(t,s) + \phi_{do}(t,s,t_{sh})}{E_o} \quad (\text{MPa})^{-1} \qquad \text{(A4.31)}$$

where

$$\phi_{bo}(t,s) = \phi_1\left(s^{-m} + 0.05\right)(t-s)^n$$

$$\phi_1 = 0.30 + 152.2\,f_c'^{-1.2}$$

$$m = 0.28 + 47.541\,f_c'^{-2}$$

$$n = 0.115 + 0.61\,f_c'^{3}\,10^{-6}$$

$$\frac{1}{E_o} = (0.0145 + 3.447\,f_c'^{-2})10^{-3} \qquad (\text{MPa}^{-1})$$

$$\phi_{do}(t,s,t_{sh}) = \phi_d'\,k_h'\,s^{-m/2}\left(1 + \frac{3\tau_{sh}}{t-s}\right)^{-0.35}$$

$$\phi_d' = \frac{1}{\sqrt{\left(1 + \dfrac{s - t_d}{10\,t_d}\right)}}\,\phi_d\,\varepsilon_{\infty sh}$$

$$\phi_d = 0.0056 + \frac{0.0189}{1+0.7r^{-1.4}} \qquad \text{for } r > 0$$

$$\phi_d = 0.0056 \qquad \text{for } r \le 0$$

$$r = 0.56\left((s/a)f_c'\right)^{0.3}(g/s)^{1.3}\left(\frac{1610(w/c)}{\varepsilon_{\infty sh}}\right)^{1.5} - 0.85$$

and $k_h' = 1 - 10^{-3}h^{1.5}$

The decrease in creep after drying component $\phi_{po}(t,s,t_{sh})$ is not included.

A4.1.5.7 Elastic Modulus (model 2)

The corresponding elastic modulus derived from the simplified Bazant and Panula creep function (i.e. (A4.31)) at (t-s) = 1 day is employed, and results in

$$E_c(s) = \frac{E_o}{1+\phi_1(s^{-m}+0.05)} \qquad \text{(MPa)} \qquad \text{(A4.32)}$$

A4.1.5.8 Shrinkage Modified (model 1)

Bazant *et al.* [127] further refined the shrinkage expression in the original Bazant and Panula model [66] (i.e. (A4.24)). This modified formula is

$$\varepsilon_{sh}(t_d) = k_h\varepsilon_{\infty sh}\left(1+\left(\frac{\tau_{sh}}{t_d}\right)^r\right)^{\frac{-1}{2r}} \qquad (\mu\text{strains}) \qquad \text{(A4.33)}$$

For **r** = 1, the previous equation results in the original Bazant and Panula formula (i.e. (A4.24)), where **r** is a material constant. The value of **r** for improved predictions of shrinkage range from 0.95 to 0.75 [64]. A statistical study of shrinkage [127] has concluded that a value of **r** = 0.75 improved predictions.

A4.1.5.9 Creep - Double Power Logarithmic Law

The prediction of short-term creep is good when employing the double power law, but experimental data for long-term creep do not agree [75]. Bazant and Chern [73-75] pointed out that the error is not due to randomness of concrete, but is systematic. To compensate for this systematic error, Bazant and Chern [73] proposed the following modification to the basic creep constituent in the BP model

$$\left.\begin{aligned} \phi_{bo}(t,s) &= \phi_1(s^{-m}+\alpha)(t-s)^n && \text{for } (t-s) \le \Theta_L \\ \phi_{bo}(t,s) &= \phi_L + n\phi_L \ln\left(\frac{t-s}{\Theta_L}\right) && \text{for } (t-s) > \Theta_L \end{aligned}\right\} \quad \text{(A4.34)}$$

where

$$\Theta_L = \sqrt[n]{\left(\frac{\phi_L}{\phi_1(s^{-m}+\alpha)}\right)}$$

and $$\phi_L = \frac{\phi_1}{1.53+0.008702\,f_c'}$$

This model is designated by *'BPdpll'*.

A4.1.5.10 Creep - Triple Power Law

The triple power law proposed by Bazant and Chern [75] improves long-term predictions of creep. The basic creep component defined by Bazant and Chern is

$$\phi_{bo}(t,s) = \phi_T(s_e^{-m}+\alpha)\left[(t-s)^{n_T} - B(t,s;n_T)\right] \quad \text{(A4.35)}$$

where

$$B(t,s;n) = n\int_{\zeta=0}^{\zeta=t-s}\left(1-\left(\frac{s}{s+\zeta}\right)^n\right)\zeta^{n-1}d\zeta = \text{binomial integral}$$

and $$\zeta = (t-s) \text{ days}$$

This model is denoted by *'BPtpl'*. Determining the binomial integral is only possible by approximate numerical procedures, for which four routines are outlined in [75]. One of these methods is the power series approach, and this is used here. The binomial integral can then be obtained from

$$B(t,s;n) = n s^n\left(\frac{\beta^{-n}-1}{n} + \ln\beta + \sum_{k=1}^{\infty}\left[\binom{n-1}{k}(-1)^k\left(\frac{\beta^{k-n}-1}{n-k} - \frac{1-\beta^k}{k}\right)\right]\right) \quad \text{(A4.36)}$$

where

$$\binom{n-1}{k} = \frac{(n-1)(n-2).....(n-k)}{k!}$$

A4.1.5.11 Shrinkage - (model 3)

Bazant *et al.* [78] recently proposed an amended formula for shrinkage prediction, which is theoretically better than has been previously used [128]. The shrinkage at time t_d from onset of drying is

$$\varepsilon_{sh}(t_d) = k_h \varepsilon_{\infty sh} \tanh\left(\sqrt{\frac{t_d}{\tau_{sh}}}\right) \qquad \text{(A4.37)}$$

where

$$t_d = \int_{t_{sh}}^{t} k'_T(t')\,dt'$$

$$k'_T = \exp\left(\frac{5000}{T_o} - \frac{5000}{T}\right)$$

$$k_h = 1 - 10^{-6} h^3 \qquad \text{for } h \le 98\%$$

$$k_h = -0.2 \qquad \text{for } h = 100\%$$

$$\varepsilon_{\infty sh} = \frac{\varepsilon_{\infty s}}{G\left(17 + \frac{\tau_{sh}}{40}\right) G(12 + t_{sh})}$$

$$\varepsilon_{\infty s} = \alpha_2 \alpha_3 \left(20.10 (w/c)^{1.5} c^{1.1} f_c'^{-0.2} \left(1 - \frac{a/c}{1 + w/c + a/c}\right) \alpha_4 + 160\right) \quad (\mu\text{strains})$$

$\alpha_2 = 1.0$ for type 'A' cement

$\alpha_2 = 1.1$ for type 'C' cement

$\alpha_3 = 1.0$ for specimens cured in water or 100% relative humidity

$$\alpha_4 = 0.7 + \frac{0.3}{(a/s - 1.6)^3} \qquad \text{for } a/s > 2.6$$

$\alpha_4 = 1.0$ otherwise

$$G(x) = \sqrt{\frac{x}{4 + 0.9x}}$$

$$\tau_{sh} = \frac{0.32 (2 k_s V/S)^2}{C_1(t_{sh})}$$

$k_s = 1.25$ (a square prism)

$$C_1(t_{sh}) = 10\left(0.6 + \sqrt{\frac{4.5}{t_{sh}}}\right) \le 18$$

h = relative humidity (%)

$T_o = 296.16$ K = reference temperature (Kelvin)

T = temperature of specimen (Kelvin)

V / S = volume/surface area ratio (mm)

w / c = water/cement ratio

a / c = total aggregate/cement ratio

and $a/s =$ total aggregate/sand ratio

A4.1.5.12 Creep (model 1) - Solidification Theory

The latest proposal by Bazant *et al.* [78-83] includes a new creep model derived from solidification theory. This model is superior to previous formulas, with improved test data agreement. The proposed creep function is

$$\phi_{bp}(t,s) = q_1 + \left[\phi_{bo}(t,s) + \phi_{do}(t,s,t_{sh}) + \phi_{po}(t,s,t_{sh})\right] F(\sigma) \qquad \text{(A4.38)}$$

where

$$\phi_{bo}(t,s) = q_2\, Q(t_T, s_e) + q_3 \ln(1 + (t_T - s_e)^{0.1}) + q_4 \ln\left(\frac{t_T}{s_e}\right)$$

$$q_1 = \frac{10^6}{7099.6\sqrt{f_c'}} \qquad 10^{-6}\ \text{MPa}^{-1}$$

$$q_2 = \frac{0.065333\,(w/c)^{0.8}\, c^{1.5}\, (s/g)^{0.02}}{\sqrt{f_c'}\left(1 - \dfrac{a/c}{1 + w/c + a/c}\right)^{0.9}} - 56.563 \qquad 10^{-6}\ \text{MPa}^{-1}$$

$$q_3 = \alpha q_2 \qquad 10^{-6}\ \text{MPa}^{-1}$$

$$q_4 = 2.4668\,(w/c)^{2.3}\, c^{0.2}\left(1 - \frac{a/c}{1 + w/c + a/c}\right)^{0.39} f_c'^{0.46}\, (s/g)^{-0.73}$$

$$10^{-6}\ \text{MPa}^{-1}$$

$$s_e = \int_0^s \beta_T(t')\,dt'$$

$$t_T = s_e + \int_s^t \beta_T'(t')\,dt'$$

$$\beta_T = \exp\left(\frac{4000}{T_o} - \frac{4000}{T}\right)$$

$$\beta_T' = \exp\left((1 + 0.2\ln(1 + t - s))\left(\frac{U_o}{R}\right)\left(\frac{1}{T_o} - \frac{1}{T}\right)\right)$$

$$\frac{U_o}{R} = \frac{38967.2\, f_c'^{0.7}}{c^{0.8}\,(w/c)^{0.7}}$$

In equations defining q_2 & q_4 then $s/c \geq 1$ and $g/c \geq 1$

$$F(\sigma) = \frac{1 + 3\sqrt{\Omega}}{1 - \Omega}$$

$$\Omega = \left(\frac{\sigma}{f_c'}\right)^{10}$$

$$F(\sigma) \equiv 1 \qquad \text{for } \sigma < 0.5 f_c'$$

$$\alpha = 1.873\times10^{-5}\,c + 0.0125 \qquad \text{for } c \geq 416\,kg/m^3$$

$$\alpha = 6.242\times10^{-5}\,c - 0.005 \qquad \text{for } 240\,kg/m^3 \leq c \leq 416\,kg/m^3$$

$$\alpha = 0.01 \qquad \text{for } c \leq 240\,kg/m^3$$

$$Q(t_T, s_e) = Q_f(s_e)\left(1+\left(\frac{Q_f(s_e)}{Z(t_T, s_e)}\right)^r\right)^{-1/r}$$

$$Z(t_T, s_e) = \frac{\ln\left(1+(t_T - s_e)^{0.1}\right)}{\sqrt{s_e}}$$

$$Q_f(s_e) = \frac{1}{0.086\,s_e^{\,2/9} + 1.21\,s_e^{\,4/9}}$$

$$r = 1.7\,s_e^{\,0.12} + 8$$

$$\phi_{do}(t, s, t_{sh}) = q_5\,k_h'\,\frac{\varepsilon_{\infty sh}}{10^3}\sqrt{\tanh\left(\sqrt{\frac{t_e - t_{she}}{\tau_m}}\right) - \tanh\left(\sqrt{\frac{s_{Te} - t_{she}}{\tau_m}}\right)}$$

$$q_5 = \frac{481.72}{\sqrt{f_c'}} \quad 10^{-6}\,MPa^{-1}$$

$$k_h' = 1 - 10^{-6}\,h^3$$

$$\tau_m = \frac{2\tau_{sh}\left(1+\dfrac{3.5}{\sqrt{t_{she}}}\right)}{\left(1+\dfrac{5}{\sqrt{s_e + t_{she}}}\right)}$$

$$\phi_{po}(t, s, t_{sh}) = 0.7\,k_h''\,\phi_{bo}(t, s)\left(\frac{1}{G(7+t_{she})} - \sqrt{0.9}\right)$$

$$\times\left(\tanh\left(\sqrt{\frac{s_{Te} - t_{she}}{0.5\tau_m}}\right) - \tanh\left(\sqrt{\frac{s_{Te} - t_{she}}{5\tau_m}}\right)\right)$$

$$k_h'' = 1 - 10^{-4}\,h^2$$

$$s_{Te} = t_{sh} + \int_{t_{sh}}^{s} k_T'(t')\,dt'$$

$$t_{she} = \int_0^{t_{sh}} \beta_T(t')\,dt'$$

$$t_e = t_{she} + \int_{t_{sh}}^{t} k_T'(t')\,dt'$$

$q_1 + \phi_{bo}(t, s)\,F(\sigma)$ = elastic and basic creep components

$\phi_{do}(t, s, t_{sh})\,F(\sigma)$ = addition creep due to drying

$\phi_{po}(t, s, t_{sh})\,F(\sigma)$ = further creep increase due to pre-drying

$F(\sigma)$ = inclusion of non-linear dependence on stress

g/c = gravel to cement ratio

s/c = sand to cement ratio

σ = applied stress (MPa)

and f_c' = concrete strength (MPa)

The *'BPX'* notation denotes time-dependent behaviour according to (A4.37) and (A4.38).

A4.1.5.13 Elastic Modulus (model 3)

The corresponding elastic modulus for the creep function defined by (A4.38) is evaluated by replacing (t-s) = 0.001 days into this equation. The resulting equation is

$$E_c(s) = \left(q_1 + q_2 Q_f(s_e) \left(1 + \left(\frac{Q_f(s_e)\sqrt{s_e}}{\ln(1.5012)} \right)^r \right)^{-1/r} + q_3 \ln\left(1 + \left(\exp\left(0.001 \left(\frac{U_o}{R} \right) \left(\frac{1}{T_o} - \frac{1}{T} \right) \right) \right)^{0.1} \right) \right)^{-1} \quad \text{(MPa)} \tag{A4.39}$$

A4.1.5.14 Shrinkage (model 4)

A simplified model for predicting shrinkage was proposed by Bazant *et al.* [83]. The shrinkage at time t_d from onset of drying is given by (A4.37), where the parameters in this equation have been simplified to

$$k_h = 1 - 10^{-6} h^3 \qquad \text{for } h \le 98\%$$

$$k_h = -0.2 \qquad \text{for } h = 100\%$$

$$\varepsilon_{\infty sh} = \alpha_1 \alpha_2 \left(19.58 (w/c)^{1.5} c^{1.1} f_c'^{-0.2} \left(1 - \frac{a/c}{1 + w/c + a/c} \right) + 160 \right) \quad \text{(μstrains)}$$

$\alpha_1 = 1.0$ for type 'A' cement

$\alpha_1 = 1.1$ for type 'C' cement

$\alpha_2 = 1.0$ for specimens cured in water or 100% relative humidity

$\tau_{sh} = 0.1563 (V/S)^2$ for a long square prism

V/S = volume/surface area ratio (mm)

h = relative humidity (%)

w/c = water/cement ratio

and a/c = total aggregate/cement ratio

A4.1.5.15 Creep (model 2) - Solidification Theory

The corresponding simplified creep function [83] for the latest creep model [79-82] is given by

$$\phi_{bp}(t,s) = q_1 + \phi_{bo}(t,s) + \phi_{do}(t,s,t_{sh}) \qquad \text{(A4.40)}$$

where

$$\phi_{bo}(t,s) = q_2\, Q(t,s) + q_3 \ln(1+(t-s)^{0.1}) + q_4 \ln\left(\frac{t}{s}\right)$$

$$q_1 = \frac{10^6}{7099.6\sqrt{f_c'}} \qquad 10^{-6}\,\text{MPa}^{-1}$$

$$q_2 = \frac{0.065333(w/c)^{0.8}\, c^{1.5}}{\sqrt{f_c'}\left(1-\frac{a/c}{1+w/c+a/c}\right)^{0.9}} - 56.563 \qquad 10^{-6}\,\text{MPa}^{-1}$$

$$q_3 = 0.025 q_2 \quad 10^{-6}\,\text{MPa}^{-1}$$

$$q_4 = 2.4668(w/c)^{2.3}\, c^{0.2}\left(1-\frac{a/c}{1+w/c+a/c}\right)^{0.39} f_c'^{0.46} \qquad 10^{-6}\,\text{MPa}^{-1}$$

$$Q(t,s) = Q_f(s)\left(1+\left(\frac{Q_f(s)}{Z(t,s)}\right)^r\right)^{-1/r}$$

$$Z(t,s) = \frac{\ln\left(1+(t-s)^{0.1}\right)}{\sqrt{s}}$$

$$Q_f(s) = \frac{1}{0.086 s^{2/9} + 1.21 s^{4/9}}$$

$$r = 1.7 s^{0.12} + 8$$

$$\phi_{do}(t,s,t_{sh}) = q_5\, k_h' \frac{\varepsilon_{\infty sh}}{10^3}\sqrt{\tanh\left(\sqrt{\frac{t-t_{sh}}{2\tau_{sh}}}\right) - \tanh\left(\sqrt{\frac{s-t_{sh}}{2\tau_{sh}}}\right)}$$

$$q_5 = \frac{481.72}{\sqrt{f_c'}} \quad 10^{-6}\,\text{MPa}^{-1}$$

and $\quad k_h' = 1 - 10^{-6} h^3$

This model is designated by *'BPXs'*, and incorporates the corresponding simplified shrinkage model.

A4.1.5.16 Elastic Modulus (model 4)

The simplified elastic modulus from (A4.40), is determined by substituting (t–s)=0.001 days into this formula, and results in

$$E_c(s) = \left(q_1 + q_2 Q_f(s) \left(1 + \left(\frac{Q_f(s)\sqrt{s}}{\ln(1.5012)} \right)^r \right) \right)^{-1/r} \qquad \text{(A4.41)}$$
$$+ q_3 \ln(1 + 0.001^{0.1}) \Big)^{-1} \qquad \text{(MPa)}$$

A4.1.5.17 Shrinkage - (model 5)

In 1995, Bazant and Baweja [84-86] proposed an amended formula for shrinkage prediction, which is experimentally better than has been previously used. The shrinkage at time $\mathbf{t_d}$ from onset of drying is

$$\varepsilon_{sh}(t_d) = k_h \varepsilon_{sh\infty} \tanh\left(\sqrt{\frac{t_d}{\tau_{sh}}} \right) \qquad \text{(A4.42)}$$

where

$t_d = t - t_{sh}$

$k_h = 1 - 10^{-6} h^3 \qquad$ for $h \le 98\%$

$k_h = -0.2 \qquad$ for $h = 100\%$

$$\varepsilon_{sh\infty} = 1.08047 \varepsilon_{s\infty} \sqrt{\frac{4 + 0.85(t_{sh} + \tau_{sh})}{t_{sh} + \tau_{sh}}}$$

$$\varepsilon_{s\infty} = \alpha_1 \alpha_2 \left(0.01903 \frac{((w/c)c)^{2.1}}{(f_c')^{0.28}} + 270 \right) \qquad (\mu\text{strains})$$

$\alpha_1 = 1.0$ for type 'A' cement

$\alpha_1 = 1.1$ for type 'C' cement

$\alpha_2 = 1.0$ for specimens cured in water or 100% relative humidity

$\tau_{sh} = 0.00620 k_t (k_s V/S)^2$

$k_s = 1.25 \qquad$ (a square prism)

$$k_t = \frac{54.981 t_{sh}^{-0.08}}{f_c'^{0.25}}$$

h = relative humidity (%)

V/S = volume/surface area ratio (mm)

w/c = water/cement ratio, where $0.3 \le w/c \le 0.85$

f_c' = 28-day concrete compressive strength (MPa), where $17 \le f_c' \le 69$

and c = cement content (kg/m^3), where $160 \le c \le 721$

A4.1.5.18 Creep (model 3) - Solidification Theory B3

The latest proposal by Bazant and Baweja [84-86] includes a creep model derived from solidification theory. This model is superior to previous formulas, with improved test data agreement. The proposed creep function is

$$\phi_{bp}(t,s) = q_1 + \phi_{bo}(t,s) + \phi_{do}(t,s,t_{sh}) \qquad \text{(A4.43)}$$

where

$$\phi_{bo}(t,s) = q_2\, Q(t,s) + q_3 \ln(1+(t-s)^{0.1}) + q_4 \ln\left(\frac{t}{s}\right)$$

$$q_1 = \frac{126.8}{\sqrt{f'_c}} \quad 10^{-6}\,\text{MPa}^{-1}$$

$$q_2 = \frac{185.33\sqrt{c}}{f_c'^{0.9}} \quad 10^{-6}\,\text{MPa}^{-1}$$

$$q_3 = 0.29(w/c)^4\, q_2 \quad 10^{-6}\,\text{MPa}^{-1}$$

$$q_4 = \frac{20.305}{(a/c)^{0.7}} \quad 10^{-6}\,\text{MPa}^{-1}$$

$$Q(t,s) = Q_f(s)\left(1+\left(\frac{Q_f(s)}{Z(t,s)}\right)^{r(s)}\right)^{-1/r(s)}$$

$$Z(t,s) = \frac{\ln\left(1+(t-s)^{0.1}\right)}{\sqrt{s}}$$

$$Q_f(s) = \frac{1}{0.086 s^{2/9} + 1.21 s^{4/9}}$$

$$r(s) = 1.7 s^{0.12} + 8$$

$$\phi_{do}(t,s,t_{sh}) = q_5 \sqrt{\left\{\exp\left(\frac{-8}{100}\left[100-(100-h)\tanh\left\{\sqrt{\frac{t-t_{sh}}{\tau_{sh}}}\right\}\right]\right) - \exp\left(\frac{-8}{100}\left[100-(100-h)\tanh\left\{\sqrt{\frac{s-t_{sh}}{\tau_{sh}}}\right\}\right]\right)\right\}}$$

$$q_5 = \frac{7.57\times10^5}{f'_c \varepsilon_{sh\infty}^{0.6}} \quad 10^{-6}\,\text{MPa}^{-1}$$

$q_1 + \phi_{bo}(t,s)$ = elastic and basic creep components

$\phi_{do}(t,s,t_{sh})$ = addition creep due to drying

and a/c = total aggregate/cement ratio, where $2.5 \le a/c \le 13.5$

The *'B3'* notation denotes time-dependent behaviour according to (A4.42) and (A4.43).

A4.1.5.19 Elastic Modulus (model 5)

The corresponding elastic modulus for the creep function defined by (A4.43) is evaluated by replacing (t-s) = 0.001 days into this equation. The resulting equation is

$$E_c(s) = \left(q_1 + q_2 Q_f(s) \left(1 + \left(\frac{Q_f(s)\sqrt{s}}{\ln(1.5012)} \right)^{r(s)} \right)^{-1/r(s)} + q_3 \ln(1.5012) \right)^{-1} \quad \text{(MPa)} \tag{A4.44}$$

CHAPTER 5

CHAPTER 5

CONCRETE CONSTITUTIVE MODELS AND REINFORCED CONCRETE COLUMN MODELS

In this chapter four distinct constitutive models for concrete incorporating time-dependent behaviour are outlined. The four models are Fabers Effective Modulus Method [6], Trost-Bazant Age-Adjusted Effective Modulus Method [7], Rate of Creep Method [8] and Improved Rate of Creep Method [9]. Each constitutive model is used to derive load-deflection models for reinforced column behaviour, otherwise described as analytical column models. The column models rely on the principle of superposition permitting finite numbers of discretely applied loads, representing a monotonically increasing load history, to be analysed.

5.1 SUMMARY OF CONCRETE CONSTITUTIVE MODELS

The concrete constitutive models outlined here describe the time-dependent behaviour of the elastic, creep and shrinkage deformations and form the basis of the reinforced concrete column load-deflection equations derived later in this chapter. Four constitutive models are examined in this thesis, namely Fabers Effective Modulus Method (FEMM) [6], Trost-Bazant Age-Adjusted Effective Modulus Method (TBEMM) [7], Rate of Creep Method (RCM) [8] and Improved Rate of Creep Method (IRCM) [9]. Each constitutive model has been derived from different assumed deformation mechanisms resulting from experimental observations. Their applicability to the description of time-dependent axial shortening of reinforced concrete columns has yet to be established and some attempt to review each model is made. A brief summary is to follow with a more detailed discussion being presented in Appendix A5.1.

Each constitutive model is distinguished by unique characteristics. Firstly, the Rate of Creep Method [8] and Improved Rate of Creep Method [9] assume that all creep-time curves are parallel and shrinkage develops at the same rate as creep. Fabers Effective Modulus Method [6] employs a reduced elastic modulus in the formation of the equations, for which the aging of the concrete is neglected, and the Trost-Bazant Age-Adjusted Effective Modulus Method [7] improves the

predictions of the latter by incorporating aging. Each of the above models are well established in the literature.

In any axial shortening analysis of a tall building, reinforced concrete column elements experience changing loads applied from the above storeys during and after construction. The time-dependent shortening of columns, and the stresses within the concrete and steel are required for both the short and long-term periods. With these requirements in mind and with reference to the constitutive models reviewed in Appendix A5.1, the TBEMM would seem to be better suited from a theoretical point of view. At this stage none of the four models are rejected, as the models have as yet to be critically assessed in terms of axial shortening. This assessment is made in Chapter 8.

5.2 REINFORCED CONCRETE COLUMN MODELS

Equations for predicting the time-dependent shortening of reinforced concrete columns based on TBEMM are derived below, whilst the analytical models based on FEMM, RCM and IRCM respectively are given in Appendix A5.2. Similar analytical models have been determined by Beasley [12], Gilbert [14] and Samra [43], although the derivations below are originated here.

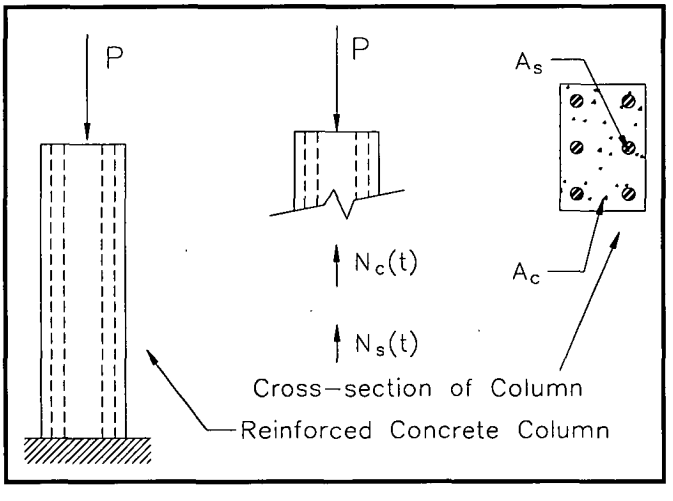

Figure 5.1 - Short symmetrically reinforced concrete column with applied load **P**.

In the formulations to follow, assumed conditions of equilibrium, compatibility and the behaviour law of the materials must be satisfied. A constant load **P** is applied to a short symmetrically reinforced concrete column at time s, refer to Figure 5.1. The load **P** must be resisted by internal forces for equilibrium, or

$$P = N_c(t) + N_s(t) \tag{5.1}$$

where

$N_c(t)$ = internal force in concrete

and $N_s(t)$ = internal force in steel

Assuming perfect bond between the reinforcement and concrete, thus total column strain compatibility between the two elements gives

$$\varepsilon(t,s) = \varepsilon_{st}(t) \tag{5.2}$$

where

$\varepsilon(t,s)$ = total column strain

and $\varepsilon_{st}(t)$ = steel strain

The steel is linear elastic and given as

$$\varepsilon_{st}(t) = \frac{\sigma_s(t)}{E_s} \tag{5.3}$$

where

E_s = elastic modulus of steel

and $\sigma_s(t)$ = stress in the steel

From the fundamental definition of stress, the internal forces which resist **P** are

$$N_c(t) = \sigma(t) A_c \tag{5.4}$$

and

$$N_s(t) = \sigma_s(t) A_s \tag{5.5}$$

where

A_c = cross-sectional area of concrete

A_s = cross-sectional area of steel

and $\sigma(t)$ = stress in the concrete

From the TBEMM, the concrete stress at time **t** can be written

$$\sigma(t) = \sigma_o + \Delta\sigma(t) \tag{5.6}$$

Here, $\Delta\sigma(t)$ is negative due to relaxation of concrete. On substituting (5.4), (5.5) and (5.6) into (5.1) and rearranging, the steel stress is given

$$\sigma_s(t) = \frac{1}{A_s}(P - (\sigma_o + \Delta\sigma(t))A_c) \tag{5.7}$$

Substituting (5.2), (5.3) and (5.7) into the TBEMM (i.e. (A5.8)), then

$$\Delta\sigma(t) = \frac{1}{1 + p_a n_e'}\left(\frac{P}{A_c} - \sigma_o(1 + p_a n_e) - \varepsilon_{sh}(t)\, p_a E_s\right) \tag{5.8}$$

where

n = modular ratio

n_e = effective modular ratio

n_e' = age-adjusted effective modular ratio

$$n = \frac{E_s}{E_c(s)}$$

$$n_e = \frac{E_s}{E_e(t,s)}$$

$$n_e' = \frac{E_s}{E_e'(t,s)}$$

and $$p_a = \frac{A_s}{A_c}$$

The initial stress σ_o is determined from a simple elastic analysis of the column, as given in Appendix A5.3. From this analysis, the value is obtained as

$$\sigma_o = \frac{P}{A_c(1 + p_a n)} \tag{5.9}$$

On substituting (5.8) and (5.9) into (A5.8), the final formula for the total column strain is

$$\begin{aligned}\varepsilon(t,s) = {} & \frac{P}{A_c E_e(t,s)(1 + p_a n)} + \frac{P}{A_c E_e'(t,s)(1 + p_a n_e')} \\ & - \frac{P(1 + p_a n_e)}{A_c E_e'(t,s)(1 + p_a n)(1 + p_a n_e')} - \varepsilon_{sh}(t)\frac{p_a n_e'}{(1 + p_a n_e')} + \varepsilon_{sh}(t)\end{aligned} \tag{5.10}$$

In the above, the first three terms represent the combined elastic and creep strain. The last term is the free shrinkage component, whilst the other term defines the reinforcement stiffening effect.

Applying the principle of superposition, where **P** becomes the incremental load $\mathbf{P}_i$ applied at time s_i, (5.10) can be rewritten

$$\begin{aligned}\varepsilon(t,s_i) = &\frac{P_i}{A_c E_e(t,s_i)(1+p_a n_i)} + \frac{P_i}{A_c E'_e(t,s_i)(1+p_a n'_{ei})} \\ &- \frac{P_i(1+p_a n_{ei})}{A_c E'_e(t,s_i)(1+p_a n_i)(1+p_a n'_{ei})} \\ &- \varepsilon_{sh}(t_d)\frac{p_a n'_{eo}}{(1+p_a n'_{eo})} + \varepsilon_{sh}(t_d)\end{aligned} \tag{5.11}$$

where

$$n_i = \frac{E_s}{E_c(s_i)}$$

$$n_{ei} = \frac{E_s}{E_e(t,s_i)}$$

$$n'_{ei} = \frac{E_s}{E'_e(t,s_i)}$$

$$n_{eo} = \frac{E_s}{E_e(t,t_{sh})}$$

$$n'_{eo} = \frac{E_s}{E'_e(t,t_{sh})}$$

t_d = drying period (days)

and t_{sh} = age at onset of drying (days)

The fourth term in (5.11) employs the elastic modulus at the onset of drying. Taking **k** incrementally applied loadings to a column of length **L**, and separating the elastic, creep, free shrinkage and reinforcement stiffening components, the final deformations are respectively

$$\delta_{elastic} = \sum_{i=1}^{k}\left(\frac{P_i L}{A_c E_c(s_i)(1+p_a n_i)}\right) \tag{5.12}$$

$$\begin{aligned}\delta_{creep} = &-\delta_{elastic} + \sum_{i=1}^{k}\left(\frac{P_i L}{A_c E_e(t,s_i)(1+p_a n_i)}\right) \\ &+ \sum_{i=1}^{k}\left(\frac{P_i L p_a (n_i - n_{ei})}{A_c E'_e(t,s_i)(1+p_a n_i)(1+p_a n'_{ei})}\right)\end{aligned} \tag{5.13}$$

$$\delta_{shrinkage} = \varepsilon_{sh}(t_d)L \tag{5.14}$$

$$\delta_{reinforcement} = -\varepsilon_{sh}(t_d)L\frac{p_a n'_{eo}}{1+p_a n'_{eo}} \tag{5.15}$$

The final absolute column shortening for a column in the **j**th storey is as follows

$$\delta_{total\ for\ j^{th}\ storey} = \delta_{elastic} + \delta_{creep} + \delta_{shrinkage} + \delta_{reinforcement} \tag{5.16}$$

The final cumulative shortening of a column in the **j**th storey is

$$\delta_{cum} = \sum_{i=1}^{j} \delta_{total\ for\ i^{th}\ storey} \tag{5.17}$$

The equations for determining the stresses in the reinforcement and concrete are now derived. Substituting (5.8) and (5.9) into (5.6), the total concrete stress due to load **P** applied at time **s** follows

$$\sigma(t) = \frac{P(p_a(n-n_e+n'_e)+1)}{A_c(1+p_a n)(1+p_a n'_e)} \tag{5.18}$$

Utilising the principle of superposition for **k** loadings, where $\mathbf{P_i}$ is applied at $\mathbf{s_i}$ to the column, the resulting concrete stresses are

$$\sigma(t)_{ec} = \sum_{i=1}^{k}\left(\frac{P_i(p_a(n_i-n_{ei}+n'_{ei})+1)}{A_c(1+p_a n_i)(1+p_a n'_{ei})}\right) \tag{5.19}$$

and

$$\sigma(t)_{sr} = \frac{-\varepsilon_{sh}(t_d)p_a E_s}{(1+p_a n'_{eo})} \tag{5.20}$$

where

$\sigma(t)_{ec}$ = total concrete stress due to elastic and creep deformations

and $\sigma(t)_{sr}$ = total concrete stress due to shrinkage

From equilibrium, the total stress in the reinforcement is

$$\sigma_s(t) = \frac{P_{total} - A_c(\sigma(t)_{ec} + \sigma(t)_{sr})}{A_s} \tag{5.21}$$

where

P_{total} = total load applied to column

and $P_{total} = \sum_{i=1}^{k} P_i$

Equations (5.12) to (5.17), and (5.19) to (5.21) inclusive represent now the complete formulation for the analysis of a reinforced concrete column based on the TBEMM.

5.3 CONCLUDING REMARKS TO CHAPTER

Four load-deflection models for time-dependent reinforced concrete column behaviour based on the constitutive models of FEMM, TBEMM, RCM and IRCM have been derived. These analytical models can accommodate a highly discretised monotonically increasing load history, such as those applied during and after the construction of a tall building. Derivation of the deterministic column models represent the first stage in developing a rational probabilistic description for axial shortening of tall concrete buildings. Probabilistic models which incorporate the randomness associated with concrete properties are developed in Chapter 6. Concrete elastic, creep and shrinkage behaviour, as required for any column model, were examined in Chapter 4.

APPENDIX

TO

CHAPTER 5

APPENDIX A5.1

A5.1.1 FABERS EFFECTIVE MODULUS METHOD (FEMM)

This method was first employed by Faber [6]. Of the four constitutive models, this is the simplest. On substituting the creep coefficient from (3.2) into (3.1), the following equation is determined

$$\varepsilon(t,s) = \frac{\sigma_o}{E_c(s)}(1+\phi(t,s)) + \varepsilon_{sh}(t) \qquad \text{(A5.1)}$$

where

σ_o = initial stress applied

and (A5.1) defines the simplest time-dependent strain which accounts for both creep and shrinkage.

The notion of *'effective'* modulus is brought into modifying (A5.1) in order that algebraic simplifications result. If the effective modulus is defined as

$$E_e(t,s) = \frac{E_c(s)}{1+\phi(t,s)} \quad \text{or} \quad \left[J(t,s) = \frac{1}{E_e(t,s)} \right] \qquad \text{(A5.2)}$$

then (A5.1) can be rewritten to include the effective modulus, or its inverse (the definition of creep function see (3.4)). The modified equation becomes

$$\varepsilon(t,s) = \frac{\sigma_o}{E_e(t,s)} + \varepsilon_{sh}(t) \qquad \text{(A5.3)}$$

or

$$\varepsilon(t,s) = \sigma_o J(t,s) + \varepsilon_{sh}(t) \qquad \text{(A5.4)}$$

Both definitions are applicable to column behaviour analysis. Creep is treated as delayed elastic strain in (A5.3), and thus the analysis is elastic with a reduced modulus (i.e. $\mathbf{E_e\,(t,s)}$).

Firstly, the term *"aging of concrete for creep"* needs defining. The model proposed by Faber for creep is dependent on the stress condition at time **t** in

(A5.1), and independent of the previous stress history. Consider two loading cases, the first case is a constant applied stress, whilst the other is a gradually applied stress of the same magnitude. Both cases are applied at time **s** to a concrete specimen, with the entire magnitude of the latter case being reached prior to time **t**. Then, the ratio of creep strains for the latter case to the previous at time **t** is equal to a factor known as the aging coefficient.

Aging of concrete for creep is not taken into account with FEMM, and is important in young concretes but negligible in mature concretes. It follows that good results can be obtained for concretes loaded at relatively older ages [14]. For young concretes with rapidly changing loads, this method might not be accurate enough. FEMM is a special case of the Trost-Bazant Age-Adjusted Effective Modulus Method [7], a more refined model. FEMM overestimates and underestimates creep strains for increasing and decreasing load histories respectively. Equation (A5.1) predicts complete creep recovery upon the removal of loads, which does not agree with experimental data [65]. If the stress in concrete is held constant, then FEMM is exact (if aging is neglected), but this rarely occurs in reinforced concrete structures [14].

A5.1.2 TROST-BAZANT AGE-ADJUSTED EFFECTIVE MODULUS METHOD (TBEMM)

This method was first introduced by Trost [129] and later refined by Bazant [7]. TBEMM is held to be a superior model to FEMM from a theoretical point of view since the aging of creep is included. In order to bring the aging of creep into the formulation, firstly let the initial stress σ_0 be applied to a concrete specimen at time **s**. This subsequently reduces to $\sigma(t)$ at time **t** (refer to Figure 3.2). The change in stress is defined by

$$\Delta\sigma(t) = \sigma_0 - \sigma(t) \tag{A5.5}$$

This change may be due to relaxation, change in applied loads, etc, which is generally unknown at the start of any creep analysis. Bazant [7] showed that the total concrete strain at time **t** can be expressed as

$$\varepsilon(t,s) = \frac{\sigma_o}{E_c(s)}(1+\phi(t,s)) + \frac{\Delta\sigma(t)}{E_c(s)}(1+\chi(t,s)\phi(t,s)) + \varepsilon_{sh}(t) \tag{A5.6}$$

Let the *'age-adjusted effective'* modulus be defined by

$$E'_e(t,s) = \frac{E_c(s)}{1+\chi(t,s)\phi(t,s)} \tag{A5.7}$$

where

$E'_e(t,s)$ = age-adjusted effective modulus

and $\chi(t,s)$ = aging coefficient

Substituting (A5.7) and the effective modulus definition (i.e. (A5.2)) into (A5.6) simplifies the latter expression to

$$\varepsilon(t,s) = \frac{\sigma_o}{E_e(t,s)} + \frac{\Delta\sigma(t)}{E'_e(t,s)} + \varepsilon_{sh}(t) \tag{A5.8}$$

This equation represents an elastic analysis, as was for the case of FEMM, except the creep coefficient is refined by the aging coefficient in the reduced elastic modulus.

The aging coefficient is generally taken to be between 0.5 to 1.0, with an average value of between 0.80 to 0.85. If the stress varied linearly between **s** and **t**, then the aging coefficient is equal to 0.5. A linear stress variation is a good assumption for very small time intervals, as has been suggested by Neville *et al.* [61]. This results in a lower limit for $\chi(t,s)$ which is 0.5. The upper limit of $\chi(t,s)$ is 1.0, and this corresponds to FEMM. Bazant [64] stated that *'TBEMM is theoretically exact for the cases in which the strains vary proportionally with the creep coefficient'*. The aging coefficient for this case must be obtained from the creep coefficient used. Determining the aging coefficient requires the following definition found in Bazant [7]

$$\chi(t,s) = \frac{E_c(s)}{E_c(s) - R(t,s)} - \frac{1}{\phi(t,s)} \tag{A5.9}$$

where the relaxation function is evaluated according to Chapter 3. The aging coefficient is determined utilising the step by step numerical procedure given in Appendix A3.1 and is referred to as the exact value here. If the approximate relaxation function of Bazant and Kim [122] is employed, the resulting aging coefficient is denoted as the approximate value.

For creep coefficients defined by continuous mathematical functions, the aging coefficient is equal to 0.5 at the instant of loading, as discussed above. The creep coefficient from the CEB-FIP 1978 code [38] is discontinuous, and this results in the initial value of unity for the aging coefficient. This discontinuity is due to the instantaneous irreversible creep component in the CEB-FIP model.

Determining the relaxation function from the actual creep coefficient using the step by step numerical procedure has led to values which are negative, for certain conditions [61]. As concrete is in compression, negative results (i.e. tensile stresses) should not be present due to relaxation, and thus **R(t,s)** must be positive.

Bastgen [130] has found that the aging coefficient based on the CEB-FIP 1978 code [38] is in best agreement with experimental results. Also, values of the relaxation function resulting from this code are always positive. From these comments, it has been suggested by Neville *et al.* [61] that the aging coefficient should be calculated from the CEB-FIP 1978 code. However, Bazant [64] comments that Bastgen's experiments were limited to short time durations, and may be inconclusive.

An empirical equation for evaluating the aging coefficient based on the CEB-FIP 1978 code is given by [14] for **s** = 2 to 100 days as follows

$$\chi(t,s) = 1 - \frac{(1-\chi^*)(t-s)}{20+(t-s)} \qquad \text{(A5.10)}$$

where

$$\chi^* = \frac{k_1 s}{k_2 + s}$$

$$k_1 = 0.78 + 0.4 e^{-1.33\phi(\infty,s)}$$

$$k_2 = 0.16 + 0.8 e^{-1.33\phi(\infty,s)}$$

and $\phi(\infty,s)$ = ultimate creep coefficient from CEB-FIP 1978 code

The ultimate aging coefficient can be taken as approximately equal to 0.8 from the curves found in [40,61], i.e.

$$\chi(\infty,s) = 0.8 \qquad \text{(A5.11)}$$

A5.1.3 RATE OF CREEP METHOD (RCM)

From experimental data on young concretes reported by Glanville [8], the basis for the RCM was established. The RCM was mathematically developed by Whitney [131], and first applied to analysis of concrete structures by Dischinger [132]. Only a single creep curve is required for this method. The RCM assumes that the change of rate of the creep coefficient is independent of loading age. The abstract interpretation of this is that the creep curves for discrete loads with respect to time are parallel, and this can be seen in Figure A5.1. Here, the tangent of the curves loaded at either s_1 or s_2 are equal, or

$$\frac{d\phi(t,s_2)}{dt} = \frac{d\phi(t,s_1)}{dt} \tag{A5.12}$$

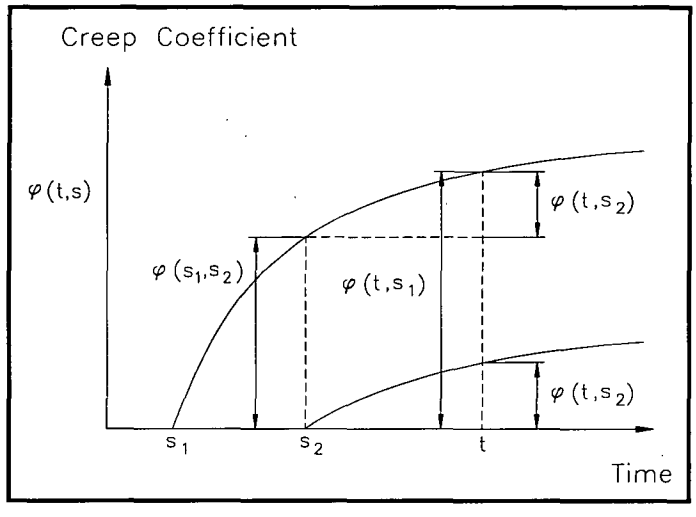

Figure A5.1 - Parallel creep curves which form the basis for developing the Rate of Creep Method.

The model further postulates that shrinkage develops at the same rate as creep, or

$$\varepsilon_{sh}(t) = \frac{\varepsilon_{sh}(\infty)}{\phi(\infty,s)}\phi(t,s) \tag{A5.13}$$

The constitutive model for the time-dependent behaviour of concrete, and known as Dischinger's equation of state, can be written

$$\frac{d\varepsilon(t,s)}{dt} = \frac{1}{E_c(s)}\frac{d\sigma(t)}{dt} + \frac{d\phi(t,s)}{dt}\left(\frac{\sigma(t)}{E_c(s)} + \frac{\varepsilon_{sh}(\infty)}{\phi(\infty,s)}\right) \tag{A5.14}$$

The assumption that creep curves are parallel is not strictly true [14]. For concretes loaded at young ages, good results are achievable, but this is not the case for more mature loading ages. The predictions from the RCM for the latter case are grossly underestimated. This led Nielsen [9] to propose a refined method, which follows.

A5.1.4 IMPROVED RATE OF CREEP METHOD (IRCM)

The inadequacy in the prediction of creep recovery employing the RCM has led Nielsen [9] to propose a modified constitutive model for concrete. This model is referred to as the Improved Rate of Creep Method (IRCM), and separates the creep component into delayed elastic and flow. The delayed elastic component is merged together with the instantaneous component, whilst flow is considered as the only creep component. Dischinger's equation of state is expanded to the form

$$\frac{d\varepsilon(t,s)}{dt} = \frac{1}{E_c'(s)}\frac{d\sigma(t)}{dt} + \frac{d\phi'(t,s)}{dt}\left(\frac{\sigma(t)}{E_c'(s)} + \frac{\varepsilon_{sh}(\infty)}{\phi'(\infty,s)}\right) \qquad \text{(A5.15)}$$

where

$$E_c'(s) = \frac{E_c(s)}{1+\phi_d}$$

$$\phi'(t,s) = \frac{\phi(t,s)-\phi_d}{1+\phi_d}$$

and $$\phi_d = \frac{\varepsilon_{de}(t,s)}{\varepsilon_e(t)}$$

The value of ϕ_d was initially given as 1/3 by Nielsen, however Rusch *et al.* [65] later refined this value to 0.4. In the IRCM, shrinkage is assumed to develop with the reduced creep coefficient.

A comparison between RCM, IRCM and the actual creep function is shown in Figure A5.2. The IRCM initially predicts a higher instantaneous strain, but this value in the long-term approaches the actual strain. Good results can be obtained by the IRCM for long-term behaviour [14], however results for short-term modelling (up to six months) are overestimated and the RCM is better applied in the latter case.

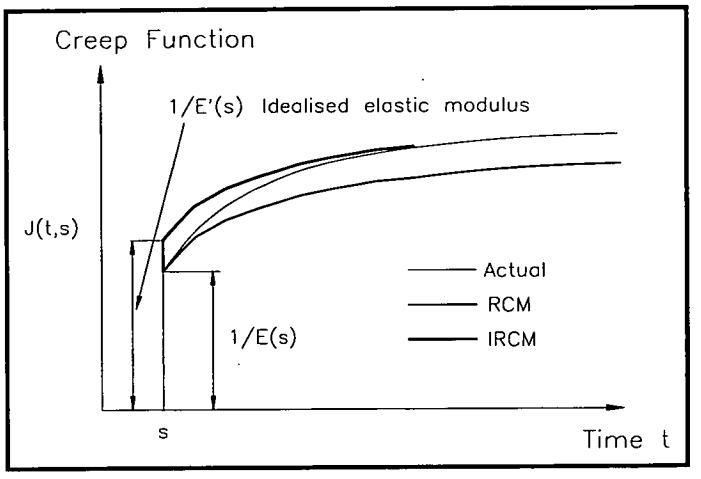

Figure A5.2 - Comparison between the Rate of Creep Method, Improved Rate of Creep Method and the actual creep of concrete.

APPENDIX A5.2

Equations for predicting the time-dependent shortening of reinforced concrete columns based on FEMM, RCM and IRCM respectively are derived below.

A5.2.1 ANALYTICAL COLUMN MODEL BASED ON FEMM

Replacing unity for the aging coefficient in the TBEMM analytical column models results in equations for FEMM, and only the final formulas are given here. This simplification transforms the age-adjusted effective modular ratio to the effective modular ratio, and the age-adjusted effective modulus is equal to the effective modulus, or

$$n_e' = n_e \tag{A5.16}$$

and $$E_e'(t,s) = E_e(t,s) \tag{A5.17}$$

The components of the column shortening are

$$\delta_{elastic} = \sum_{i=1}^{k}\left(\frac{P_i L}{A_c E_c(s_i)(1+p_a n_i)}\right) \tag{A5.18}$$

$$\delta_{creep} = \sum_{i=1}^{k}\left(\frac{P_i L(p_a n_i + \phi(t,s_i) + p_a n_i \phi(t,s_i) - p_a n_{ei})}{A_c E_c(s_i)(1+p_a n_i)(1+p_a n_{ei})}\right) \tag{A5.19}$$

$$\delta_{shrinkage} = \varepsilon_{sh}(t_d)L \tag{A5.20}$$

$$\delta_{reinforcement} = -\varepsilon_{sh}(t_d)L\frac{p_a n_{eo}}{1+p_a n_{eo}} \tag{A5.21}$$

The total concrete stress due to combined elastic and creep deformation is

$$\sigma(t)_{ec} = \sum_{i=1}^{k}\left(\frac{P_i(p_a n_i + 1)}{A_c(1+p_a n_i)(1+p_a n_{ei})}\right) \tag{A5.22}$$

and that due to shrinkage is

$$\sigma(t)_{sr} = \frac{-\varepsilon_{sh}(t_d)\, p_a E_s}{(1 + p_a n_{eo})} \qquad \text{(A5.23)}$$

The steel stress is given by (5.21).

Equations (A5.18) to (A5.23) inclusive and, (5.16), (5.17) and (5.21) represent now the complete formulation for the analysis of a reinforced concrete column based on FEMM.

A5.2.2 ANALYTICAL COLUMN MODEL BASED ON RCM

A constant load **P** is applied to a short symmetrically reinforced concrete column at time **s**, refer to Figure 5.1. The time derivative of the equilibrium equation (i.e. (5.1)) is

$$\frac{dN_c(t)}{dt} + \frac{dN_s(t)}{dt} = 0 \qquad \text{(A5.24)}$$

Differentiating the compatibility equation (i.e. (5.2)) with respect to time results in

$$\frac{d\varepsilon(t,s)}{dt} = \frac{d\varepsilon_{st}(t)}{dt} \qquad \text{(A5.25)}$$

Also differentiating with respect to time, (5.3), (5.4) and (5.5) are modified to

$$\frac{dN_c(t)}{dt} = \frac{d\sigma(t)}{dt} A_c \qquad \text{(A5.26)}$$

$$\frac{dN_s(t)}{dt} = \frac{d\sigma_s(t)}{dt} A_s \qquad \text{(A5.27)}$$

and

$$\frac{d\sigma_s(t)}{dt} = \frac{d\varepsilon_{st}(t)}{dt} E_s \qquad \text{(A5.28)}$$

Substituting (A5.25), (A5.26), (A5.27) and (A5.28) into (A5.24), yields the time derivative for concrete stress as follows

$$\frac{d\sigma(t)}{dt} = -\frac{d\varepsilon(t,s)}{dt} E_s p_a \qquad \text{(A5.29)}$$

After replacing (5.2), (5.3), (5.4) and (5.5) into (5.1), the concrete stress can be found from

$$\sigma(t) = \frac{1}{A_c}(P - \varepsilon(t,s) E_s A_s) \tag{A5.30}$$

Substituting (A5.29) and (A5.30) into the RCM (i.e. (A5.14) yields the linear first order differential equation

$$\frac{d\varepsilon(t,s)}{dt} + a_{rcm} \frac{d\phi(t,s)}{dt} \varepsilon(t,s) = b_{rcm} \frac{d\phi(t,s)}{dt} \tag{A5.31}$$

where

$$a_{rcm} = \frac{p_a n}{1 + p_a n}$$

and $$b_{rcm} = \frac{\left(\frac{P}{A_c E_c(s)} + \frac{\varepsilon_{sh}(\infty)}{\phi(\infty,s)} \right)}{1 + p_a n}$$

The solution of (A5.31) requires knowledge of the integration constant, and can be found from the boundary condition of the problem. At the time of loading, the column shortening is entirely elastic and the boundary condition is established. The total column strain is

$$\varepsilon(t,s) = \frac{P\left(1 - e^{-a_{rcm}\phi(t,s)}\right)}{A_c E_c(s) p_a n} + \frac{P e^{-a_{rcm}\phi(t,s)}}{A_c E_c(s)(1 + p_a n)} + \frac{\varepsilon_{sh}(\infty)}{\phi(\infty,s) p_a n}\left(1 - e^{-a_{rcm}\phi(t,s)}\right) \tag{A5.32}$$

Applying the principle of superposition, the column shortening components due to **k** applied loadings are

$$\delta_{elastic} = \sum_{i=1}^{k} \left(\frac{P_i L}{A_c E_c(s_i)(1 + p_a n_i)} \right) \tag{A5.33}$$

$$\delta_{creep} = -\delta_{elastic} + \sum_{i=1}^{k} \left(\frac{P_i L\left(1 - e^{-a_{rcmi}\phi(t,s_i)}\right)}{A_c E_c(s_i) p_a n_i} \right) + \sum_{i=1}^{k} \left(\frac{P_i L e^{-a_{rcmi}\phi(t,s_i)}}{A_c E_c(s_i)(1 + p_a n_i)} \right) \tag{A5.34}$$

$$\delta_{shrinkage} = \frac{\varepsilon_{sh}(\infty)}{\phi(\infty, t_{sh})}\phi(t, t_{sh})L \tag{A5.35}$$

$$\delta_{reinforcement} = -\delta_{shrinkage} + \frac{\varepsilon_{sh}(\infty)L\left(1-e^{-a_{rcmo}\phi(t,t_{sh})}\right)}{\phi(\infty, t_{sh})p_a n_o} \tag{A5.36}$$

where

$$n_o = \frac{E_s}{E_c(t_{sh})}$$

$$a_{rcmi} = \frac{p_a n_i}{1+p_a n_i}$$

and $$a_{rcmo} = \frac{p_a n_o}{1+p_a n_o}$$

The stresses in the steel and concrete are now determined. Replacing (A5.26) and (A5.27) into (A5.24), the time derivative of the reinforcement stress is

$$\frac{d\sigma_s(t)}{dt} = -\frac{d\sigma(t)}{dt}\frac{1}{p_a} \tag{A5.37}$$

Substituting (A5.37) into (A5.28), and subsequently substituting this formula into (A5.25) combined with the RCM (i.e. (A5.14)), the resulting differential equation follows

$$\frac{\frac{d\sigma(t)}{dt}}{\left(\sigma(t)+\frac{\varepsilon_{sh}(\infty)E_c(s)}{\phi(\infty,s)}\right)} = -\frac{d\phi(t,s)}{dt}\left(\frac{p_a n}{1+p_a n}\right) \tag{A5.38}$$

Incorporating the previous boundary condition, and utilising the principle of superposition for **k** applied loadings to the column, the final stress in the concrete attributed to the combined elastic and creep deformation is

$$\sigma(t)_{ec} = \sum_{i=1}^{k}\left(\frac{P_i\, e^{\left(\frac{-p_a n_i\,\phi(t,s_i)}{1+p_a n_i}\right)}}{A_c(1+p_a n_i)}\right) \tag{A5.39}$$

and the stress due to shrinkage is

$$\sigma(t)_{sr} = \frac{\varepsilon_{sh}(\infty)E_c(t_{sh})}{\phi(\infty,t_{sh})}\left(e^{\left(\frac{-p_a n_o \phi(t,t_{sh})}{1+p_a n_o}\right)} - 1\right) \tag{A5.40}$$

The steel stress if given by (5.21).

Equations (A5.33) to (A5.36) inclusive and, (A5.39), (A5.40) and (5.21) represent now the complete formulation for the analysis of a reinforced concrete column based on RCM.

A5.2.3 ANALYTICAL COLUMN MODEL BASED ON IRCM

Derivation of the IRCM column shortening model is similar to that of the RCM, except modified values of creep coefficients and elastic modulus are necessary. Only the final equations are given here. The components of column shortening due to **k** applied loadings are

$$\delta_{elastic} = \sum_{i=1}^{k}\left(\frac{P_i L}{A_c E_c'(s_i)(1+p_a n_i')}\right) \tag{A5.41}$$

$$\delta_{creep} = -\delta_{elastic} + \sum_{i=1}^{k}\left(\frac{P_i L\left(1-e^{-a'_{rcmi}\phi'(t,s_i)}\right)}{A_c E_c'(s_i) p_a n_i'}\right) + \sum_{i=1}^{k}\left(\frac{P_i L e^{-a'_{rcmi}\phi'(t,s_i)}}{A_c E_c'(s_i)(1+p_a n_i')}\right) \tag{A5.42}$$

$$\delta_{shrinkage} = \frac{\varepsilon_{sh}(\infty)}{\phi'(\infty,t_{sh})}\phi'(t,t_{sh})L \tag{A5.43}$$

$$\delta_{reinforcement} = -\delta_{shrinkage} + \frac{\varepsilon_{sh}(\infty)L\left(1-e^{-a'_{rcmo}\phi'(t,t_{sh})}\right)}{\phi'(\infty,t_{sh})p_a n_o'} \tag{A5.44}$$

The total concrete stress due to the combined elastic and creep deformation is

$$\sigma(t)_{ec} = \sum_{i=1}^{k}\left(\frac{P_i e^{\left(\frac{-p_a n_i' \phi'(t,s_i)}{1+p_a n_i'}\right)}}{A_c(1+p_a n_i')}\right) \tag{A5.45}$$

whilst the total concrete stress attributed to shrinkage is

$$\sigma(t)_{sr} = \frac{\varepsilon_{sh}(\infty)E'_c(t_{sh})}{\phi'(\infty,t_{sh})}\left(e^{\left(\frac{-p_a n'_o \phi'(t,t_{sh})}{1+p_a n'_o}\right)} - 1\right) \tag{A5.46}$$

The reinforcement stress is given by (5.21). Modified parameters and values in the previous analysis are as follows

$$E'_c(s_i) = \frac{E_c(s_i)}{1.4} \tag{A5.47}$$

$$\phi'(t,s_i) = \frac{\phi(t,s_i) - 0.4}{1.4} \tag{A5.48}$$

$$a'_{rcmi} = \frac{p_a n'_i}{1+p_a n'_i} \tag{A5.49}$$

$$a'_{rcmo} = \frac{p_a n'_o}{1+p_a n'_o} \tag{A5.50}$$

$$n'_i = \frac{E_s}{E'_c(s_i)} \tag{A5.51}$$

and $$n'_o = \frac{E_s}{E'_c(t_{sh})} \tag{A5.52}$$

Equations (A5.41) to (A5.46) inclusive and (5.21) represent now the complete formulation for the analysis of a reinforced concrete column based on IRCM.

APPENDIX A5.3

An elastic analysis of a short symmetrically reinforced concrete column (Figure 5.1) with a constant applied load **P** is derived below. The total column strain is

$$\varepsilon(t,s) = \varepsilon(t) = \frac{\sigma(t)}{E_c(s)} + \varepsilon_{sh}(t) \tag{A5.53}$$

Substituting (5.3), (5.4) and (5.5) into (5.1), and employing the compatibility equation (i.e. (5.2)), the resulting concrete stress is

$$\sigma(t) = \frac{1}{A_c}(P - \varepsilon(t) E_s A_s) \tag{A5.54}$$

Substituting (A5.54) into (A5.53), the elastic strain follows

$$\varepsilon_{elastic} = \frac{P}{A_c E_c(s)(1 + p_a n)} \tag{A5.55}$$

The corresponding initial concrete stress is

$$\sigma_o = \frac{P}{A_c(1 + p_a n)} \tag{A5.56}$$

CHAPTER 6

CHAPTER 6

PROBABILISTIC MODELS OF AXIAL SHORTENING

In this chapter, the deterministic reinforced concrete column models of Chapter 5 are extended to probabilistic format in order to incorporate variability of the concrete properties, in particular the elastic modulus, creep coefficient and basic shrinkage strain. Each of these parameters are examined in the context of probabilistic modelling, and are finally described by independent Gaussian distributions. A first- and second-order moment analysis is developed, as well as a Monte Carlo simulation which forms part of any tall building analysis. Finally, comparisons are made between the probabilistic procedures to confirm accuracy of the results.

6.1 RANDOM PARAMETERS IN AXIAL SHORTENING

In the probabilistic models of axial shortening, derived later in this chapter, the concrete properties are modelled as independent Gaussian random parameters. These properties are the elastic modulus, creep coefficient and basic shrinkage strain. Madsen and Bazant [133] reported that creep and shrinkage are the most uncertain mechanical properties of concrete and it therefore would appear that both of these parameters warrant probabilistic descriptions in the shortening models. Further, the concrete modulus is also assumed random. The geometric properties of the reinforced concrete columns (i.e. column and reinforcement areas, and column lengths) are assumed to remain fixed and therefore deterministic.

The applied loads which consist of a live load portion exhibit variability and could for reasons of comprehensiveness be modelled as random. However, the aim of the thesis is to examine the natural uncertainty of concrete constitutive behaviour within any axial shortening analysis, that is, comparing total axial shortening of columns with other model predictions and experimental results to ascertain differences in the concrete properties. Constitutive behaviour being an implicit uncertainty, whilst loading is explicit. Uncertainty of the individual floor loads is not assumed to influence the average total loads applied to the building and therefore is not modelled as random in the thesis to fulfil the objectives of the

work. Applied loads, environmental humidity and temperature are assumed to be deterministic in all probabilistic methods, with the loads being estimated average values from real building project data. All other remaining variables in the axial shortening models do not exhibit significant natural variability to be reasonably assumed as probabilistic.

Before formulating the probabilistic axial shortening models, the characteristic uncertainties of random concrete properties are firstly investigated. It has been generally accepted that the probability density function (PDF) of the compressive strength is normally distributed [134,135]. Mirza *et al.* [136] have suggested that this description is adequate, although Stewart [137] has found the log-normal PDF to be better fit. A study by Drysdale [138] of concrete compressive strengths in existing buildings, employing non-destructive testing techniques, has concluded that good quality control of concrete results in Gaussian PDFs. However, a noted skewness was present with poor to satisfactory control. Further studies by Mirza *et al.* [136] have suggested that the initial tangent modulus for concrete, based on tests conducted by others, to be normal. Whilst limited test data for the secant modulus were available, this parameter can be assumed to be Gaussian [136].

Bazant *et al.* [127,139,140] have reported a statistical study of experimental shrinkage data for concrete. It was concluded there that the PDF of shrinkage strains exhibited a slight skewness. Whilst the Gaussian distribution was determined to be acceptable empirically, the gamma or log-normal distributions tend to describe shrinkage strains somewhat better. From the studies of Bazant *et al.* [127], it can be seen that the coefficient of variation (COV) for shrinkage strains remain fairly constant during standard drying periods (i.e. from 5 days). To the author's knowledge there have been no definitive statistical studies undertaken to describe the PDF of creep strains, and Gaussian distribution is assumed to characterise this variable. Thus all random variables throughout the analysis are assumed to be normal.

Establishing a procedure for deducing the outcomes of the expected value and variance of each random parameter employed by the probabilistic algorithms, is necessary. Each random variable is modelled by a Gaussian PDF in which the value obtained deterministically is equated to the mean. The variance is then derived from the COV. In addressing the choice of the numerical values for various COVs of the independent parameters, the results of Bazant *et al.* [78-83] have been adopted (for all models except B3). The COV for creep strain was

17.05%, whilst for the shrinkage strain 27.0% was reported. The B3 model parameters used were 23.6% and 34.3% respectively [84,85].

In the absence of definitive data, the COV for the elastic modulus was determined by a retrospective investigation of the set of benchmark data from which the ACI [37] recommendations on elastic modulus were obtained. For the purpose here, a linear regression was carried out to obtain values for the elastic modulus based partially on the work of Pauw [112]. Not all experimental data was available to the present author, although those of Hanson [141], Shideler [142] and Kluge *et al.* [143] were obtained. The resulting equation was determined to be

$$E_c(s) = \rho^{1.5}\, 0.0374\sqrt{f_c(s)} \tag{6.1}$$

This results in values for $\mathbf{E_c(s)}$ approximately 13% less than those proposed by Pauw. The COV for the elastic modulus was derived from the scatter of the experimental data about the regression line given by (6.1) and was found to be 17.96%, see Figure 6.1. Values of the COV for concrete strength (employed by Madsen and Bazant [133]) and other random concrete properties are summarised in Table 6.1.

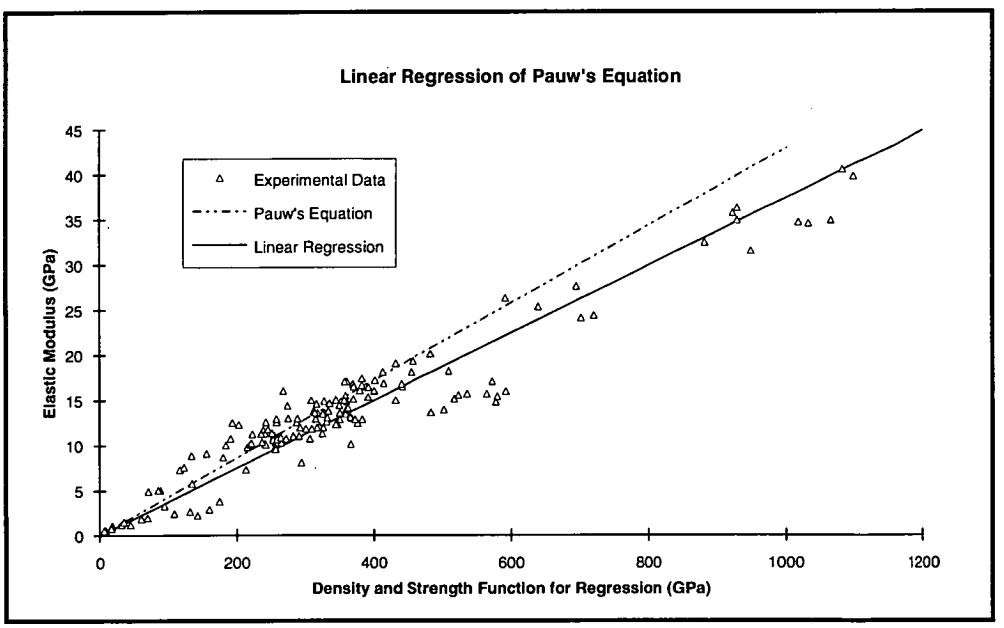

Figure 6.1 - Summary graph of linear regression of available data set used by Pauw [112] to derive ACI [37] elastic modulus model for concrete.

Parameter	COV
Creep Coefficient	17.05 %
Shrinkage Strain	27.0 %
Elastic Modulus	17.96 %
Concrete Strength	10 %

Table 6.1 - Numeric values of COV for the random parameters.

6.2 COLUMN MODELS BASED ON MONTE CARLO SIMULATION

Solutions based on a rigorous n^{th}-order moment formulation embody the variability of the independent parameters in moment form which in turn propagates through the analysis. However, the simplifying assumptions which are used in the derivation of the theory cause uncertainty in the outcome of such analyses. These restrictions can be overcome by casting the analysis in Monte Carlo form [144,145] to obtain the required probabilistic outcomes. A special case of this simulation is the method of realisations. The latter procedure is employed by Melerski [146,147], and in short the input random parameter distributions are discretised into a number of intervals (i.e. realisations). As the number of realisations tend towards infinity, this method approaches the Monte Carlo process.

The Monte Carlo simulation (MCS) adopted here resolves the approximation errors in the second-order moment analysis, though at the expense of increased computational time. In the MCS the algorithm firstly generates a random value for each of the independent variables, according to a specified probability density function. A single outcome from the deterministic analysis is subsequently obtained. This process is then repeated a large number of times. On completion the results can be presented in histogram form or, alternatively, a statistical analysis can be performed to obtain the characteristic moments of the PDF. The mean, variance, relative skewness and relative kurtosis of the statistical data are obtained for **n** data points respectively according to

$$\mu = \frac{1}{n}\sum_{i=1}^{n} x_i \qquad (6.2)$$

$$\sigma^2 = \frac{\sum_{i=1}^{n}(x_i - \mu)^2}{(n-1)} \tag{6.3}$$

$$SK_{rel} = \frac{\sum_{i=1}^{n}(x_i - \mu)^3}{\sigma^3} \tag{6.4}$$

and $$K_{rel} = \frac{\sum_{i=1}^{n}(x_i - \mu)^4}{\sigma^4} \tag{6.5}$$

where $\mathbf{x}_i$ is the i^{th} deterministic output result. For highly complex cases, for example, the presence of a large number of storeys in a building, the solution time is consuming. For an infinite number of simulations, the values obtained from (6.2) to (6.5) inclusive become *"exact"*.

An efficient random number generator for a specified PDF is required in order to lead to efficiencies with the MCS model for problem solving. A Gaussian distribution random number generator has been considered here, as all random variables are normally distributed. Software which includes a uniform random number generator on the interval (0,1) is readily available. The procedure adopted here was to convert the random number outcomes to a Gaussian distribution using the Box-Muller method [148]. This method is outlined in Appendix A6.1 where three independent standardised random numbers are determined, namely $\mathbf{Z}_1$, $\mathbf{Z}_2$ and $\mathbf{Z}_3$, which are transformed to random characteristic values of concrete elastic modulus, creep coefficient and basic shrinkage strain by utilising the posterior modification based on the Gaussian distribution

$$E_c(s) = E[E_c(s)] + Z_1\sqrt{Var[E_c(s)]} \tag{6.6}$$

$$\phi(t,s) = E[\phi(t,s)] + Z_2\sqrt{Var[\phi(t,s)]} \tag{6.7}$$

and $$\varepsilon_{sh}(t_d) = E[\varepsilon_{sh}(t_d)] + Z_3\sqrt{Var[\varepsilon_{sh}(t_d)]} \tag{6.8}$$

where the operators E[•] and Var[•] are defined to be the expected value and variance, respectively.

Exploring the MCS analysis a little further, the initial outcome for a generated random variable such as concrete modulus is described as the base value, with each subsequent value of the modulus being related to it. This being a time-dependent relation, or in other words the modulus can be considered having characteristics of a time series. This principle is extended to the generation of the concrete properties as follows

$$E_c(t_i) = \sqrt{\frac{Var[E_c(t_i)]}{Var[E_c(t)]}}(E_c(t) - E[E_c(t)]) + E[E_c(t_i)] \tag{6.9}$$

$$\phi(t_i, s_j) = \sqrt{\frac{Var[\phi(t_i, s_j)]}{Var[\phi(t,s)]}}(\phi(t,s) - E[\phi(t,s)]) + E[\phi(t_i, s_j)] \tag{6.10}$$

and $$\varepsilon_{sh}(t_{di}) = \sqrt{\frac{Var[\varepsilon_{sh}(t_{di})]}{Var[\varepsilon_{sh}(t_d)]}}(\varepsilon_{sh}(t_d) - E[\varepsilon_{sh}(t_d)]) + E[\varepsilon_{sh}(t_{di})] \tag{6.11}$$

where $\mathbf{t_i}$, $\mathbf{s_j}$ and $\mathbf{t_{di}}$ are the total age, loading age and drying time respectively at some other point in time.

The COV, defined to be the ratio of the standard deviation to expected value of each random parameter, is assumed to be invariant with respect to time, and that the correlation coefficient between each is unity. With the latter assumption, each concrete property can be viewed as being modelled by a Gaussian process (i.e. stochastic process). Thus the variation of each random parameter with respect to time is modelled by the analysis in a very simplified manner. The Gaussian distribution encompasses negative values which have no physical meaning in the present context, therefore each PDF is truncated at zero.

The above MCS procedure is employed in conjunction with the deterministic column models based on FEMM, TBEMM, RCM and IRCM determined in Chapter 5. In the MCS analysis, the expected values, variances, minimum and maximum values, and some higher order moments of axial shortening are determined, with the concrete properties being independent, random and Gaussian. Temperature and humidity have also been modelled as independent, random and Gaussian in the MCS, but their uncertainty associated with axial shortening has not been investigated here.

Once having developed the MCS, the task of ensuring that the numbers generated by the Box-Muller method are random, and thus that the MCS is valid, is a

requirement of the overall procedure. To this end, a goodness of fit test was carried out to test that the random numbers produced were in fact Gaussian. The Kolmogorov-Smirnov (K-S) and chi-squared (χ^2) goodness of fit tests [144,145,149] (refer to Appendix A6.2 for details) were made, at the 95% level of significance, confirming the application of the MCS. Software (STATS) was developed here which incorporates these goodness of fit tests, and details are given in Chapter 7. For the tests conducted, 5 groups of 100,000 and 30 groups of 10,000 random numbers were generated utilising the Box-Muller approach, for which μ=100 and σ=20. A summary of these tests can be found in Appendix A6.3. Histograms of 10,000 and 100,000 Gaussian generated numbers can be seen in Figures 6.2 and 6.3 respectively, where the theoretical PDFs are also shown.

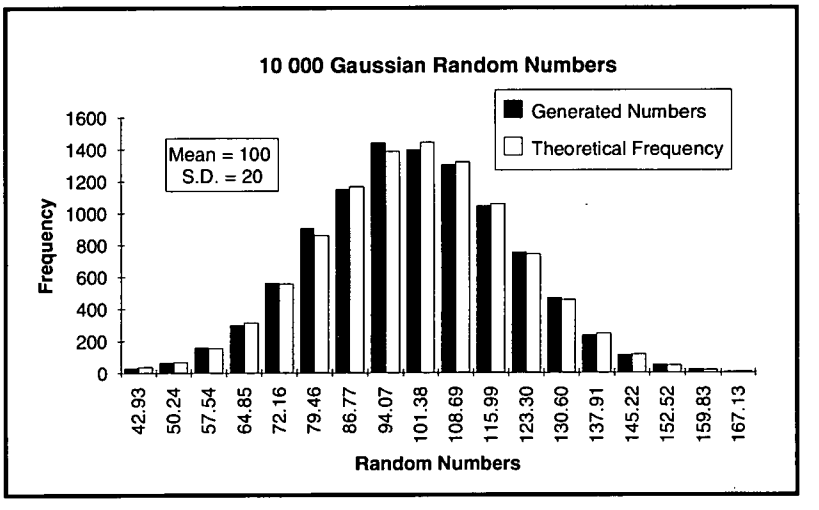

Figure 6.2 - 10,000 Gaussian random numbers generated employing Box-Muller approach with μ=100 and σ=20.

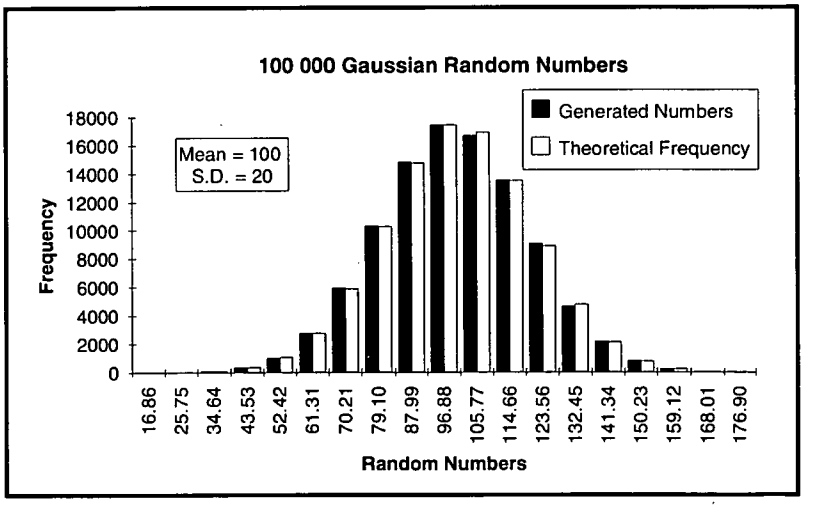

Figure 6.3 - 100,000 Gaussian random numbers generated employing Box-Muller approach with μ=100 and σ=20.

6.3 COLUMN MODELS BASED ON FIRST- AND SECOND-ORDER MOMENT ANALYSES

The first- and second-order moment equations for axial shortening are now derived, extending the previous deterministic column models based on FEMM, TBEMM, RCM and IRCM. In the moment analysis, only the expected values and corresponding variances of axial shortening are determined, with the concrete properties being independent, random and Gaussian.

The governing expressions for describing uncertainty in output results based on first- and second-order moment formulations for a general function with a finite number of random variables are derived in Appendix A6.4. These expressions are not readily available in the form required here and were derived from first principles. Also, well known properties of the Gaussian distribution as applied in this thesis are given in Appendix A6.5.

First- and second-order moment analyses are not applicable for PDFs with large values of the COV, and this aspect is examined later to check that the Taylor series approximation is adequate. A second-order moment formulation embodies to a large extent the non-linearity of the general function **Y** defined in Appendix A6.4, however, consideration of higher-order moments to improve the non-linear description is avoided due to algebraic complexity. It is important to note that the expected value of **Y** for a third-order moment analysis is identical to the second-order equation (as the Gaussian PDF is symmetrical). Thus in applying the second-order expected value expression, the third-order formulation is actually being employed.

6.3.1 Moment Analysis Based on FEMM and TBEMM

First-order moment equations are firstly derived for the TBEMM, whilst FEMM can be evaluated by equating the aging coefficients in these final expressions to unity. As for the case of the MCS, subsequent values for each random variable in terms of the base value are defined as follows for the creep coefficient, elastic modulus and basic shrinkage strain respectively

$$E_c(s_i) = K_{Ei}\, E_c(s) \tag{6.12}$$

$$\phi(t_i, s_j) = K_{Cij}\, \phi(t,s) \tag{6.13}$$

and $$\varepsilon_{sh}(t_{di}) = K_{Si}\, \varepsilon_{sh}(t_d) \tag{6.14}$$

Here, $\mathbf{E_c(s)}$, ϕ**(t,s)** and $\varepsilon_{sh}(t_d)$ are the basic random variables, whilst $\mathbf{K_{Ei}}$, $\mathbf{K_{Cij}}$ and $\mathbf{K_{Si}}$ are constant multipliers given by the ratio of a specific random parameter such as elastic modulus, creep coefficient and shrinkage to the basic random variable for each of the concrete properties respectively.

Alternatively, the time-dependent modelling described above can be explained as follows. Each random concrete property can be modelled as deterministic and multiplied by a random Gaussian PDF in the deterministic column models. These random PDFs would have correlation coefficients equal to zero for the cases of correlating different concrete properties, and unity when correlating each property at subsequent times.

Substitution of the deterministic column models into (A6.13) and (A6.14), results in the final first-order moment expressions which follow. For $\mathbf{k_j}$ loads applied on the $\mathbf{j^{th}}$ storey column, the expected value and variance of the total cumulative shortening are respectively

$$E[\delta_{cum}] = \delta_{cum} \tag{6.15}$$

and

$$\begin{aligned} Var[\delta_{cum}] = {} & Var[\phi(t,s)]\left(\frac{\partial \delta_{cum}}{\partial \phi(t,s)}\right)^2 + Var[E_c(s)]\left(\frac{\partial \delta_{cum}}{\partial E_c(s)}\right)^2 \\ & + Var[\varepsilon_{sh}(t_d)]\left(\frac{\partial \delta_{cum}}{\partial \varepsilon_{sh}(t_d)}\right)^2 \end{aligned} \tag{6.16}$$

Here, δ_{cum} is obtained from (5.17) based on TBEMM. The first-order derivatives in the two previous equations are

$$\frac{\partial \delta_{cum}}{\partial \varepsilon_{sh}(t_d)} = \sum_{i=1}^{j}\left(\frac{\partial \delta_i}{\partial \varepsilon_{sh}(t_d)}\right) \tag{6.17}$$

$$\frac{\partial \delta_{cum}}{\partial E_c(s)} = \sum_{i=1}^{j}\left(\frac{\partial \delta_i}{\partial E_c(s)}\right) + \sum_{i=1}^{j}\sum_{h=1}^{k_j}\left(\frac{\partial \delta_{ih}}{\partial E_c(s)}\right) \tag{6.18}$$

$$\frac{\partial \delta_{cum}}{\partial \phi(t,s)} = \sum_{i=1}^{j}\left(\frac{\partial \delta_i}{\partial \phi(t,s)}\right) + \sum_{i=1}^{j}\sum_{h=1}^{k_j}\left(\frac{\partial \delta_{ih}}{\partial \phi(t,s)}\right) \tag{6.19}$$

$$\frac{\partial \delta_i}{\partial \varepsilon_{sh}(t_d)} = \frac{L_i E_{ci}(t_{sh}) K_{Si}}{d_{3i}(t_i, t_{sh})} \tag{6.20}$$

$$\frac{\partial \delta_i}{\partial E_c(s)} = \frac{L_i p_{ai} E_s \varepsilon_{shi}(t_i) d_{1i}(t_i, t_{sh}) K_{Ei}}{d_{3i}(t_i, t_{sh})^2} \tag{6.21}$$

$$\frac{\partial \delta_{ih}}{\partial E_c(s)} = \frac{-P_{ih} L_i K_{Eih}}{A_{ci} d_{2i}(s_{ih})^2} - \frac{P_{ih} L_i \phi_i(t_i, s_{ih}) [E_{ci}(s_{ih})^2 - p_{ai}{}^2 E_s{}^2 d_{1i}(t_i, s_{ih})] K_{Eih}}{A_{ci} d_{2i}(s_{ih})^2 d_{3i}(t_i, s_{ih})^2} \tag{6.22}$$

$$\frac{\partial \delta_i}{\partial \phi(t,s)} = \frac{-\varepsilon_{shi}(t_i) L_i E_{ci}(t_{sh}) p_{ai} E_s \chi_i(t_i, t_{sh}) K_{Ci}}{d_{3i}(t_i, t_{sh})^2} \tag{6.23}$$

$$\frac{\partial \delta_{ih}}{\partial \phi(t,s)} = \frac{P_{ih} L_i E_{ci}(s_{ih}) K_{Cih}}{A_{ci} d_{3i}(t_i, s_{ih})^2} \tag{6.24}$$

$$K_{Si} = \frac{\varepsilon_{shi}(t_i)}{\varepsilon_{sh}(t_d)} \tag{6.25}$$

$$K_{Ei} = \frac{E_{ci}(t_{sh})}{E_c(s)} \tag{6.26}$$

$$K_{Eih} = \frac{E_{ci}(s_{ih})}{E_c(s)} \tag{6.27}$$

$$K_{Ci} = \frac{\phi_i(t_i, t_{sh})}{\phi(t,s)} \tag{6.28}$$

$$K_{Cih} = \frac{\phi_i(t_i, s_{ih})}{\phi(t,s)} \tag{6.29}$$

$$d_{1i}(x,y) = 1 + \chi_i(x,y)\phi_i(x,y) \tag{6.30}$$

$$d_{2i}(x) = E_{ci}(x) + p_{ai} E_s \tag{6.31}$$

$$d_{3i}(x,y) = E_{ci}(y) + p_{ai} E_s d_{1i}(x,y) \tag{6.32}$$

and $$p_{ai} = \frac{A_{si}}{A_{ci}} \tag{6.33}$$

where

A_{si} = cross-sectional area of steel in column in i^{th} storey

A_{ci} = cross-sectional area of concrete in column in i^{th} storey

L_i = length of column in i^{th} storey

t_i = total age of column in i^{th} storey

s_{ih} = loading age of column in i^{th} storey due to h^{th} load

P_{ih} = the h^{th} load applied to column in i^{th} storey

$E_{ci}(x)$ = concrete elastic modulus of column in i^{th} storey at time x days

$\chi_i(x,y)$ = aging coefficient of column in i^{th} storey with a total column age of x days and a loading age of y days

$\phi_i(x,y)$ = creep coefficient of column in i^{th} storey with a total column age of x days and a loading age of y days

and $\varepsilon_{shi}(x)$ = free shrinkage strain of column in i^{th} storey at time x days

The second-order moment equations for the TBEMM can similarly be obtained. The expected value and variance of the total cumulative shortening due to $\mathbf{k}_j$ loads applied on the $\mathbf{j}^{th}$ storey column are respectively

$$E[\delta_{cum}] = \delta_{cum} + \frac{1}{2}Var[\phi(t,s)]\left(\frac{\partial^2\delta_{cum}}{\partial\phi(t,s)^2}\right) + \frac{1}{2}Var[E_c(s)]\left(\frac{\partial^2\delta_{cum}}{\partial E_c(s)^2}\right) + \frac{1}{2}Var[\varepsilon_{sh}(t_d)]\left(\frac{\partial^2\delta_{cum}}{\partial\varepsilon_{sh}(t_d)^2}\right) \tag{6.34}$$

and

$$Var[\delta_{cum}] = Var[\phi(t,s)]\left(\frac{\partial\delta_{cum}}{\partial\phi(t,s)}\right)^2 + Var[E_c(s)]\left(\frac{\partial\delta_{cum}}{\partial E_c(s)}\right)^2 + Var[\varepsilon_{sh}(t_d)]\left(\frac{\partial\delta_{cum}}{\partial\varepsilon_{sh}(t_d)}\right)^2 + \frac{1}{2}Var^2[\phi(t,s)]\left(\frac{\partial^2\delta_{cum}}{\partial\phi(t,s)^2}\right)^2 + \frac{1}{2}Var^2[E_c(s)]\left(\frac{\partial^2\delta_{cum}}{\partial E_c(s)^2}\right)^2 + \frac{1}{2}Var^2[\varepsilon_{sh}(t_d)]\left(\frac{\partial^2\delta_{cum}}{\partial\varepsilon_{sh}(t_d)^2}\right)^2 \tag{6.35}$$

The second-order derivatives in the two previous equations are

$$\frac{\partial^2 \delta_{cum}}{\partial \varepsilon_{sh}(t_d)^2} = 0 \tag{6.36}$$

$$\frac{\partial^2 \delta_{cum}}{\partial E_c(s)^2} = \sum_{i=1}^{j}\left(\frac{\partial^2 \delta_i}{\partial E_c(s)^2}\right) + \sum_{i=1}^{j}\sum_{h=1}^{k_j}\left(\frac{\partial^2 \delta_{ih}}{\partial E_c(s)^2}\right) \tag{6.37}$$

$$\frac{\partial^2 \delta_{cum}}{\partial \phi(t,s)^2} = \sum_{i=1}^{j}\left(\frac{\partial^2 \delta_i}{\partial \phi(t,s)^2}\right) + \sum_{i=1}^{j}\sum_{h=1}^{k_j}\left(\frac{\partial^2 \delta_{ih}}{\partial \phi(t,s)^2}\right) \tag{6.38}$$

$$\frac{\partial^2 \delta_i}{\partial E_c(s)^2} = \frac{-2L_i p_{ai} E_s \varepsilon_{shi}(t_i) d_{1i}(t_i, t_{sh}) K_{Ei}^2}{d_{3i}(t_i, t_{sh})^3} \tag{6.39}$$

$$\begin{aligned}\frac{\partial^2 \delta_{ih}}{\partial E_c(s)^2} = {} & \frac{2P_{ih}L_i K_{Eih}^2}{A_{ci} d_{2i}(s_{ih})^3} - \frac{2P_{ih}L_i \phi_i(t_i, s_{ih}) E_{ci}(s_{ih}) K_{Eih}^2}{A_{ci} d_{2i}(s_{ih})^2 d_{3i}(t_i, s_{ih})^2} \\ & + \frac{2P_{ih}L_i \phi_i(t_i, s_{ih})[E_{ci}(s_{ih})^2 - p_{ai}^2 E_s^2 d_{1i}(t_i, s_{ih})]}{A_{ci} d_{2i}(s_{ih})^3 d_{3i}(t_i, s_{ih})^3} \\ & \times [d_{2i}(s_{ih}) + d_{3i}(t_i, s_{ih})] K_{Eih}^2\end{aligned} \tag{6.40}$$

$$\frac{\partial^2 \delta_i}{\partial \phi(t,s)^2} = \frac{2\varepsilon_{shi}(t_i) L_i E_{ci}(t_{sh}) p_{ai}^2 E_s^2 \chi_i(t_i, t_{sh})^2 K_{Ci}^2}{d_{3i}(t_i, t_{sh})^3} \tag{6.41}$$

and

$$\frac{\partial^2 \delta_{ih}}{\partial \phi(t,s)^2} = \frac{-2P_{ih}L_i E_{ci}(s_{ih}) p_{ai} E_s \chi_i(t_i, s_{ih}) K_{Cih}^2}{A_{ci} d_{3i}(t_i, s_{ih})^3} \tag{6.42}$$

6.3.2 Moment Analysis Based on RCM and IRCM

The first-order moment equations based on the RCM or IRCM can also similarly be obtained. For either method, the expected value and variance of the total cumulative shortening due to $\mathbf{k_j}$ loads applied on the $\mathbf{j^{th}}$ storey column are respectively

$$E[\delta_{cum}] = \delta_{cum} \tag{6.43}$$

and

$$\mathrm{Var}[\delta_{cum}] = \mathrm{Var}[\phi(t,s)]\left(\frac{\partial \delta_{cum}}{\partial \phi(t,s)}\right)^2 + \mathrm{Var}[E_c(s)]\left(\frac{\partial \delta_{cum}}{\partial E_c(s)}\right)^2 + \mathrm{Var}[\varepsilon_{sh}(\infty)]\left(\frac{\partial \delta_{cum}}{\partial \varepsilon_{sh}(\infty)}\right)^2 \tag{6.44}$$

Here, δ_{cum} is obtained from (5.17) based on either the RCM or IRCM. The first-order derivatives in the two previous equations are

$$\frac{\partial \delta_{cum}}{\partial \varepsilon_{sh}(\infty)} = \sum_{i=1}^{j}\left(\frac{\partial \delta_i}{\partial \varepsilon_{sh}(\infty)}\right) \tag{6.45}$$

$$\frac{\partial \delta_{cum}}{\partial E_c(s)} = \sum_{i=1}^{j}\left(\frac{\partial \delta_i}{\partial E_c(s)}\right) + \sum_{i=1}^{j}\sum_{h=1}^{k_j}\left(\frac{\partial \delta_{ih}}{\partial E_c(s)}\right) \tag{6.46}$$

$$\frac{\partial \delta_{cum}}{\partial \phi(t,s)} = \sum_{i=1}^{j}\left(\frac{\partial \delta_i}{\partial \phi(t,s)}\right) + \sum_{i=1}^{j}\sum_{h=1}^{k_j}\left(\frac{\partial \delta_{ih}}{\partial \phi(t,s)}\right) \tag{6.47}$$

$$\frac{\partial \delta_i}{\partial \varepsilon_{sh}(\infty)} = \frac{L_i E_{ci}(t_{sh})[1-d_{8i}(t_i,t_{sh})]K_{S\infty i}}{p_{ai}E_s[a_i(t_i,t_{sh})\phi_i(t_i,t_{sh})-d_4]} \tag{6.48}$$

$$\frac{\partial \delta_i}{\partial E_c(s)} = \frac{L_i \varepsilon_{shi}(\infty)[1-d_{8i}(t_i,t_{sh})]K_{Ei}}{p_{ai}E_s[a_i(t_i,t_{sh})\phi_i(t_i,t_{sh})-d_4]} - \frac{\varepsilon_{shi}(\infty)L_i E_{ci}(t_{sh})[\phi_i(t_i,t_{sh})-d_4]d_{8i}(t_i,t_{sh})K_{Ei}}{d_{7i}(t_{sh})^2[a_i(t_i,t_{sh})\phi_i(t_i,t_{sh})-d_4]} \tag{6.49}$$

$$\frac{\partial \delta_{ih}}{\partial E_c(s)} = \frac{-P_{ih}L_i\, d_{8i}(t_i,s_{ih})K_{Eih}}{A_{ci}d_{7i}(s_{ih})^3} \times\left(d_{2i}(s_{ih})+\phi_i(t_i,s_{ih})E_{ci}(s_{ih})+0.96\,d_6\,p_{ai}E_s\right) \tag{6.50}$$

$$\frac{\partial \delta_i}{\partial \phi(t,s)} = \frac{a_i(t_i,t_{sh})\varepsilon_{shi}(\infty)L_i E_{ci}(t_{sh})[d_{8i}(t_i,t_{sh})-1]K_{Ci}}{[a_i(t_i,t_{sh})\phi_i(t_i,t_{sh})-d_4]^2 p_{ai}E_s} + \frac{\varepsilon_{shi}(\infty)L_i E_{ci}(t_{sh})d_{8i}(t_i,t_{sh})K_{Ci}}{[a_i(t_i,t_{sh})\phi_i(t_i,t_{sh})-d_4]d_{7i}(t_{sh})} \tag{6.51}$$

$$\frac{\partial \delta_{ih}}{\partial \phi(t,s)} = \frac{P_{ih}L_i E_{ci}(s_{ih})d_{8i}(t_i,s_{ih})K_{Cih}}{A_{ci}d_{7i}(s_{ih})^2} \tag{6.52}$$

$$a_i(x,y) = \frac{\phi(\infty,y)}{\phi(x,y)} \tag{6.53}$$

$$K_{S\infty i} = \frac{\varepsilon_{shi}(\infty)}{\varepsilon_{sh}(\infty)} \tag{6.54}$$

$$\left.\begin{array}{ll} d_4 = 0 & (\text{for RCM}) \\ d_4 = 0.4 & (\text{for IRCM}) \end{array}\right\} \tag{6.55}$$

$$\left.\begin{array}{ll} d_5 = 1 & (\text{for RCM}) \\ d_5 = 1.4 & (\text{for IRCM}) \end{array}\right\} \tag{6.56}$$

$$\left.\begin{array}{ll} d_6 = 0 & (\text{for RCM}) \\ d_6 = 1 & (\text{for IRCM}) \end{array}\right\} \tag{6.57}$$

$$d_{7i}(x) = E_{ci}(x) + d_5 p_{ai} E_s \tag{6.58}$$

and $$d_{8i}(x,y) = e^{\left(\frac{-p_{ai}E_s(\phi_i(x,y)-d_4)}{d_{7i}(y)}\right)} \tag{6.59}$$

The second-order moment equations for the RCM or IRCM also follow. The expected value and variance of the total cumulative shortening due to $\mathbf{k}_j$ loads applied on the $\mathbf{j}^{th}$ storey column are respectively

$$\begin{aligned} E[\delta_{cum}] = \delta_{cum} &+ \frac{1}{2}\text{Var}[\phi(t,s)]\left(\frac{\partial^2\delta_{cum}}{\partial\phi(t,s)^2}\right) \\ &+ \frac{1}{2}\text{Var}[E_c(s)]\left(\frac{\partial^2\delta_{cum}}{\partial E_c(s)^2}\right) + \frac{1}{2}\text{Var}[\varepsilon_{sh}(\infty)]\left(\frac{\partial^2\delta_{cum}}{\partial\varepsilon_{sh}(\infty)^2}\right) \end{aligned} \tag{6.60}$$

and

$$\begin{aligned} \text{Var}[\delta_{cum}] = &\text{Var}[\phi(t,s)]\left(\frac{\partial\delta_{cum}}{\partial\phi(t,s)}\right)^2 + \text{Var}[E_c(s)]\left(\frac{\partial\delta_{cum}}{\partial E_c(s)}\right)^2 \\ &+ \text{Var}[\varepsilon_{sh}(\infty)]\left(\frac{\partial\delta_{cum}}{\partial\varepsilon_{sh}(\infty)}\right)^2 + \frac{1}{2}\text{Var}^2[\phi(t,s)]\left(\frac{\partial^2\delta_{cum}}{\partial\phi(t,s)^2}\right)^2 \\ &+ \frac{1}{2}\text{Var}^2[E_c(s)]\left(\frac{\partial^2\delta_{cum}}{\partial E_c(s)^2}\right)^2 + \frac{1}{2}\text{Var}^2[\varepsilon_{sh}(\infty)]\left(\frac{\partial^2\delta_{cum}}{\partial\varepsilon_{sh}(\infty)^2}\right)^2 \end{aligned} \tag{6.61}$$

The second-order derivatives in the two previous equations are

$$\frac{\partial^2 \delta_{cum}}{\partial \varepsilon_{sh}(\infty)^2} = 0 \tag{6.62}$$

$$\frac{\partial^2 \delta_{cum}}{\partial E_c(s)^2} = \sum_{i=1}^{j}\left(\frac{\partial^2 \delta_i}{\partial E_c(s)^2}\right) + \sum_{i=1}^{j}\sum_{h=1}^{k_j}\left(\frac{\partial^2 \delta_{ih}}{\partial E_c(s)^2}\right) \tag{6.63}$$

$$\frac{\partial^2 \delta_{cum}}{\partial \phi(t,s)^2} = \sum_{i=1}^{j}\left(\frac{\partial^2 \delta_i}{\partial \phi(t,s)^2}\right) + \sum_{i=1}^{j}\sum_{h=1}^{k_j}\left(\frac{\partial^2 \delta_{ih}}{\partial \phi(t,s)^2}\right) \tag{6.64}$$

$$\begin{aligned}\frac{\partial^2 \delta_i}{\partial E_c(s)^2} &= \frac{2\varepsilon_{shi}(\infty) L_i E_{ci}(t_{sh})[\phi_i(t_i,t_{sh}) - d_4] d_{8i}(t_i,t_{sh}) K_{Ei}^2}{d_{7i}(t_{sh})^3 [a_i(t_i,t_{sh})\phi_i(t_i,t_{sh}) - d_4]} \\ &- \frac{\varepsilon_{shi}(\infty) L_i E_{ci}(t_{sh}) p_{ai} E_s [\phi_i(t_i,t_{sh}) - d_4]^2 d_{8i}(t_i,t_{sh}) K_{Ei}^2}{d_{7i}(t_{sh})^4 [a_i(t_i,t_{sh})\phi_i(t_i,t_{sh}) - d_4]} \\ &- \frac{2\varepsilon_{shi}(\infty) L_i [\phi_i(t_i,t_{sh}) - d_4] d_{8i}(t_i,t_{sh}) K_{Ei}^2}{d_{7i}(t_{sh})^2 [a_i(t_i,t_{sh})\phi_i(t_i,t_{sh}) - d_4]}\end{aligned} \tag{6.65}$$

$$\begin{aligned}\frac{\partial^2 \delta_{ih}}{\partial E_c(s)^2} &= \frac{2 P_{ih} L_i\, d_{8i}(t_i,s_{ih}) K_{Eih}^2}{A_{ci} d_{7i}(s_{ih})^3} \\ &+ \frac{2\phi_i(t_i,s_{ih}) P_{ih} L_i\, d_{8i}(t_i,s_{ih})[E_{ci}(s_{ih}) - d_5\, p_{ai} E_s] K_{Eih}^2}{A_{ci} d_{7i}(s_{ih})^4} \\ &+ \left(\frac{d_6\, d_{8i}(t_i,s_{ih}) P_{ih} L_i\, p_{ai} E_s\, K_{Eih}^2}{A_{ci} d_{7i}(s_{ih})^5}\right) \\ &\times \left(2.08 E_{ci}(s_{ih}) + 3.136 p_{ai} E_s + 0.8 E_{ci}(s_{ih})\phi_i(t_i,s_{ih})\right) \\ &- \frac{P_{ih} L_i\, p_{ai} E_s\, E_{ci}(s_{ih}) d_{8i}(t_i,s_{ih})\phi_i(t_i,s_{ih})^2 K_{Eih}^2}{A_{ci} d_{7i}(s_{ih})^5}\end{aligned} \tag{6.66}$$

$$\begin{aligned}\frac{\partial^2 \delta_i}{\partial \phi(t,s)^2} &= \frac{2 a_i(t_i,t_{sh})^2 \varepsilon_{shi}(\infty) L_i E_{ci}(t_{sh})[1 - d_{8i}(t_i,t_{sh})] K_{Ci}^2}{p_{ai} E_s [a_i(t_i,t_{sh})\phi_i(t_i,t_{sh}) - d_4]^3} \\ &- \frac{2 a_i(t_i,t_{sh}) \varepsilon_{shi}(\infty) L_i E_{ci}(t_{sh}) d_{8i}(t_i,t_{sh}) K_{Ci}^2}{d_{7i}(t_{sh})[a_i(t_i,t_{sh})\phi_i(t_i,t_{sh}) - d_4]^2} \\ &- \frac{\varepsilon_{shi}(\infty) L_i E_{ci}(t_{sh}) p_{ai} E_s\, d_{8i}(t_i,t_{sh}) K_{Ci}^2}{d_{7i}(t_{sh})^2 [a_i(t_i,t_{sh})\phi_i(t_i,t_{sh}) - d_4]}\end{aligned} \tag{6.67}$$

and $$\frac{\partial^2 \delta_{ih}}{\partial \phi(t,s)^2} = \frac{-P_{ih} L_i E_{ci}(s_{ih}) p_{ai} E_s d_{8i}(t_i, s_{ih}) K_{Cih}^2}{A_{ci} d_{7i}(s_{ih})^3} \quad (6.68)$$

First- and second-order moment equations for axial shortening of reinforced concrete columns have been derived, it now being necessary to verify the approximations used in these models (i.e. the Taylor series approximation). This is done by comparing numerical shortening results from first- and second order moment analyses with those obtained from a MCS.

6.4 COMPARISON OF PROBABILISTIC MODELS

The numerical rigour of the three probabilistic axial shortening prediction methods developed here is examined. Numerical values employed for the random concrete properties in the probabilistic models are those initially given in this chapter, together with the models proposed by ACI [37], CEB-FIP [38,58], AS-3600 [39] and Bazant *et al.* [66-84]. All four reinforced concrete column models developed have been tested. In these tests, the long-term axial shortening predictions of an example 39 storey building were determined. The data for this building is given in Appendix A6.6. From the tests it can be concluded that, ***"significant difference of the mean and standard deviation predictions between a first-order moment analysis and MCS exist"***. This difference is present due to the non-linear random parameters (i.e. creep coefficient and concrete modulus) in the axial shortening models. Also, ***"results from a second-order moment analysis and MCS show close agreement"***. As the probabilistic methods depend on the COV values employed, comparisons of these methods, taking into account the effect of each random variable in separate analyses, was also necessary. Again the conclusion drawn was, ***"results from a MCS and second-order moment analysis are comparable"***.

A summary for one test is shown in Figures 6.4 to 6.9 inclusive, where the column model of FEMM is employed with the ACI recommendations, in this case for the 39 storey building analysis. Figures 6.4 and 6.5 show the expected values for a first- and second-order moment analysis, and MCS for the long-term axial shortening of the 39th storey service core and outer spandrel frame column respectively, whilst Figures 6.6 and 6.7 show the corresponding standard deviations respectively. Stability of the MCS is achieved as the number of simulations increase, and can be seen in the previous four diagrams. In Figures 6.8 and 6.9, the MCS histograms for 1000 runs are shown for the long-term axial

shortening of the 39th storey service core and outer spandrel frame column respectively.

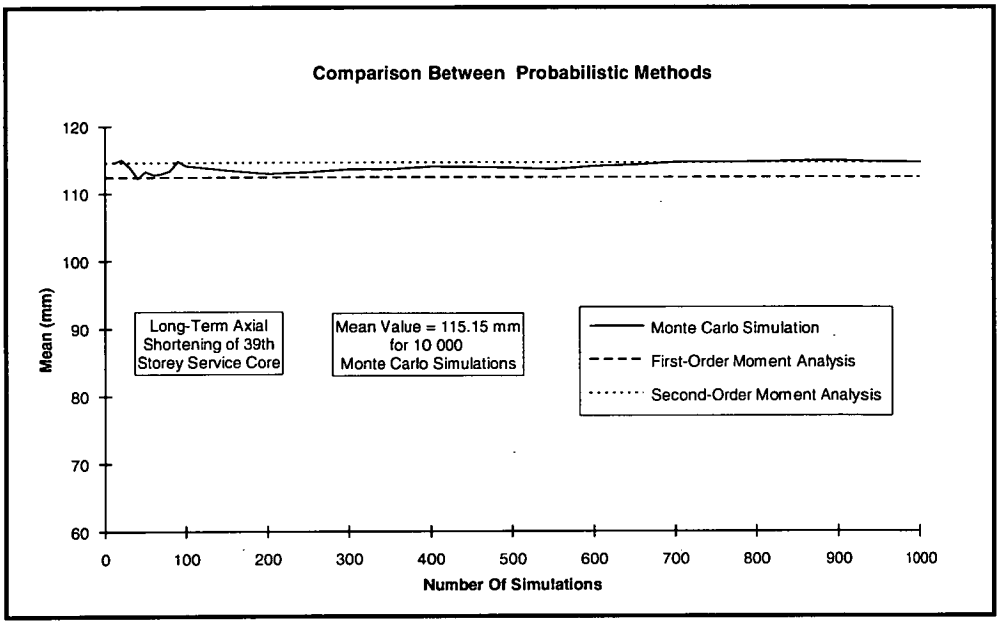

Figure 6.4 - Comparison between first- and second-order moment analysis, and the Monte Carlo simulation for expected value of long-term axial shortening of 39th storey service core.

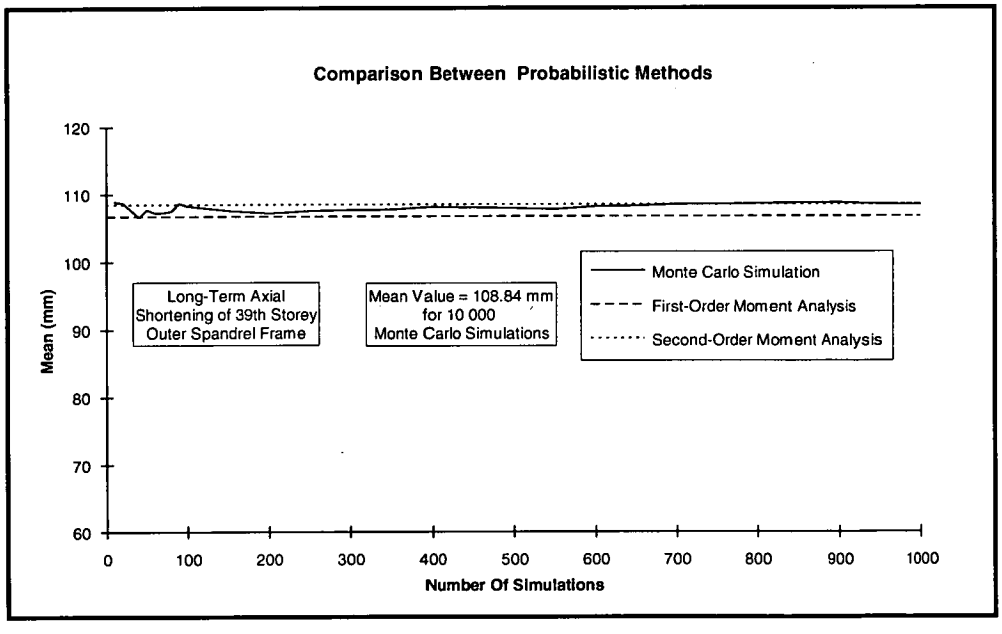

Figure 6.5 - Comparison between first- and second-order moment analysis, and the Monte Carlo simulation for expected value of long-term axial shortening of 39th storey outer spandrel frame column.

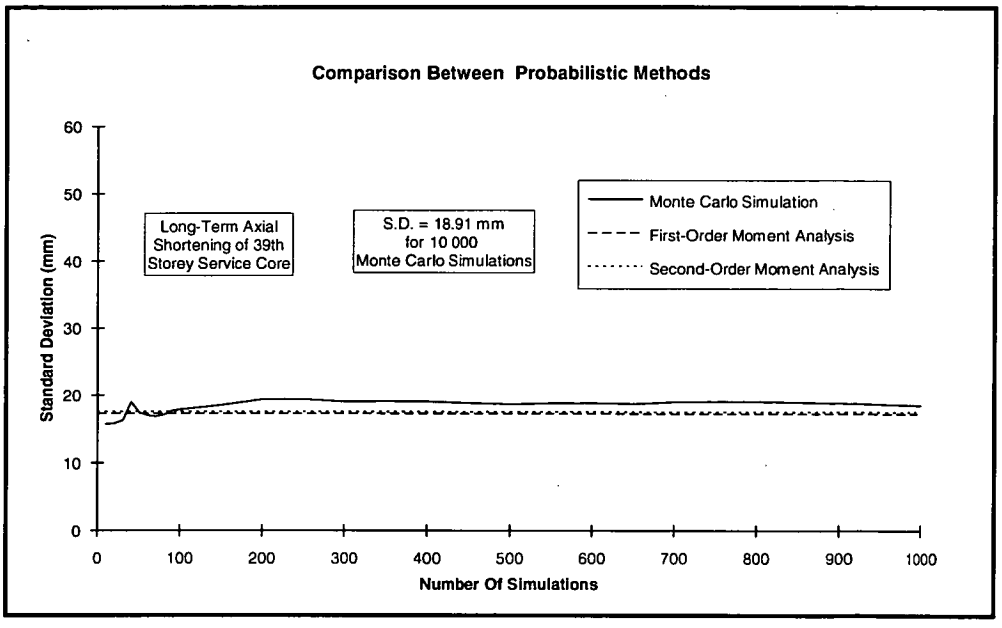

Figure 6.6 - Comparison between first- and second-order moment analysis, and the Monte Carlo simulation for standard deviation of long-term axial shortening of 39th storey service core.

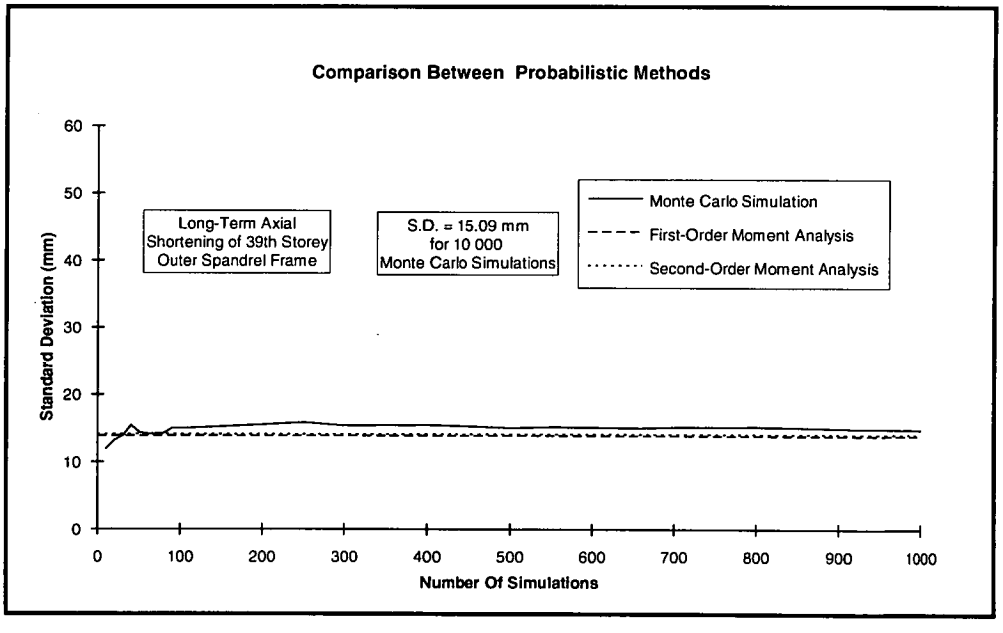

Figure 6.7 - Comparison between first- and second-order moment analysis, and the Monte Carlo simulation for standard deviation of long-term axial shortening of 39th storey outer spandrel frame column.

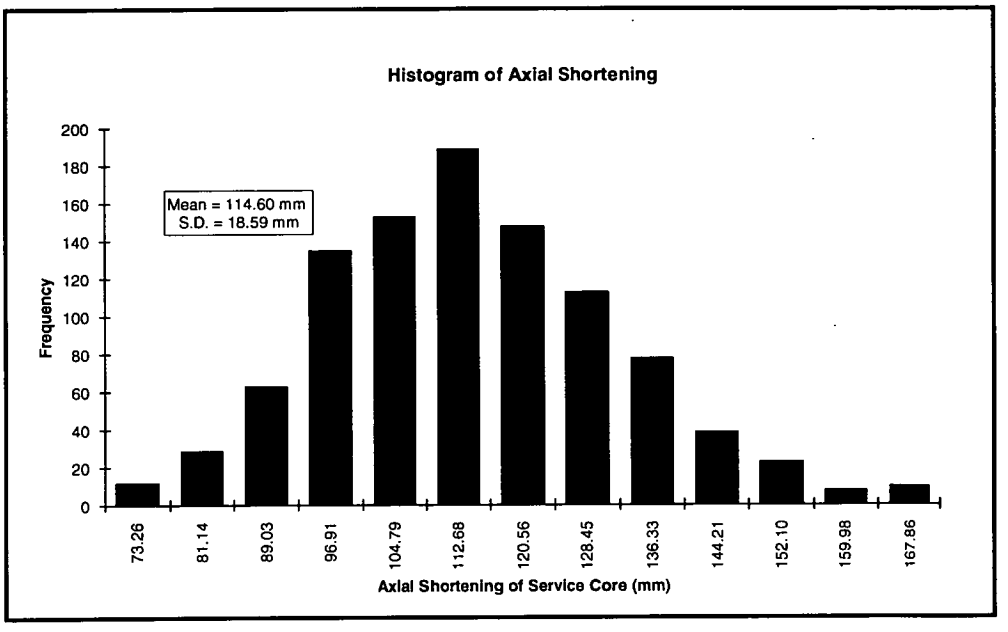

Figure 6.8 - MCS histogram of long-term axial shortening of 39th storey service core.

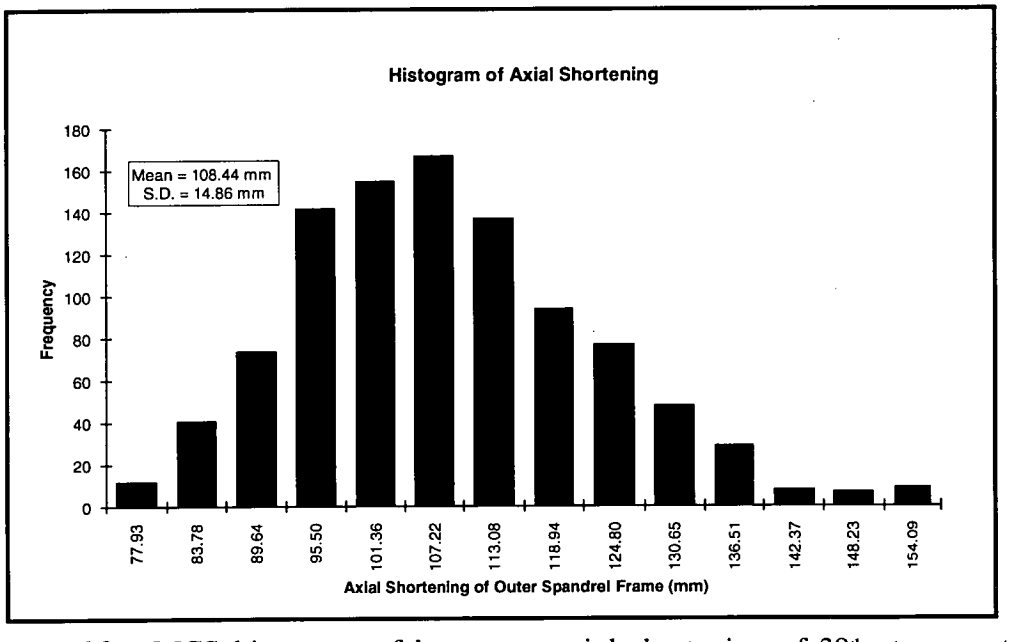

Figure 6.9 - MCS histogram of long-term axial shortening of 39th storey outer spandrel frame column.

6.5 STOCHASTIC MODELS OF AXIAL SHORTENING

In this section, the probabilistic axial shortening column models derived at the start of this chapter are further developed. First- and second-order moment approaches are employed in this new analysis, as well as Monte Carlo simulation, which allow for the stochastic modelling of each random concrete property, i.e. creep coefficient, basic shrinkage strain and elastic modulus, by independent

Gaussian processes. This is a significant advance over the previous models since stochastic variations are incorporated.

6.5.1 Stochastic Concrete Property Modelling

The probabilistic, time-dependent, load-deflection column equations previously derived describe the concrete properties as either having correlation coefficients equal to zero or unity with respect to other random properties or time. This assumption is investigated.

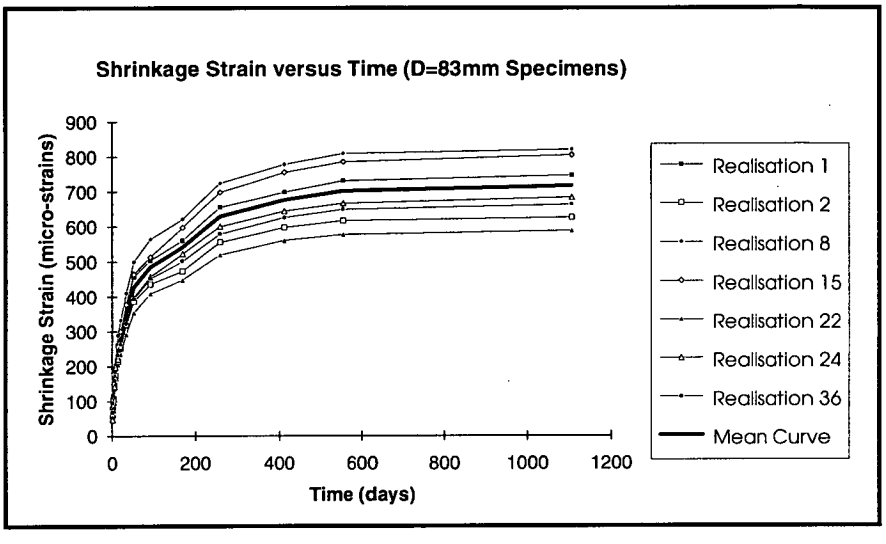

Figure 6.10 - Shows some of the D=83mm cylinder shrinkage data realisations reported in [127].

Bazant *et al.* [127] reported the time-dependent concrete shrinkage strains of 36 test cylinders (83mm dia.) and a further 35 cylinders (160mm dia.). Figure 6.10 shows some of the 83mm cylinder shrinkage data. It is apparent that the causal relationship between points on the data curve is not wholly deterministic and any refined model must necessarily include a stochastic interpretation of the data. The test data was standardised according to $z=(x-\mu)/\sigma$ where z, x, μ and σ are the standardised shrinkage data, unstandardised shrinkage data from [127], data mean value and data standard deviation respectively. Figure 6.11 shows the 83mm standardised shrinkage data results indicating a reasonably high time-dependent correlation for the shrinkage data. In addition, it can be observed that the correlation becomes consistent in the long-term.

From the above studies the author has determined the correlation coefficients for shrinkage strains (for both the 83mm and 160mm test cylinder series) within the context of a stochastic process. It was found that the coefficients between

shrinkages at two different long drying times (i.e. both drying times greater than 34 days) were between 0.9 to 0.95, this is shown in Table 6.2 and 6.3 for the 83mm and 160mm specimens respectively. In the axial shortening model a constant correlation coefficient is adopted for long-term shrinkage predictions based on the above experimental observations. It should be noted that correlation coefficients for creep at different times and loading ages and for concrete moduli at different times could not be determined from the literature.

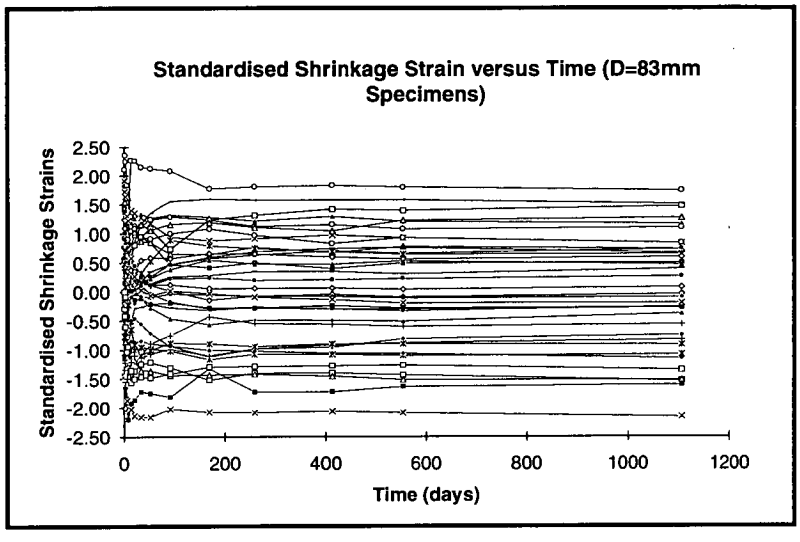

Figure 6.11 - Shows all of the D=83mm standardised cylinder shrinkage data realisations.

t_d	1	2	3	6	8	14	21	34	52	91	169	258	412	554	1105
1	1														
2	0.96	1													
3	0.94	0.98	1												
6	0.81	0.89	0.94	1											
8	0.78	0.87	0.93	1.00	1										
14	0.58	0.71	0.77	0.91	0.92	1									
21	0.49	0.63	0.70	0.87	0.88	0.99	1								
34	0.47	0.61	0.68	0.85	0.87	0.98	0.99	1							
52	0.45	0.58	0.65	0.83	0.85	0.96	0.98	0.99	1						
91	0.48	0.60	0.66	0.83	0.86	0.95	0.96	0.97	0.99	1					
169	0.48	0.59	0.64	0.81	0.83	0.91	0.93	0.95	0.97	0.99	1				
258	0.46	0.58	0.63	0.80	0.83	0.92	0.94	0.96	0.98	0.99	1.00	1			
412	0.45	0.56	0.62	0.79	0.82	0.91	0.93	0.96	0.98	0.99	0.99	1.00	1		
554	0.45	0.57	0.63	0.80	0.82	0.91	0.94	0.96	0.98	0.98	0.99	1.00	1.00	1	
1105	0.45	0.56	0.62	0.79	0.82	0.91	0.94	0.96	0.98	0.98	0.99	1.00	1.00	1.00	1

Table 6.2 - Correlation coefficients between basic shrinkage strains at different drying periods $\mathbf{t_d}$ determined from the experimental data of Bazant *et al.* [127] for specimen size D=83mm (note that table is symmetric).

t_d	1	2	3	6	8	14	21	34	52	91	169	258	412	554	1105
1	1														
2	0.95	1													
3	0.94	0.98	1												
6	0.87	0.95	0.98	1											
8	0.85	0.93	0.97	0.99	1										
14	0.65	0.74	0.76	0.81	0.79	1									
21	0.72	0.85	0.89	0.95	0.96	0.77	1								
34	0.67	0.80	0.84	0.91	0.94	0.75	0.99	1							
52	0.57	0.69	0.72	0.77	0.79	0.64	0.87	0.89	1						
91	0.57	0.71	0.75	0.83	0.86	0.68	0.95	0.98	0.91	1					
169	0.51	0.65	0.69	0.78	0.82	0.62	0.92	0.95	0.88	0.99	1				
258	0.44	0.55	0.60	0.69	0.73	0.53	0.84	0.87	0.82	0.93	0.95	1			
412	0.43	0.56	0.60	0.70	0.74	0.55	0.86	0.90	0.84	0.96	0.98	0.94	1		
554	0.39	0.52	0.57	0.67	0.72	0.52	0.84	0.89	0.84	0.95	0.98	0.94	0.99	1	
1105	0.37	0.50	0.56	0.67	0.71	0.52	0.85	0.89	0.84	0.94	0.97	0.94	0.98	0.99	1

Table 6.3 - Correlation coefficients between basic shrinkage strains at different drying periods $\mathbf{t_d}$ determined from the experimental data of Bazant *et al.* [127] for specimen size D=160mm (note that table is symmetric).

In summary, it is assumed that the correlation coefficients between shrinkage at different times, creep coefficient at different times and modulus at different times are all constant at 0.9. Further, it is assumed that correlations between any remaining concrete properties are zero. Also, it can be assumed that time-dependent properties of different concrete mixes are statistically independent, due to the absence of causality.

For the purpose of the computational model below each concrete property is modelled as a Gaussian process. As only a finite number of random parameter values are required for each continuous Gaussian process, shrinkage, creep coefficient and concrete modulus is described by a multivariate normal distribution. As is well known, this distribution can be completely described by its mean vector and covariance matrix. Determination of expected values and standard deviations were discussed in this chapter, whilst the covariance between any two time-dependent random variables for one particular concrete property is evaluated from the correlation coefficient and the two respective standard deviations.

6.5.2 Monte Carlo and First- and Second-Order Moment Stochastic Column Models

First- and second-order moment equations are derived for the TBEMM, whilst the FEMM can be considered a subset of this with the aging coefficient set to unity. The derivations and equations can be found in Appendix A6.7. A probabilistic reinforced concrete column shortening model based on Monte Carlo simulation is also outlined in Appendix A6.7, together with a brief description of software implementing new analysis and comparisons of output results.

6.5.3 Comparison of New Improved Probabilistic Models

A comparison is made between the "simpler" models developed in Section 6.2 and 6.3 and those developed in Appendix A6.7. Figure 6.12 shows the long-term axial shortening results of the service core obtained by second-order moment analyses. It can be observed that there is no significant difference between the "simpler" models and the new improved models. One could suggest that the improved models are not necessary, however, it should be remembered that accurate stochastic data for the elastic/inelastic variables such as the creep coefficient and elastic modulus are currently not available in the literature.

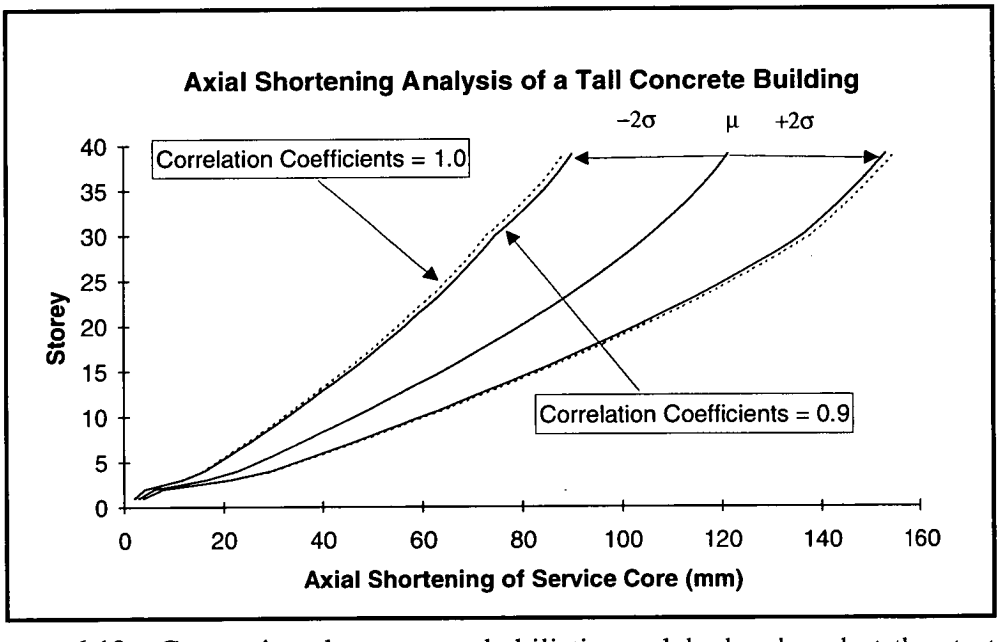

Figure 6.12 - Comparison between probabilistic models developed at the start of Chapter 6 (Section 6.2 and 6.3, ρ=1.0) and those derived in Appendix A6.7 (ρ =0.9).

6.5.4 Concluding Remarks for New Stochastic Models

First- and second-order moment analyses, and a Monte Carlo simulation for reinforced concrete column behaviour were developed. In these models the concrete properties were modelled as independent Gaussian processes. The results from a second-order moment model were found to agree well with those from a Monte Carlo simulation. Although these new analysis methods allow for a random stochastic description of the input parameters, tall building computational times are far greater than when employing the relatively simpler probabilistic models derived earlier in this chapter. Finally, the new models and the "simpler" models result in close correlations between axial shortening predictions, and for this reason the "simpler" models of analysis are employed in subsequent chapter in preference to the new models.

6.6 CONCLUDING REMARKS TO CHAPTER

A first- and second-order moment analysis, and a Monte Carlo simulation for reinforced concrete column behaviour were developed. In these models the concrete properties, namely the elastic modulus, creep coefficient and basic shrinkage strain, were modelled as independent, random and Gaussian. The first-order moment column shortening equations were found to produce inaccurate results when compared to the output from the more rigorous MCS method. Both the Monte Carlo simulation and second-order moment analysis gave comparable results, thus verifying that the Taylor series approximation in the latter method is sufficient. The Monte Carlo simulation was found to be time consuming and not suited as a design tool. For the case-studies presented in Chapter 8, both the second-order moment procedure and MCS are used.

APPENDIX

TO

CHAPTER 6

APPENDIX A6.1

A Gaussian distribution random number generator, which has been implemented into the MCS, is described here. Software which includes a uniform random number generator on the interval (0,1) is readily available. The procedure adopted here was to convert the random number outcomes to a Gaussian distribution using the Box-Muller method [148]. This is now outlined. For example, two independent random numbers are generated from the standard uniform distribution (i.e. $\mathbf{U}_1$ and $\mathbf{U}_2$), which represent deviates in a unit square. These are both transformed on to an interval (-1,1) by

$$V_1 = 2U_1 - 1 \tag{A6.1}$$

and $$V_2 = 2U_2 - 1 \tag{A6.2}$$

Next, $\mathbf{V}_1$ and $\mathbf{V}_2$ are considered to lie within a circle of unit radius. A value for the radial dimension of the transformed deviates $\mathbf{V}_1$ and $\mathbf{V}_2$ is then defined by $\mathbf{S}$ according to

$$S = V_1^2 + V_2^2 \tag{A6.3}$$

$\mathbf{S}$ must be less than or equal to unity to lie within the circle, otherwise, the above process is repeated until this is satisfied. Next, two intermediate independent random numbers from a standard Gaussian distribution (i.e. $\mu = 0$ and $\sigma = 1$) can be evaluated using the previously determined values of $\mathbf{S}$, $\mathbf{V}_1$ and $\mathbf{V}_2$. These standardised random parameters are $\mathbf{Z}_1$ and $\mathbf{Z}_2$ which are obtained from the expressions determined by Box-Muller as follows

$$Z_1 = V_1 \sqrt{\frac{-2\ln(S)}{S}} \tag{A6.4}$$

and $$Z_2 = V_2 \sqrt{\frac{-2\ln(S)}{S}} \tag{A6.5}$$

A further pair of independent standardised random variables are also generated using the above approach, denoted by $\mathbf{Z}_3$ and $\mathbf{Z}_4$, for which the latter is discarded. The remaining three standardised random numbers (i.e. $\mathbf{Z}_1$, $\mathbf{Z}_2$ and $\mathbf{Z}_3$) are employed in deriving probabilistic axial shortening models based on the MCS.

APPENDIX A6.2

To check the goodness of fit of the data to any PDF, the chi-squared (χ^2) or Kolmogorov-Smirnov (K-S) tests [144,145,149] are necessary. Examining the χ^2 test firstly, the data points are grouped into **k** classes such that each class has at least 5 members. The χ^2 value for the data can then be evaluated by

$$\chi^2 = \sum_{i=1}^{n} \left(\frac{(\text{Freq(data)} - \text{Freq(theory)})^2}{\text{Freq(theory)}} \right) \tag{A6.6}$$

where

Freq(data) = frequency of the data

and Freq(theory) = frequency obtained from the PDF

To disprove the null hypothesis (i.e. the fit of the data to the specified distribution can be rejected), the following condition has to be satisfied

$$\chi^2 > \chi^2_{\alpha,\text{dof}} \tag{A6.7}$$

where

$\text{dof} = k - 1 - p$

α = level of significance (%)

p = number of parameters estimated from data

and $\chi^2_{\alpha,\text{dof}}$ = chi-squared limiting value for testing hypothesis

With the χ^2 test, the data must be grouped into classes and the test depends on an underlining distribution. These requirements are not a condition of the K-S test. This test basically compares the observed cumulative distribution with that from the PDF to be fitted. The K-S statistic is defined by

$$D_n(x) = S_n(x) - F_o(x) \tag{A6.8}$$

where

$S_n(x)$ = portion of samples less than x

and $F_o(x)$ = cumulative distribution of PDF up to x

The following condition has to be satisfied to disprove the null hypothesis

$$D_n(x) > D_{n,\alpha} \tag{A6.9}$$

where $\mathbf{D}_{n,\alpha}$ is the critical value.

APPENDIX A6.3

To check that the random numbers generated by the Box-Muller approach [148] were Gaussian, the χ^2 and K-S tests [144,145,149] were utilised. For the tests conducted, 5 groups of 100,000 and 30 groups of 10,000 random numbers were generated utilising the Box-Muller routine, for which μ=100 and σ=20. A normal distribution has a relative skewness and kurtosis of 0 and 3 respectively. From these tests, the number sets generated were normally distributed. A summary of results are in Table A6.1, where the following definitions are made

n = number of random numbers tested
μ = mean
σ = standard deviation
SK = relative skewness
K = relative kurtosis
$\chi^2 = \chi^2$ test value
$\chi^2_{95\%}$ = maximum acceptable χ^2 value
D_n = K-S statistic
and $D_{n,95\%}$ = maximum acceptable K-S statistic

n	μ	σ	SK	K	χ^2	$\chi^2_{95\%}$	D_n	$D_{n.95\%}$
10^4	100.03	20.01	0.04	2.95	11.79	25.00	0.0079	0.0136
10^4	100.03	20.02	-0.04	3.01	14.42	23.68	0.0086	0.0136
10^4	100.03	19.85	0.03	3.00	12.33	25.00	0.0071	0.0136
10^4	100.18	19.96	0.05	2.98	17.06	25.00	0.0081	0.0136
10^4	99.61	19.75	-0.01	2.94	11.37	25.00	0.0050	0.0136
10^4	100.37	19.97	0.00	3.02	16.53	27.59	0.0060	0.0136
10^4	99.87	19.93	0.01	2.99	8.06	25.00	0.0052	0.0136
10^4	100.05	20.04	0.05	2.95	18.44	23.68	0.0081	0.0136
10^4	100.38	19.89	0.03	2.99	10.94	25.00	0.0067	0.0136
10^4	99.87	19.90	0.00	3.10	20.91	26.30	0.0064	0.0136
10^4	99.61	20.03	0.00	2.94	13.09	23.68	0.0055	0.0136
10^4	99.89	20.04	0.02	2.98	5.99	26.30	0.0075	0.0136
10^4	100.05	19.93	0.00	3.00	18.04	26.30	0.0066	0.0136
10^4	100.11	20.05	-0.01	2.98	19.87	25.00	0.0085	0.0136
10^4	100.05	20.08	0.02	3.00	13.99	25.00	0.0091	0.0136
10^4	99.87	19.95	0.03	3.00	14.14	25.00	0.0090	0.0136
10^4	99.83	20.13	-0.03	3.01	16.86	26.30	0.0056	0.0136
10^4	100.04	19.96	0.01	3.00	16.75	22.36	0.0056	0.0136
10^4	100.22	20.19	-0.01	2.94	12.95	23.68	0.0052	0.0136
10^4	100.03	20.20	0.04	3.04	15.41	25.00	0.0071	0.0136
10^4	100.25	20.05	0.02	2.94	11.88	26.30	0.0040	0.0136
10^4	100.06	20.09	0.02	3.03	15.67	27.59	0.0063	0.0136
10^4	100.02	20.02	0.02	2.98	8.90	25.00	0.0059	0.0136
10^4	99.66	19.97	-0.02	3.03	21.17	25.00	0.0049	0.0136
10^4	100.23	20.07	-0.01	2.95	16.16	26.30	0.0052	0.0136
10^4	99.97	19.99	-0.01	3.04	18.07	26.30	0.0060	0.0136
10^4	100.07	19.99	-0.01	2.97	15.79	25.00	0.0080	0.0136
10^4	99.95	19.97	0.02	3.01	7.23	23.68	0.0047	0.0136
10^4	99.80	19.99	0.03	2.97	9.81	25.00	0.0069	0.0136
10^4	99.95	19.88	0.00	2.99	9.95	26.30	0.0050	0.0136
10^5	99.99	19.94	0.00	3.00	22.88	26.30	0.0017	0.0043
10^5	99.86	20.04	0.00	3.02	7.01	26.30	0.0019	0.0043
10^5	99.95	20.04	0.00	3.00	16.86	25.00	0.0020	0.0043
10^5	100.04	20.03	0.01	3.00	10.84	25.00	0.0018	0.0043
10^5	100.00	19.99	0.01	3.01	9.32	26.30	0.0013	0.0043

Table A6.1 - Summary of tests conducted on random numbers generated by Box-Muller method.

APPENDIX A6.4

Consider a continuous general function **Y** of **n** random variables (X_i) such that all X_i's are statistically independent. Then the expected value and variance are defined by

$$E[Y] = \int_{-\infty}^{\infty}\int_{-\infty}^{\infty}\cdots\int_{-\infty}^{\infty} Y f_{x1}(X_1)\cdots f_{xn}(X_n)\,dX_1\cdots dX_n \qquad \text{(A6.10)}$$

and

$$Var[Y] = \int_{-\infty}^{\infty}\int_{-\infty}^{\infty}\cdots\int_{-\infty}^{\infty} (Y - E[Y])^2 f_{x1}(X_1)\cdots f_{xn}(X_n)\,dX_1\cdots dX_n \qquad \text{(A6.11)}$$

where

$Y = g(X_1, X_2, X_3, \ldots, X_n)$

X_i = i^{th} random variable

and $f_{xi}(X_i)$ = probability density function of X_i

The solution of the expected value and variance, (A6.10) and (A6.11), of the general function **Y** with **n** independent random variables is complex and in general cannot be obtained in closed form. It is therefore necessary to the solutions to approximate these equations. One method is to approximate the general function by the Taylor series expansion [144,145]. A second is to use a polynomial approximation. The latter is not employed here, but the process is outlined in [150,151]. For a Taylor series approximation, complete knowledge of the PDF is not required.

The Taylor series expansion of the general function **Y**, about the mean value is

$$Y = g(\mu_{x1},\mu_{x2},\mu_{x3},\ldots,\mu_{xn}) + \sum_{i=1}^{n}\left((X_i-\mu_{xi})\frac{\partial g}{\partial X_i}\right) + \frac{1}{2}\sum_{i=1}^{n}\sum_{j=1}^{n}\left((X_i-\mu_{xi})(X_j-\mu_{xj})\frac{\partial^2 g}{\partial X_i \partial X_j}\right) + \frac{1}{6}\sum_{i=1}^{n}\sum_{j=1}^{n}\sum_{k=1}^{n}\left((X_i-\mu_{xi})(X_j-\mu_{xj})(X_k-\mu_{xk})\frac{\partial^3 g}{\partial X_i \partial X_j \partial X_k}\right) + \ldots \quad \text{(A6.12)}$$

For a first-order moment analysis, only the first two terms of (A6.12) are used which are then substituted into the basic moment equations (i.e. (A6.10) and (A6.11)). The final expressions for the expected value and variance reduce respectively to

$$E[Y] = g(\mu_{x1},\ldots,\mu_{xn}) \quad \text{(A6.13)}$$

and

$$Var[Y] = \sum_{i=1}^{n}\left(Var[X_i]\left(\frac{\partial g}{\partial X_i}\right)^2\right) \quad \text{(A6.14)}$$

For a second-order moment analysis, the first three terms of (A6.12) are utilised, for which the resulting equations for expected value and variance are respectively

$$E[Y] = g(\mu_{x1},\ldots,\mu_{xn}) + \frac{1}{2}\sum_{i=1}^{n}\left(Var[X_i]\frac{\partial^2 g}{\partial X_i^{\,2}}\right) \quad \text{(A6.15)}$$

and

$$Var[Y] = \sum_{i=1}^{n}\left(Var[X_i]\left(\frac{\partial g}{\partial X_i}\right)^2\right) + \frac{1}{4}\sum_{i=1}^{n}\left(K[X_i]\left(\frac{\partial^2 g}{\partial X_i^{\,2}}\right)^2\right) - \frac{1}{4}\sum_{i=1}^{n}\left(Var^2[X_i]\left(\frac{\partial^2 g}{\partial X_i^{\,2}}\right)^2\right) + \sum_{i=1}^{n}\left(SK[X_i]\left(\frac{\partial^2 g}{\partial X_i^{\,2}}\right)\left(\frac{\partial g}{\partial X_i}\right)\right) \quad \text{(A6.16)}$$

As the PDFs are normally distributed (Gaussian properties are given in Appendix A6.5), (A6.19) is incorporated into the latter expression which simplifies to

$$\mathrm{Var}[Y] = \sum_{i=1}^{n}\left(\mathrm{Var}[X_i]\left(\frac{\partial g}{\partial X_i}\right)^2\right) + \frac{1}{2}\sum_{i=1}^{n}\left(\mathrm{Var}^2[X_i]\left(\frac{\partial^2 g}{\partial X_i{}^2}\right)^2\right) \qquad \text{(A6.17)}$$

The second-order moment analysis is not applicable for PDFs with large values of the coefficient of variation (COV). This formulation embodies to a large extent the non-linearity of the general function, however, consideration of higher-order moments to improve the non-linear description is avoided due to algebraic complexity. As the Gaussian PDF is symmetrical, the expected value of **Y** for a third-order moment analysis is identical to the second-order equation.

APPENDIX A6.5

The Gaussian probability density function is given by

$$f_x(X) = \frac{1}{\sigma\sqrt{2\pi}} e^{\left(-\frac{1}{2}\left(\frac{X-\mu}{\sigma}\right)^2\right)} \qquad \text{(A6.18)}$$

where

σ = standard deviation

μ = mean

and $-\infty < X < \infty$

The expected value, variance, relative skewness and relative kurtosis for this distribution follow respectively

$$\left.\begin{aligned} E[X] &= \mu \\ Var[X] &= \sigma^2 \\ SK_{rel}[X] &= 0 \\ K_{rel}[X] &= 3 \end{aligned}\right\} \qquad \text{(A6.19)}$$

APPENDIX A6.6

A 39 storey building constructed in Brisbane at a height of 162m was completed in 1990 [2]. The axial shortening case-studies, examined in Chapter 8 of this thesis, are based on the data of this building and its construction.

The construction cycle period T_c is 10 days, with 20 days delay in start of the outer frame. The in-service loads are applied 180 days after completion of each floor. Long-term axial shortening predictions are made 1000 days after the level one service core was poured. Temperature and relative humidity of the environment are constant at 20°C and 50% respectively. All loads are estimated average values obtained from the consultant involved in the design of the building. A list of concrete and column properties of, and loads applied to the service core are summarised in the tables to follow, where the following definitions are made

ρ = concrete density (kg/m^3)
c = cement content (kg/m^3)
w / c = water-cement ratio of concrete
a / c = total aggregate-cement ratio of concrete
s / c = sand-cement ratio of concrete
a = percentage air in concrete by volume (%)
A_t = cross-sectional column area (m^2)
p_a = steel reinforcement ratio (%)
L = length of column (m)
and u = perimeter of column (m)

Storeys	Concrete Mix	ρ (kg/m^3)	c (kg/m^3)
1 to 30	40 MPa	2450	395
31 to 39	30 MPa	2450	325

Storeys	w/c ratio	a/c ratio	s/c ratio
1 to 30	0.43	4.8	1.68
31 to 39	0.52	5.91	2.31

Storeys	a (%)	Slump (mm)	Aggregate type
1 to 30	2.5	100	Basalt
31 to 39	3.5	100	Basalt

Storeys	A_t (m^2)	p_a (%)	L (m)	u (m)
1 to 2	10.74	0.2	3	41.9
3	10.74	0.2	10.8	41.9
4	8.53	0.2	5.4	41.1
5 to 39	8.53	0.2	3.6	41.1

Storeys	Construction load (kN)	In-Service load (kN)	Self-weight (kN)
1	1829.4	322.8	777.81
2	2003.6	353.6	777.81
3	5444.2	960.7	2800.10
4	3177.3	560.7	1111.96
5 to 15	2485.1	438.5	741.31
16 to 17	2876.1	507.5	741.31
18	2557.4	451.3	741.31
19 to 27	2485.1	438.5	741.31
28 to 29	3938.6	695	741.31
30	3896.1	687.5	741.31
31 to 38	2485.1	438.5	741.31
39	6467.4	1141.3	741.31

A list of concrete and column properties of, and loads applied to the outer spandrel frame columns are summarised in the tables to follow

Storeys	Concrete Mix	ρ (kg/m^3)	c (kg/m^3)
1 to 2	40 MPa	2450	395
3	50 MPa	2450	485
4 to 9	60 MPa	2450	520
10 to 30	50 MPa	2450	485
31 to 39	30 MPa	2450	325

Storeys	w/c ratio	a/c ratio	s/c ratio
1 to 2	0.43	4.8	1.68
3	0.35	3.79	1.13
4 to 9	0.33	3.47	0.99
10 to 30	0.35	3.79	1.13
31 to 39	0.52	5.91	2.31

Storeys	a (%)	Slump (mm)	Aggregate type
1 to 2	2.5	100	Basalt
3	2	100	Basalt
4 to 9	1.5	100	Basalt
10 to 30	2	100	Basalt
31 to 39	3.5	100	Basalt

Storeys	A_t (m^2)	p_a (%)	L (m)	u (m)
1 to 2	1.43	1	3	4.24
3	1.43	1	10.8	4.24
4	0.87	2.8	5.4	3.3
5 to 10	0.87	2.8	3.6	3.3
11 to 30	0.87	2.4	3.6	3.3
31 to 39	0.87	1.1	3.6	3.3

Storeys	Construction load (kN)	In-Service load (kN)	Self-weight (kN)
1	768.9	135.7	105.38
2	836.9	147.7	105.38
3	247	43.6	379.37
4	399.6	70.5	119.88
5 to 10	433.6	76.5	79.92
11 to 15	434.1	76.6	79.26
16 to 17	468.1	82.6	79.26
18 to 27	434.1	76.6	79.26
28 to 30	757.1	133.6	79.26
31 to 38	436	76.9	77.10
39	1184	208.9	77.10

APPENDIX A6.7

A6.7.1 FIRST- AND SECOND-ORDER MOMENT STOCHASTIC COLUMN MODELS

First-order moment equations are firstly derived for the TBEMM, whilst the FEMM can be considered a subset of this with the aging coefficient set to unity.

The governing expressions for describing uncertainty in the output results, based on first- and second-order moment formulations for a general function with a finite number of correlated random variables, are derived in Appendix A6.8. These expressions are not readily available in the form required here and were derived from first principles. Also, well known properties of the multivariate Gaussian distribution are given in Appendix A6.9.

Substitution of the deterministic column models into (A6.46) and (A6.47) results in the final first-order moment expressions which follow. For $\mathbf{k}_j$ loads applied on the $\mathbf{j}^{th}$ storey column, the expected value and variance of the total cumulative shortening are respectively

$$E[\delta_{long,j,a}] = \delta_{long,j,a} \tag{A6.20}$$

and

$$Var[\delta_{long,j,a}] = Var[\varepsilon'_{sh}(t_d)] + Var[\phi'(t,s)] + Var[E'_c(s)] \tag{A6.21}$$

where

$\delta_{long,j,a}$ = long-term cumulative shortening of j^{th} storey Column "a"

$k_{all,long,j,a} = \sum_{i=1}^{j} k_{long,i,a}$

$k_{all,long,j,a}$ = entire load set applied between levels 1 and j to Column "a" for determining long-term cumulative shortening

$k_{long,i,a}$ = load set applied at level i to Column "a" for determining long-term cumulative shortening

st(x) = corresponding level and column for applied load x

E[X] = expected value of X

Var[X] = variance of X

and Var[X′] = variance of first-order X terms

Here, $\delta_{long,j,a}$ is obtained from (5.17) based on the TBEMM.

The first-order variance approximation terms due to each independent random parameter (i.e. basic shrinkage strain, creep coefficient and elastic modulus) which are employed in (A6.21) are given to be respectively

$$Var[\varepsilon'_{sh}(t_d)] = \sum_{x=1}^{j}\sum_{y=1}^{j}\left(\eta_x\eta_y Cov[\zeta_x,\zeta_y]\right) \tag{A6.22}$$

$$Var[\phi'(t,s)] = \sum_{x=1}^{k_{all,long,j,a}}\sum_{y=1}^{k_{all,long,j,a}}\left(\lambda_x\lambda_y Cov[\theta_x,\theta_y]\right) \tag{A6.23}$$

$$Var[E'_c(s)] = \sum_{x=1}^{k_{all,long,j,a}}\sum_{y=1}^{k_{all,long,j,a}}\left(\xi_x\xi_y Cov[\tau_x,\tau_y]\right) \tag{A6.24}$$

where

$$\zeta_x = \varepsilon_{sh}(t_{d,x})$$

$$\theta_x = \phi(t_{st(x)}, s_{st(x)})$$

$$\tau_x = E_c(s_{st(x)})$$

$$\eta_x = \frac{L_x E_c(t_{sh,x})}{d_3(t_x, t_{sh,x})}$$

for first loading:

$$\lambda_x = \frac{P_{st(x)}L_{st(x)}E_c(s_{st(x)})}{A_{c,st(x)}d_3(t_{st(x)},s_{st(x)})^2} - \frac{\varepsilon_{sh}(t_{st(x)})L_{st(x)}E_c(t_{sh,st(x)})p_{a,st(x)}E_s\chi(t_{st(x)},t_{sh,st(x)})}{d_3(t_{st(x)},t_{sh,st(x)})^2}$$

$$\xi_x = \frac{L_{st(x)}p_{a,st(x)}E_s\varepsilon_{sh}(t_{st(x)})d_1(t_{st(x)},t_{sh,st(x)})}{d_3(t_{st(x)},t_{sh,st(x)})^2} - \frac{P_{st(x)}L_{st(x)}}{A_{c,st(x)}d_2(s_{st(x)})^2} - \frac{P_{st(x)}L_{st(x)}\phi(t_{st(x)},s_{st(x)})[E_c(s_{st(x)})^2 - p_{a,st(x)}{}^2E_s{}^2d_1(t_{st(x)},s_{st(x)})]}{A_{c,st(x)}d_2(s_{st(x)})^2 d_3(t_{st(x)},s_{st(x)})^2}$$

and for subsequent loading:

$$\lambda_x = \frac{P_{st(x)}L_{st(x)}E_c(s_{st(x)})}{A_{c,st(x)}d_3(t_{st(x)},s_{st(x)})^2}$$

$$\xi_x = \frac{-P_{st(x)}L_{st(x)}}{A_{c,st(x)}d_2(s_{st(x)})^2} - \frac{P_{st(x)}L_{st(x)}\phi(t_{st(x)},s_{st(x)})[E_c(s_{st(x)})^2 - p_{a,st(x)}{}^2E_s{}^2d_1(t_{st(x)},s_{st(x)})]}{A_{c,st(x)}d_2(s_{st(x)})^2 d_3(t_{st(x)},s_{st(x)})^2}$$

where

$d_1(x,y) = 1+\chi(x,y)\phi(x,y)$

$d_2(x) = E_c(x)+p_aE_s$

$d_3(x,y) = E_c(y)+p_aE_sd_1(x,y)$

$p_a = \frac{A_s}{A_c}$

$p_{a,st(x)} = \frac{A_{s,st(x)}}{A_{c,st(x)}}$

$t_{d,st(x)} = t_{st(x)} - t_{sh,st(x)}$

A_s = cross-sectional area of steel

A_c = cross-sectional area of concrete

$A_{s,st(x)}$ = cross-sectional area of steel in column st(x)

$A_{c,st(x)}$ = cross-sectional area of concrete in column st(x)

$Cov[X,Y]$ = covariance of X and Y

$E_c(x)$ = concrete elastic modulus at time x days

E_s = steel reinforcement elastic modulus

$L_{st(x)}$ = length of column st(x)

$s_{st(x)}$ = loading age of column st(x)

$P_{st(x)}$ = load applied to column st(x)

$t_{d,st(x)}$ = drying period of column st(x)

$t_{st(x)}$ = total age of column st(x)

$t_{sh,st(x)}$ = age of column st(x) at onset of drying

$\chi(x,y)$ = aging coefficient with a total column age of x days and a loading age of y days

$\phi(x,y)$ = creep coefficient with a total column age of x days and a loading age of y days

and $\varepsilon_{sh}(x)$ = free shrinkage strain at time x days

The second-order moment equations for the TBEMM can similarly be obtained. The expected value and variance of the total cumulative shortening due to $\mathbf{k}_j$ loads applied on the $\mathbf{j}^{th}$ storey column are respectively

$$E[\delta_{long,j,a}] = \delta_{long,j,a} + E[\phi''(t,s)] + E[E_c''(s)] \tag{A6.25}$$

and

$$\begin{aligned} Var[\delta_{long,j,a}] = {} & Var[\varepsilon'_{sh}(t_d)] + Var[\phi'(t,s)] + Var[E'_c(s)] \\ & + Var[\phi''(t,s)] + Var[E''_c(s)] \end{aligned} \tag{A6.26}$$

where

$E[X'']$ = expected value of second-order X terms

and $Var[X'']$ = variance of second-order X terms

The additional second-order variance approximation terms due to each independent random parameter (i.e. creep coefficient and elastic modulus) which are employed in (A6.26) are given to be respectively

$$Var[\phi''(t,s)] = \frac{1}{2}\sum_{x=1}^{k_{all,long,j,a}}\sum_{y=1}^{k_{all,long,j,a}}\left(\alpha_x \alpha_y Cov^2[\theta_x, \theta_y]\right) \tag{A6.27}$$

$$Var[E_c''(s)] = \frac{1}{2}\sum_{x=1}^{k_{all,long,j,a}}\sum_{y=1}^{k_{all,long,j,a}}\left(\psi_x \psi_y Cov^2[\tau_x, \tau_y]\right) \tag{A6.28}$$

where for first loading:

$$\begin{aligned} \alpha_x = {} & \frac{2\varepsilon_{sh}(t_{st(x)})L_{st(x)}E_c(t_{sh,st(x)})p_{a,st(x)}{}^2E_s{}^2\chi(t_{st(x)},t_{sh,st(x)})^2}{d_3(t_{st(x)},t_{sh,st(x)})^3} \\ & - \frac{2P_{st(x)}L_{st(x)}E_c(s_{st(x)})p_{a,st(x)}E_s\chi(t_{st(x)},s_{st(x)})}{A_{c,st(x)}d_3(t_{st(x)},s_{st(x)})^3} \end{aligned}$$

$$\begin{aligned} \psi_x = {} & \frac{-2L_{st(x)}p_{a,st(x)}E_s\varepsilon_{sh}(t_{st(x)})d_1(t_{st(x)},t_{sh,st(x)})}{d_3(t_{st(x)},t_{sh,st(x)})^3} \\ & + \frac{2P_{st(x)}L_{st(x)}}{A_{c,st(x)}d_2(s_{st(x)})^3} - \frac{2P_{st(x)}L_{st(x)}\phi(t_{st(x)},s_{st(x)})E_c(s_{st(x)})}{A_{c,st(x)}d_2(s_{st(x)})^2d_3(t_{st(x)},s_{st(x)})^2} \\ & + \frac{2P_{st(x)}L_{st(x)}\phi(t_{st(x)},s_{st(x)})[E_c(s_{st(x)})^2 - p_{a,st(x)}{}^2E_s{}^2d_1(t_{st(x)},s_{st(x)})]}{A_{c,st(x)}d_2(s_{st(x)})^3d_3(t_{st(x)},s_{st(x)})^3} \\ & \times [d_2(s_{st(x)}) + d_3(t_{st(x)},s_{st(x)})] \end{aligned}$$

and for subsequent loading:

$$\alpha_x = \frac{-2P_{st(x)}L_{st(x)}E_c(s_{st(x)})p_{a,st(x)}E_s\chi(t_{st(x)},s_{st(x)})}{A_{c,st(x)}d_3(t_{st(x)},s_{st(x)})^3}$$

$$\psi_x = \frac{2P_{st(x)}L_{st(x)}}{A_{c,st(x)}d_2(s_{st(x)})^3} - \frac{2P_{st(x)}L_{st(x)}\phi(t_{st(x)},s_{st(x)})E_c(s_{st(x)})}{A_{c,st(x)}d_2(s_{st(x)})^2 d_3(t_{st(x)},s_{st(x)})^2}$$
$$+ \frac{2P_{st(x)}L_{st(x)}\phi(t_{st(x)},s_{st(x)})[E_c(s_{st(x)})^2 - p_{a,st(x)}{}^2E_s{}^2d_1(t_{st(x)},s_{st(x)})]}{A_{c,st(x)}d_2(s_{st(x)})^3 d_3(t_{st(x)},s_{st(x)})^3}$$
$$\times [d_2(s_{st(x)}) + d_3(t_{st(x)},s_{st(x)})]$$

The additional second-order expected value approximation terms due to each independent random parameter (i.e. creep coefficient and elastic modulus) which are employed in (A6.25) are given to be respectively

$$E[\phi''(t,s)] = \frac{1}{2}\sum_{x=1}^{k_{all,long,j,a}}(\alpha_x Var[\theta_x]) \qquad \text{(A6.29)}$$

$$E[E_c''(s)] = \frac{1}{2}\sum_{x=1}^{k_{all,long,j,a}}(\psi_x Var[\tau_x]) \qquad \text{(A6.30)}$$

Considering a first-order moment differential analysis between column pairs, the expected value and variance of differential movement at the **j**th storey level are respectively

$$E[\Delta_{f,j}] = \delta_{long,j,1} - \delta_{long,j,2} \qquad \text{(A6.31)}$$

and

$$Var[\Delta_{f,j}] = Var[\varepsilon'_{sh}(t_d)] + Var[\phi'(t,s)] + Var[E'_c(s)] \qquad \text{(A6.32)}$$

where

$\Delta_{f,j} = \delta_{long,j,1} - \delta_{long,j,2}$

$\Delta_{f,j}$ = long-term differential column shortening at jth storey

$k_{all,long,j,a+b} = \sum_{i=1}^{j}(k_{long,i,a} + k_{long,i,b})$

and $k_{all,long,j,a+b}$ = entire load set applied between levels 1 and j to Columns "a" and "b" for determining long-term cumulative shortening

The first-order variance approximation terms due to each independent random parameter (i.e. basic shrinkage strain, creep coefficient and elastic modulus) which are employed in (A6.32) are given to be respectively

$$\mathrm{Var}[\varepsilon'_{sh}(t_d)] = \sum_{x=1}^{2j}\sum_{y=1}^{2j}\left(\eta_x \eta_y \mathrm{Cov}[\zeta_x, \zeta_y]\right) \tag{A6.33}$$

$$\mathrm{Var}[\phi'(t,s)] = \sum_{x=1}^{k_{all,long,j,a+b}}\sum_{y=1}^{k_{all,long,j,a+b}}\left(\lambda_x \lambda_y \mathrm{Cov}[\theta_x, \theta_y]\right) \tag{A6.34}$$

$$\mathrm{Var}[E'_c(s)] = \sum_{x=1}^{k_{all,long,j,a+b}}\sum_{y=1}^{k_{all,long,j,a+b}}\left(\xi_x \xi_y \mathrm{Cov}[\tau_x, \tau_y]\right) \tag{A6.35}$$

where

$$\zeta_x = \varepsilon_{sh}(t_{d,\bar{x}})$$

$$\eta_x = \overline{\eta}_x \qquad x \le j$$
$$\eta_x = -\overline{\eta}_x \qquad x > j$$

$$\overline{\eta}_x = \frac{L_{\bar{x}} E_c(t_{sh,\bar{x}})}{d_3(t_{\bar{x}}, t_{sh,\bar{x}})}$$

$$\left.\begin{array}{ll} \bar{x} = x & x \le j \\ \bar{x} = x - j & x > j \end{array}\right\} \text{ for Equation (A6.33)}$$

$$\theta_x = \phi(t_{st(\bar{x})}, s_{st(\bar{x})})$$

$$\lambda_x = \overline{\lambda}_x \qquad x \le k_{all,long,j,a}$$
$$\lambda_x = -\overline{\lambda}_x \qquad x > k_{all,long,j,a}$$

$$\tau_x = E_c(s_{st(\bar{x})})$$

$$\xi_x = \overline{\xi}_x \qquad x \le k_{all,long,j,a}$$
$$\xi_x = -\overline{\xi}_x \qquad x > k_{all,long,j,a}$$

$$\left.\begin{array}{ll} \bar{x} = x & x \le k_{all,long,j,a} \\ \bar{x} = x - k_{all,long,j,a} & x > k_{all,long,j,a} \end{array}\right\} \text{ for Equations (A6.34) and (A6.35)}$$

where for first loading:

$$\bar{\lambda}_x = \frac{P_{st(\bar{x})} L_{st(\bar{x})} E_c(s_{st(\bar{x})})}{A_{c,st(\bar{x})} d_3(t_{st(\bar{x})}, s_{st(\bar{x})})^2} - \frac{\varepsilon_{sh}(t_{st(\bar{x})}) L_{st(\bar{x})} E_c(t_{sh,st(\bar{x})}) p_{a,st(\bar{x})} E_s \chi(t_{st(\bar{x})}, t_{sh,st(\bar{x})})}{d_3(t_{st(\bar{x})}, t_{sh,st(\bar{x})})^2}$$

$$\bar{\xi}_x = \frac{L_{st(\bar{x})} p_{a,st(\bar{x})} E_s \varepsilon_{sh}(t_{st(\bar{x})}) d_1(t_{st(\bar{x})}, t_{sh,st(\bar{x})})}{d_3(t_{st(\bar{x})}, t_{sh,st(\bar{x})})^2} - \frac{P_{st(\bar{x})} L_{st(\bar{x})}}{A_{c,st(\bar{x})} d_2(s_{st(\bar{x})})^2} - \frac{P_{st(\bar{x})} L_{st(\bar{x})} \phi(t_{st(\bar{x})}, s_{st(\bar{x})}) [E_c(s_{st(\bar{x})})^2 - p_{a,st(\bar{x})}{}^2 E_s{}^2 d_1(t_{st(\bar{x})}, s_{st(\bar{x})})]}{A_{c,st(\bar{x})} d_2(s_{st(\bar{x})})^2 d_3(t_{st(\bar{x})}, s_{st(\bar{x})})^2}$$

and for subsequent loading:

$$\bar{\lambda}_x = \frac{P_{st(\bar{x})} L_{st(\bar{x})} E_c(s_{st(\bar{x})})}{A_{c,st(\bar{x})} d_3(t_{st(\bar{x})}, s_{st(\bar{x})})^2}$$

$$\bar{\xi}_x = \frac{-P_{st(\bar{x})} L_{st(\bar{x})}}{A_{c,st(\bar{x})} d_2(s_{st(\bar{x})})^2} - \frac{P_{st(\bar{x})} L_{st(\bar{x})} \phi(t_{st(\bar{x})}, s_{st(\bar{x})}) [E_c(s_{st(\bar{x})})^2 - p_{a,st(\bar{x})}{}^2 E_s{}^2 d_1(t_{st(\bar{x})}, s_{st(\bar{x})})]}{A_{c,st(\bar{x})} d_2(s_{st(\bar{x})})^2 d_3(t_{st(\bar{x})}, s_{st(\bar{x})})^2}$$

Considering a second-order moment differential analysis between column pairs, the expected value and variance of differential movement at the **j**th storey level are given to be

$$E[\Delta_{f,j}] = \delta_{long,j,1} - \delta_{long,j,2} + E[\phi''(t,s)] + E[E_c''(s)] \tag{A6.36}$$

and

$$\begin{aligned} Var[\Delta_{f,j}] = {} & Var[\varepsilon_{sh}'(t_d)] + Var[\phi'(t,s)] + Var[E_c'(s)] \\ & + Var[\phi''(t,s)] + Var[E_c''(s)] \end{aligned} \tag{A6.37}$$

The additional second-order variance approximation terms due to each independent random parameter (i.e. creep coefficient and elastic modulus) which are employed in (A6.37) are given to be respectively

$$\mathrm{Var}[\phi''(t,s)] = \frac{1}{2}\sum_{x=1}^{k_{all,long,j,a+b}}\sum_{y=1}^{k_{all,long,j,a+b}}\left(\alpha_x\alpha_y \mathrm{Cov}^2[\theta_x,\theta_y]\right) \tag{A6.38}$$

$$\mathrm{Var}[E_c''(s)] = \frac{1}{2}\sum_{x=1}^{k_{all,long,j,a+b}}\sum_{y=1}^{k_{all,long,j,a+b}}\left(\psi_x\psi_y \mathrm{Cov}^2[\tau_x,\tau_y]\right) \tag{A6.39}$$

where

$$\alpha_x = \overline{\alpha}_x \qquad x \le k_{all,long,j,a}$$
$$\alpha_x = -\overline{\alpha}_x \qquad x > k_{all,long,j,a}$$

$$\psi_x = \overline{\psi}_x \qquad x \le k_{all,long,j,a}$$
$$\psi_x = -\overline{\psi}_x \qquad x > k_{all,long,j,a}$$

$$\overline{x} = x \qquad x \le k_{all,long,j,a}$$
$$\overline{x} = x - k_{all,long,j,a} \qquad x > k_{all,long,j,a}$$

where for first loading:

$$\overline{\alpha}_x = \frac{2\varepsilon_{sh}(t_{st(\overline{x})})L_{st(\overline{x})}E_c(t_{sh,st(\overline{x})})p_{a,st(\overline{x})}{}^2E_s{}^2\chi(t_{st(\overline{x})},t_{sh,st(\overline{x})})^2}{d_3(t_{st(\overline{x})},t_{sh,st(\overline{x})})^3} - \frac{2P_{st(\overline{x})}L_{st(\overline{x})}E_c(s_{st(\overline{x})})p_{a,st(\overline{x})}E_s\chi(t_{st(\overline{x})},s_{st(\overline{x})})}{A_{c,st(\overline{x})}d_3(t_{st(\overline{x})},s_{st(\overline{x})})^3}$$

$$\overline{\psi}_x = \frac{-2L_{st(\overline{x})}p_{a,st(\overline{x})}E_s\varepsilon_{sh}(t_{st(\overline{x})})d_1(t_{st(\overline{x})},t_{sh,st(\overline{x})})}{d_3(t_{st(\overline{x})},t_{sh,st(\overline{x})})^3} + \frac{2P_{st(\overline{x})}L_{st(\overline{x})}}{A_{c,st(\overline{x})}d_2(s_{st(\overline{x})})^3} - \frac{2P_{st(\overline{x})}L_{st(\overline{x})}\phi(t_{st(\overline{x})},s_{st(\overline{x})})E_c(s_{st(\overline{x})})}{A_{c,st(\overline{x})}d_2(s_{st(\overline{x})})^2d_3(t_{st(\overline{x})},s_{st(\overline{x})})^2}$$
$$+ \frac{2P_{st(\overline{x})}L_{st(\overline{x})}\phi(t_{st(\overline{x})},s_{st(\overline{x})})[E_c(s_{st(\overline{x})})^2 - p_{a,st(\overline{x})}{}^2E_s{}^2d_1(t_{st(\overline{x})},s_{st(\overline{x})})]}{A_{c,st(\overline{x})}d_2(s_{st(\overline{x})})^3d_3(t_{st(\overline{x})},s_{st(\overline{x})})^3}$$
$$\times\ [d_2(s_{st(\overline{x})}) + d_3(t_{st(\overline{x})},s_{st(\overline{x})})]$$

and for subsequent loading:

$$\overline{\alpha}_x = \frac{-2P_{st(\overline{x})}L_{st(\overline{x})}E_c(s_{st(\overline{x})})p_{a,st(\overline{x})}E_s\chi(t_{st(\overline{x})},s_{st(\overline{x})})}{A_{c,st(\overline{x})}d_3(t_{st(\overline{x})},s_{st(\overline{x})})^3}$$

$$\overline{\psi}_x = \frac{2P_{st(\bar{x})}L_{st(\bar{x})}}{A_{c,st(\bar{x})}d_2(s_{st(\bar{x})})^3} - \frac{2P_{st(\bar{x})}L_{st(\bar{x})}\phi(t_{st(\bar{x})},s_{st(\bar{x})})E_c(s_{st(\bar{x})})}{A_{c,st(\bar{x})}d_2(s_{st(\bar{x})})^2 d_3(t_{st(\bar{x})},s_{st(\bar{x})})^2}$$
$$+\frac{2P_{st(\bar{x})}L_{st(\bar{x})}\phi(t_{st(\bar{x})},s_{st(\bar{x})})[E_c(s_{st(\bar{x})})^2 - p_{a,st(\bar{x})}{}^2E_s{}^2d_1(t_{st(\bar{x})},s_{st(\bar{x})})]}{A_{c,st(\bar{x})}d_2(s_{st(\bar{x})})^3 d_3(t_{st(\bar{x})},s_{st(\bar{x})})^3}$$
$$\times [d_2(s_{st(\bar{x})}) + d_3(t_{st(\bar{x})},s_{st(\bar{x})})]$$

The additional second-order expected value approximation terms due to each independent random parameter (i.e. creep coefficient and elastic modulus) which are employed in (A6.36) are given to be respectively

$$E[\phi''(t,s)] = \frac{1}{2}\sum_{x=1}^{k_{all,long,j,a+b}}(\alpha_x \mathrm{Var}[\theta_x]) \tag{A6.40}$$

$$E[E_c''(s)] = \frac{1}{2}\sum_{x=1}^{k_{all,long,j,a+b}}(\psi_x \mathrm{Var}[\tau_x]) \tag{A6.41}$$

All of the above expressions describe the first- and second-order moment equations for axial shortening of reinforced concrete columns and the differential behaviour between column pairs. The concrete properties, i.e. the creep coefficient, basic shrinkage strain and modulus, are modelled as Gaussian processes in which each process is statistically independent. Thus, time series correlations within each property are accounted for in the advanced model analysis.

A6.7.2 MONTE CARLO STOCHASTIC COLUMN MODELS

A probabilistic reinforced concrete column shortening model based on Monte Carlo simulation (MCS) is outlined here. The output shortening results are used for comparison with those from both a first- and second-order moment analysis. As in Chapter 6, the simplifying assumption of a Taylor series approximation in the derivation is assessed.

With a Monte Carlo model, numerous deterministic runs are required where, in each run, the random parameter values used are those generated from a Gaussian process. The result is that the set of deterministic output values obtained represent a sample of the true population.

The MCS application requires an efficient Gaussian process number generator. Since only a finite number of locations within each stochastic process are necessary for any shortening analysis, a multivariate Gaussian random number generator can be used (for example, as supplied with any FORTRAN subroutine library). The approach employed by the subroutine basically determines the Cholesky decomposition matrix from the input covariance matrix first, then determines a vector with random outcomes from a standard multivariate normal distribution and finally transforms this vector to outcomes from a general distribution.

A6.7.3 COMPUTATIONAL ALGORITHM

The complex loading history and building structure idealisations made in Chapter 2 are merged with the probabilistic column model developed in this chapter and have subsequently been incorporated into an algorithm. Comparisons between the deterministic results from the software written in FORTRAN and those produced from Beasley's program [13] show good agreement (see Figure A6.1).

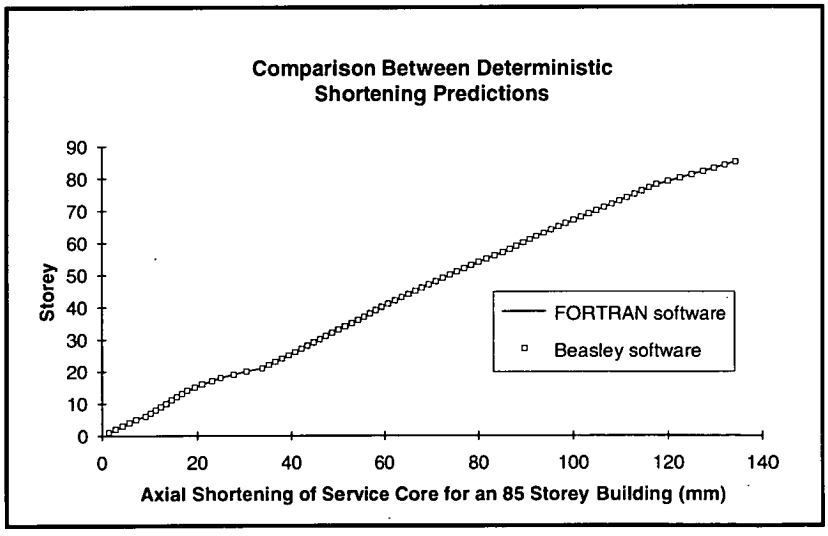

Figure A6.1 - Comparison of deterministic axial shortening values obtained from the software developed here and that from Beasley [13] for an example 85 storey building.

Employing a 486-66DX2 machine with 20 Mbytes RAM the second-order moment analysis of a 40 storey building takes approximately twenty three hours, whilst this time is reduced to eight CPU hours on a Sun 670/514MP station with 4x50MHz Supersparc processors running a Solaris 2.3 operating system. For comparison, a tall building analysis based on a second-order moment probabilistic column model developed at the start of Chapter 6 requires 4 seconds of CPU time

on the PC (see Table 7.1). Figure A6.2 shows the CPU analysis time for a second-order moment analysis as a function of storey levels for the case of the three random parameters in the analysis, namely creep, shrinkage and modulus. Figure A6.3 shows the CPU computational times for a 40 storey building analysis employing the Monte Carlo method. Here, determination of the Cholesky decomposition matrices need only be done once at the beginning of the analysis, taking approximately 84 CPU minutes for 40 storeys.

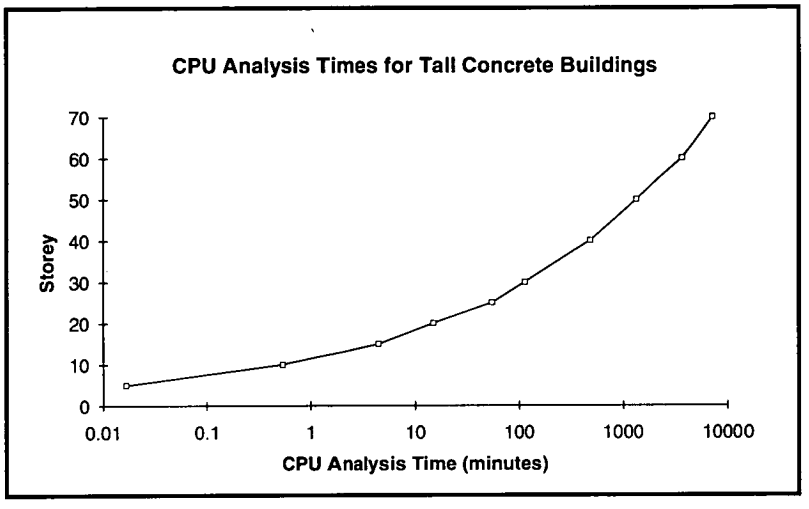

Figure A6.2 - Tall building analysis times employing second-order moment theory on a Sun 670/514MP station.

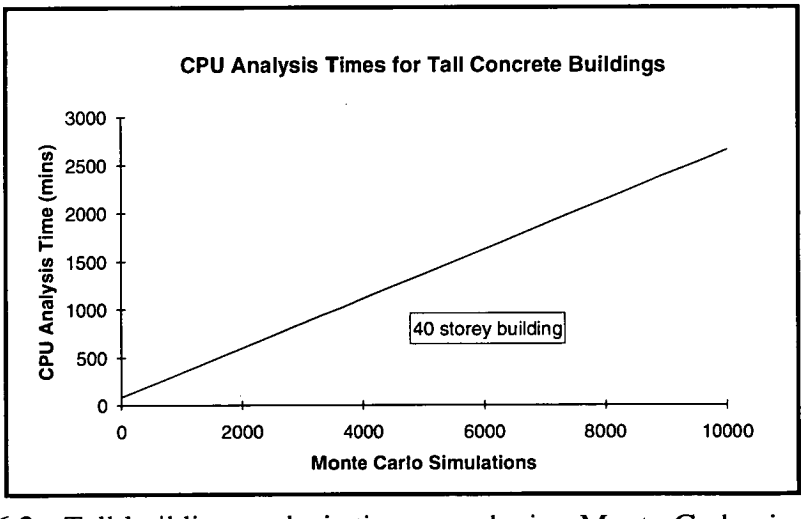

Figure A6.3 - Tall building analysis times employing Monte Carlo simulation on a Sun 670/514MP station.

The array sizes employed in the analyses prompted the use of a workstation FORTRAN compiler in preference to a PC compiler. Considering a 40 storey building with 3 instantaneously applied loads per storey, 120 separate loads for each of the column pairs in the structural system need to be processed (see

Chapter 2). To calculate the axial shortening at the top storey for both column pairs using MCS requires four 3.1×10^6 square covariance matrices with four 3.1×10^6 length mean vectors for the elastic/inelastic random variables, whilst two 800 square covariance matrices with two 800 length mean vectors for the shrinkage random variables. For a 100 storey building, four 114.8×10^6 square matrices, four 114.8×10^6 length vectors, two 5050 square matrices and two 5050 length vectors respectively, are necessary.

The majority of the MCS analysis time is spent calculating the Cholesky decomposition matrices from the covariance matrices. For the same 40 storey building above, the number of computations necessary to predict variances of axial shortenings using the second-order moment equations developed here is interesting. To determine the variance of total shortening at every level for both column pairs requires 10.4×10^8 numeric calculations, whilst additional 20.9×10^8 numeric calculations are necessary for differential shortening predictions also. For a 100 storey building the number of computations are 39.3×10^8 and 78.7×10^8 respectively.

The main steps involved in a first- or second-order moment analysis, for the prediction of total shortening and differential movement between column pairs, are as follows:

- Load input data from file
- Determine column and loading ages
- Calculate deterministic long-term total and differential shortening values
- Calculate numeric first-order shrinkage derivatives
- Calculate numeric first- and second-order creep derivatives
- Calculate numeric first- and second-order modulus derivatives
- Cumulate numeric first- and second-order derivatives for both column pairs
- Calculate expected values and variances of total and differential shortening between column pairs
- Write output data to file

Whilst the steps for a MCS analysis are:

- Load input data from file
- Determine column and loading ages
- Determine mean vectors for shrinkage, creep and modulus
- Determine covariance matrix for shrinkage, creep and modulus
- Generate random vectors for shrinkage, creep and modulus

- Calculate random long-term total and differential shortening values
- Repeat above procedure the required number of simulations
- Calculate expected values, variances, relative skewness, relative kurtosis, minimum and maximum values of total and differential shortening between column pairs
- Write output data to file

A6.7.4 EXAMPLE APPLICATION OF NEW MODELS

An example 39 storey building is used to illustrate the outcomes of the probabilistic column models developed here. Long-term shortening predictions of the service core and the spandrel columns are determined.

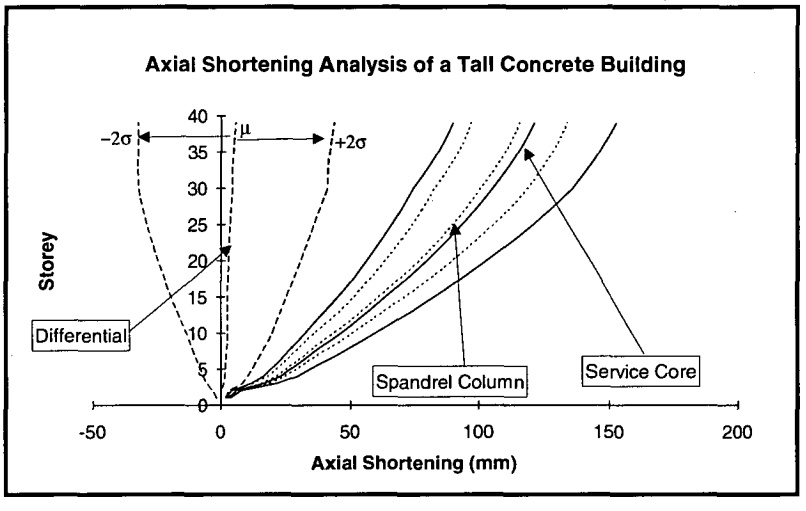

Figure A6.4 - Axial shortening of example 39 storey building showing the ($\mu \pm 2\sigma$) region, for shortening of the service core and spandrel columns.

Figure A6.4 shows the ($\mu \pm 2\sigma$) region of a second-order moment analysis of total and differential shortening, where the ACI recommendations on creep, shrinkage and modulus [37] are modelled as random, with statistical information assumed from Section A6.7.1. The validity of the Taylor series approximation was checked by comparing first- and second-order moment results with Monte Carlo predictions. See Figures A6.5 and A6.6 for comparisons of total shortening of the 39th storey core and spandrel column respectively. The predictions of expected values and corresponding standard deviations show close correlation, thus verifying the preference for second-order moment analyses for tall buildings.

Monte Carlo histograms (10000 simulations) of total shortening for the 39th storey core and spandrel column are shown in Figures A6.7 and A6.8 respectively. It can

be observed that the shortenings are approximately symmetrical and similar to a Gaussian shape. Further, the variation of relative skewness and relative kurtosis (Gaussian values are 0 and 3 respectively) as a function of Monte Carlo runs are shown in Figure A6.9 for the 39th level core and spandrel column. Figures A6.5, A6.6 and A6.9 show how the Monte Carlo results become more stable with increased simulations.

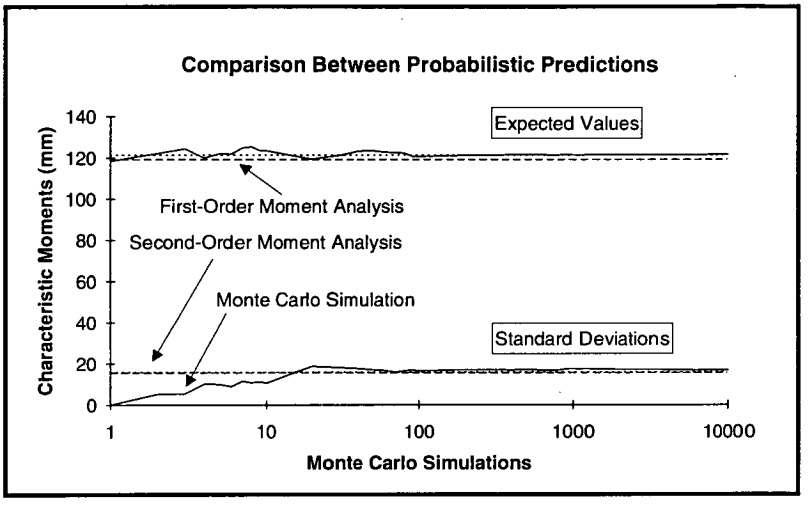

Figure A6.5 - Comparisons between first- and second-order moment theory, and Monte Carlo simulation predictions of total shortening for 39th level core of example 39 storey building.

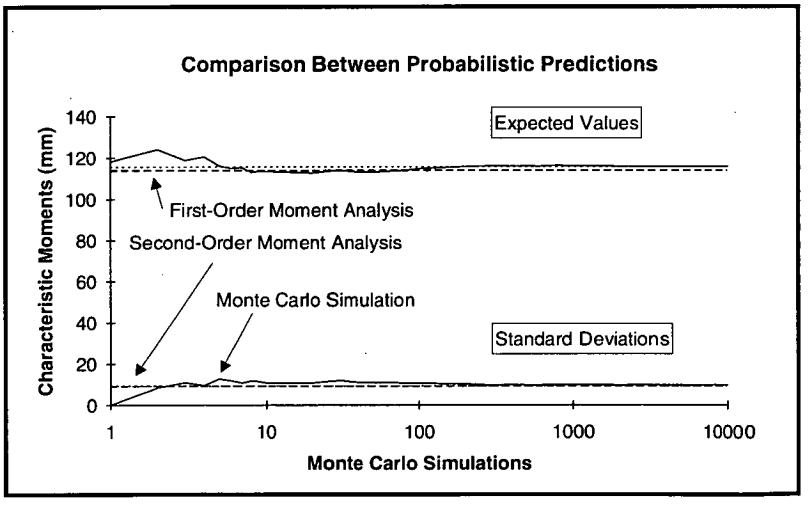

Figure A6.6 - Comparisons between first- and second-order moment theory, and Monte Carlo simulation predictions of total shortening for 39th level spandrel column of example 39 storey building.

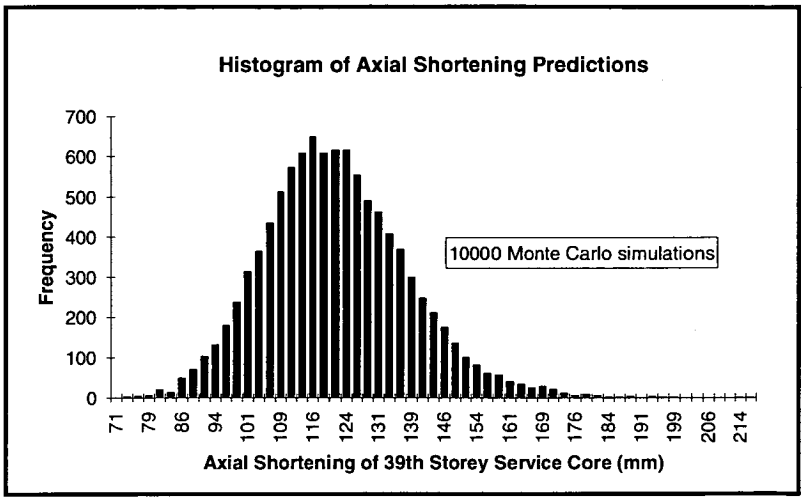

Figure A6.7 - Monte Carlo histogram (10000 simulations) of total shortening for 39th level core of example 39 storey building.

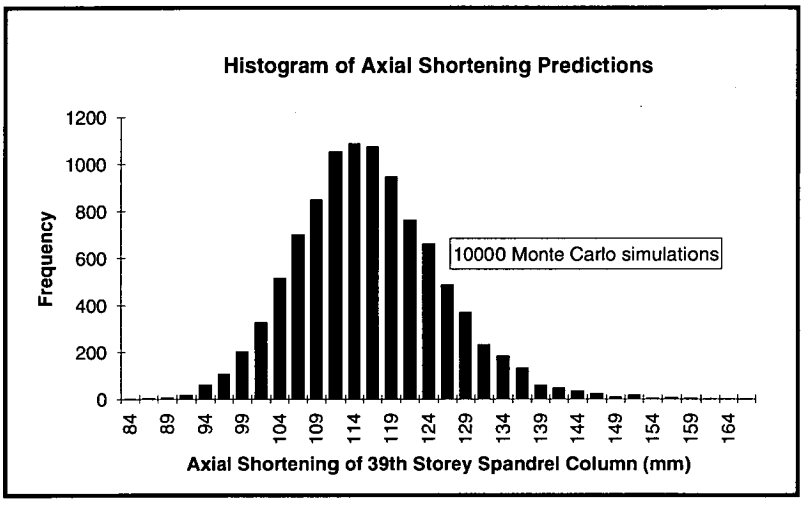

Figure A6.8 - Monte Carlo histogram (10000 simulations) of total shortening for 39th level spandrel column of example 39 storey building.

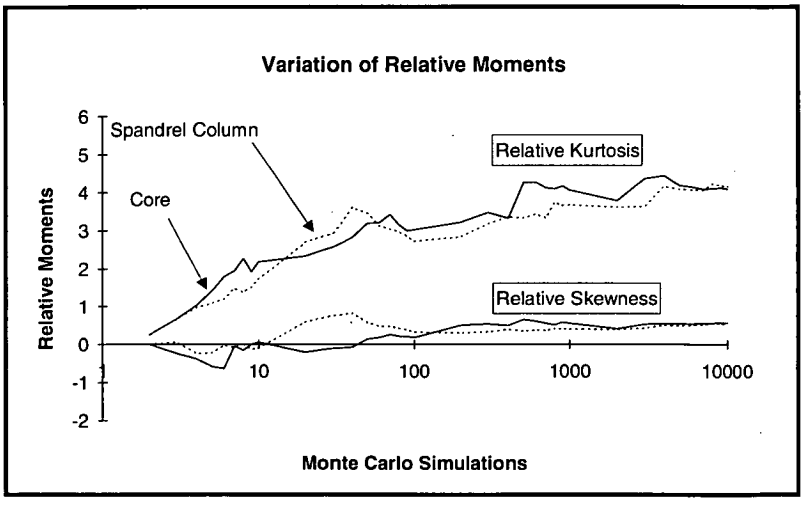

Figure A6.9 - The variation of relative skewness and relative kurtosis of total shortening for 39th level core and spandrel column of example 39 storey building.

APPENDIX A6.8

Consider **Y** as a general function of **n** series such that series 1 has n_1 random variables, series 2 has n_2 random variables, etc, to series n which has n_n random variables. It is further assumed that correlations between different series do not exist, whilst within a series they do. Then the expected value and variance are defined by

$$E[Y] = \int_{-\infty}^{\infty}\int_{-\infty}^{\infty}\cdots\int_{-\infty}^{\infty} Y\, f_{xn}(X_{11},\ldots,X_{n_n n})\, dX_{11}\ldots dX_{n_n n} \tag{A6.42}$$

and

$$Var[Y] = \int_{-\infty}^{\infty}\int_{-\infty}^{\infty}\cdots\int_{-\infty}^{\infty} (Y - E[Y])^2\, f_{xn}(X_{11},\ldots,X_{n_n n})\, dX_{11}\ldots dX_{n_n n} \tag{A6.43}$$

where

$$Y = g\begin{pmatrix} X_{11}, & X_{21}, & \cdots & X_{n_1 1}, \\ X_{12}, & X_{22}, & \cdots & X_{n_2 2}, \\ \vdots & \vdots & & \vdots \\ X_{1n}, & X_{2n}, & \cdots & X_{n_n n} \end{pmatrix} = g(X_{11},\ldots,X_{n_n n})$$

X_{ij} = ij^{th} random variable (i = 1 to n_j, j = 1 to n)

n = total number of random series

n_j = number of random variables in j^{th} series

and $f_{xn}(X_{11},\ldots,X_{n_n n})$ = multivariate probability density function

Equations (A6.42) and (A6.43) have been defined in order to develop a model for each time-dependent random variable (i.e. creep coefficient, shrinkage strain and modulus) in terms of a series.

In addition, the form of **Y** can be expressed as

$$\begin{aligned} g(X_{11},\ldots,X_{n_n n}) = {} & g(X_{11},\ldots,X_{1n}) + g(X_{21},\ldots,X_{2n}) \\ & + g(X_{31},\ldots,X_{3n}) + g(X_{41},\ldots,X_{4n}) + \ldots. \end{aligned} \tag{A6.44}$$

The format of (A6.44) is directly applicable to shortening analyses, as each function (i.e. $g_i(X_{i1}, X_{i2}, X_{i3},\ldots, X_{in})$) on the right hand side represents, for example, the deformations of a reinforced concrete column due to a single instantaneously

applied load. Each function, g_i, is dependent on only one creep coefficient, basic shrinkage strain and elastic modulus parameter, thus explaining the format of (A6.44). In addition, the following partial derivatives are zero, i.e.

$$\frac{\partial^2 g}{\partial X_{ij} X_{kj}} = 0 \quad \text{for any i, j and k } (i \neq k) \tag{A6.45}$$

The solution of the expected value and variance, (A6.42) and (A6.43), of the general function **Y** is complex and in general cannot be obtained in closed form. Employing the Taylor series approximation given by (A6.12), a first-order moment analysis requires the first two terms of this equation and are substituted into the basic moment equations (i.e. (A6.42) and (A6.43)) together with (A6.45) and the properties of a multivariate Gaussian distribution (see Appendix A6.9). The final expressions for the expected value and variance of **Y** respectively can be derived as

$$E[Y] = g(\mu_{x11}, \ldots, \mu_{xn_n n}) \tag{A6.46}$$

and

$$\mathrm{Var}[Y] = \sum_{i=1}^{n} \sum_{j=1}^{n_i} \sum_{k=1}^{n_i} \left(\mathrm{Cov}[X_{ji}, X_{ki}] \left(\frac{\partial g}{\partial X_{ji}} \right) \left(\frac{\partial g}{\partial X_{ki}} \right) \right) \tag{A6.47}$$

where

$\mathrm{Cov}[X_{ji}, X_{ki}]$ = covariance of X_{ji} and X_{ki}

$\mathrm{Cov}[X_{ji}, X_{ji}] = \mathrm{Var}[X_{ji}]$

and μ_{xij} = expected value of X_{ij}

For a second-order moment analysis, the first three terms of (A6.12) are utilised, for which the resulting equations for expected value and variance are respectively

$$E[Y] = g(\mu_{x11}, \ldots, \mu_{xn_n n}) + \frac{1}{2} \sum_{i=1}^{n} \sum_{j=1}^{n_i} \left(\mathrm{Var}[X_{ji}] \frac{\partial^2 g}{\partial X_{ji}^2} \right) \tag{A6.48}$$

and

$$\mathrm{Var}[Y] = \sum_{i=1}^{n}\sum_{j=1}^{n_i}\sum_{k=1}^{n_i}\left(\mathrm{Cov}[X_{ji}, X_{ki}]\left(\frac{\partial g}{\partial X_{ji}}\right)\left(\frac{\partial g}{\partial X_{ki}}\right)\right) + \frac{1}{2}\sum_{i=1}^{n}\sum_{j=1}^{n_i}\sum_{k=1}^{n_i}\left(\mathrm{Cov}^2[X_{ji}, X_{ki}]\left(\frac{\partial^2 g}{\partial X_{ji}^{\,2}}\right)\left(\frac{\partial^2 g}{\partial X_{ki}^{\,2}}\right)\right) \tag{A6.49}$$

As the multivariate Gaussian probability density function is symmetrical, the expected value of **Y** for a third-order moment analysis is identical to the second-order equation. The forms of (A6.46) to (A6.49) inclusive are such that the effects of each independent random parameter (in this case creep, shrinkage and modulus) accumulate independently through the axial shortening analysis. Thus, probabilistic shortening results obtained for each random parameter considered separately, can be obtained with little addition to the computational time. This point is of particular importance as computational times are critical in tall building analyses.

APPENDIX A6.9

The multivariate Gaussian probability density function is given by

$$f_{xn}(X) = \frac{1}{(2\pi)^{\frac{n}{2}}\sqrt{\det|V|}} e^{\left(-\frac{1}{2}(X-\mu)^T V^{-1}(X-\mu)\right)} \tag{A6.50}$$

where

V = n×n covariance matrix

$\det|V|$ = determinant of covariance matrix

μ^T = transpose operation on n×1 mean vector

$\mu = \{\mu_{x1},\ldots,\mu_{xn}\}^T$ = n×1 mean vector

and $X = \{X_1,\ldots,X_n\}^T$ = n×1 random vector

Some product-moments of the multivariate Gaussian distribution are as follows

$$\left.\begin{aligned}&\int_{-\infty}^{\infty}\int_{-\infty}^{\infty}\ldots\int_{-\infty}^{\infty}(X_i-\mu_{xi})(X_j-\mu_{xj})f_{xn}(X_1,\ldots,X_n)dX_1\ldots dX_n\\&=\mathrm{Cov}[X_i,X_j]\end{aligned}\right\} \tag{A6.51}$$

$$\int_{-\infty}^{\infty}\int_{-\infty}^{\infty}\ldots\int_{-\infty}^{\infty}(X_i-\mu_{xi})^2(X_j-\mu_{xj})f_{xn}(X_1,\ldots,X_n)dX_1\ldots dX_n=0 \tag{A6.52}$$

$$\left.\begin{aligned}&\int_{-\infty}^{\infty}\int_{-\infty}^{\infty}\ldots\int_{-\infty}^{\infty}(X_i-\mu_{xi})^2(X_j-\mu_{xj})^2 f_{xn}(X_1,\ldots,X_n)dX_1\ldots dX_n\\&=\mathrm{Var}[X_i]\mathrm{Var}[X_j]+2\mathrm{Cov}^2[X_i,X_j]\end{aligned}\right\} \tag{A6.53}$$

CHAPTER 7

CHAPTER 7

SOFTWARE DEVELOPMENT

In this chapter two computer programs which have been written a) to predict the axial shortening of columns in tall concrete buildings, and b) to statistically analyse and fit Monte Carlo output data to common distributions, are described. These programs are referred to as AXS and STATS respectively. AXS implements the four column models describing reinforced column behaviour, coupled with concrete property models for creep and shrinkage which have been presented in Chapter 4. The column models allow for either deterministic or probabilistic approaches in determining axial shortening values in columns, and three probabilistic methods outlined in Chapter 6 are incorporated. STATS was developed to statistically analyse Monte Carlo data with the important moment characteristic values determined. Also embodied here are two standard goodness of fit tests to check various PDFs fitted to the data, where these distributions include normal, log-normal, gamma and beta.

7.1 AXIAL SHORTENING SOFTWARE PACKAGE (AXS)

7.1.1 Introduction

AXS has been developed on an IBM-compatible machine with the executable file size being approximately 380 Kbytes in the DOS system. AXS requires at least 580 Kbytes to run, with a maths co-processor recommended. The program listing contains a main segment with sixteen supporting units, which are given in [28]. The language is TurboPascal [152-161].

The analysis segment of AXS was tested against that developed by Beasley [12,13]. For these tests, the deterministic analysis of both programs gave comparable results (see Figure 7.1). The results from a Monte Carlo simulation and second-order moment analysis in AXS also show close agreement (see Section 6.4).

For a 486-66DX2 machine, some of the CPU analysis times for a 39 storey building are given in Table 7.1. The method of analysis used here was FEMM

together with the proposals of ACI [37], CEB-FIP 1978 [38], AS-3600 [39] and BPX [66-82] models on creep and shrinkage.

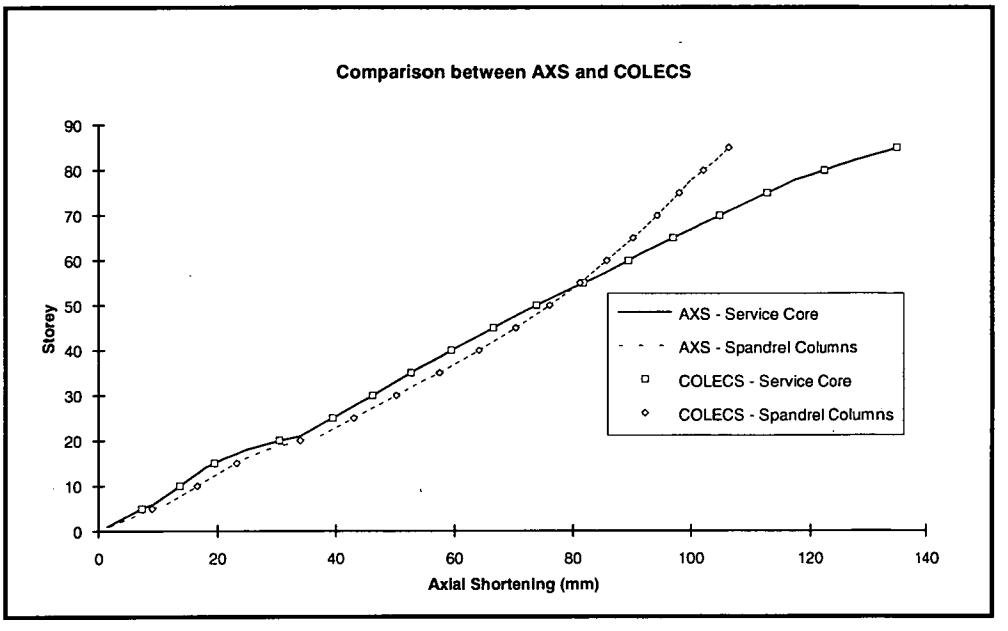

Figure 7.1 - Comparison of deterministic values obtained from AXS and COLECS (Beasley [12,13]) for an 85 storey building.

Concrete Property Models	Times for Deterministic Analysis	Times for Second-Order Moment Analysis
ACI [37]	14 sec	4 sec
CEB-FIP 1978 [38]	33 sec	8 sec
AS-3600 [39]	14 sec	4 sec
BPX [66-82]	1 min 8 sec	13 sec

Table 7.1 - Summary of CPU analysis times for 39 storey building.

A more detailed description of AXS can be found in [28]. In the section to follow, the analysis procedures of the program are summarised.

7.1.2 Main Program

The flow charts for the different types of analyses are shown in Figures 7.2 to 7.5 inclusive. For a deterministic analysis, Figures 7.2 and 7.3, the output results obtained are the cumulative shortening of two adjacent column pairs, slab cambers and the steel and concrete stresses in these columns.

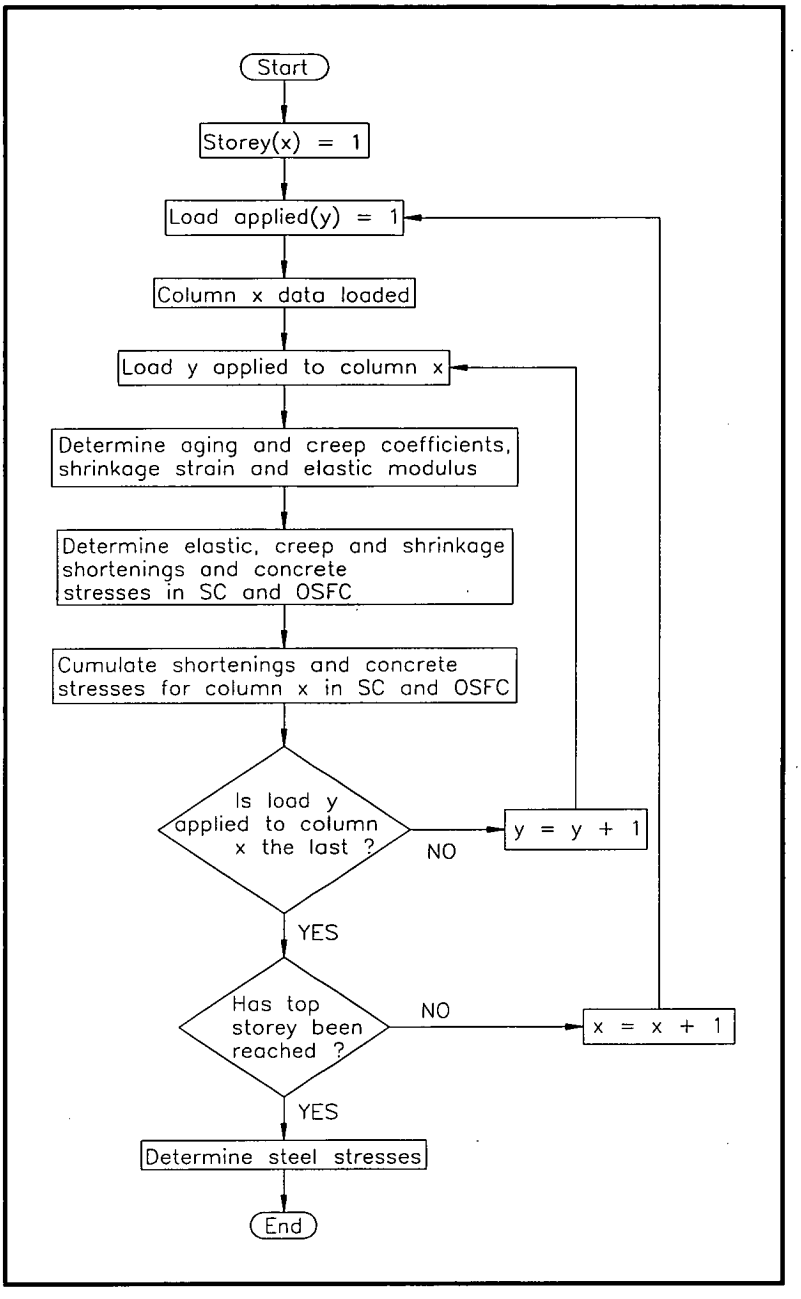

Figure 7.2 - Deterministic analysis flow chart employed by AXS in determining cumulative shortening of, and steel and concrete stresses in service core (SC) and outer spandrel frame columns (OSFC).

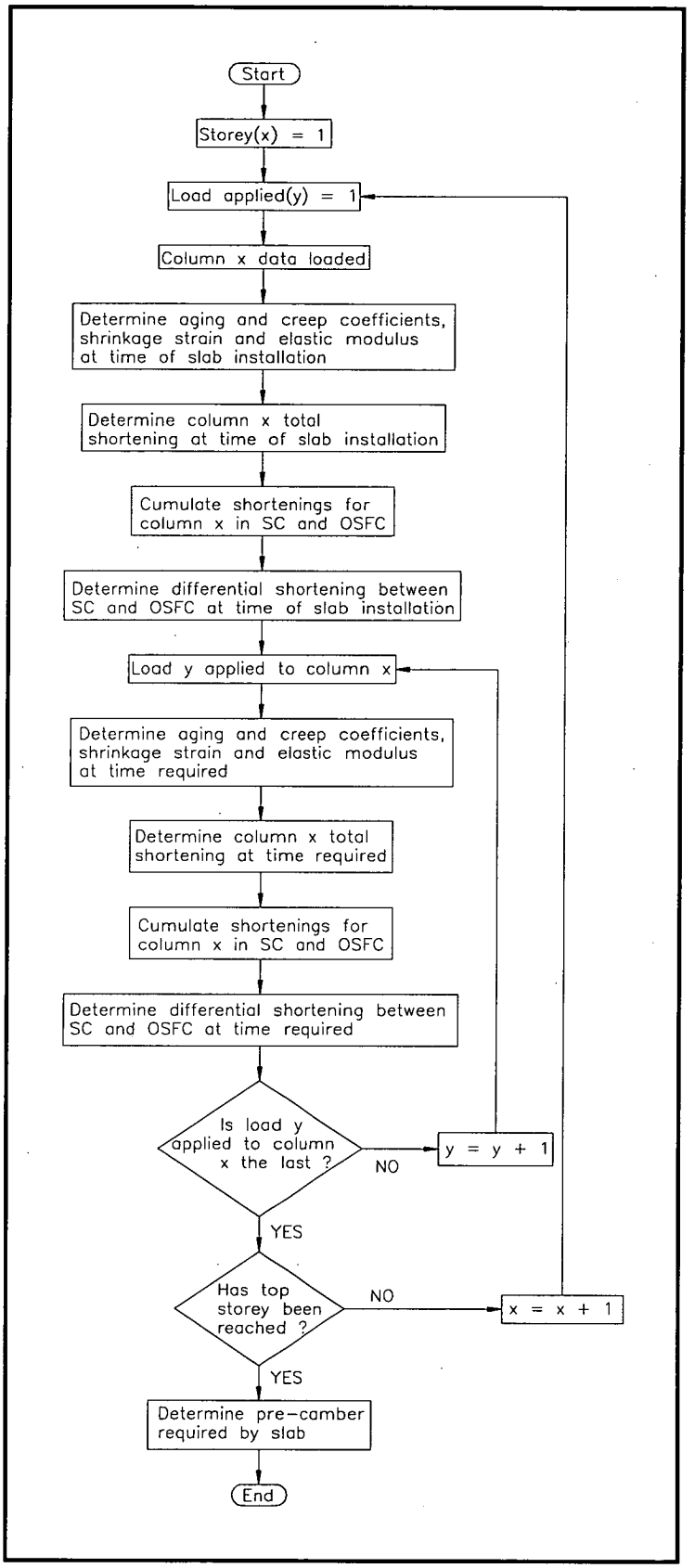

Figure 7.3 - Deterministic analysis flow chart employed by AXS in determining slab cambers of building.

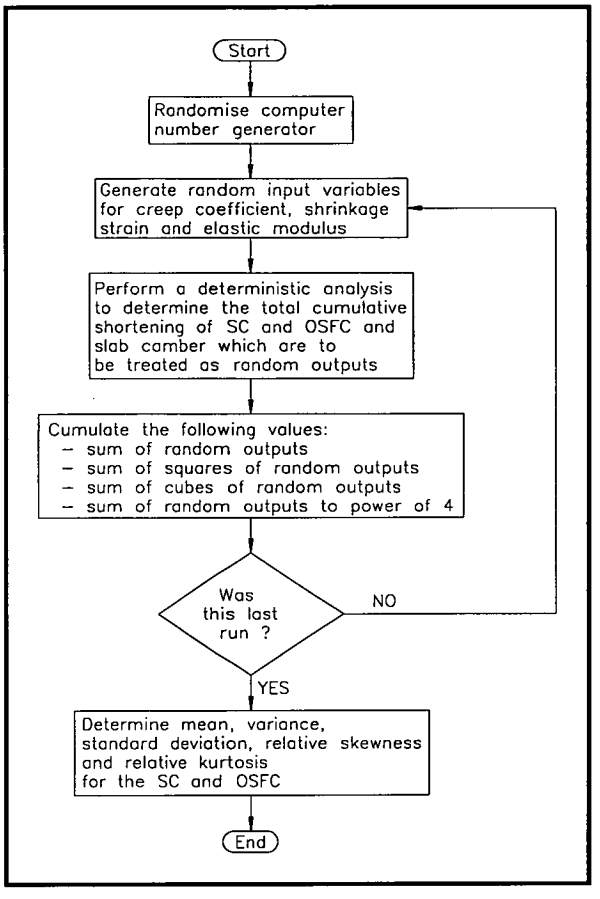

Figure 7.4 - Monte Carlo simulation flow chart employed by AXS in determining cumulative shortening of service core (SC) and outer spandrel frame columns (OSFC), and slab cambers of building.

The flow chart routine employed by Monte Carlo simulation is shown in Figure 7.4. From this type of analysis, the output results obtained are the expected value, standard deviation, relative skewness, relative kurtosis, minimum and maximum values of slab cambers and cumulative shortening of both column pairs. The Gaussian random number generator implemented in the Monte Carlo simulation is described in Chapter 6.

The main procedure utilised by AXS for a first- or second-order moment analysis is shown in the flow chart given in Figure 7.5. From these two types of analyses, the expected value and standard deviation of cumulative shortening of both column pairs are determined. Example output files from AXS for a deterministic analysis, Monte Carlo simulation and second-order moment analysis can be found in [28].

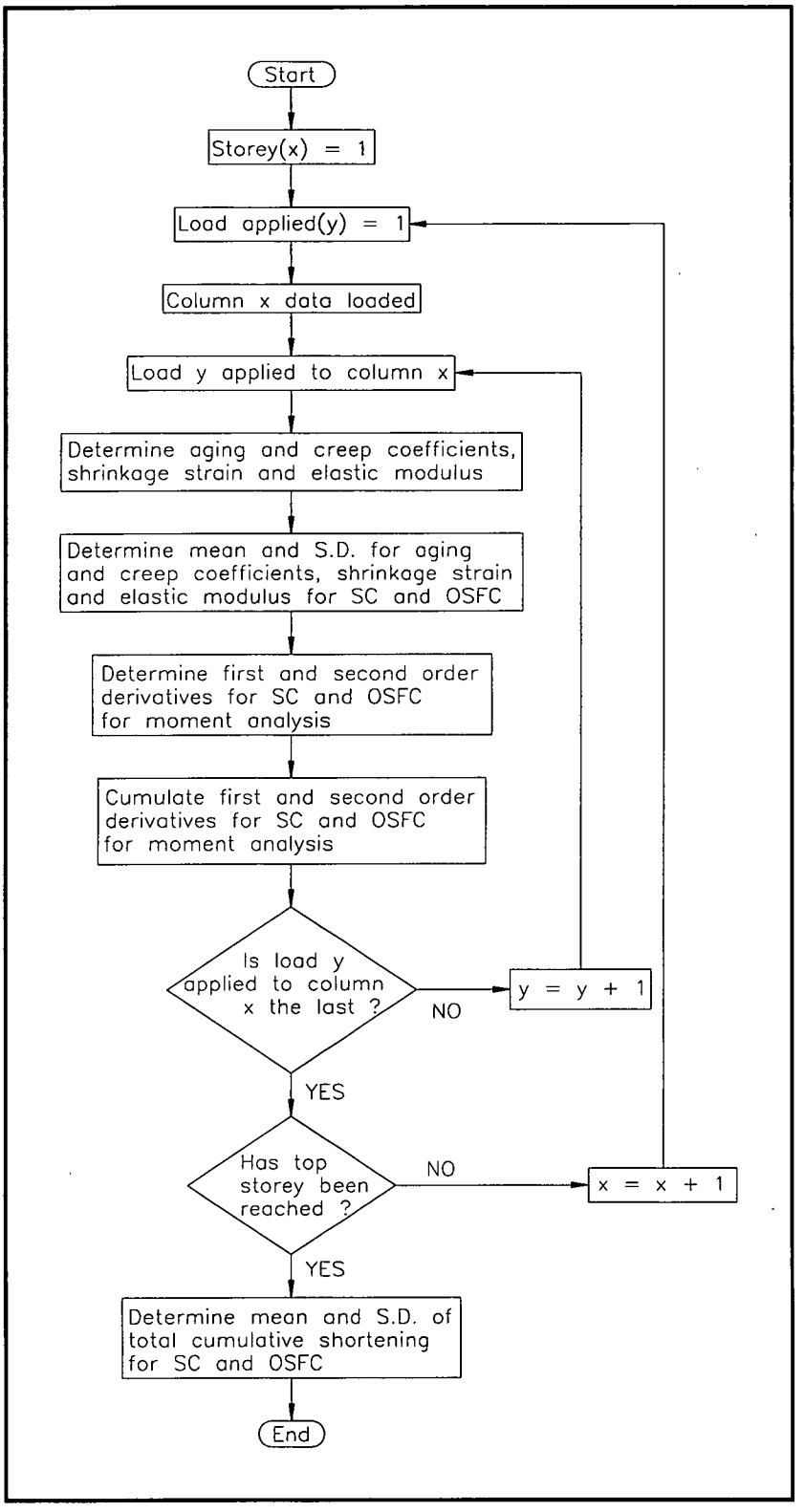

Figure 7.5 - Flow chart of first- and second-order moment analyses employed by AXS in determining mean and standard deviation of cumulative shortening of service core (SC) and outer spandrel frame columns (OSFC).

7.2 STATISTICAL SOFTWARE PACKAGE (STATS)

7.2.1 Introduction

Current software which analyses univariate data, specifically Monte Carlo axial shortening data sets, to determine characteristic moments and optimal normal, log-normal, gamma and beta distribution best fits are not readily available. For this reason the author has developed STATS.

STATS was developed utilising TurboPascal programming language [152-161] with the main objective being to analyse the probabilistic input and output data involved in axial shortening predictive methods. The program was written as one main file which is listed in [27].

STATS requires an IBM-compatible machine with the size of the executable file (STATS.EXE) being approximately 100 Kbytes. This program is best run with a maths co-processor, and ideally a 486-66DX2 computer is recommended. With this set-up the CPU time is approximately 2 to 3 minutes to analyse 1000 data points, while 10000 data points requires between 15 to 20 minutes.

7.2.2 Main Program

The general flow chart for STATS is shown in Figure 7.6.

On execution (refer to Figure 7.6) the maximum acceptable values for the χ^2 test at 95% level of significance are initialised. The data are then analysed with the expected value, standard deviation, variance, relative skewness, relative kurtosis, 5^{th} to 10^{th} order relative central moments, minimum and maximum values being determined. Employing a simple algorithm, the data are then sorted in order of increasing values. From the sorted data, the 95% confidence limits for these data points are then determined such that the interval lies between the 2.5% upper and lower tail regions.

From the previously determined parameters describing the data, four initial PDFs are then defined namely the normal, log-normal, gamma and beta distributions. To check that the data fits to the chosen PDFs, the χ^2 and K-S tests [144,145,149] are utilised at the 95% level of significance.

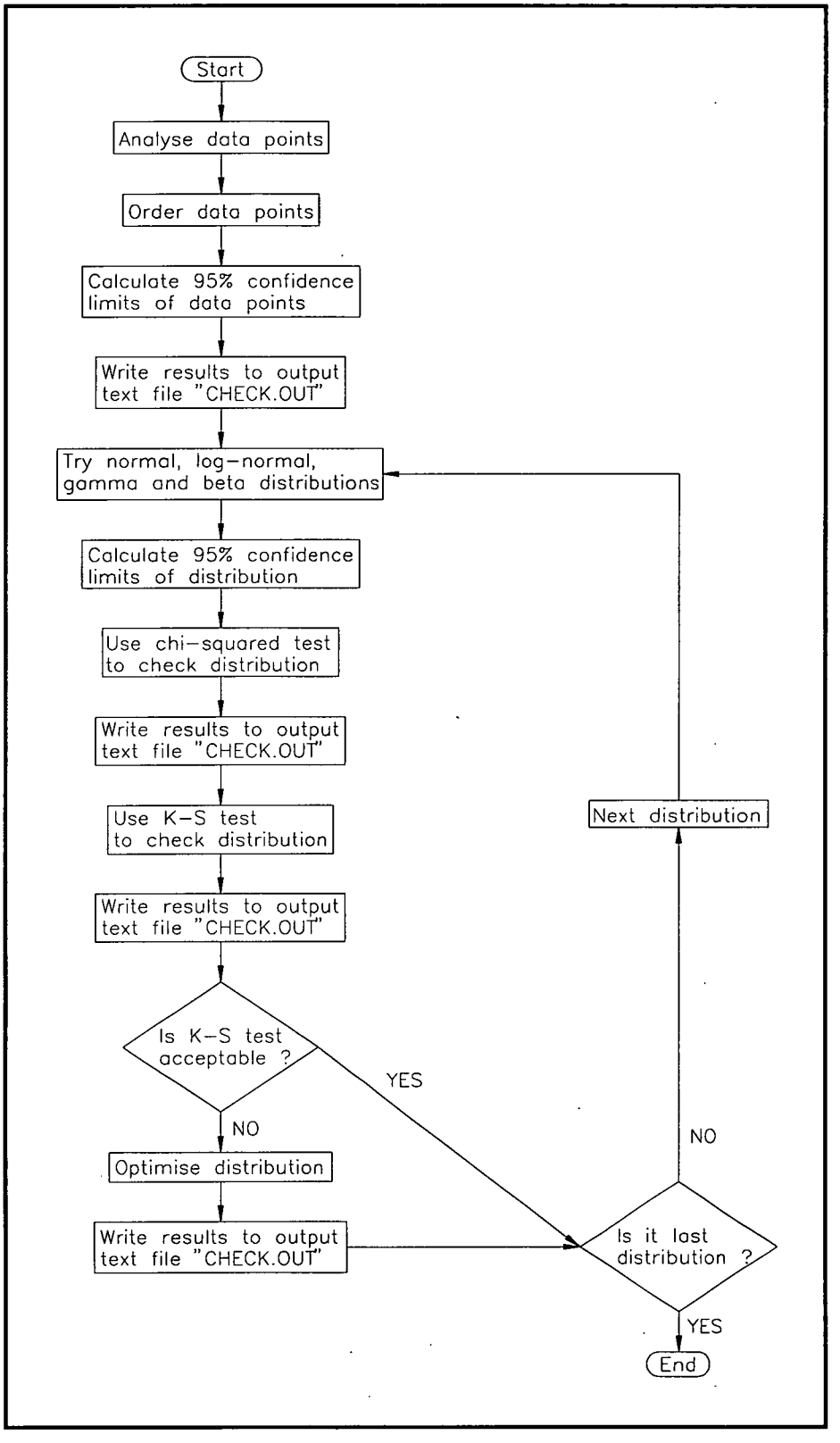

Figure 7.6 - Main flow chart for the computer program STATS.

The initial parameters for the normal PDF are the expected value and the standard deviation of the data. Using the method of bisections [162], the 95% confidence limits of the initial normal distribution are then determined. To verify that the

lower and upper limits are correct, a numerical integration is carried out between these limits. The χ^2 and K-S tests are then used to confirm the fit of the normal PDF. As the K-S test does not rely on an underlying distribution and the method compares the difference between the two cumulative distributions, this test is used as the basis for acceptance of the fits. If an acceptable PDF fit results, STATS then continues with the next distribution, else a minimisation procedure otherwise described as pattern search [162] is implemented. This process attempts to minimise the K-S statistic according to the two variables, namely the expected value and the standard deviation of the normal distribution. The routine continues until either the PDF fit is acceptable or not acceptable.

After the normal distribution fit has been completed, then the log-normal, gamma and beta distributions are fitted in turn. The initial values for the log-normal distribution fit are the expected value and standard deviation of the data. For the gamma and beta distribution fits, the expected value, standard deviation and minimum of the data and, the expected value, standard deviation, minimum and maximum of the data are used as the initial parameters respectively. A similar algorithm is followed for each distribution as was the case for the normal PDF. The program run finishes on completion of the beta distribution analysis. A summary of all the analyses performed by STATS can be found in the output text file, refer to [27] for example.

7.3 CONCLUDING REMARKS TO CHAPTER

AXS and STATS was briefly described in this chapter with further details available in [27,28]. Both packages have been extensively employed in the work of Chapter 8.

CHAPTER 8

CHAPTER 8

SENSITIVITY ANALYSIS AND COMPARISON OF AXIAL SHORTENING PREDICTION METHODS

This chapter firstly defines an approach for assessing possible significant differences between the probability density functions which characterise long-term axial shortening outputs. The random characteristics of axial shortenings are determined by fitting a set of distributions to the Monte Carlo output data, including normal, log-normal, gamma and beta PDFs. After determining the types of distributions thought applicable to modelling most shortenings, further comparisons of the column models are performed at a probabilistic level utilising the general comparison procedure defined here. The second part of the chapter compares probabilistic theoretical column shortening predictions with a set of experimental data. To conclude an analysis is performed on the input parameters of the concrete properties to rank the sensitivities of each of these parameters.

8.1 A TEST FOR COMPARING DISTRIBUTIONS

Output results from a probabilistic analysis are graphically displayed by PDFs. When comparing two PDFs, referring to Figure 8.1, the common area represents the percentage of over-lap. This in turn forms the basis for the comparisons to follow.

Defining a procedure for comparing probabilistic outcomes requires designating some rational form of limiting values. Here, the limiting values are specified as ranges, as no other clear criteria are available. Defining the appropriate ranges has proved difficult and the following measures have been adopted.

Region A is defined as suggesting no significant differences between the PDFs, and essentially predict the same statistical population. Region B is defined as a transition, where small significant differences are present. In region C, definite differences between the PDFs are apparent. The boundaries between regions are arbitrary, however, conclusions made later are not so dependent on these boundaries.

To characterise each region, the percentage of over-lap values have been defined as,

region A - 90% to 100%,

region B - 75% to 90%, and

region C - up to 75%.

Over-lap percentages at the boundary regions can be seen in Figures 8.2 and 8.3.

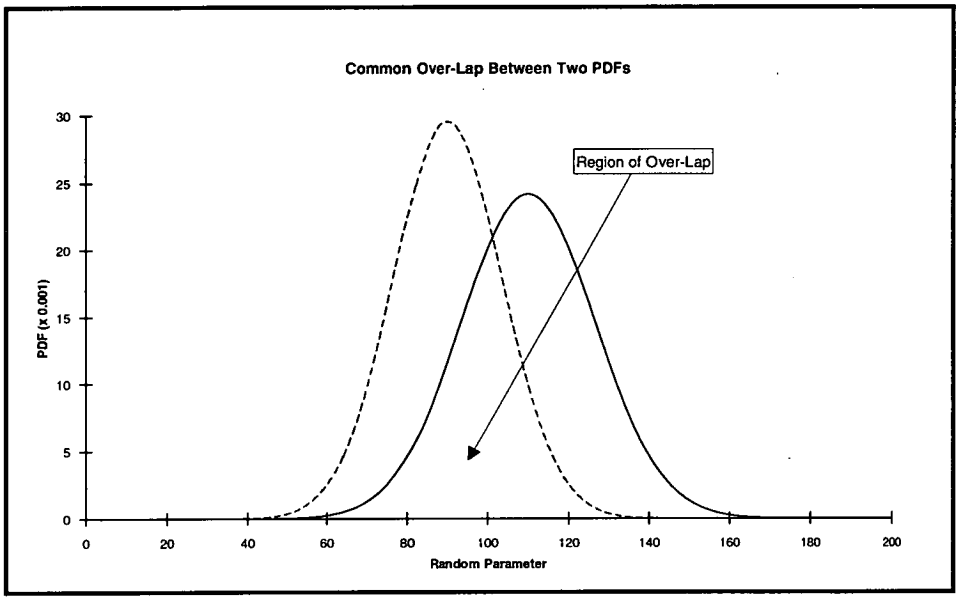

Figure 8.1 - Region of over-lap between two PDFs.

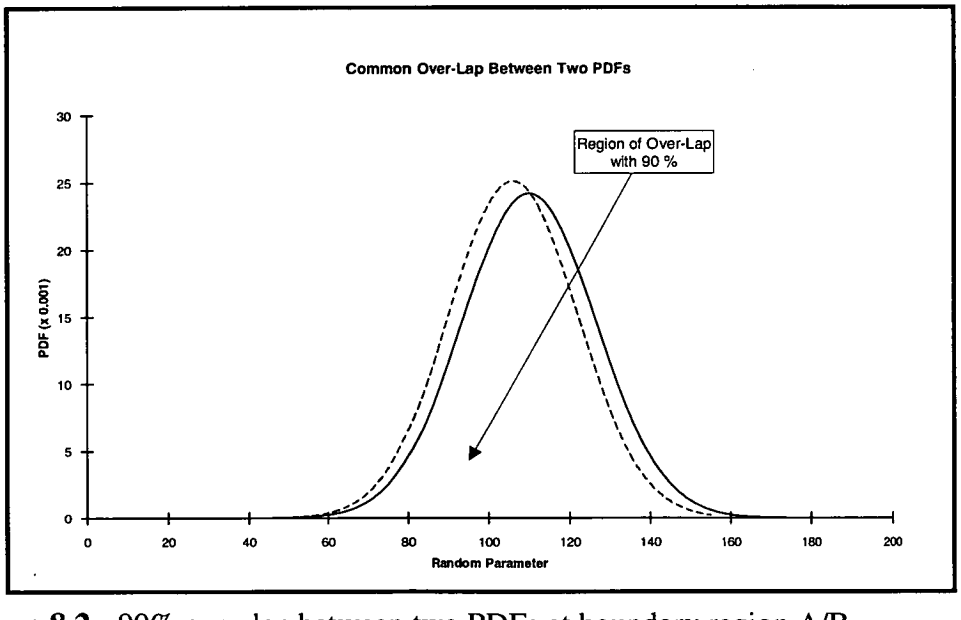

Figure 8.2 - 90% over-lap between two PDFs at boundary region A/B.

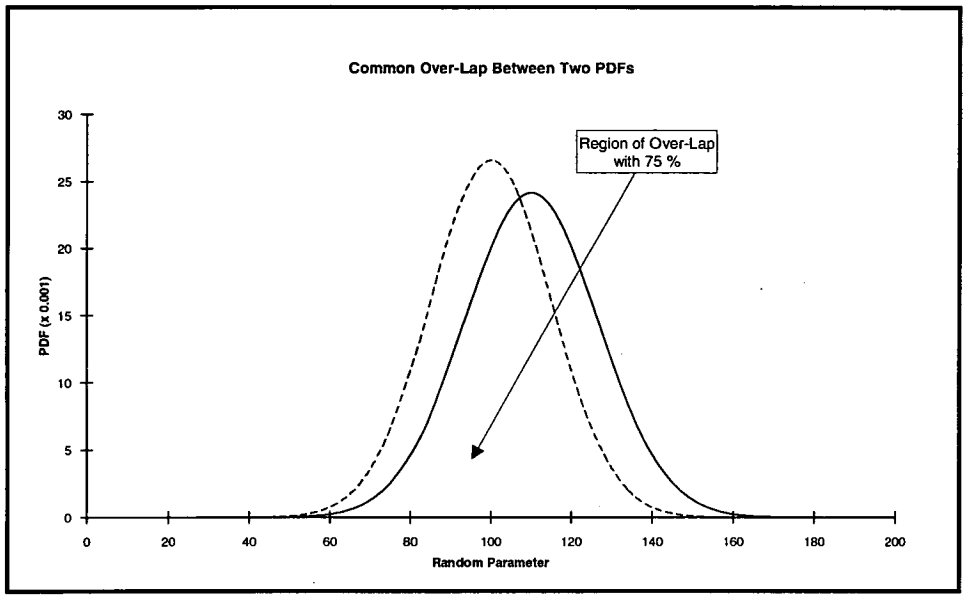

Figure 8.3 - 75% over-lap between two PDFs at boundary region B/C.

8.2 DETERMINING OUTPUT AXIAL SHORTENING PDFs

The results obtained from a second-order moment analysis are in the form of expected values and corresponding variances for long-term column shortening of the service core (SC) and outer spandrel frame columns (OSFC). It remains however that being based on characteristic parameters only, as a second-order moment analysis is, little information regarding the respective PDFs is available, for example, whether they are Gaussian or otherwise. To assess these distributions, the Monte Carlo simulation approach developed in Chapter 6 is adopted, and subsequently combined with the Kolmogorov-Smirnov (K-S) goodness of fit test [144,145,149] at the 95% level of significance to establish the PDFs of "best fit". The statistical analysis program (STATS) developed in Chapter 7 is employed here.

Shortening distributions were determined for each of the column models based on the range of concrete property models in Chapter 4. Here, the example 39 storey building given in Appendix A6.6 was employed as the case-study. From these investigations, it was concluded that long-term axial shortenings conform to Gaussian distributions with moments for these distributions determined from a second-order moment approach. The coefficient of variation values adopted to describe each random concrete property in the shortening analyses are those values employed in Chapter 6.

With the MCS output data further studies to check fits with other PDF types were made. These included the log-normal, gamma and beta distributions. For all K-S tests conducted at the 95% level of significance, the latter three distributions were also statistically admissible. However, for simplicity, the Gaussian description has been adopted in all subsequent studies. Figure 8.4 illustrates four of the numerous distribution fits to a set of MCS data. In these curves, the axial shortening outcomes for the 39th storey service core are shown. The FEMM column model and the ACI recommendations on creep and shrinkage have been used here.

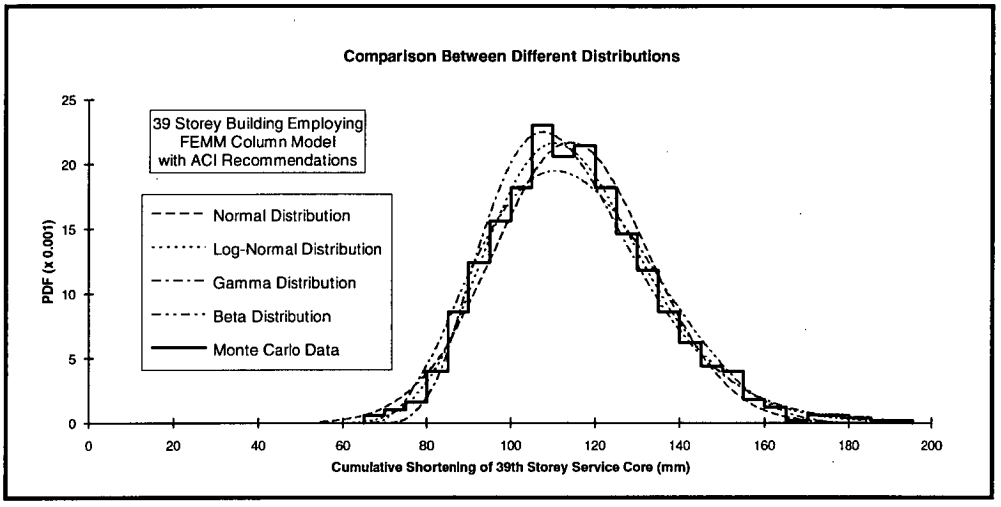

Figure 8.4 - Comparison between normal, log-normal, gamma and beta distributions fitted to MCS axial shortenings.

MCS results from the analysis of differential long-term axial shortening between the columns and core of the 39 storey building were examined to determine a suitable distribution. Employing the K-S test at the 95% level of significance, it was found that the Gaussian PDF is an adequate description for the uncertainty in differential shortening. However, it was also observed (see Figure A6.4) that the differential distributions had low mean values with relatively larger standard deviations. This in effect would mean that the differential predictions are impractical for design purposes, but one should remember that it has been assumed that concrete test data is unavailable and thus the probabilistic column models employ random concrete parameters with high COV values.

Modelling of the output axial shortening results by a Gaussian PDF is valid only for the specified values of the COVs employed here, or for those in close proximity to them. The basic shrinkage strain is linear in the time-dependent analysis, as given by axial column models, and the remaining two random parameters are non-linear. As is well known, a linear transformation of a Gaussian

PDF results in the same distribution. This would suggest that the COV of the basic shrinkage strain has a dominant effect on the PDF of the output results, as was found to be the case, when the effect of each random variable was taken into account in separate analyses.

The work in Sections 8.3, 8.4, 8.5 and 8.6 investigate total axial shortening predictions of the core and internal columns in preference to using differential predictions. This has been mainly due to one of two reasons. The first being that differential shortening predictions had high COV values which make them unsuitable. Secondly, the discrepancies between two probabilistic differential predictions would not be so apparent, as comparisons between values are made are relative rather than absolute.

8.3 COMPARISON OF PREDICTION METHODS

Comparisons in which the random nature of the concrete properties are modelled, within a rational structural analysis of a tall building, have not, to the best of the author's knowledge, been done at all.

The principal objective here is to assess the constitutive and property models in the context of a tall building analysis, based on the predictive accuracy of the models. For example, Bazant [7] stated that the TBEMM is "theoretically superior" to the FEMM, whilst Bazant *et al.* [184] have suggested that their property models describing creep and shrinkage are experimentally and theoretically more exact than other models given in Chapter 4.

Using the probabilistic comparison technique defined in Section 8.1, column model comparisons are made. These were carried out for the long-term cumulative shortening of the service core and outer frame of the example 39 storey building using the different concrete properties combined with each of the column models. In this part of the work, a second-order moment analysis of axial shortenings was employed.

8.3.1 Comparison of Column Models

The four column models in combination with all of the specified concrete property models were tested for long-term axial shortening. As the TBEMM column model is theoretically more advanced, although in the context here not necessarily more definitive, this was used as the base model for comparison. For FEMM it was

found that the percentage of overlap of the PDFs fell in the upper half of region A (i.e. 95% to 100%), whilst for the RCM this area on average was in the lower half of region A (i.e. 90% to 95%). The IRCM comparisons were deemed to be on the boundary region A/B (i.e. 85% to 95%). The FEMM predictions show closer agreement to the column model of TBEMM, as would be expected since the two previous models differ only by the inclusion of a refined aging coefficient. The IRCM predictions show some significant differences. See Figure 8.5 for one of the many comparisons utilising the ACI properties.

After determining the percentage of over-lap between the RCM and the IRCM, it can be concluded that there are no significant differences between these two models. The region in which these comparisons fell were the lower half of region A (i.e. 90% to 95%).

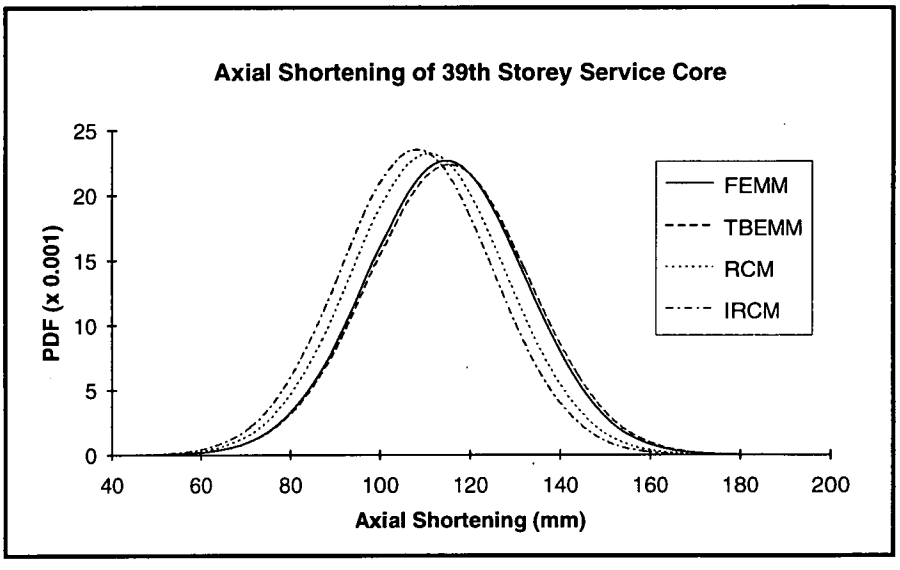

Figure 8.5 - Comparison between different column models for predicting long-term axial shortening of example 39th storey service core.

8.3.2 Comparison of Aging Coefficient Models

As mentioned in Chapter 5 the TBEMM column model includes an aging coefficient parameter, the definition of which is given in (A5.9). To make the study of the TBEMM more comprehensive four separate aging coefficient models have been identified and implemented into the study here. These are; 0.8 average value, the CEB-FIP 1978 model [40], and the "approximate" and "exact" models as outlined in Bazant and Kim [122]. Here, the approximate aging coefficient can be determined by using an approximate relaxation function given by (3.23) together with (A5.9), whilst the exact model can be evaluated utilising a step by step numerical process, as described in Appendix A3.1. It is noted here that

incorporating the latter model in an axial shortening analysis, relative to adopting the 0.8 average value, increases CPU analysis time, at least on the author's PC, by as much as 4000 times.

The exact aging coefficient model was used as a base for comparison of the other models. From the axial shortening analyses which included incorporating all concrete property models in turn, the percentage of over-lap on average fell in the top third of region A (i.e. 97% to 100%). The results of this study indicate that all of the four aging models used with the TBEMM show extremely close agreement. One might even argue that the aging coefficient parameter is, for practical purposes, redundant. The 0.8 average value which remained constant throughout the analysis has therefore been adopted in subsequent axial shortening applications. See Figure 8.6 for one of the many comparisons utilising the ACI properties.

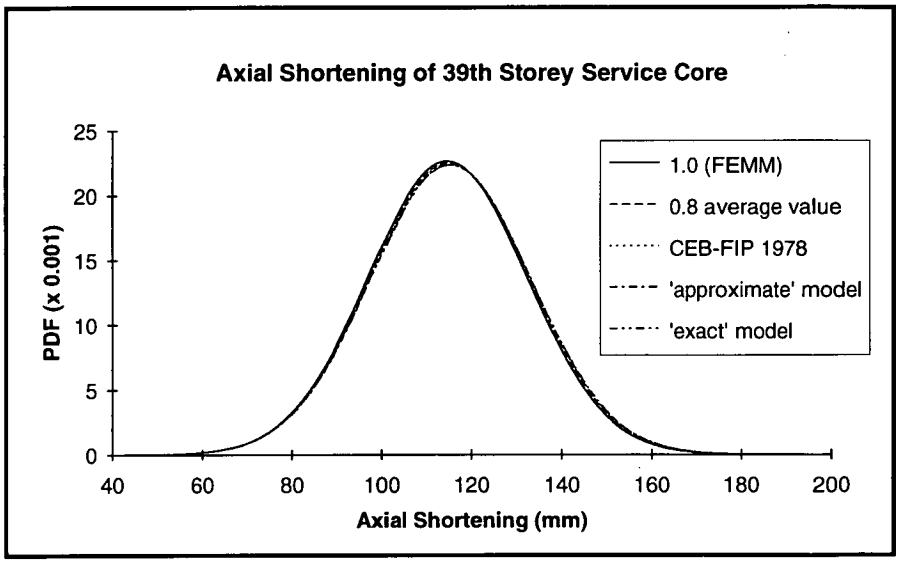

Figure 8.6 - Comparison between different aging coefficient models for predicting long-term axial shortening of example 39th storey service core.

8.3.3 Comparison of the CEB-FIP 1978 Recommendations on Concrete Properties

Expressions found in [14] and [40] for describing the concrete properties recommended by CEB-FIP 1978 code [38] were tested in conjunction with the four column models. On average, the percentage of over-lap between these two sets of equations, resulting in axial shortening predictions of the 39 storey building, were in the lower half of region A (i.e. 90% to 95%). In effect, it can be concluded that both sets of expressions result in essentially the same predictions.

See Figure 8.7 for one of the many comparisons utilising the TBEMM column model.

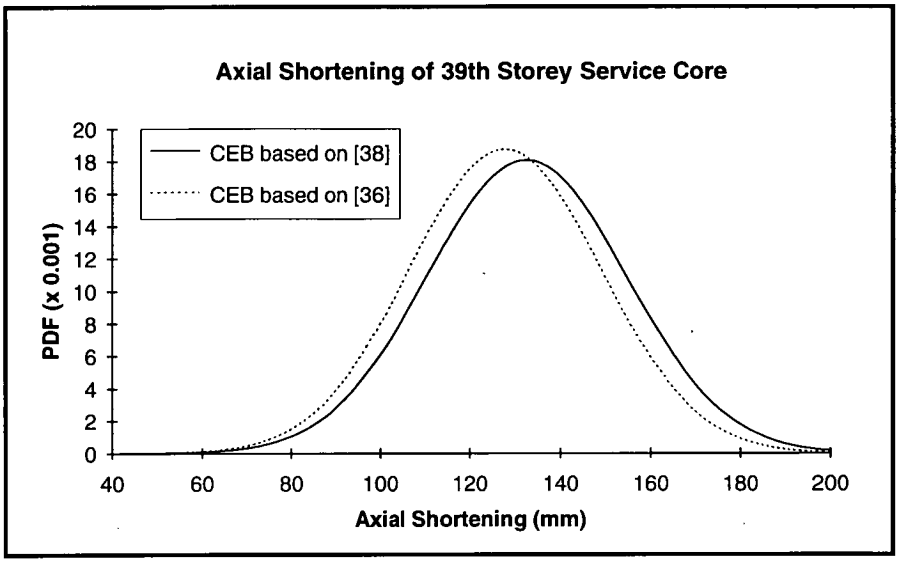

Figure 8.7 - Comparison between different CEB-FIP 1978 concrete property model equations for predicting long-term axial shortening of example 39th storey service core.

8.3.4 Comparison of Concrete Strength Models

The concrete strength models proposed by the ACI 1978 [37] and CEB-FIP 1978 [38] standards were also studied. The strength equations are used in determining the elastic modulus, which is critical to an axial shortening analysis, however this forms an independent assessment as described in the next section. Concrete strength values are also required by the AS-3600, BP and BPX models for predicting creep and shrinkage. The analysis of all four column models, combined with the concrete properties of ACI, CEB-FIP and AS-3600 in turn, indicated that the percentage of over-lap in the PDFs was in the lower half of region A (i.e. 90% to 95%). Thus, it would appear, based on the criteria above, that there is not a significant difference between axial shortening outcomes from either of the concrete strength models. See Figure 8.8 for one of the many comparisons utilising the TBEMM column model coupled with the ACI properties.

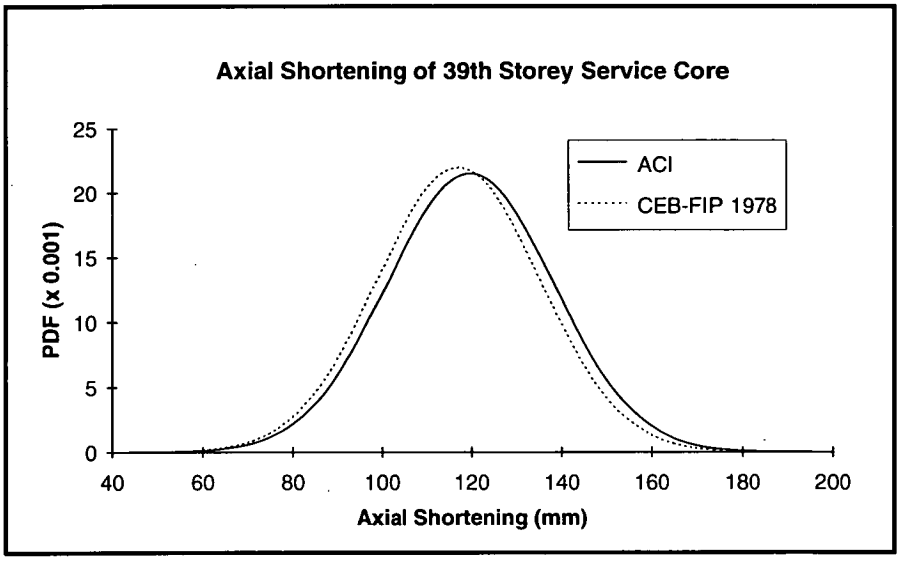

Figure 8.8 - Comparison between different concrete strength models for predicting long-term axial shortening of example 39th storey service core.

8.3.5 Comparison of Elastic Modulus Models

The elastic modulus proposed by Pauw [112], given by (3.15), was historically based mainly on light-weight concretes, however more work recently on higher strength concretes has found that this equation is not always adequate [114]. The Pauw model however is adopted as the base model for axial shortening comparisons. Models of elastic modulus for either normal, or both normal and high strength concretes have been proposed by Jobse and Moustafa [117], Ahmad and Shah [118] and can also be obtained for ACI High Strength Concrete [57] and CEB-FIP 1978 [38] standards. In examining the four column models, combined with each of the concrete property models, the percentage of over-lap of the PDFs was found to vary from 55% to 90% for axial shortenings. The classification of these comparisons were in regions B and C. Thus, there are significant differences between the outcomes of axial shortening which use higher strength modulus equations, as would be expected (since deformation equates directly, though inversely, to modulus). Selection therefore of a representative model for elastic modulus is therefore critical to predictive accuracy. Given the downstream implications of imprecise values in any analysis, laboratory data for specific concrete mixes should be considered essential. See Figure 8.9 for one of the many comparisons utilising the TBEMM column model coupled with the ACI properties.

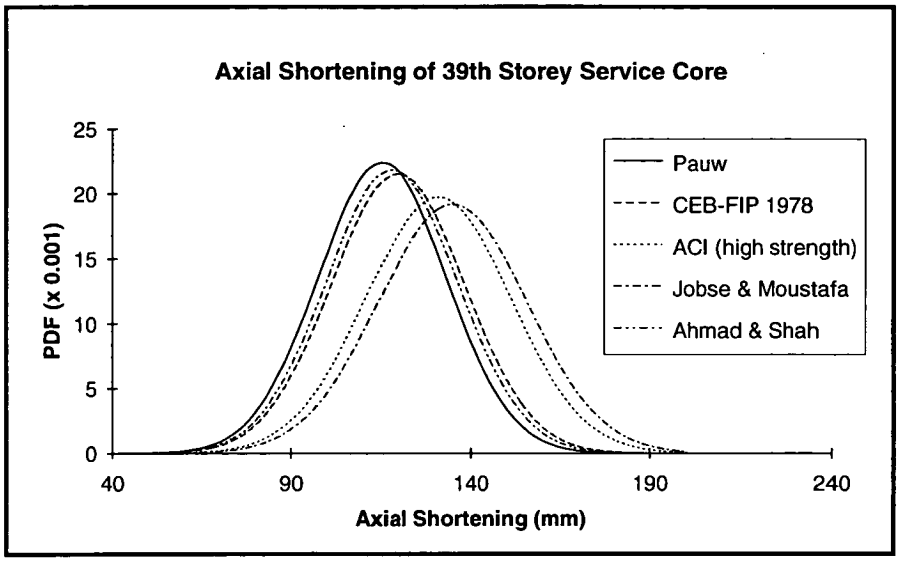

Figure 8.9 - Comparison between different elastic modulus models for predicting long-term axial shortening of example 39th storey service core.

8.3.6 Comparison of the BP Concrete Property Models

The original BP (Bazant-Panula) model for describing the concrete properties [66-68] has been extended to incorporate the effects of high strength concretes [72], temperature [66-68] and cyclic humidity [71]. The simplified BPs model [69,70] is also examined here. The BP model was adopted as the base model for these comparisons. Here, the column models of FEMM and TBEMM (i.e. aging coefficient values of 1.0 and 0.8 respectively) incorporating the BP concrete properties and modifications for the simplified version, high strength concrete, temperature and cyclic humidity, were tested for axial shortenings. The BPs model resulted in comparisons for overlap of the PDFs being in the top two thirds of region B (i.e. 80% to 90%). This would suggest that there are small significant differences between the models, and the simpler model might be inappropriate. The percentage over-laps for the other extensions of the BP model were; for temperature in top quarter of region A (i.e. 97% to 100%), for high strength concretes in the top third of region B (i.e. 85% to 90%) and for cyclic humidity in the mid-region of A (i.e. 93% to 97%). Temperature and cyclic humidity in this case are deemed not to be a significant influence on shortening outcomes and therefore do not constitute a useful pair of independent parameters to refine the predictions. The incorporation of high strength concrete parameters is however a different matter and should be accounted for in any shortening analysis when a building includes elements of high strength concrete.

Improvements to the original BP model via an improved shrinkage expression [127], and refined laws for creep which employ either double power logarithmic

or triple power laws [73,75] instead of the original double power law, can be made. As shown in [73,75,127] these refinements agree better with long-term test data. Adopting the triple power law over the double power law increases the CPU analysis time for the example 39 storey building by approximately 4000 times, whilst the double power logarithmic law has been proposed to reduce this analysis time. The column models of FEMM and TBEMM for axial shortenings were tested, where the BP model was utilised as the base model for comparisons. The percentage of over-lap for these creep and shrinkage refinements fell in the top half of region A (i.e. 95% to 100%). In summary, these improved models seem to be predicting essentially the same axial shortenings as the unmodified version. It is pointed out that the original BP model with all its refinements has been superseded by the improved model of Bazant *et al.* [76-83] and is examined in the next section.

8.3.7 Comparison of Concrete Property Models

Bazant *et al.* [78-82] proposed a more recent concrete property model using substantially more experimental data than the original BP model. For comparison purposes the improved BPX model was utilised as the base for axial shortening outcomes. The BPX model included a simpler BPXs model [83], which is also studied here. Tests on the column models of FEMM and TBEMM coupled together with the concrete property models of ACI, CEB-FIP, AS-3600, BP and BPXs in turn were made. The percentage of over-lap of the PDFs for the BPXs model was in region A (i.e. 93% to 100%). This simpler version would suggest that there are no significant differences between this and the more comprehensive BPX model. When comparing the BP and BPX models, it was found that there were definite significant differences in the predictions. The percentage of over-lap on average fell well in region C (i.e. 15% to 60%). In conclusion, the original BP model shows significant differences in shortening predictions to the BPX model and care is required with its application. However, this cannot also be said in regard to the application of the simplified version of the improved BP model (i.e. BPXs).

Other property models tested included; CEB-FIP 1970 [58], CEB-FIP 1978 [38], ACI [37] with elastic modulus of Pauw [112] and the ACI high strength concrete model [57] of elastic modulus, and AS-3600 [39] with same two elastic modulus models. The percentage of over-lap for CEB-FIP 1970 code was at the bottom of region C (i.e. 35% to 50%). Here, a definite significant difference between the output results can be observed, concluding that this model would be inappropriate

for the present application. The model also has been superseded by CEB-FIP 1978. The remaining comparisons gave percentage over-laps as follows; CEB-FIP 1978 standard was in region C (i.e. 25% to 40%), ACI code with model of Pauw in regions B and C (i.e. 70% to 85%) and ACI high strength concrete model in region C (i.e. 35% to 45%), and finally AS-3600 standard with model of Pauw or ACI high strength concrete with values ranging from 80% to 95% (i.e. regions A and B) or 45% to 65% (i.e. region C) respectively. In summary, there seems to be significant differences in some cases and less differences in others. The selection of creep and shrinkage properties for concrete are critical, and again laboratory data would appear to be essential to obtaining a meaningful analysis of a tall building.

Following on from the above, the objective now is to assess the B3 property model in the context of a tall building analysis, based on the predictive accuracy of the model. The probabilistic comparisons were carried out for the long-term cumulative shortening of the service core and outer frame of the example 39 storey building using the B3 concrete properties, combined with either FEMM or TBEMM column models.

For comparison purposes the revised B3 model was utilised as the base for axial shortening outcomes. Tests on the column models of FEMM and TBEMM coupled together with the property models of BPX, BPXs and BP in turn were made. The percentage of over-lap of the PDFs for the BPX, BPXs and BP models were in regions A and B (i.e. 70% to 95%), region A (i.e. 90% to 95%) and region C (i.e. 20% to 50%) respectively. It can be concluded that the original BP model shows significant differences in shortening predictions to the B3 model, whilst the BPX model showed moderate discrepancies and BPXs was shown to be predicting the same population. See Figure 8.10 for one of the many comparisons utilising the TBEMM column model.

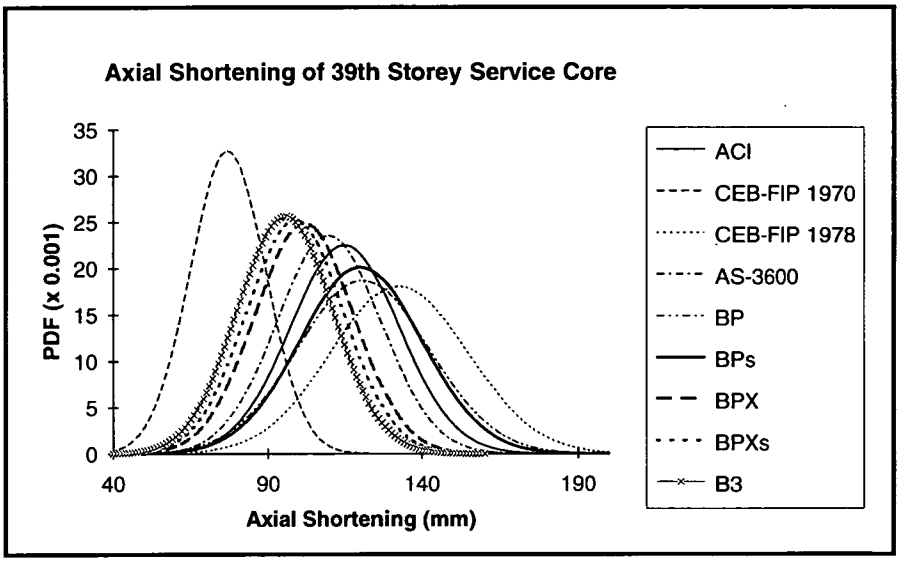

Figure 8.10 - Comparison between different Bazant *et al.* concrete property models for predicting long-term axial shortening of example 39th storey service core.

8.3.8 Comparisons of Construction Cycle Variations

Having investigated the respective sets of concrete property and column models, the storey cycle which is typical of tall building construction is examined for various assumed cycle times. From this, its influence on long-term axial shortening is investigated. For the analyses undertaken, again the column models of FEMM and TBEMM together with the concrete property models of ACI, CEB-FIP 1978, AS-3600, BPX, BPXs and B3 in turn were tested. The cycle time per storey level was the single variable parameter in these comparisons, with ±2 day variations being the limiting times, where an assumed constant construction rate of 10 days per storey was used as the basis for comparison. Loading ages for each column element are affected by varying the cycle period, with young loading ages having a more significant influence on the inelastic deformations than the more mature loading ages. For a variation of ±1 day, the percentage of over-lap was in the top half of region A (i.e. 95% to 100%), whilst for ±2 days these comparisons were in the bottom half of region A (i.e. 90% to 95%). Thus, variations in the construction cycle of ±2 days does not significantly alter the axial shortenings for the example building considered. See Figure 8.11 for one of the many comparisons utilising the TBEMM column model coupled with the ACI properties.

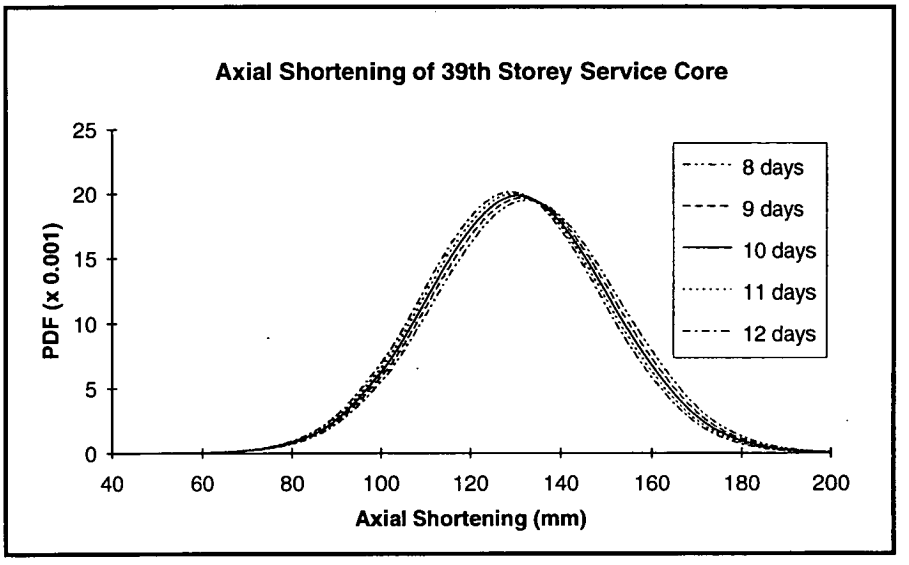

Figure 8.11 - Comparison of TBEMM column model with varying construction rates for predicting long-term axial shortening of example 39th storey service core.

8.4 COMPARISON OF THEORETICAL AND EXPERIMENTAL SHORTENINGS

In testing the probabilistic shortening models developed Chapter 6 against real building data, only single-valued experimental data has been available to the author through [29]. Ideally, probabilistic experimental data would have provided better comparisons for quantifying the uncertainty of theoretical shortenings, however, to the best of the author's knowledge no such data is available in the literature.

In [29] Brady describes the application of different surveying procedures which have been used to measure the axial shortening of columns in the University of Technology Sydney building. This building, with a total height of 146m, contains 24 storeys in the main tower, and was completed in 1978 [123]. Wire gauges embedded in the columns were used to obtain the necessary strain readings. From the column strain measurements of Brady, Cridland *et al.* [123] compared these results with several deterministic time-dependent shortening models. Cridland *et al.* found that when employing test data for creep, shrinkage, elastic modulus and concrete strength in the theoretical models, the comparisons with those measured, resulted in closer agreement than if no test data had been incorporated.

Other experimental and theoretical comparisons were made by Pfeifer *et al.* [163] on a 197m high building with 70 storeys known as the Lake Point Tower in Chicago. The columns and core of the building were designed for normal weight

concretes using characteristic strengths of 50, 40, 35 and 25 MPa. Not all input variables needed for an axial shortening analysis were given for this building and thus the test data could not be employed here.

The total absolute shortening strains of three columns located within different storeys were measured by Brady [29]. These columns are designated by their storey levels of 8, 12 and 20 respectively. The input data available for a shortening analysis from these three columns included concrete mix parameters, column geometric properties, applied loads and loading ages, and experimentally determined values of concrete strength and modulus. It should be noted that the applied loads were estimated from the design dead and live loads, not the measured loads in the building. All data for the three columns can be found in Appendix A8.1. The self-weight of each column is assumed to apply at the end of the initial column curing period.

In accordance with Section 8.3.5 the elastic modulus model used in determining the theoretical shortenings is assumed to be critical. Applying the modulus model of Pauw [112], with the measured values of concrete strength, the resulting calculated modulus values were found to be in very close agreement with measured values. Thus, the model of Pauw was used, reducing to some extent, the uncertainty of the shortening analysis. Creep and shrinkage test data were not included as part of the raw data supplied to the computer model.

The axial shortening column strains were measured to be 516, 475 and 400 micro-strains for the columns on storey 8, 12 and 20 respectively. Comparison of these values with some probabilistic predictions are shown in Figure 8.12 for each of the levels. The column model of TBEMM incorporating the exact aging coefficient was used in this analysis. This model is coupled with the concrete properties of the ACI [37], AS-3600 [39], CEB-FIP 1978 [38], and the models of Bazant *et al.* (BPXs) [83], Bazant *et al.* (BPX) [78-82] and Bazant *et al.* (B3) [84] in turn. For the tests conducted, the experimental strains are observed to be in good agreement with the theoretical column models, Figure 8.12. The strain measured on storey 12 is somewhat lower when compared to the predictions and no explanation is offered, other than to point out that the measured value falls within the theoretical distributions.

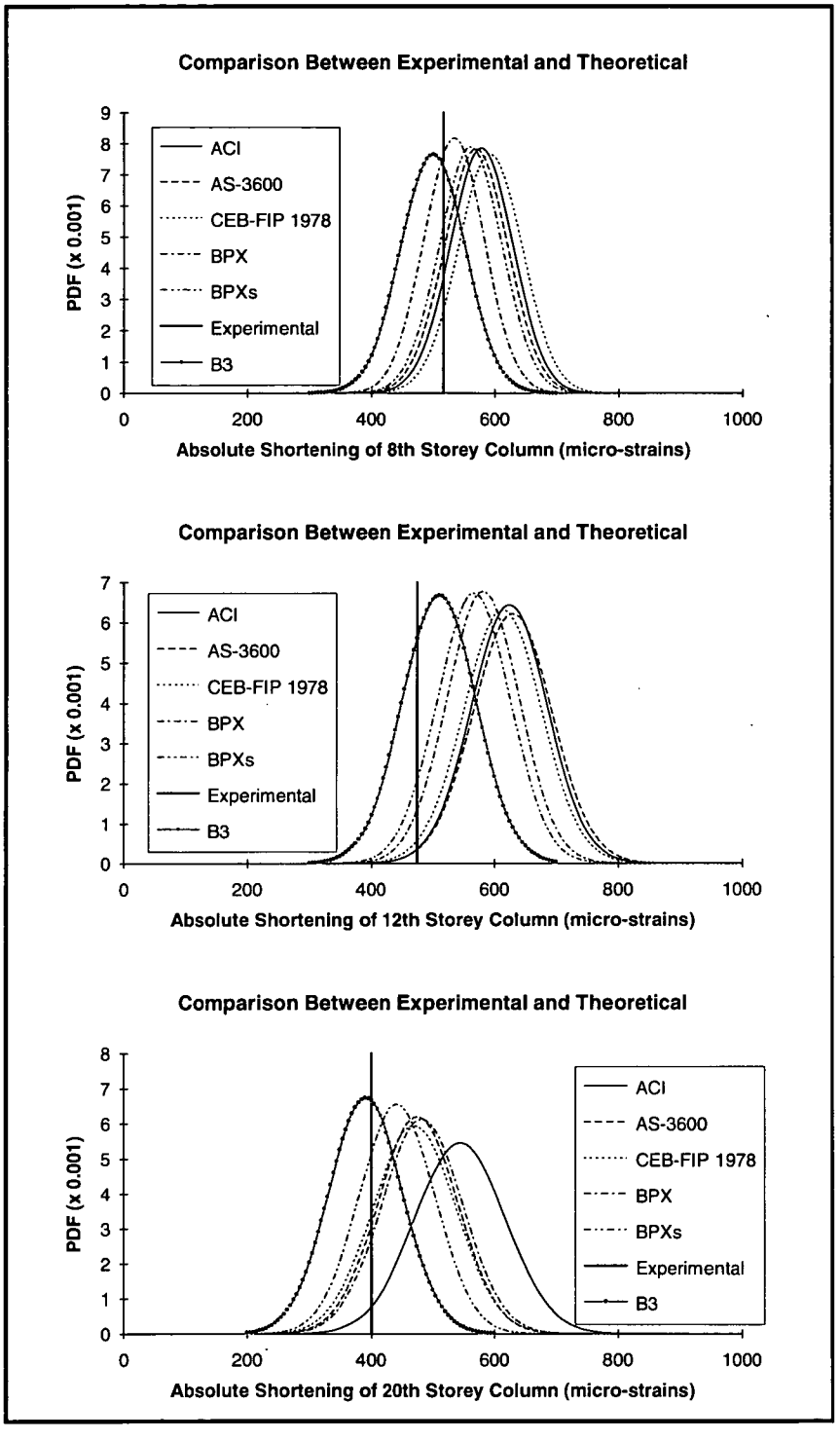

Figure 8.12 - Comparisons of probabilistic predictions and strain measurements of Brady [29] on columns in University of Technology Sydney building.

The shortening predictions of a TBEMM column model combined with the B3 model [84] are compared to the experimental shortening of the three columns, where the expected values were determined to be 500, 511 and 392 micro-strains for the columns on level 8, 12 and 20 respectively as compared with 516, 475 and 400 micro-strains. From all shortening predictions made in this section, the B3

model predictions showed the best agreement and were within ±7% of the test data, see Figure 8.12.

8.5 SENSITIVITY ANALYSIS

8.5.1 Introduction

The overall axial shortening analysis can be reduced to three hierarchical levels of parameters. Referring to Figure 8.13, the first level considers the primary input variables which are required as input into the models for the creep coefficient, basic shrinkage strain and elastic modulus. These level one variables may include some or all of the environment parameters such as humidity and temperature. Also, column properties and concrete mix variables are at this level. The creep coefficient, basic shrinkage strain and elastic modulus are considered as the level two parameters or intermediate variables. Finally, level three variables represent the final axial shortening outcomes.

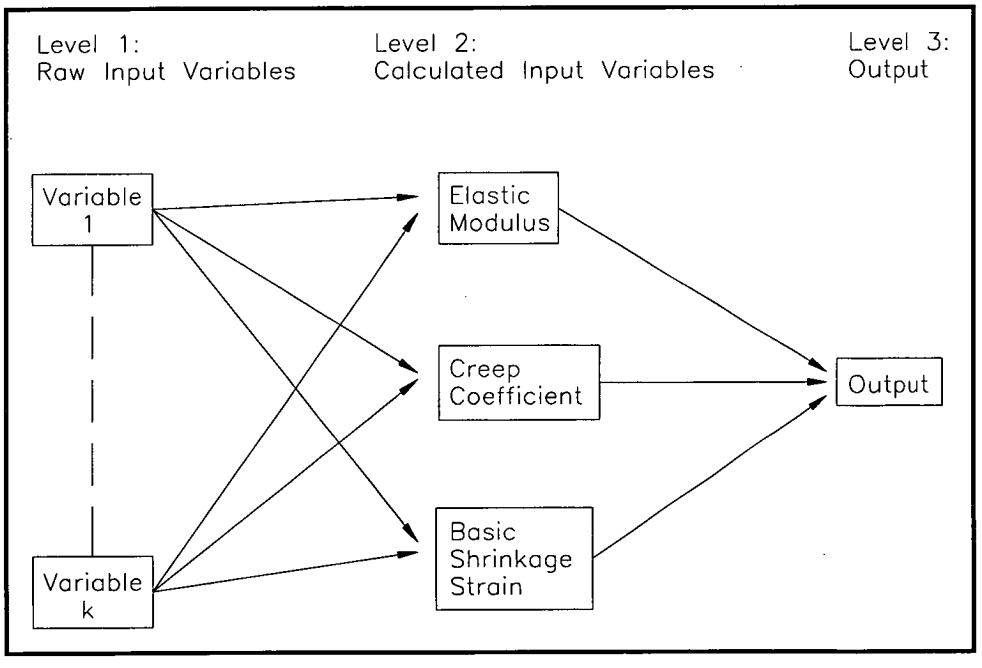

Figure 8.13 - Diagrammatic representation of the numerical processes involved in an axial shortening analysis, as required for a sensitivity analysis.

The sensitivity of a given variable depends on the level at which it is being measured. For example, a variable beginning at level one, whilst having a significant influence on the next level variable, in the context of the overall results may in fact not be at all significant. This depends on how the column model incorporates each variable and the internal processes which treat the variable.

In the work to follow, the FEMM column model was combined with a selection of different concrete property models. Here, each combined model was tested for variable sensitivity. The example 39 storey building was used for this study also and the long-term shortenings of the service core and spandrel frame respectively were determined. One example of the many correlations, in this case, the sensitivity of relative humidity on the computed creep coefficient is shown in Figure 8.14.

The sensitivity of each parameter was carried out between the ±50% limits of the base value to determine the stability of the column model equations, whilst ±20% limits were used in establishing sensitivity. The variability of the column geometric properties were not considered in the sensitivity analyses. This agrees with Madsen and Bazant [133].

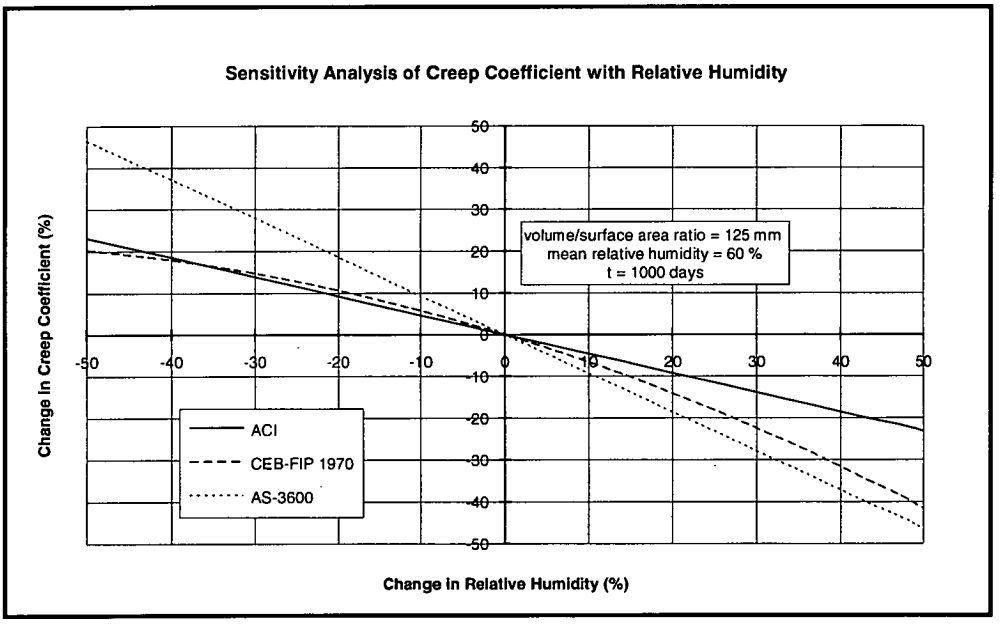

Figure 8.14 - Sensitivity analysis of creep coefficient with respect to environment relative humidity.

In the sections to follow a number of concrete property models are considered and the respective independent input parameters to each are evaluated.

8.5.2 ACI Code

An analysis of the FEMM column model with the ACI code [37,57] consisted of varying each level one independent parameter by ±20% respectively, resulting in axial shortening variations as follows:

	air content	±0.5%
	cement content	±1%
	concrete slump	±2%
	fine aggregate content	±4%
	concrete strength	∓5%
and	environment humidity	∓5%

On the basis of these findings one could conclude that the input mix parameters, excluding the fine aggregate content, have no significant effect on shortening outcomes. It is observed that ±20% variation of humidity content resulted in the creep coefficient and shrinkage strain varying some ∓9% and ∓15% respectively. Also ±20% modification of fine aggregate content resulted in the same parameters varying by ±2% and ±12% respectively. Thus, humidity in this case is shown to be the most sensitive of the variables, with concrete strength and fine aggregate content following.

The variation of the level two parameters, i.e. elastic modulus, creep coefficient and basic shrinkage, within the ±20% limits, caused the shortening results to vary by (-10%,+20%), (+15,-10%) and (+10%,-10%) respectively. Here, the first number in the brackets is the output result due to +20% fluctuation of input variable.

The stability of the FEMM column model was tested by varying each input parameter independently by ±50% for the ACI code, as well as testing the elastic modulus, creep coefficient and basic shrinkage strain independently. Within these limits the equations did not result in axial shortening values becoming unstable.

8.5.3 CEB-FIP 1978 Code

The FEMM column model was also combined with the CEB-FIP 1978 standard [38]. In similar manner to the above, variations of ±20% on each parameter were trialed including concrete strength and humidity. This resulted in axial shortening deviations of ∓5% and (-10%,+2%) respectively. It is clear that both variables in this instance require judicious selection for use in shortening analyses.

Variations of the elastic modulus, creep coefficient and basic shrinkage strain within the ±20% limits resulted in shortenings fluctuating by (-10%,+20%), ±10%

and ±5% respectively. Again, the stability of the column model based on input variables and concrete properties was kept within ±50% limits.

8.5.4 AS-3600 Code

The FEMM column model with AS-3600 code [39] and the high strength concrete modulus model of ACI [57] were combined for this analysis. Modifying humidity and concrete strength, by ±20% respectively resulted in axial shortenings varying by ∓10% and (-10%,+20). Concrete strength especially would appear to have a significant effect on the creep component.

The deviation of elastic modulus, creep coefficient and basic shrinkage within the ±20% limits caused the shortenings to differ by (-10%,+15%), ±7% and ±5% respectively. The stability of the FEMM column model was again retained within ±50% limits.

8.5.5 BPX Model

Here the FEMM column model was combined with the Bàzant *et al.* [78-82] concrete properties (i.e. BPX model) with a ±20% variation being again applied to each relevant level one parameter. The results for axial shortenings varied respectively by:

	sand-cement ratio	±2%
	total aggregate-cement ratio	∓4%
	environment humidity	∓4%
	concrete strength	∓10%
	environment temperature	±10%
	cement content	±15%
and	water-cement ratio	±20%

It would appear that the cement content and water-cement ratio are extremely sensitive to this combined BPX model, with water-cement ratio being equally significant in creep and shrinkage components, whilst of lesser importance in their significance on the modulus parameter. Temperature and concrete strength are also critical though less sensitive than the two previous variables. Humidity and total aggregate-cement ratio are critical to the shrinkage component, but in the overall context axial shortenings appear to be less significant. Thus, cement content and water-cement ratio in this case appear to be the most sensitive parameters, requiring careful selection for a shortening analysis.

The variation of elastic modulus, creep coefficient and basic shrinkage within the ±20% limits caused the shortenings to vary by (-12%,+18%), ±8% and ±5% respectively. The stability of the column model analysed here again was held within ±50% limits.

8.5.6 B3 Model

The FEMM column model was combined with the Bazant and Baweja concrete properties (i.e. B3 model) with a ±20% variation being applied to each relevant level one parameter. The results for axial shortenings varied respectively by:

	total aggregate-cement ratio	±3%
	environment humidity	∓4%
	cement content	±5%
	water-cement ratio	±5%
and	concrete strength	∓10%

It would appear that the concrete strength is moderately sensitive to this combined B3 model, whilst water-cement ratio, cement content, humidity and total aggregate-cement ratio are less sensitive. Thus, concrete strength in this case appears to be the most sensitive parameter, requiring careful selection for a shortening analysis. In addition, it was observed that the sensitivities of the output shortenings based on the B3 model are significantly less than those for the BPX model.

The variation of elastic modulus, creep coefficient and basic shrinkage within the ±20% limits caused the shortenings to vary by (-13%,+20%), ±8% and ±4% respectively. The stability of the column model analysed here was held within ±50% limits.

8.5.7 Summary

For the combined column models tested, the effects of the independent constitutive parameters on axial shortening were ranked above. For the level two variables, the sensitivities in descending order are given to be elastic modulus, creep coefficient and basic shrinkage strain, irrespective of which concrete property model is used. It is interesting to note that decreasing the modulus resulted in a different measure of its sensitivity than increasing it. One can conclude that a degree of caution is required in the choice of design values for

concrete modulus, especially if one is underestimating values. Also, the axial shortenings were moderately proportional to both creep and shrinkage, that is, almost linear relationships were observed to exist between creep coefficient and shortening, whilst shrinkage is linear in the main column shortening equations. The level two order of sensitivity defined here is important in determining the accuracy of expected values in a probabilistic analysis.

8.5.8 Load History of Columns

Column weights are required for partially defining the load history of any tall building (see Chapter 2) and subsequently used for predicting axial shortening. A sensitivity analysis was performed on the concrete density, as applied to determining the load histories of the 39 storey building. Modifying this parameter by ±20% resulted in axial shortenings varying by ±1%. Here, the concrete density is not crucial, but this depends on the magnitudes of the other loads assumed in the load histories. The column weights contribute 20% and 13% of the entire loads applied to the core and spandrel columns respectively in the case-study considered here. In conclusion, the concrete density obligates cautious selection only if the other building loads are of most equal magnitude or less than the column weights.

8.6 FINAL RECOMMENDATIONS ON AXIAL SHORTENING OF TALL CONCRETE BUILDINGS

It was found from the literature review that axial shortening can cause problems in tall concrete buildings and should be considered by the analyst at the design stage. Deterministic methods of analysis are currently available for predicting time-dependent shortening. It has been recommended by various standards that the uncertainty of the elastic modulus, creep coefficient and basic shrinkage strain need to be incorporated in design, for example, AS-3600 requires that variations of ±20% for the modulus and ±30% for both creep and shrinkage. Incorporating the concrete properties in this manner is rather crude. To improve on this aspect, the description of each random property is modelled by a Gaussian distribution which propagates through any Monte Carlo simulation or any n^{th}-order moment analysis. Consequently, predictions can more reliably be employed in design. These models do, however, represent a preliminary stage of development and could be further improved to embody more complex random variables as discussed in Chapter 9.

From the deterministic and probabilistic comparisons made in Chapters 4 and 8 respectively, the examination of the concrete property models and constitutive stress-strain laws (Chapters 4 and 5 respectively), the sensitivity analyses in Chapter 8 and the experimental comparisons also in Chapter 8, a final recommendation on the long-term axial shortening of columns and cores in tall concrete buildings can be made.

Bazant [7] has stated that the Trost-Bazant Age-Adjusted Effective Modulus Method is a theoretically superior model for analysis, and Bazant and Baweja [84] have recommend this model for the analysis of tall buildings. The probabilistic comparisons (Section 8.3.1) with other constitutive models for axial shortening have been shown to result in some differences with the less rigorous RCM and IRCM models. Thus, it can be suggested that the two latter models are inappropriate for tall building analyses.

Employing the TBEMM requires the use of an aging coefficient which is obtained from the creep coefficient and elastic modulus (i.e. the stress-dependent elastic and inelastic concrete behaviour) used in the analysis [7]. Adopting a 0.8 average value for aging throughout a long-term shortening analysis rather than the exact value, the probabilistic comparisons showed no significant differences in predictions (Section 8.3.2).

Bazant and Baweja [84] recommend the B3 model, on the basis of its more advanced theoretical and statistical characteristics. In addition, the B3 model accommodates concretes which, for example, may have equal strengths but unrelated creep and/or shrinkage properties. Significant differences have been observed with shortening predictions employing various creep and shrinkage models (Sections 8.3.6 and 8.3.7). Currently available concrete property models are limited with respect to the range of conditions that can be handled (Section 4.2), however the B3 model has a wider applicability range. From the sensitivity of axial shortenings, it was found that the input parameters required for the B3 model are not quite as sensitive to the output shortening relative to the input parameters for the BPX model (Sections 8.5.5 and 8.5.6). Comparison of predicted column shortenings with test data showed that the B3 model gave the best results. All were within ±7% (Section 8.4, Figure 8.12).

In conclusion, the Trost-Bazant Age-Adjusted Effective Modulus Method combined with the 0.8 average value aging coefficient and the B3 concrete

property model is potentially the most sophisticated of all approaches at present to the analysis of long-term axial shortening in tall concrete buildings.

Interpretation of the results obtained from any probabilistic analysis of total and differential shortening in the columns and core of a tall building needs some discussion. On obtaining the probability density functions describing shortening, Gaussian distributions in this case, the analyst selects the confidence limits that gives a measure of safety in serviceability and strength design. If selecting the 95% limits for differential shortening, both the upper and lower portion of the distribution's rejected tail would each contain 2.5%. A maximum and minimum value is then obtained corresponding to the distribution's tails. Both of these limits need to be considered in design as the worst case does not necessarily occur at the maximum value. For example, the minimum differential shortening could be negative implying that the beam/slab connection to the column and core may require additional negative and/or positive reinforcement. In selecting the 95% limits for total shortening, the upper portion of the distribution's rejected tail would be 5%. A conservative maximum value is then obtained which is important in ultimate design consideration, for example, the maximum total shortening of the core may be necessary when designing for the installation of lift guide rails.

The author is not able to recommend on the selection of input parameters for the design of buildings since each parameter is governed by a number of factors. These factors relate to the height of the building, the layout of columns and core, the floor to floor heights, the columns and core geometric cross-sections, amount of reinforcement and the concrete mixes used. Based on the arguments in Section 6.1, the applied loads are estimated average values obtained from a project when any differential shortening analysis is required, whilst conservative loads may need to be considered with absolute shortening of either columns or cores. The concrete mixes and properties of the vertical elements are obtained directly from the design data. Further, actual concrete mix parameters can be used at the preliminary design stage for predicting concrete properties (i.e. creep, shrinkage and elastic modulus) with coefficient of variations for each random variable described in Section 6.1. Concrete test data however should be incorporated when available at a later stage.

Finally, the limitations of the models developed in Chapter 6 are examined. Firstly, restriction of the input concrete mix parameters as required for predictions of creep, shrinkage and elastic modulus obtained from the B3 model are noted in

Chapter 4. The construction cycle model developed in Chapter 2 is quite general and can accommodate any construction sequence which groups all loads into three main classes, namely vertical element self-weights, construction and in-service (i.e. three loads per storey are added to the overall building system). Each load application occurs instantaneously. The idealised structural configuration of the building does not allow for frame-type actions or load transfers, and only free column shortening is accounted for. Any second-order moment analysis is approximate and predictions need to be checked with Monte Carlo results initially, and subsequently when coefficient of variation values are varied for each random parameter for different analyses. Monte Carlo analyses are time consuming and are not recommended as a primary tool of analysis, but only to confirm n^{th}-order moment predictions. The uncertainty of the concrete properties only are incorporated in the probabilistic models as normally distributed, whilst all other input variables are modelled as deterministic.

8.7 CONCLUDING REMARKS TO CHAPTER

Numerous combinations of concrete property models with column models were tested and the resulting output axial shortenings were shown to conform to Gaussian distributions with the characteristic moments determined from a second-order moment analysis. Other distributions were tested and shown also to be statistically admissible. The axial shortening predictions were compared for different column and property models where both significant and slight differences were observed. Comparisons of the probabilistic column models with field data showed good agreement. The sensitivity analysis determined the effects of the independent constitutive parameters on axial shortening, which were then ranked. Interpretation of the results of this study should not be seen to be conclusive, as the case-study adopted indicates specific outcomes and not necessarily applying to all tall concrete buildings. Finally, a recommendation based on the work of Chapters 4, 5 and 8 on long-term axial shortening of tall concrete buildings was made. Conclusions drawn from this chapter are elaborated in Chapter 9.

APPENDIX

TO

CHAPTER 8

APPENDIX A8.1

Listed below are input axial shortening data for the three columns where strains were measured by Brady [29] in the survey project of the University of Technology Sydney building. For information not available for a theoretical comparison, the following values for the respective variables have been assumed; percentage of air in mix: 2.5%, water-cement ratio for mix in level 20 column: 0.5, concrete density: 2400 kg/m^3, environment humidity: 65%, environment temperature: 20°C. For the level 8 column:

Variable	Value
Concrete Strength	48.1 MPa
Water-Cement Ratio	0.4
Sand-Cement Ratio	1.02
Total Aggregate-Cement Ratio	3.53
Percentage of Fines	28.8 %
Cement Content	496 kg/m^3
Slump	90 mm
Rock Type	Basalt
Area of Column	1.2871 m^2
Percentage of Steel	7.7 %
Perimeter of Column	5.44 m
Period of Analysis	1582 days

Loading Age (days)	Loads (kN)	Loading Age (days)	Loads (kN)
29	120	851	330
60	120	910	1240
121	300	971	2180
180	820	1032	1260
242	670	1094	1050
302	830	1155	1350
364	1310	1216	1100
425	960	1276	1980
486	410	1337	2400
545	670	1398	1130
606	570	1460	290
667	690	1521	680
729	960	1582	400
790	480		

For the level 12 column:

Variable	Value
Concrete Strength	38.6 MPa
Water-Cement Ratio	0.48
Sand-Cement Ratio	1.77
Total Aggregate-Cement Ratio	4.89
Percentage of Fines	36.1 %
Cement Content	386 kg/m^3
Slump	90 mm
Rock Type	Basalt
Area of Column	1.2871 m^2
Percentage of Steel	5.0 %
Perimeter of Column	5.44 m
Period of Analysis	1376 days

Loading Age (days)	Loads (kN)	Loading Age (days)	Loads (kN)
37	67	767	2182
98	294	828	1261
160	1081	890	1055
221	533	951	1344
282	0	1012	1101
341	669	1072	2012
402	360	1133	2408
463	658	1194	1090
525	940	1256	290
586	422	1317	681
647	333	1376	394
706	1237		

For the level 20 column:

Variable	Value
Concrete Strength	39.6 MPa
Water-Cement Ratio	0.5
Sand-Cement Ratio	2.05
Total Aggregate-Cement Ratio	4.8
Percentage of Fines	42.8 %
Cement Content	375 kg/m^3
Slump	80 mm
Rock Type	Basalt
Area of Column	1.2871 m^2
Percentage of Steel	1.2 %
Perimeter of Column	5.44 m
Period of Analysis	658 days

Loading Age (days)	Loads (kN)	Loading Age (days)	Loads (kN)
47	190	413	2360
108	810	474	1090
170	870	536	290
231	1050	597	680
292	1050	658	390
352	2000		

CHAPTER 9

CHAPTER 9

CONCLUSIONS

Consideration of the variability of the concrete properties within the context of a probabilistic axial shortening analysis of tall buildings helps to quantify the uncertainty associated with selecting specific codified values. Choosing representative parametric values in any analysis for which accuracy rather than conservatism is desirable, must be done cautiously. For tall buildings differential axial shortening values result from the difference of at least two significantly large numbers (the absolute values of shortening in each of two columns), requiring at least some knowledge of the error associated with the solutions for design purposes. It has been demonstrated that some of the key parameters, namely the creep coefficient, the basic shrinkage strain and the elastic modulus, can be incorporated into a probabilistic analysis from which rational estimates of values can be made and consequent effects evaluated.

From the work of this thesis, it can be seen that the long-term axial shortening of columns and cores in tall concrete buildings can be effectively and rationally characterised according to the recommendations of Section 8.6. This can be summarised as follows: *the Trost-Bazant Age-Adjusted Effective Modulus Method combined with the 0.8 average value aging coefficient and the Bazant and Baweja (B3) concrete property model is potentially the most sophisticated of methods presently available for analysing long-term axial shortening in tall concrete* buildings. As has been demonstrated by the author, when resolved into probabilistic format, this form of analysis represents a tool which can be considered useful in both research and design.

The project involved investigations in four major stages which were necessary in order to arrive at the final recommendations. These stages were: (i) the development of probabilistic models for predicting time-dependent shortening of column elements and the implementation of the developed deterministic and probabilistic models of analysis into software, (ii) an assessment of concrete property and constitutive models and, the assumptions associated with the application to tall building shortening analyses, and the theoretical probabilistic comparisons between different predictive methods, (iii) a parametric study to rank

the sensitivities of the input variable with respect to the computed axial shortenings, and (iv) the comparisons of the theoretical column models with experimental shortening data. A number of conclusions have been drawn from each stage and are presented below.

STAGE (i)

The probabilistic solutions undertaken here have included a Monte Carlo simulation, and first- and second-order moment analyses. With results from the software (AXS) embodying the probabilistic analyses, the following observations can be made:

- the Monte Carlo method is more quantitative in terms of its output than a n^{th}-order moment analysis, however it is a computationally time consuming method (Section 6.2). This can be equally applied to the solution in any probabilistic mechanics problem however.

- comparable output results were obtained from a Monte Carlo simulation and a second-order moment analysis, whilst a first-order moment analysis was found to be inadequate for representing characteristic moments of shortening distributions (Section 6.4). This warranted the application of the second-order moment analyses in Chapter 8.

- assuming Gaussian PDFs for the representation of concrete properties, the output axial shortening PDFs are shown to conform to the same distribution with characteristic moments determined from a second-order moment analysis. Refer to Section 8.2. This aspect further reinforces the use of the second-order moment analyses in Chapter 8.

- the gamma and beta distributions are also shown to be capable of modelling the output axial shortening PDFs, however, the complex characteristic descriptions of these distributions make them difficult to readily employ as design tools (Section 8.2). For this reason the Gaussian description was preferred in Chapter 8.

- the probabilistic analysis of the axial shortening predictions can be classified as being close to linear (for the COVs values employed here, see Section 6.1), as the basic shrinkage strain variation, which is linear, has a dominant effect and propagates through the analysis (Section 8.2). This reinforces the idea that the output shortening distributions can be modelled by Gaussian distributions.

The probabilistic axial shortening column models derived in Section 6.2 and 6.3 ("simpler" models) are further developed in Appendix A6.7. First- and second-order moment approaches were developed in this new analysis, as well as Monte Carlo simulation, which allow for the stochastic modelling of each random concrete property, that is, creep coefficient, basic shrinkage strain and elastic modulus, by independent Gaussian processes. This is a significant advance (in terms of mathematical modelling) over the "simpler" models of Chapter 6 since stochastic variations are incorporated. Based on the tall building analyses performed here, comparable output results were obtained from the Monte Carlo simulation and the second-order moment analysis (Appendix A6.7). It can be concluded that the rigour of the refined second-order moment equations is sufficiently accurate for the analysis of tall buildings, where concrete properties only are randomised. Comparisons between the "simpler" and new models showed no significant differences.

STAGE (ii)

There are a number of conclusions which can be drawn from the comprehensive probabilistic comparisons and sensitivity analyses of the 39 storey building case-study. However, the interpretation of the results of this study is not definitive, since it deals with specific outcomes and does not necessarily apply to all tall concrete buildings.

The following observations for long-term axial shortening analyses can be made from the probabilistic comparisons assessed here. These should not overshadow the recommendations made earlier, but give a more complete picture of currently available models which predict column shortening. Specifically:

- large discrepancies between concrete property models for predicting creep, shrinkage and instantaneous deformations were shown to exist at a deterministic level (Section 4.3). This was a significant reason for the study which was focussed on improving design standards and more rigorously quantifying the shortening phenomena of tall building performance.

- the differences between the column models indicate less of an influence on the axial shortening outcomes than the differences between the concrete property models. That is, selection of appropriate concrete properties would appear to be more critical than the selection of column model (Sections 8.3.1 and 8.3.7). Thus, the focus of the project has been to more closely examine the concrete properties which are used in predicting column shortening.

- predictions from the TBEMM column model, when coupled with any of the prescribed aging coefficient models, gave essentially the same results, thus the 0.8 average value appears to be equally suited in shortening applications (Section 8.3.2). This serves to inform of a possible simplification to the overall shortening analysis without loss of prediction accuracy.

- no real significant differences were noted between the column models of FEMM and TBEMM. The first is algebraically simpler, and in certain cases can be better applied (Section 8.3.1). One example being to obtain higher order moment analyses of column shortening.

- two complete sets of independent expressions required for describing both creep and shrinkage (one set is found in Comite Euro-International du Beton [40] and the other in Gilbert [14]) according to the CEB-FIP 1978 code [38] are predicting in essence the same shortenings (Section 8.3.3). This has direct application to the design of buildings which use concretes with characteristics more aptly described by the CEB-FIP 1978 code than other available code models.

- no real significant differences are observed in predictions when using the concrete strength formulae of either ACI [37] or CEB-FIP 1978 [38] codes (Section 8.3.4).

- care is needed when selecting appropriate elastic modulus, creep coefficient and shrinkage models for long-term axial shortenings (Sections 8.3.5 and 8.3.7).

- modifications to the original BP model [66-68] for cyclic humidity [71], temperature [66-68] and better long-term predictions proved to have a minor effect on overall shortenings, whilst the high strength modification in [72] is significant (Section 8.3.6). This has direct application to the analysis of buildings which use high strength concretes characterised by the BP model.

- large disparities were noted between the original BP model [66-68] and the revised version [78-82,84] for shortenings (Section 8.3.7).

STAGE (iii)

The sensitivities of the concrete properties in an axial shortening analysis was shown to vary. In descending order of apparent importance these were found to be the elastic modulus, creep coefficient and basic shrinkage strain, irrespective of which concrete property model is used (see Section 8.5.7). Here, the order is important when evaluating mean and deterministic axial shortening values, whilst the coefficients of variation play a significant role in the dispersion of shortening distributions. From the sensitivity analyses, the following conclusions can be drawn in respect of long-term axial shortenings:

- ACI Standard (209R-82, 363R-84) [37,57]; fine aggregate content, concrete strength and humidity had a significant effect on axial shortening outcomes for the example 39 storey building. Conversely air content, cement content and concrete slump showed as having little effect on outcomes. Refer to Section 8.5.2.

- CEB-FIP 1978 Standard [38]; concrete strength and humidity are the most significant of the parameters to influence axial shortening (Section 8.5.3).

- AS-3600 1988 Standard [39]; as for CEB-FIP. See Section 8.5.4.

- Bazant *et al.* model [78-83]; sand-cement ratio was shown not to be a sensitive variable; total aggregate-cement ratio, humidity, concrete strength and environment temperature were moderately influential; cement content and water-cement ratio are shown to be a critical inclusion in any shortening analysis. Refer to Section 8.5.5.

- Bazant and Baweja model [84-86]; concrete strength is moderately sensitive; water-cement ratio, cement content, humidity and total aggregate-cement ratio are less sensitive. It was observed that the sensitivities of the output shortenings based on the Bazant and Baweja model are significantly less than those for the Bazant *et al.* model [78-82]. Refer to Section 8.5.6.

- the stability of FEMM column model combined with either the ACI, CEB-FIP 1978, AS-3600, Bazant *et al.* [78-82] or Bazant and Baweja [84-86] concrete property models was held, where the applicable independent input parameters were tested within ±50% range (Sections 8.5.7). This is a measure of the stability of the procedures adopted.

STAGE (iv)

Comparisons of the probabilistic models with field data were limited. The measured values fell within the majority of the predictive distributions, which is seen as encouraging with respect to the validity of the analytical procedures used. For the models tested, the experimental results fell within ($\mu \pm 3\sigma$) for all comparisons, whilst comparisons involving columns on level 8 and level 20 at the University of Technology Sydney building were seen to be more accurate, with results falling within a range ($\mu \pm 2\sigma$). Refer to Section 8.4. From additional shortening predictions also made in this section, the B3 model predictions showed best agreement and were within ±7% of the test data, see Figure 8.12.

FUTURE WORK

The work in this thesis has concentrated on the development of rigorous probabilistic procedures for the analysis of time-dependent shortening in the columns and core of tall concrete buildings, as well as a case-study to assess the different predictive methods. Future work on this topic can proceed in a number of areas, where each is described in turn.

The first relates to the development of a complete statistical description for elastic, creep and shrinkage behaviour of concrete. This would require extensive long-term experimental investigations. The author has derived probabilistic models (see Chapter 6) based on the available statistical data in the literature. New information will govern the type of probabilistic models applicable to the analysis of tall buildings, where these models may require highly complex stochastic analyses.

The second would permit the incorporation of other random parameters into the models. These could include environmental humidity and temperature (as well as their time-dependent variations), time-dependent loading of the building, the quality control involved in the construction (i.e. the standard and consistency of the concrete mixes, the geometric setting-up and construction of columns) and the construction time of each level. Each of these parameters may in addition be non-normally distributed. Methods of analysis may in such cases be limited to Monte Carlo simulation or the method of realisations [146,147], leaving a standard n^{th}-order analysis as impractical due to intractable complexity.

Finally, recasting the problem of axial shortening to incorporate structural interactions between adjacent column elements would advance the field substantially. The column models developed in Chapter 5 assume a monotonically increasing load history where each load is applied instantaneously, however, inclusion of structural interactions cause the load history of each column element to be time-dependent instead. Thus, the current models can be used for describing deformations in columns with the only modification being to discretise the history into a number of intervals where each interval has a constant load associated with it. Then, computational times for any modified structural interaction model would be dependent on the total number of discretised load history intervals.

It can be seen from the above that the probabilistic models developed by the author in Chapter 6 can be considered preliminary research, with future areas of work being rather fertile.

REFERENCES

REFERENCES

1. Steel Reinforcement Institute of Australia (1989), - Tall Buildings : An Overview, *Reinforced Concrete Digest 7*, Concrete Publishing Pty Ltd, Sydney, October.
2. Steel Reinforcement Institute of Australia (1994), - Australia's 100 Tallest Buildings, *Reinforced Concrete Digest 16*, Concrete Publishing Pty Ltd, Sydney, September.
3. Steel Reinforcement Institute of Australia (1991), - 311 South Wacker Drive, *Reinforced Concrete Digest 13*, Concrete Publishing Pty Ltd, Sydney, July.
4. Kelsey J (1993), - World's Tallest RC Building Completed in Record Time, *Concrete International*, December, pages 46-48.
5. Fintel M, Ghosh S.K. (1984), - High Rise Design : Accounting for Column Length Changes, *Civil Engineering ASCE*, April, pages 55-59.
6. Faber O (1927), - Plastic Yield, Shrinkage and Other Problems of Concrete and Their Effects on Design, *Minutes of Proceedings of the Institution of Civil Engineers*, 225, Part I, London, pages 27-73.
7. Bazant Z.P. (1972), - Prediction of Concrete Creep Effects Using Age-Adjusted Effective Modulus Method, *ACI Journal*, Volume 69, April, pages 212-217.
8. Glanville W.H. (1930), - Studies in Reinforced Concrete III : The Creep or Flow of Concrete Under Load, *Building Research Technical Paper Number 12*, Department of Scientific and Industrial Research, London, pages 39.
9. Nielsen L.F. (1970), - Kriechen und Relaxation des Betons, *Beton - und Stahlbetonbau*, 65, pages 272-275.
10. Fintel M, Khan F.R. (1969), - Effects of Column Creep and Shrinkage in Tall Structures - Prediction of Inelastic Column Shortening, *ACI Journal*, Volume 66, December, pages 957-967.
11. Warner R.F. (1976), - Axial Shortening in Reinforced Concrete Columns, *Australian Civil Engineering Transactions*, pages 15-19.
12. Beasley A.J. (1987), - COLECS : A Numerical Solution for the Prediction of Elastic, Creep, Shrinkage and Thermal Deformations in the Columns and Cores of Tall Concrete Buildings, *Research Report CM 87/2*, Department of Civil and Mechanical Engineering, University of Tasmania - Hobart, Tasmania.

13. Beasley A.J. (1987), - COLECS : A Computer Program for the Analysis of Elastic, Creep, Shrinkage and Thermal Deformations in the Columns and Cores of Tall Concrete Buildings, *Research Report CM 87/3*, Department of Civil and Mechanical Engineering, University of Tasmania - Hobart, Tasmania.
14. Gilbert R.I. (1988), - *Time Effects in Concrete Structures*, Elsevier Science Publishers, New York.
15. McAdam P.S., Behan J.E. (1989), - Time Dependent Shortening of Reinforced Concrete Columns, August, *Civil Engineering Research Report, Research Report CE105*, Department of Civil Engineering, University of Queensland, Queensland.
16. Koutsoukis M (1991), - Effect of Creep and Shrinkage in Tall Concrete Buildings, *Honours Thesis CM 91/3*, Department of Civil and Mechanical Engineering, University of Tasmania - Hobart, Tasmania.
17. Pan L.B., Liu P.C., Bakoss S.L. (1993), - Long-Term Shortening of Concrete Columns in Tall Buildings, *Journal of the Structural Engineering*, Volume 119, Number 7, July, pages 2258-2262.
18. Koutsoukis M, Beasley A.J. (1994), - Monte Carlo Analysis of Tall Concrete Structures, Presented at the Second International Conference on Computational Structures Technology 30th August - 1st September 1994 in Athens, *CST 1994 Proceedings*, Civil-Comp Ltd, Edinburgh, Advances in Non-Linear Finite Element Methods, pages 129-134.
19. Koutsoukis M, Beasley A.J. (1994), - Probabilistic Shortening of Tall Concrete Buildings, Presented at the Australasian Structural Engineering Conference 21st-23rd September 1994 in Sydney, *ASEC 1994 Proceedings*, Institution of Engineers Australia, Canberra, Volume 1, pages 595-600.
20. Koutsoukis M, Beasley A.J. (1995), - Second-Order Moment Dischinger Model for the Axial Shortening in Tall Concrete Buildings, Presented at the Fifth East Asia-Pacific Conference on Structural Engineering and Construction 25th-27th July 1995 in Gold Coast, *EASEC-5 Proceedings*, Gold Coast University College of Griffith University, Gold Coast, Volume 1, pages 525-530.
21. Koutsoukis M, Beasley A.J. (1995), - Idealising the Construction Cycle of Tall Concrete Buildings for Axial Shortening Analyses, Presented at the Concrete 95 Toward Better Concrete Structures Conference 4th-7th September 1995 in Brisbane, *Concrete-95 Proceedings*, Concrete Institute of Australia, Brisbane, Volume 1, pages 447-453.

22. Koutsoukis M, Beasley A.J. (1995), - Axial Shortening Prediction Methods for Tall Concrete Buildings Part I : Comparison of Theoretical Methods, Presented at the Fourteenth Australasian Conference on the Mechanics of Structures and Materials 11th-13th December 1995 in Hobart, *14ACMSM Proceedings*, University of Tasmania, Hobart, Volume 2, pages 528-534.
23. Koutsoukis M, Beasley A.J. (1995), - Axial Shortening Prediction Methods for Tall Concrete Buildings Part II : Sensitivity Analysis and Experimental Comparisons, Presented at the Fourteenth Australasian Conference on the Mechanics of Structures and Materials 11th-13th December 1995 in Hobart, *14ACMSM Proceedings*, University of Tasmania, Hobart, Volume 2, pages 535-540.
24. Koutsoukis M, Beasley A.J. (1996), - Characteristics of Random Axial Shortening in RC Columns using Second-Order Moment Theory, Accepted for presentation at the Second International Conference Multi-Purpose High-Rise Towers and Tall Buildings 30th-31st July 1996 in Singapore, *Conference Proceedings*, Singapore, Volume ?, pages ?-?.
25. Koutsoukis M, Beasley A.J. (1992), - Effect of Elastic, Creep and Shrinkage Deformations in the Columns of Concrete Buildings, Presented at the Movement in Structures Seminar 29th April 1992 in Hobart, *CIA Proceedings*, Concrete Institute of Australia (Tasmanian Division), pages 17.
26. Koutsoukis M, Melerski E.S. (1996), - Random Elastic Response Characteristics of Bar Structures by Monte Carlo Simulation, Accepted for presentation at the Seventh ASCE Speciality Conference on Probabilistic Mechanics and Structural Reliability 7th-9th August 1996 in Worcester USA, *ASCE Conference Proceedings*, ASCE, New York, Volume ?, pages ?-?.
27. Koutsoukis M (1995), - STATS : Statistical Analysis Package (Version 1.0), *Research Report CM 95/1*, Department of Civil and Mechanical Engineering, University of Tasmania - Hobart, Tasmania, pages 41.
28. Koutsoukis M (1995), - AXS : Axial Shortening Analysis Package (Version 2.0), *Research Report CM 95/2*, Department of Civil and Mechanical Engineering, University of Tasmania - Hobart, Tasmania, pages 148.
29. Brady E.A. (1980), - The Measurement of Shortening of Reinforced Concrete Columns and Core in a Tall Building by Surveying Methods, *Civil Engineering Monograph C.E. 80/1 S*, The New South Wales Institute of Technology, Sydney.

30. Fintel M (1988), - Creep and Shrinkage Shortenings in Tall Structures and Their Compensation, *Concrete in Australia*, Concrete Institute of Australia, Volume 14, Number 2, December, pages 11-14.
31. Tomasetti R.L. (1994), - Current Evolution of Tall Building Structures, Australasian Structural Engineering Conference 21st-23rd September 1994 in Sydney, *ASEC 1994 Proceedings*, Institution of Engineers Australia, Canberra, Volume 1, pages 9-22.
32. Council on Tall Buildings and Urban Habitat (1978), - *Structural Design of Tall Concrete and Masonry Buildings*, American Society of Civil Engineers, New York.
33. Heiman J.L. (1973), - Long-Term Deformations in the Tower Building Australia Square Sydney, *ACI Journal*, Volume 70, April, pages 279-284.
34. Lukkunaprasit P, Zyhajlo E, Levy C (1995), - Differential Column Shortening of Baiyoke II Tower, Fifth East Asia-Pacific Conference on Structural Engineering and Construction 25th-27th July 1995 in Gold Coast, *EASEC-5 Proceedings*, Gold Coast University College of Griffith University, Gold Coast, Volume 1, pages 211-216.
35. Zyhajlo E, Levy C, Burnett I (1995), - Construction of a 90 Storey Building in Bangkok, Concrete 95 Toward Better Concrete Structures Conference 4th-7th September 1995 in Brisbane, *Concrete-95 Proceedings*, Concrete Institute of Australia, Brisbane, Volume 2, pages 691-699.
36. Fintel M, Khan F.R. (1971), - Effects of Column Creep and Shrinkage in Tall Structures - Analysis for Differential Shortening of Columns and Field Observation of Structures, *Designing for Effects of Creep, Shrinkage and Temperature in Concrete Structures*, Special Publication Number 27, ACI, Michigan, pages 95-119.
37. American Concrete Institute 209R-82 (1986), - Prediction of Creep, Shrinkage and Temperature Effects in Concrete Structure, *ACI Manual of Concrete Practice*, ACI, Michigan.
38. Comite Euro-International du Beton (1978), - *CEB-FIP Code for Concrete Structures*, English Translation, CEB.
39. Standards Association of Australia (1988), - *Australian Standard AS 3600-1988 Concrete Structures*, Standards Association of Australia, Sydney.
40. Comite Euro-International du Beton (1984), *Structural Effects of Time Dependent Behaviour of Concrete*, Georgi Publishing Company, Saint-Saphorin.

41. Manual R.F. MacGregor J.G. (1967), - Analysis of Restrained Reinforced Concrete Columns Under Sustained Load, *ACI Journal*, Volume 64, January, pages 12-23.
42. Samra R.M. (1989), - Creep Model for Reinforced Concrete Columns, *ACI Structural Journal*, Volume 86, January-February, pages 77-82.
43. Samra R.M. (1995), - New Analysis for Creep Behaviour in Concrete Columns, *Journal of Structural Engineering ASCE*, Number 3, Volume 121, March, pages 399-407.
44. Mauch S, Holley M.J. (1963), - Creep Buckling of Reinforced Concrete Columns, *Journal of the Structural Division ASCE*, Volume 89, August, pages 451-481.
45. Rangan B.V. (1990), - Strength of Reinforced Concrete Slender Columns, *ACI Structural Journal*, Volume 87, January-February, pages 32-38.
46. Gilbert R.I. (1989), - A Procedure for the Analysis of Slender Concrete Columns Under Sustained Eccentric Loading, *Australian Civil Engineering Transactions*, pages 39-46.
47. Gao Z, Bradford M.A. (1993), - Time-Dependent Shortening of Slender RC Columns, *Journal of Engineering Mechanics*, Volume 119, Number 10, October, pages 2036-2051.
48. Bradford M.A., Gilbert R.I. (1992), - Analysis of Circular RC Columns for Short- and Long-Term Deformations, *Journal of Structural Engineering*, Volume 118, Number 3, March, pages 669-683.
49. Spanos P.D. (1988), - *Probabilistic Methods in Civil Engineering*, American Society of Civil Engineers, New York.
50. Warner R.F., Kabaila A.P. (1968), - Monte Carlo Study of Structural Safety, *Journal of the Structural Division ASCE*, Number 12, Volume 94, December, pages 2847-2859.
51. Cornell C.A. (1969), - Structural Safety Specifications Based on Second-Moment Reliability Analysis, *IABSE Final Report*, London, pages 235-245.
52. Ravindra M.K., Lind N.C., Siu W (1974), - Illustrations of Reliability-Based Design, *Journal of the Structural Division ASCE*, Number 9, Volume 100, September, pages 1789-1811.
53. Benjamin J.R., Cornell C.A., Gabrielsen B.E. (1965), - A Stochastic Model for the Creep Deflection of Reinforced Concrete Beams, International Symposium on the Flexural Mechanics of Reinforced Concrete, *Conference Proceedings SP-12*, American Concrete Institute, Detroit, Michigan, pages 557-580.

54. Zundelevich S, Benjamin J.K. (1972), - Probabilistic Analysis of Deflections of Reinforced Concrete Beams, Probabilistic Design of Reinforced Concrete Buildings, *Conference Proceedings SP-31*, American Concrete Institute, Detroit, Michigan, pages 223-246.

55. Ditlevsen O (1982), - Stochastic Visco-Elastic Strain Modeled as a Second Moment White Noise Process, *International Journal of Solids and Structures*, Number 1, Volume 18, pages 23-25.

56. Stewart M.G. (1994), - Probability of Serviceability Failure of Reinforced Concrete Office Floor Beams, *Research Report 099.07.1994*, Department of Civil Engineering and Surveying, University of Newcastle, NSW.

57. American Concrete Institute 363R-84 (1986), - State of the Art Report on High Strength Concrete, *ACI Manual of Concrete Practice*, ACI, Michigan.

58. Comite Euro-International du Beton (1970), - *CEB-FIP International Recommendations for the Design and Construction of Concrete Structures*, CEB, Paris-London.

59. Taranath B.S. (1988), - *Structural Analysis and Design of Tall Buildings*, McGraw-Hill Book Company, New York.

60. Council on Tall Buildings and Urban Habitat (1980), - *Tall Building Systems and Concepts*, American Society of Civil Engineers, New York.

61. Neville A.M., Dilger W.H., Brooks J.J. (1983), - *Creep of Plain and Structural Concrete*, Construction Press, London.

62. Backstrom S (1956), - Creep and Creep Recovery of Cement Mortar, IABSE, 5th Congress, *Preliminary Report*, Lisbon.

63. Smerda Z, Kristek V (1988), - *Creep and Shrinkage of Concrete Elements and Structures*, Elsevier Science Publishers, New York.

64. Bazant Z.P. (1988), - *Mathematical Modelling of Creep and Shrinkage of Concrete*, Anchor Press Ltd, Tiptree, Essex.

65. Rusch H, Jungwirth D, Hilsdorf H.K. (1983), - *Creep and Shrinkage : Their Effect on the Behavior of Concrete Structures*, R.R. Donnelley and Sons, Harrisonburg.

66. Bazant Z.P., Panula L (1978), - Practical Prediction of Time-Dependent Deformations of Concrete, *Materials and Structures*, Part 1 and 2, Volume 11, Issue 65, pages 307-328.

67. Bazant Z.P., Panula L (1978), - Practical Prediction of Time-Dependent Deformations of Concrete, *Materials and Structures*, Part 3 and 4, Volume 11, Issue 66, pages 415-434.

68. Bazant Z.P., Panula L (1979), - Practical Prediction of Time-Dependent Deformations of Concrete, *Materials and Structures*, Part 5 and 6, Volume 12, Issue 69, pages 169-183.
69. Bazant Z.P., Panula L (1978), - Simplified Prediction of Concrete Creep and Shrinkage From Strength and Mix, *Structural Engineering Report number 78-10/640s*, Northwestern University, Illinois.
70. Bazant Z.P., Panula L (1980), - Creep and Shrinkage Characterization for Analysing Prestressed Concrete Structures, *PCI Journal*, Volume 25, Issue 3, May-June, pages 86-122.
71. Bazant Z.P., Wang T.S. (1985), - Practical Prediction of Cyclic Humidity Effect in Creep and Shrinkage of Concrete, *Materials and Structures*, Volume 18, Issue 106, pages 274-252.
72. Bazant Z.P., Panula L (1984), - Practical Prediction of Creep and Shrinkage of High Strength Concrete, *Materials and Structures*, Number 101, Volume 17, pages 375-378.
73. Bazant Z.P., Chern J.C. (1984), - Double Power Logarithmic Law for Concrete Creep, *Cement and Concrete Research*, Volume 14, Issue 6, pages 793-806.
74. Bazant Z.P., Chern J.C. (1985), - Log Double Power Law for Concrete Creep, *ACI Journal*, Volume 82, September-October, pages 665-675.
75. Bazant Z.P., Chern J.C. (1985), - Triple Power Law for Concrete Creep, *Journal of Engineering Mechanics ASCE*, Volume 111, January, pages 63-83.
76. Bazant Z.P., Prasannan S (1989), - Solidification Theory for Concrete Creep : Formulation, *Journal of Engineering Mechanics*, Volume 115, Issue 8, August, pages 1691-1703.
77. Bazant Z.P., Prasannan S (1989), - Solidification Theory for Concrete Creep : Verification and Applications, *Journal of Engineering Mechanics*, Volume 115, Issue 8, August, pages 1704-1725.
78. Bazant Z.P., Kim J.K., Panula L (1991), - Improved Prediction Model for Time-Dependent Deformations of Concrete : Part 1 : Shrinkage, *Materials and Structures*, Volume 24, pages 327-345.
79. Bazant Z.P., Kim J.K. (1991), - Improved Prediction Model for Time-Dependent Deformations of Concrete : Part 2 : Basic Creep, *Materials and Structures*, Volume 24, pages 409-421.
80. Bazant Z.P., Kim J.K. (1992), - Improved Prediction Model for Time-Dependent Deformations of Concrete : Part 3 : Creep at Drying, *Materials and Structures*, Volume 25, pages 21-28.

81. Bazant Z.P., Kim J.K. (1992), - Improved Prediction Model for Time-Dependent Deformations of Concrete : Part 4 : Temperature Effects, *Materials and Structures*, Volume 25, pages 84-94.
82. Bazant Z.P., Kim J.K. (1992), - Improved Prediction Model for Time-Dependent Deformations of Concrete : Part 5 : Cyclic Load and Cyclic Humidity, *Materials and Structures*, Volume 25, pages 163-169.
83. Bazant Z.P., Panula L, Kim J.K., Xi Y (1992), - Improved Prediction Model for Time-Dependent Deformations of Concrete : Part 6 : Simplified Code-Type Formulation, *Materials and Structures*, Volume 25, pages 219-223.
84. Bazant Z.P., Baweja S (1995), - Creep and Shrinkage Prediction Model for Analysis and Design of Concrete Structures - Model B3, *Materials and Structures*, Volume 28, pages 357-365.
85. Bazant Z.P., Baweja S (1995), - Justification and Refinements of Model B3 for Concrete Creep and Shrinkage - 1 Statistics and Sensitivity, *Materials and Structures*, Volume 28, pages 415-430.
86. Bazant Z.P., Baweja S (1995), - Justification and Refinements of Model B3 for Concrete Creep and Shrinkage - 2 Updating and Theoretical Basis, *Materials and Structures*, Volume 28, pages 488-495.
87. Freyssinet E (1936), - *Une Revolution dans les Techniques du Beton*, Eyrolles, Paris, pages 118.
88. Freyssinet E (1951), - The Deformation of Concrete, *Magazine of Concrete Research*, Volume 3, Number 8, pages 49-56.
89. Bingham E.C., Reiner M (1933), - Rheological Properties of Cement and Cement-Mortar-Stone, *Physics*, Volume 4, pages 88-96.
90. Glanville W.H., Thomas F.G. (1939), - Studies in Reinforced Concrete IV : Further Investigations on Creep or Flow of Concrete Under Load, *Building Research Technical Paper Number 21*, Department of Scientific and Industrial Research, London, pages 44.
91. Jensen R.S., Richart F.E. (1938), - Short-Time Creep Tests on Concrete in Compression, *Proceedings of ASTM*, Volume 38, pages 410-417.
92. Lynam C.G. (1934), - *Growth and Movement in Portland Cement Concrete*, Oxford University Press, London, pages 139.
93. Vogt F (1935), - *On the Flow and Extensibility of Concrete*, Norges Tekniske Hoiskole, pages 349-374.
94. Arnstein A, Reiner M (1945), - Creep of Cement, Cement-Mortar and Concrete, *Civil Engineering and Public Works Review*, Volume 40, pages 198-202.

95. Thomas F.G. (1937), - Creep of Concrete Under Load, *International Association of Testing Materials*, London Congress, April, pages 292-294.
96. Reiner M (1949), - On Volume or Isotropic Flow as Exemplified in the Creep of Concrete, *Research : A Journal of Science and its Applications*, Volume A1, pages 475-488.
97. Hansen T.C. (1960), - Creep and Stress Relaxation of Concrete, *Proceeding 31*, Swedish Cement and Concrete Research Institute, Stockholm, pages 112.
98. Lea F.M., Lee C.R. (1946), - Shrinkage and Creep in Concrete, Symposium on the Shrinkage and Cracking of Cementive Materials, *The Society of Chemical Industry*, London, May, pages 7-17.
99. Seed H.B. (1948), - Creep and Shrinkage in Reinforced Concrete Structures, *Reinforced Concrete Review*, Volume 1, Number 8, May, pages 253-267.
100. Vaishnav R.N., Kesler C.E. (1961), - Correlation of Creep of Concrete with its Dynamic Properties, *T. and A.M. Report Number 603*, University of Illinois, pages 194.
101. Ali I, Kesler C.E. (1963), - Creep in Concrete with and without Exchange of Moisture with the Environment, *T. and A.M. Report Number 641*, University of Illinois, pages 71.
102. Ruetz W (1968), - The Two Different Physical Mechanisms of Creep in Concrete, *Proceedings of the International Conference on the Structure of Concrete*, Cement and Concrete Association, London, pages 146-153.
103. Ruetz W (1968), - A Hypothesis for the Creep of Hardened Cement Paste and the Influence of Simultaneous Shrinkage, *Proceedings of the International Conference on the Structure of Concrete*, Cement and Concrete Association, London, pages 365-387.
104. Cilosani Z.N. (1964), - On the Probable Mechanism of Creep of Concrete, *Beton i Zhelezobeton*, Number 2, Moscow, pages 75-78.
105. Powers T.C. (1966), - Some Observations on the Interpretation of Creep Data, *RILEM Bulletin*, Number 33, December, pages 381-391.
106. Powers T.C. (1968), - The Thermodynamics of Volume Change and Creep, *Materials and Structures*, Volume 1, Number 6, pages 487-507.
107. Bazant Z.P. (1976), - Theory of Creep and Shrinkage in Concrete Structures : a Precis of Recent Developments, *Mechanics Today*, pages 1-93.
108. American Concrete Institute 209R Subcommittee III (1972), - *Mechanisms of Creep and Shrinkage*, ACI, Detroit, September, pages 105.

109. Marzouk H (1991), - Creep of High-Strength Concrete and Normal-Strength Concrete, *Magazine of Concrete Research*, Volume 45, Number 115, June, pages 121-126.
110. L'Hermite R, Grieu J.J. (1952), - Etude Experimentales Recentes sur le Retrait des Ciments et des Betons, *Annales ITBTP*, Volume 5(52-3), pages 494-514.
111. Neville A.M. (1981), - *Properties of Concrete*, Pitman Publishing Limited, London.
112. Pauw A (1960), - Static Modulus of Elasticity of Concrete as Affected by Density, *ACI Journal*, Volume 57, December, pages 679-687.
113. Hansen T.C. (1965), - Influence of Aggregate and Voids on Modulus of Elasticity of Concrete, Cement Mortar and Cement Paste, *ACI Journal*, Volume 62, February, pages 193-215.
114. Setunge S, Attard M.M., Darvall P.LeP. (1990), - Static Modulus of Elasticity and Poisson's Ratio of Very High Strength Concrete, *Civil Engineering Research Report 1/1990*, Monash University.
115. La Rue H.A. (1946), - Modulus of Elasticity of Aggregate and its Effect on Concrete, *ASTM Journal*, Volume 46, pages 1298-1309.
116. Carrasquillo R.L., Nilson A.H., Slate F.O. (1981), - Properties of High Strength Concrete Subject to Short-Term Loads, *ACI Journal*, Volume 78, May-June, pages 171-178.
117. Jobse H.J., Moustafa S.E. (1984), - Applications of High Strength Concrete for Highway Bridges, *PCI Journal*, May-June, pages 44-73.
118. Ahmad S.H., Shah S.P. (1985), - Structural Properties of High Strength Concrete and its Implications for Precast Prestressed Concrete, *PCI Journal*, November-December, pages 92-119.
119. Boltzmann Z (1876), - Zur Theorie der Elastischen Nachwirkung, *Sitzber. Akad. Wiss., Wiener Bericht 70, Wiss. Abh.*, Volume 1, pages 279-306.
120. Volterra V (1913), - *Lecons sur les Fonctions de Ligne*, Gauthier-Villars, Paris.
121. McHenry D (1943), - A New Aspect of Creep in Concrete and its Application to Design, *Proceedings of ASTM*, Volume 43, pages 1069-1086.
122. Bazant Z.P., Kim S.S (1979), - Approximate Relaxation Function for Concrete, *Journal of the Structural Division ASCE*, December, pages 2695-2705.

123. Cridland L, Heiman J.L., Bakoss S.L., Burfit A.J. (1979), - Measured and Predicted Strains and Deformations in a Column of a Tall Reinforced Concrete Building, *Civil Engineering Monograph C.E. 79/1 ST E*, The New South Wales Institute of Technology, Sydney.

124. Comite Euro-International du Beton (1990), - Evaluation of the Time Dependent Behavior of Concrete, *Bulletin D'Information*, Number 199, CEB, Lausanne.

125. Hilsdorf H.K., Muller H.S. (1979), - Comparison of Methods to Predict Time-Dependent Strains of Concrete, Institut fur Baustofftechnologie, Universitat Karlsruhe (TH), 91 pages.

126. Branson D.E., Meyers B.L., Kripanarayanan K.M. (1970), - Loss of Prestress, Camber, and Deflection of Non-Composite and Composite Structures Using Different Weight Concretes, *Final Report No. 70-6*, Iowa Highway Commission, August.

127. Bazant Z.P., Wittmann F.H., Kim J.K., Alou F (1987), - Statistical Extrapolation of Shrinkage Data: Part 1 Regression, *ACI Materials Journal*, Volume 84, January-February, pages 20-34.

128. Bazant Z.P., Kim J.K. (1991), - Consequences of Diffusion Theory for Shrinkage of Concrete, *Materials and Structures*, Volume 24, pages 323-326.

129. Trost H (1967), - Auswirkungen des Superpositionsprinzips auf Kriech- und Relaxations-Probleme bei Beton und Spannbeton, *Beton- und Stahlbetonbau*, Volume 62, Number 10, pages 230-238, Number 11 pages 261-269.

130. Bastgen K.J. (1979) - Zum Spannungs-Dehnungs-Zeit-Verhalten von Beton, Relaxation, Kriechen und deren Wechsel Wirkung, *Dissertation*, Rheinisch-Westfalische Technische Hochschule Aachen, pages 122.

131. Whitney C.S. (1932) - Plain and Reinforced Concrete Arches, *ACI Journal*, Volume 28, pages 479-519.

132. Dischinger F (1937) - Untersuchungen uber die Knicksicherheit, die Elastische Verformung und das Kriechen des Betons bei Bogenbrucken, *Der Bouingenieur*, Volume 18, Number 33/34, pages 487-520, Number 35/36, pages 539-552, Number 39/40, pages 595-621.

133. Madsen H.O., Bazant Z.P. (1983), - Uncertainty Analysis of Creep and Shrinkage Effects in Concrete Structures, *ACI Journal*, Volume 80, March-April, pages 116-127.

134. Warner R.F., Rangan B.V., Hall A.S. (1989), - *Reinforced Concrete*, Longman Cheshire Pty Ltd, Melbourne.

135. Darvall P.LeP. (1988), - *Reinforced and Prestressed Concrete*, The Macmillan Company of Australia, Melbourne.
136. Mirza S.A., Hatzinikolas M, MacGregor J.G. (1979), - Statistical Description of Strength of Concrete, *Journal of the Structural Engineering*, Volume 105, Number 6, June, pages 1021-1037.
137. Stewart M.G. (1994), - Concrete Quality, Workmanship and Probabilistic Models of Concrete Compressive Strength, *Research Report 089.01.1994*, Department of Civil Engineering and Surveying, University of Newcastle, NSW.
138. Drysdale R.G. (1973), - Variation of Concrete Strength in Existing Buildings, *Magazine of Concrete Research*, Volume 25, Number 85, December, pages 201-207.
139. Bazant Z.P., Wittmann F.H., Kim J.K., Alou F (1988), - Statistics of Concrete Test Data, *Probabilistic Methods in Civil Engineering*, American Society of Civil Engineers, Spanos P.D., New York, pages 104-107.
140. Bazant Z.P., Wittmann F.H., Kim J.K., Alou F (1987), - Statistical Extrapolation of Shrinkage Data: Part 2 Bayesian Updating, *ACI Materials Journal*, Volume 84, March-April, pages 83-91.
141. Hanson J.A. (1958), - Shear Strength of Lightweight Reinforced Concrete Beams, *ACI Journal*, Volume 55, September, pages 387-403.
142. Shideler J.J. (1957), - Lightweight-Aggregate Concrete for Structural Use, *ACI Journal*, Volume 54, October, pages 299-328.
143. Kluge R.W., Sparks M.M., Tuma E.C. (1949), - Lightweight-Aggregate Concrete, *ACI Journal*, Volume 45, May, pages 625-642.
144. Ang A.H. Tang W.H. (1975), - *Probability Concepts in Engineering Planning and Design: Volume 1: Basic Principles*, John Wiley and Sons Inc, New York.
145. Ang A.H. Tang W.H. (1984), - *Probability Concepts in Engineering Planning and Design: Volume 2: Decision Risk and Reliability*, John Wiley and Sons Inc, New York.
146. Melerski E.S. (1988), - Thin Shell Foundation Resting on Stochastic Soil, *Journal of Structural Engineering ASCE*, Number 12, Volume 114, December, pages 2692-2709.
147. Melerski E.S. (1992), - Probabilistic Computer Analysis of Circular Rafts by the Method of Realizations, *Computer and Structures*, Number 6, Volume 43, pages 1075-1083.
148. Box G.E.P., Muller M.E. (1958) - A Note on the Generation of Normal Deviates, *Annals of Mathematical Statistics*, Volume 29, pages 610-611.

149. Canavos G.C. (1984), - *Applied Probability and Statistical Methods*, Little Brown and Company Limited, Canada.
150. Evans D.H. (1967), - An Application of Numerical Integration Techniques to Statistical Tolerancing, *Technometrics*, Number 3, Volume 9, August, pages 441-456.
151. Evans D.H. (1972), - An Application of Numerical Integration Techniques to Statistical Tolerancing: General Distributions, *Technometrics*, Number 1, Volume 14, February, pages 23-35.
152. Borland (1990), - *TurboPascal 6.0 User's Guide*, Borland, USA.
153. Borland (1990), - *TurboPascal 6.0 Programmer's Guide*, Borland, USA.
154. Borland (1990), - *TurboPascal 6.0 Turbo Vision Guide*, Borland, USA.
155. Borland (1990), - *TurboPascal 6.0 Library Reference Guide*, Borland, USA.
156. O'Brien S (1991), - *TurboPascal 6 The Complete Reference*, California, McGraw-Hill.
157. Palmer D.P. (1991), - *Mastering TurboPascal 6*, California, Sybex Inc.
158. Borland (1992), - *TurboPascal 7.0 User's Guide*, Borland, USA.
159. Borland (1992), - *TurboPascal 7.0 Language Guide*, Borland, USA.
160. Borland (1992), - *TurboPascal 7.0 Programmer's Guide*, Borland, USA.
161. Borland (1992), - *TurboVision Programming Guide*, Borland, USA.
162. Press W.H., Flannery B.P., Teukolsky S.A., Vetterling W.T. (1987), - *Numerical Recipes*, Press Syndicate of the University of Cambridge, USA.
163. Pfeifer D.W., Magura D.D., Russell H.G., Corley W.G. (1971), - Time Dependent Deformations in a 70 Story Structure, *Designing for Effects of Creep, Shrinkage and Temperature in Concrete Structures*, Special Publication Number 27, ACI, Michigan, pages 159-185.

NOTATION

NOTATION

General

COV	- Coefficient of variation
FEMM	- Fabers Effective Modulus Method
IRCM	- Improved Rate of Creep Method
MCS	- Monte Carlo simulation
PDF	- Probability density function
RCM	- Rate of Creep Method
TBEMM	- Trost-Bazant Age-Adjusted Effective Modulus Method

Chapter 2

C_{ab}	- Column "a" (i.e. either column 1 or 2) on storey "b"
DL	- Total dead load component
LL	- Total live load component
T_a	- Total age of the building (days)
T_c	- Construction cycle period of the building (days)
α_1	- Portion of construction dead load
α_2	- Portion of in-service dead load
β_1	- Portion of construction live load
β_2	- Portion of in-service live load

Chapter 3

C(t,s)	- Specific creep at time t with a loading age of s
$E_a(t)$	- Elastic modulus of coarse aggregate at time t
$E_c(s)$	- Elastic modulus of concrete at time s
$E_m(t)$	- Elastic modulus of cement mortar at time t
$f_c(s)$	- Concrete strength at time s
J(t,s)	- Creep function at time t with a loading age of s
k_{dc}	- Creep modification factor due to drying environment
R(t,s)	- Relaxation function at time t with a unit deformation applied at age s
V_a	- Volume fraction of coarse aggregate in concrete
V_m	- Volume fraction of cement mortar in concrete

β_a - Aggregate type coefficient for elastic modulus (3.17)
$\varepsilon(t)$ - Total concrete strain at time t
$\varepsilon_{bc}(t)$ - Basic creep strain at time t
$\varepsilon_c(t)$ - Creep strain at time t
$\varepsilon_c(t,s)$ - Creep strain at time t with a loading age of s
$\varepsilon_{dc}(t)$ - Drying creep strain at time t
$\varepsilon_{de}(t)$ - Delayed elastic creep strain at time t
$\varepsilon_e(t)$ - Instantaneous (elastic) concrete strain at time t
$\varepsilon_f(t)$ - Flow creep strain at time t
$\varepsilon_{fb}(t)$ - Basic flow creep strain at time t
$\varepsilon_{fd}(t)$ - Drying flow creep strain at time t
$\varepsilon_{if}(t)$ - Initial rapid flow creep strain at time t
$\varepsilon_{sh}(t)$ - Concrete shrinkage strain at time t
$\varepsilon_{shc}(t)$ - Carbonation shrinkage strain at time t
$\varepsilon_{shcp}(t)$ - Capillary shrinkage strain at time t
$\varepsilon_{shd}(t)$ - Drying shrinkage strain at time t
$\varepsilon_{shh}(t)$ - Hydration shrinkage strain at time t
ρ - Concrete density
$\sigma(t)$ - Concrete stress at time t, or
- Applied stress
$\phi(t,s)$ - Creep coefficient at time t with a loading age of s

Chapter 4

$E_c(s)$ - Elastic modulus of concrete at time s
E_o - Intermediate value used in BP model
$f_c(s)$ - Concrete strength at time s
f'_c - 28 day concrete strength
f'_{cc} - 28 day characteristic concrete strength
$F(\sigma)$ - Intermediate variable used in BPX model
k_h - Intermediate variable used in BP model
k_1 - Intermediate variable used in CEB-FIP 1970 code, or
- Intermediate variable used in AS-3600 code
k^*_1 - Intermediate variable used in CEB-FIP 1970 code
k_2 - Intermediate variable used in CEB-FIP 1970 code, or
- Intermediate variable used in AS-3600 code
k_3 - Intermediate variable used in CEB-FIP 1970 code, or
- Intermediate variable used in AS-3600 code
k_4 - Intermediate variable used in CEB-FIP 1970 code

k^*_4 - Intermediate variable used in CEB-FIP 1970 code

k_5 - Intermediate variable used in CEB-FIP 1970 code

m - Intermediate variable used in BP model

n - Intermediate variable used in BPtpl model

n_T - Intermediate variable used in BP code

$Q_f(s)$ - Intermediate variable used in BPX model

q_1 - Intermediate variable used in BPX model

q_2 - Intermediate variable used in BPX model

r - Intermediate variable used in BP model

s - Loading age of concrete

t - Total age of concrete

t_d - Age of concrete from onset of drying

t_{sh} - Age of concrete when drying begins

α - Constant used in ACI code, or

- Intermediate variable used in BP model

β - Constant used in ACI code

$\beta_a(t\text{-}s)$ - Intermediate variable used in CEB-FIP code

$\beta_d(t\text{-}s)$ - Intermediate variable used in CEB-FIP code

$\beta_f(s)$ - Intermediate variable used in CEB-FIP code

$\beta_f(t)$ - Intermediate variable used in CEB-FIP code

$\beta_{sh}(t)$ - Intermediate variable used in CEB-FIP code

$\beta_{sh}(t_{sh})$ - Intermediate variable used in CEB-FIP code

γ_a - Modification factor for ACI code

γ_s - Modification factor for ACI code

$\gamma_{v/s}$ - Modification factor for ACI code

γ_λ - Modification factor for ACI code

γ_ξ - Modification factor for ACI code

γ_ψ - Modification factor for ACI code

γ'_a - Modification factor for ACI code

γ'_c - Modification factor for ACI code

γ'_{cp} - Modification factor for ACI code

$\gamma'_{v/s}$ - Modification factor for ACI code

γ'_λ - Modification factor for ACI code

γ'_ξ - Modification factor for ACI code

γ'_ψ - Modification factor for ACI code

ε_{sh0} - Intermediate variable used in CEB-FIP code

$\varepsilon_{sh}(t_d)$ - Shrinkage strain at time t_d from onset of drying

$\varepsilon_{sh}(t,t_{sh})$ - Intermediate variable used in CEB-FIP code

$(\varepsilon_{sh})_t$ - Shrinkage strain at time t in μstrains for ACI code

$(\varepsilon_{sh})_u$ - Ultimate shrinkage strain in μstrains for ACI code

$\varepsilon_{\infty sh}$ - Intermediate variable used in BP model

ζ - Used in binomial integral definition

Θ_L - Intermediate variable used in BPdpll model

μ_t - Creep coefficient at time t for ACI code

μ_u - Ultimate creep coefficient for ACI code

ρ - Concrete density

σ_o - Constant stress applied at time s

τ_{sh} - Intermediate variable used in BP model

$\phi_{bo}(t,s)$ - Intermediate variable used in BP and BPX models

$\phi_{bp}(t,s)$ - Creep function of Bazant at time t with a loading age of s

$\phi_{cc.b}$ - Intermediate variable used in AS-3600 code

ϕ_d - Intermediate variable used in CEB-FIP code

$\phi_{do}(t,s,t_{sh})$ - Intermediate variable used in BP and BPX models

ϕ_f - Intermediate variable used in CEB-FIP code

ϕ_L - Intermediate variable used in BPdpll model

$\phi_{po}(t,s,t_{sh})$ - Intermediate variable used in BP and BPX models

ϕ_T - Intermediate variable used in BP model

$\phi(t,s)$ - Creep coefficient at time t with a loading age of s

$\phi(t,s)_{CEB}$ - Creep coefficient at time t with a loading age of s defined by CEB-FIP codes

ϕ_1 - Intermediate variable used in BP model

Chapter 5

A_c - Cross-sectional area of concrete in a reinforced concrete column

A_s - Cross-sectional area of steel in a reinforced concrete column

$E_c(s)$ - Elastic modulus of concrete at time s

$E'_c(s)$ - Modified elastic modulus of concrete at time s

$E_e(t,s)$ - Effective elastic modulus of concrete at time t with a loading age of s

$E'_e(t,s)$ - Age-adjusted effective elastic modulus of concrete at time t with a loading age of s

E_s - Elastic modulus of steel reinforcement

$J(t,s)$ - Creep function at time t with a loading age of s

k_1 - Intermediate constant used in (A4.10)

k_2 - Intermediate constant used in (A4.10)

L - Length of a reinforced concrete column

n - Modular ratio

$N_c(t)$ Internal force in concrete in a reinforced concrete column at time t

n_e - Effective modular ratio

n'_e - Age-adjusted effective modular ratio

$N_s(t)$ Internal force in steel in a reinforced concrete column at time t

P - Load applied to a reinforced concrete column at time s

p_a - Ratio of cross-sectional areas of steel to concrete

P_i - i^{th} load applied to a reinforced concrete column at time s_i

P_{total} - Total load applied to a reinforced concrete column

R(t,s) - Relaxation function at time t with a unit deformation applied at age s

s - Age of concrete when load is applied

s_i - Age of concrete when i^{th} load is applied

t - Total age of concrete

t_d - Drying period for concrete

t_{sh} - Age of concrete at the onset of drying

δ_{creep} - Creep shortening component of a reinforced concrete column

δ_{cum} - Cumulative shortening of a reinforced concrete column on the j^{th} storey

$\delta_{elastic}$ - Elastic (instantaneous) shortening component of a reinforced concrete column

$\delta_{reinforcement}$ -Reinforcement stiffening effect on shrinkage shortening of a reinforced concrete column

$\delta_{shrinkage}$ - Free shrinkage shortening component of a reinforced concrete column

δ_{total} - Total shortening of a reinforced concrete column

$\Delta\sigma(t)$ - Change in concrete stress at time t due concrete relaxation

$\varepsilon(t,s)$ - Total concrete strain at time t for a loading age of s, or
- Total strain of a reinforced concrete column at time t for a loading age of s

$\varepsilon_{de}(t)$ - Delayed elastic creep strain at time t

$\varepsilon_e(t)$ - Elastic concrete strain at time t

$\varepsilon_{sh}(t)$ - Concrete shrinkage strain at time t

$\varepsilon_{st}(t)$ - Steel strain in a reinforced concrete column at time t

σ_o - Initial stress applied to concrete specimen

$\sigma(t)$ - Concrete stress at time t, or
- Stress of concrete in a reinforced concrete column at time t

$\sigma(t)_{ec}$ - Concrete stress due to elastic and creep shortening components of a reinforced concrete column at time t

$\sigma(t)_{sr}$ - Concrete stress due to shrinkage shortening component of a reinforced concrete column at time t

$\sigma_s(t)$ - Steel stress in a reinforced concrete column at time t

$\phi(t,s)$ - Creep coefficient at time t with a loading age of s

ϕ_d - Ratio of delayed elastic concrete strain to elastic concrete

$\phi'(t,s)$ - Modified creep coefficient at time t with a loading age of s

$\chi(t,s)$ - Aging coefficient of concrete at time t with a loading age of s

χ^* - Intermediate constant used in (A4.10)

Chapter 6

A_c - Cross-sectional area of concrete

A_{ci} - Cross-sectional area of concrete in i^{th} storey column

$A_{c,st(x)}$ - Cross-sectional area of concrete in column st(x)

A_s - Cross-sectional area of steel

A_{si} - Cross-sectional area of steel in i^{th} storey column

$A_{s,st(x)}$ - Cross-sectional area of steel in column st(x)

Cov[X,Y] - Covariance of X and Y

d_4 - Variable used in RCM and IRCM column models

d_5 - Variable used in RCM and IRCM column models

d_6 - Variable used in RCM and IRCM column models

$E_c(x)$ - Concrete elastic modulus at time x days

$E_{ci}(x)$ - Concrete elastic modulus of i^{th} storey column at time x

$E_c(s)$ - Random concrete elastic modulus at time s

E_s - Steel reinforcement elastic modulus

E[X] - Expected value of X

E[X″] - Expected value of second-order X terms

$f_{xi}(X_i)$ - Probability density function of X_i

$f_{xn}(X_{11},\ldots,X_{n_n n})$ - Multivariate probability density function

$g(X_1, X_2,\ldots, X_n)$ - General function of n random variables

$k_{all,long,j,a}$ - Entire load set applied between levels 1 and j to Column "a" for determining long-term cumulative shortening

$k_{all,long,j,a+b}$ - Entire load set applied between levels 1 and j to Columns "a" and "b" for determining long-term cumulative shortening

$k_{long,i,a}$ - Load set applied at level i to Column "a" for determining long-term cumulative shortening

K_{rel} - Relative kurtosis of data points

k_j - Number of loads applied on j^{th} storey column

$K_{rel}[X]$ - Relative kurtosis of X

L_i - Length of i^{th} storey column

$L_{st(x)}$ - Length of column st(x)

n - Total number of random series

n_j - Number of random variables in j^{th} series

p_{ai} - Ratio of cross-sectional area of concrete to steel in i^{th} storey column

P_{ih} - h^{th} load applied to column on i^{th} storey

$P_{st(x)}$ - Load applied to column st(x)

S - Used in Box-Muller approach for Gaussian generated random numbers

s_{ih} - Loading age of column in i^{th} storey due to h^{th} applied load

SK_{rel} - Relative skewness of data points

$SK_{rel}[X]$ - Relative skewness of X

$s_{st(x)}$ - Loading age of column st(x)

st(x) - Corresponding level and column for applied load x

$t_{d,st(x)}$ - Drying period of column st(x)

t_i - Total age of i^{th} storey column

$t_{sh,st(x)}$ - Age of column st(x) at onset of drying

$t_{st(x)}$ - Total age of column st(x)

U_1 - Used in Box-Muller approach for Gaussian generated random numbers

U_2 - Used in Box-Muller approach for Gaussian generated random numbers

V - n×n covariance matrix

Var[X] - Variance of X

Var[X′] - Variance of first-order X terms

Var[X″] - Variance of second-order X terms

V_1 - Used in Box-Muller approach for Gaussian generated random numbers

V_2 - Used in Box-Muller approach for Gaussian generated random numbers

X	- n×1 random vector
X_i	- i^{th} random variable
X_{ij}	- ij^{th} random variable
Z_1	- Used in Box-Muller approach for Gaussian generated random numbers
Z_2	- Used in Box-Muller approach for Gaussian generated random numbers
Z_3	- Used in Box-Muller approach for Gaussian generated random numbers
$\delta_{long,j,a}$	- Long-term cumulative shortening of j^{th} storey Column "a"
$\Delta_{f,j}$	- Long-term differential column shortening at j^{th} storey
$\varepsilon_{sh}(t_d)$	- Random shrinkage strain at time t_d from onset of drying
$\varepsilon_{shi}(x)$	- Free shrinkage strain of i^{th} storey column at time x
$\varepsilon_{sh(x)}$	- Free shrinkage strain at time x days
μ	- Mean, or - n×1 mean vector
μ_{xij}	- Expected value of X_{ij}
σ	- Standard deviation
$\phi(x,y)$	- Creep coefficient with a total column age of x days and a loading age of y days
$\phi_i(x,y)$	- Creep coefficient of i^{th} storey column with a column age of x and a loading age of y
$\phi(t,s)$	- Random creep coefficient at time t with a loading age of s
$\chi(x,y)$	- Aging coefficient with a total column age of x days and a loading age of y days
$\chi_i(x,y)$	- Aging coefficient of i^{th} storey column with a column age of x and a loading age of y

PREFACE

Volume 2 consists of published material that is not able to be communicated. We have added the contents pages to volume 2 here.

Volume 2 contains conference papers and research reports which form part of this submission, with the following included here:

Conference Papers

Koutsoukis M, Beasley A.J. (1994), - Monte Carlo Analysis of Tall Concrete Structures, Presented at the Second International Conference on Computational Structures Technology 30th August - 1st September 1994 in Athens, *CST 1994 Proceedings*, Civil-Comp Ltd, Edinburgh, Advances in Non-Linear Finite Element Methods, pages 129-134.

Koutsoukis M, Beasley A.J. (1994), - Probabilistic Shortening of Tall Concrete Buildings, Presented at the Australasian Structural Engineering Conference 21st-23rd September 1994 in Sydney, *ASEC 1994 Proceedings*, Institution of Engineers Australia, Canberra, Volume 1, pages 595-600.

Koutsoukis M, Beasley A.J. (1995), - Second-Order Moment Dischinger Model for the Axial Shortening in Tall Concrete Buildings, Presented at the Fifth East Asia-Pacific Conference on Structural Engineering and Construction 25th-27th July 1995 in Gold Coast, *EASEC-5 Proceedings*, Gold Coast University College of Griffith University, Gold Coast, Volume 1, pages 525-530.

Koutsoukis M, Beasley A.J. (1995), - Idealising the Construction Cycle of Tall Concrete Buildings for Axial Shortening Analyses, Presented at the Concrete 95 Toward Better Concrete Structures Conference 4th-7th September 1995 in Brisbane, *Concrete-95 Proceedings*, Concrete Institute of Australia, Brisbane, Volume 1, pages 447-453.

Koutsoukis M, Beasley A.J. (1995), - Axial Shortening Prediction Methods for Tall Concrete Buildings Part I : Comparison of Theoretical Methods, Presented at the Fourteenth Australasian Conference on the Mechanics of Structures and Materials 11th-13th December 1995 in Hobart, *14ACMSM Proceedings*, University of Tasmania, Hobart, Volume 2, pages 528-534.

Koutsoukis M, Beasley A.J. (1995), - Axial Shortening Prediction Methods for Tall Concrete Buildings Part II : Sensitivity Analysis and Experimental Comparisons, Presented at the Fourteenth Australasian Conference on the Mechanics of Structures and Materials 11th-13th December 1995 in Hobart, *14ACMSM Proceedings*, University of Tasmania, Hobart, Volume 2, pages 535-540.

Koutsoukis M, Beasley A.J. (1996), - Characteristics of Random Axial Shortening in RC Columns using Second-Order Moment Theory, Accepted for presentation at the Second International Conference Multi-Purpose High-Rise Towers and Tall Buildings 30th-31st July 1996 in Singapore, *Conference Proceedings*, Singapore, Volume ?, pages ?-?.

Koutsoukis M, Melerski E.S. (1996), - Random Elastic Response Characteristics of Bar Structures by Monte Carlo Simulation, Accepted for presentation at the Seventh ASCE Speciality Conference on Probabilistic Mechanics and Structural Reliability 7th-9th August 1996 in Worcester USA, *ASCE Conference Proceedings*, ASCE, New York, Volume ?, pages ?-?.

Seminar Papers

Koutsoukis M, Beasley A.J. (1992), - Effect of Elastic, Creep and Shrinkage Deformations in the Columns of Concrete Buildings, Presented at the Movement in Structures Seminar for the Concrete Institute of Australia (Tasmanian Division) 29th April 1992 in Hobart, *CIA Proceedings*, pages 17.

Research Reports

Koutsoukis M (1995), - STATS : Statistical Analysis Package (Version 1.0), *Research Report CM 95/1*, Department of Civil and Mechanical Engineering, University of Tasmania - Hobart, Tasmania.

Koutsoukis M (1995), - AXS : Axial Shortening Analysis Package (Version 2.0), *Research Report CM 95/2*, Department of Civil and Mechanical Engineering, University of Tasmania - Hobart, Tasmania.